A Design Scheme of Energy Management,Control,Optimisation System for Hybrid Solar-Wind and Battery Energy Storages System

A Thesis Submitted for the Degree of Doctor of Philosophy

by

RANJIT SINGH SARBAN SINGH

ELECTRONIC & COMPUTER ENGINEERING DEPARTMENT

COLLEGE OF ENGINEERING, DESIGN AND PHYSICAL SCIENCES

BRUNEL UNIVERSITY LONDON

UNITED KINGDOM

OCTOBER 2016

ABSTRACT

Hybrid renewable energy system was introduced to improve the individual renewable energy power system's productivity and operation-ability. This circumstance has led towards an extensive technological study and analysis on the hybrid renewable energy system. The extensive technological study is conducted using many different approaches, but in this research the linear programming, artificial intelligence and smart grid approaches are studied.

This thesis proposed a complete hardware system development, implementation and construction of real-time DC Hybrid Renewable Energy System for solar-wind-battery energy source integrated with grid network support. The proposed real-time DC HRES hardware system adopts the hybrid renewable energy system concept which is composed of solar photovoltaic, wind energy system, battery energy storage system and grid network support. The real-time DC HRES hardware system research work is divided into three stages. Stage 1 involves modelling and simulation of the proposed system using MATLAB Simulink/Stateflow software. During this stage, system's methodological design and development is emphasised. The obtained results are considered as fundamental finding to design, develop, integrate, implement and construct the real-time DC HRES hardware system. Stage II is designing and developing the electronic circuits for the real-time DC HRES hardware system using PROTEUS software. Real time simulation is performed on the electronic circuits to study and analyse the circuit's behaviour. This stage also involves embedded software application development for the microcontroller PIC16F877A. Thus, continuous dynamic decision-making algorithm is developed and incorporated into microcontroller PIC16F877A. Next, electronic circuits and continuous dynamic decision-making algorithm are integrated with the microcontroller PIC16F877A as a real-time DC HRES hardware system to perform real time simulation. The real-time DC HRES hardware system simulation results are studied, analysed and compared with the results obtained in Stage 1. Any indifference between the obtained results in Stage 1 and Stage 2 are analysed and necessary changes are made. Stage 3 involves integrating, implementation and construction of real-time DC HRES. The continuous dynamic decision-making algorithm is also incorporated into the real microcontroller PCI16F877A development board. Real-time DC HRES's

experimental results have successfully demonstrated the system's ability to perform supervision, coordination, management and control of all the available energy sources with lease dependency on the grid network. The obtained results demonstrated the energy management and optimisation of the available energy sources as primary power source deliver.

ACKNOWLEDGEMENTS

Firstly, I am grateful and highly indebted to the Ministry of Higher Education of Malaysia and Universiti Teknikal Malaysia Melaka (UTeM) for giving me the opportunity to pursue my PhD study at Brunel University London, United Kingdom.

Secondly, I would like to express my sincere gratitude to my supervisors, Dr Maysam Abbod and Professor Wamadeva Balachandran from Department of Electronic and Computer Engineering, Brunel University London for their undivided support, advice and help.

All of this would not have been possible without the morale support and encouragement from my family members, especially my parents, my brothers and by inlaws. I also would like to give a very big thank you to my beloved wife who stood with me, next to me throughout my PhD studies.

Last but not least, I would like to thank all the others who have known me either from Malaysia or the United Kingdom for their invaluable support for my meaningful journey.

Thank you all again, would not be possible with all the encouragement and support from everyone.

TABLE OF CONTENTS

LIST OF TABLES

LIST OF FIGURES

ABBREVIATIONS

AC	Alternating Current
ADC	Analogue to Digital Conversion
ASEAN	The Association of Southeast Asian Nation
BATT	Battery
BC	Boost Converter
BESS	Battery Energy Storage System
CPU	Central Processing Unit
CSP	Concentrating Solar Power
DC	Direct Current
DE	Differential Evolution
DisCh	Discharging
DL	Dump Load
FC	Fuel Cells
FF	Fill Factor
FL	Fuzzy Logic
GA	Genetic Algorithm
HCC	Hybrid Charge Controller
HOMER	Hybrid Optimization of Multiple Energy Resources
HRES	Hybrid Renewable Energy System
IC	Integrated Circuit
HEP	Hydroelectric Power
LCD	Liquid Crystal Display
LED	Light Emitting Diodes
MCLR	Master Clear Unit
MGT	Micro Gas Turbine
MPPT	Maximum Power Point Tracker
NC	Normally Closed
NN	Neural Network
NO	Normally Open
OWC	Oscillating Water Column
PCB	Printed Circuit Board
PEMFC	Proton Exchange Membrane Fuel Cell
PSO	Particle Swarm Optimisation
PV	Solar Photovoltaic
PWM	Pulse Width Modulation
RESs	Renewable Energy Sources
RETs	Renewable Energy Technologies
RPM	Revolutions Per Minute
SCADA	Supervisory Control and Data Acquisition
SoC	State of Charge
SVP	Solar Ventilation Preheating
TSR	Tip Speed Ratio
UK	United Kingdom
VRs	Variable Resistors

VSM	Virtual System Modelling
WT	Wind Turbine

DECLARATION

This work was produced by the author unless otherwise stated and duly acknowledged.

Signed: …….

Date: …….

CHAPTER 1

INTRODUCTION

Renewable energy sources have been available since many years ago. Renewable energy sources usually come from the natural sources such as sunlight, wind, rain water, tides, waves, geothermal heat and much more. These renewable energy sources can be used as replenishment to the depleting fossil fuels for electricity generation. The concern of depleting fossil fuels has encouraged the industries to explore or to increase the electricity productivity using the available renewable energy sources. Also, recent concerns on the concentrations of greenhouse gasses because of fossil fuels combustion have also encouraged the industries to look into new alternative sources for electricity generation. Alternative sources such as solar and wind power have been looked as notable renewable energy sources to support the diminishing conventional fossil fuels for electricity generation. Over the past 10 years, solar and wind power energies made a significant rise. Ever since solar and wind power is seen able to promisingly take over on the fossil fuels for electricity generation, many countries and local governments invested a lot of money into renewable energy electricity generation and distribution systems.

As the solar and wind power systems are growing into large-scale, the energy researchers, scientists and practitioners are looking into continuity research to improve the overall system performances, operation and reducing the financial risks. First, renewable energy sources such as solar and wind is always dependent on the geographical area, periodic climate change and greater energy production probability may disperse from the load locations. Neither solar nor wind power systems have the capability to fully satisfy the load demand and consumption due to the geographical area and periodic climate changes. Hence, solar and wind energies are combined to complement each another as hybrid power system to increase the electricity power generation, production and reduce the greenhouse gas emission impact on the environment. With the development of complementary hybrid power system, the power intermittency issue which greatly reflects on the climate condition can be probably resolved or improved. Theoretically, solar and wind complementary hybrid power systems have got more

advantages compare to any other single renewable energy source power system. Solar Wind Energy Tower article [1] mentioned about the latest development of solar and wind complementary hybrid power system, which is also known as Hybrid Renewable Energy System (HRES). This development has emphasised on the optimisation of the hybrid system design for reliable economy costing. In it's comparison the designed and developed complementary or hybrid solar - wind power system have shown a significant reduction in the installation area and costing while increasing the lifetime of the overall system performances [2]. This indicates that the deployment of renewable energy sources as complementary or hybrid power system could economically increase many involved parameters for a better performance [3]. Looking at the design and development in [1], this research hypothesised that complementary or hybrid renewable energy sources presents the cost-effective electricity power generation scheme to accommodate the increasing power supply demand and optimised the system operation.

This research work is divided into three stages; 1) modelling and simulating the concept of solar-wind renewable energy sources using the self-intervention method to supervise, coordinate, manage and control the available sources for an optimal system operation and integrating charging and discharging process for the Battery Energy Storage System (BESS) using MATLAB Simulink/Stateflow Software. 2) Designing, developing and simulating electronic circuits for solar-wind renewable energy sources and BESS to perform the self-intervention method for optimal system controllability and operation, incorporating microcontroller PIC16F877A to supervise, coordinate, manage and control the BESS charging and discharging process using PROTEUS Software. 3) Development, implementation, integration and construction of solar-wind renewable energy sources and BESS as a complete hardware system for real-time testing.

This research work is conducted in three stages are to fundamentally study the concept of supervising, coordinating, managing and controlling the solar-wind renewable energy sources and BESS for optimal operation with least dependency on the power source supply from the grid network. Each stage is presented with system performance analysis results, obtained results in stage one and two are categorised as preliminary results to validate the self-intervention of solar-wind renewable energy sources and BESS for charging or discharging process. The obtained preliminary results in stage one demonstrated the supervision,

coordinating, managing and controlling of solar-wind renewable energy sources and BESS charging or discharging using the MATLAB Simulink/Stateflow software.

Once the obtained preliminary results in stage one are studied and analysed, then the research is proceed to second stage. In the second stage, the electronic circuits PROTEUS software is used to design, develop and simulate the modelled system in stage one. All the modelled subsystems in stage one are designed, developed and simulated based on the real-time condition. The PROTEUS software is used to design and develop the electronics circuit and integrate the electronic circuits with microcontroller PIC16F877A to perform supervision, coordinating, managing and controlling the solar-wind renewable energy sources and BESS charging or discharging process. Prior to that, the embedded software application is designed and developed for microcontroller PIC16F877A. The embedded software application is important to be incorporated into microcontroller PIC16F877A to perform mathematical calculation on the available voltages to allow the microcontroller PIC16F877A intelligently supervise, coordinate, manage and control the solar-wind renewable energy sources and BESS charging or discharging process. This also will assist the system to optimise the solar-wind renewable energy sources and BESS utilisation for the connected Alternating Current (AC) load with least dependency on the grid network. The obtained results during the system simulation using the electronic circuits PROTEUS software is compared, analysed and validated with the obtained preliminary results in stage one. After these results are satisfied, then the hardware development, implementation, integration and construction is carried out. For a good hardware performance, it is necessary to realize a good preliminary work, clear feasible study which will be an indication for optimal technical solution for hardware development, implementation, integration and construction.

1.1 POWER ELECTRONICS ADVANCEMENT

Among the DC HRES, solar and wind energies are utilised broadly due to the extensive research in the system and technology development. Power electronics engineering research field have impacted in smoothing the overall performances of DC HRES for a continuous reliability of power generation, overall system operational optimisation and energy delivery/transfer between available sources/loads. Although many large HRES have been and are still under construction all around the globe, small scale HRES have seen increasing in

numbers and getting more focus in the recent years. Small scale HRES such as DC based are getting attention due to their lower impact on the landscape, avoid synchronisation process such as in AC based system, their ability to operate separately from the grid (islanded) and also able to operate with the grid network (non-islanded). In general, there is huge potential of usage for small scale DC HRES with strategic supervision, coordination, management and control of the available power from renewable energy sources and BESS for optimum power delivery, each subsystem to operate together and efficient self-intervention performance between renewable energy sources and switching between BESS for charging or discharging process. All of these advantages are not possible with all the advancements in the power electronics engineering field.

1.2 MOTIVATIONS

Solar and wind energies are being utilized broadly as source to electricity generation due to the advance development in the renewable energy sector and technology, their freely available energy characteristics at no extra cost, independency from fossil fuels and cost reduction in the individual system development have gained interest from many sectors. The work to develop indigenous Direct Current (DC) HRES using solar and wind to harvest the available energies from the sun and wind to generate electricity requires proper technologies integration. Even though the solar and wind DC HRES have improved significantly in terms of design and development, there are still challenges involved in many subareas of the HRES. One of the challenges or constraints exist in the HRES are the power management control strategy, to harness the DC energies as maximum as possible to optimise the freely available power source as primary supply for the connected AC load. Therefore, a strategic power supervision, coordination, management and control from the input sources to the connected load and BESS for charging or discharging are necessary. In addition, these challenges and constraints need to be address due to HRES dependency on the weather that would cause the intermittency of power delivery and operation optimisation. The increase research and advancement in power electronics engineering have provided the flexibility to address the challenges and constraints of smoothing the power delivery via an effective supervision, coordination, management and control at the DC HRES.

1.3 PROBLEM STATEMENT

At this point, the integration of solar and wind renewable energy sources as a system is gaining popularity due to their limitation to perform satisfactorily as an individual source. Due to the intermittent climate nature, individual solar or wind energy power systems are unable to perform and satisfactorily meet the load demand. Hence, integrating solar and wind renewable energy sources can improve the system complementary operation for maximum power delivery. With additional of some sources and sinks, counter balance the system intermittency could be achieved. The rapid development in the renewable energy and power electronics technology, reduced costing of the energy storages and broad microgrid system applications, various different system control strategies for optimum operation of power delivery and management has managed to achieved an effective energy distribution from the sources to the load of a HRES [4].

The concept of having two renewable energy sources is no longer new and have gained popularity in recent years such as been discussed in [5 - 10]. HRES is aimed to increase the system power delivery efficiency, optimise system operation and increase the power utilisation mainly from HRES. In general, HRES have huge potential for utilising the renewable energy sources to maximize the electricity power generation and distribution for increasing electricity demand around the globe. However, HRES encounter several technical challenges which are mainly associated to the intermittent climate and nature of the renewable energy sources. Thus, the technical challenges associated with HRES require an extensive research in several areas. The areas that have been identified are:

Proper sources self-intervention to achieve system operational optimisation for power management strategy and utilisation – It is to ensure that the power produced by solar-wind renewable energy sources can be optimised as much as possible without switching to the grid network. Also, to assist the HRES to operate at minimum production level but still would be able to perform at optimum performance when intermittent nature condition occurs.

Proper supervision, coordination, management and control of each subsystem that is connected via the control system – The HRES requires a proper supervision, coordination, management and control among each of the subsystem during a complete system operational. Therefore, the control system has to supervise, coordinate, manage and control different task

assigned for each subsystem in order to perform different type of system operation and functionality. With proper supervision, coordination, management and control of all the subsystem and control system, the overall system would achieve high system efficiency in terms of its operation and functionality.

Proper BESS selection for charging or discharging process – BESS is integrated as necessary component in HRES. The importance of integrating BESS into HRES is to have the continue supply of electricity during not available period of the renewable energy sources. In contrast to that, BESS is important to store the access energy during peak period of the renewable energy sources. With this, excessive energy could be stored and used during the sudden event of not available period of the renewable energy sources.

Looking at the problem statements, this research focus on designing, developing, implementing, integrating and constructing a real-time DC HRES hardware system to effectively supervise, coordinate, manage and control the solar-wind renewable energy sources power delivery and BESS charging or discharging process. Incorporating an effective supervision, coordination, management and controlling task would optimise the power delivery and energy management strategy for the real-time DC HRES hardware system. There are different types of techniques and methods that have been integrated into the previously developed DC HRES to achieve the maximum power deliverability while ensuring technical challenges are addressed. The aim and objectives section will briefly discuss on the techniques and methods that are proposed for the real-time DC HRES hardware system. These techniques and methods are integrated to address and overcome the technical challenges in this research to achieve an effective supervision, coordination, management and control of the solar-wind renewable energy sources and BESS charging or discharging self-intervention process. Whilst, this will also assist the proposed real-time DC HRES hardware system to deliver power effectively and strategically manage all the input and output resources.

1.4 AIM AND OBJECTIVES

The propose of this research is to develop, integrate, implement and construct a real-time DC HRES hardware system to supervise, coordinate, manage and control the solar-wind renewable energy sources and BESS charging or discharging self-intervention process. To perform the self-intervention process, voltage based self-intervention approach is integrated

with the microcontroller PIC16F877A which will help to predict the increment or decrement regulated output voltages or climate change between the solar-wind renewable energy sources. The objectives of this research are to:

Modelling and simulating the complete real-time DC HRES hardware system using MATLAB Simulink/Stateflow software. The modelling and simulating process in MATLAB Simulink/Stateflow software is used as a fundamental methodology for next stage.

Designing, developing and simulating the complete real-time DC HRES hardware system using PROTEUS software. The designing, developing and simulation is conducted to understand the electronic circuits characteristics via virtual real-time simulation before proceeding to next stage.

Integrating, implementing and constructing the complete real-time DC HRES hardware system for real-time system testing. This stage is concentrating to develop a complete real-time DC HRES hardware system and conducting a test on the complete hardware.

1.5 RESEARCH METHODOLOGY

This section will describe the research methodology used to develop the complete real-time DC HRES hardware system. The development, implementation and construct of the real-time DC HRES hardware system are divided into three stages. Each stage is described as in the following:

Stage I is involving the modelling and simulation using MATLAB Simulink/Stateflow software. The MATLAB Simulink software is used to model the electronic base subsystems, whilst, the MATLAB Stateflow software is used to develop the dynamic decision making controllers. The electronic base subsystems are modelled to perform the supervision, coordination, management and control of the solar-wind renewable energy sources as power source supplier and BESS for charging or discharging process. Whereas, the dynamic decision making controllers are developed to continuously sense the current condition of each respective subsystem and to perform any changes if the sensed and measured condition changed. Thus, the electronic base subsystems and continuous dynamic decision making controllers are integrated together to study the proposed real-time DC HRES hardware system

performances. Other than having the electronic base subsystems attached together in the real-time DC HRES hardware system, DC to DC BC and DC to AC Inverter is also modelled as a part of the proposed system. The DC to DC BC and DC to AC Inverter is modelled using the MATLAB Simulink software. DC to DC BC is used to step-up the 7~12 Volt regulated output voltages from the solar-wind renewable energy sources to a desired output voltage for either as a power source supply via the DC to AC Interver to the connected AC load or charging the BESS. The DC to AC Inverter is integrated to step-up and converts the 12~15 Volt regulated output voltage from the renewable energy sources and BESS into an AC voltage. The operation of DC to AC Inverter is controlled using the PWM signal.

Stage II of this research is involving designing, developing and simulating the electronic circuits using PROTEUS software. This stage can only be executed after the completion of Stage I. At the beginning of Stage II, PROTEUS software is used to model and design the electronic circuits, whereas, PCWH CCS C Compiler embedded software application is used to develop decision making algorithm for the microcontroller PIC16F877A. The electronic circuits that are modelled and designed using the PROTEUS software are as listed:

- Voltage based self-intervention circuitries (4 Units)
- Microcontroller PIC16F877A development board (1 Unit)
- Relay base switching circuitries (17 Units)
- DC to DC BC (4 Units)
- DC to AC Inverter (1 Unit)

The voltage based self-intervention approach is a concept of voltage divider circuit which is used to sense and measure the voltages changes at the solar-wind renewable energy sources and BESS. Microcontroller PIC16F877A development board is modelled and designed to integrate all the electronic circuitries which are controlled via the embedded software application incorporated in microcontroller PIC16F877A. The relay base switching circuitries are divided into two, which are: a) relay switching and control modules which are used to perform the self-intervention between the regulated output voltages from the solar-wind renewable energy sources and b) charging/discharging switching circuits which are used to

perform the self-intervention during the charging or discharging process. These relay base circuitries are controlled via the embedded software application incorporated in microcontroller PIC16F877A. The embedded software application algorithm incorporated in microcontroller PIC16F877A is developed to continuously perform switching based on the sensed and measured voltages at the solar-wind renewable energy sources and BESS. Therefore, the embedded software application developed is named as continuous dynamic decision making algorithm. DC to DC BC is modelled to step-up the 7~12 Volt regulated output voltages from the solar-wind renewable energy sources. The stepped-up voltages are used as a primary power source supply to the connected AC load or BESS charging. DC to AC Inverter is modelled and integrated at the load input. Thus, 12~15 Volt voltage is step-up and converted into an AC voltage for the connected AC load. The electronic circuitries modelled and designed using PROTEUS software are virtually connected to each other and perform the real-time simulation to analyse the real-time DC HRES hardware system operation and performance.

Stage III of the real-time DC HRES hardware system is transforming the designed and developed methodologies in Stage I and II into a complete hardware system. Therefore, after studying the designed and developed methodologies in Stage I and II, all the hardware modules except for the voltage based self-intervention are purchased to develop, integrate, implement and construct the real-time DC HRES hardware system. All of the hardware modules are integrated together with the microcontroller PIC16F877A to implement and construct the real-time DC HRES hardware system as a complete system. Then, the continuous dynamic decision making algorithm is incorporated into the microcontroller PIC16F877A to perform the supervision, coordination, management and controlling for all the connected subsystems. The effective supervision, coordination, management and controlling of the available sources via real-time DC HRES hardware system has successfully utilised and optimised the power source delivery to the connected AC load. Besides that, the real-time DC HRES hardware system also effectively managed the BESS charging or discharging process, stepping-up 7~12 Volt regulated output voltages from the solar-wind renewable energy sources to a desired output voltage and converting 12~15 Volt into an AC voltage for the connected AC load.

1.6 CONTRIBUTIONS TO KNOWLEDGE

The aim and objectives addressed are to overcome the technical challenges described in the problem statement in Section 1.3. The major contributions of this thesis are described below:

Modelling and simulation of the real-time DC HRES hardware system which is composed with DC to DC BC and DC to AC Inverter is performed using MATLAB Simulink/Stateflow software. The modelling of the real-time DC HRES hardware system is constructed using the MATLAB Simulink and Stateflow toolbox. Two continuous dynamic decision making controllers are modelled using the Stateflow toolbox which function is to detect the voltage changes from the solar-wind renewable energy sources and BESS. The Simulink toolbox is used to model all the electronic circuitries that are used to supervise, coordinate, manage and control the switching between the solar-wind renewable energy sources and BESS for charging or discharging process. All the Simulink and Stateflow based modelled subsystems are integrated together and successfully supervised, coordinated, managed and control the real-time DC HRES hardware system.

Next contribution is development and simulation of electronic circuits using PROTEUS software. Each part modelled using MATLAB Simulink/Sateflow is developed in PROTEUS software environment. To simulate the real-time DC HRES hardware system, continuous decision making algorithm is designed and developed using the PCWH CCS C Compiler embedded software. The development of continuous decision making algorithm using PCWH CCS C Compiler embedded software reduces the electronic circuitries modelled using MATLAB Simulink/Stateflow. The continuous decision making algorithm in incorporated into the microcontroller PIC16F877A to demonstrate the supervision, coordination, management and control to optimise the real-time DC HRES hardware system operation and at the same time optimise the sources power delivery without dependency on the grid network.

Final contribution is commencing the real-time DC HRES hardware system development, implementation, integration and construction based on the obtained results from MATLAB Simulink/Stateflow and PROTEUS software simulation. This contribution is critically important to demonstrate the proposed real-time DC HRES hardware system can operate as it is described during the real-time DC HRES system development process.

1.7 THESIS STRUCTURE

This thesis has been organised into seven chapters, which are organised as follows:

CHAPTER 2 – LITERATURE REVIEW

This chapter discusses about the available HRES structures which can be used to configure the renewable energy sources as standalone or grid-connected HRES. Brief descriptions for each component available in Solar Photovoltaic (PV) and wind HRES is also presented. In addition, technical reviews and contributions of previously and recently developed HRES are discussed to understand the system's controllability and operability.

CHAPTER 3 – MATLAB-SIMULINK MODELLING OF REAL-TIME DC HRES HARDWARE SYSTEM

The initial modelling and simulation of real-time DC HRES hardware system is discussed in this chapter. The voltage based self-intervention, voltage base controller, voltage switching subsystem controller, circuit breaker switching, group conditions and BESS charging/discharging switching circuit, DC to DC BC and DC to AC Inverter are modelled and simulated. The determined results from the conducted modelling and simulation are used as preliminary findings and reference prior to hardware implementation, integration and constructions.

CHAPTER 4 – DESIGN AND DEVELOPMENT METHODOLOGY OF HARDWARE SYSTEM SIMULATION: PROTEUS SOFTWARE

The voltage based self-intervention, relay switching and control module, charging-discharging switching circuit, GRID connection/LOAD switching circuit, DC to DC BC, DC to AC Inverter and microcontroller PIC16F877A system development using PROTEUS software is discussed in this chapter. The simulation determined results are compared with the preliminary results in Chapter 3 to validate the hardware system operation.

CHAPTER 5 – EMBEDDED SOFTWARE APPLICATION ALGORITHM FOR MICROCONTROLLER PIC16F877A

This chapter deals with the embedded software application development for the microcontroller PIC16F877A. The embedded software application develops the continuous dynamic decision making algorithm for the microcontroller PIC16F877A.

CHAPTER 6 – HARDWARE IMPLEMENTATION AND CONSTRUCTION – RESULTS, ANALYSIS, VALIDATION and DISCUSSION

This chapter describes the hardware implementation and constructions. The developed methodology in Chapters 4 and 5 are used to implement and construct the real-time DC HRES hardware system. The hardware system is tested and commissioned to achieve the best output results. These results are analysed, compared and validated with the obtained results in Chapters 3 and 4. This chapter also includes discussion and summary for overall achieved results for the modelling, simulation, integration, implementation and construction of real-time DC HRES hardware system.

CHAPTER 7 – CONCLUSIONS AND FUTURE WORK

This chapter will provide a conclusion and describe the future prospects of this research.

1.8 LIST OF PUBLICATIONS

Conference papers:

1. Ranjit Singh, Maysam Abbod, and W. Balachandran, Renewable Energy Resource Self-Intervention Control Technique using Simulink/Stateflow Modelling. UPEC2015, September 1st - 4th, 2015 | Staffordshire University, UK.

2. Ranjit Singh, Maysam Abbod, and W. Balachandran, Low Voltage Hybrid Renewable Energy System Management for Energy Storage Charging-Discharging. ENERGYCON 2016 April 4rd - 8th, 2016 | Leuven, Belgium.

3. Ranjit Singh, Maysam Abbod, and W. Balachandran, Simulation of a New Proposed Voltage-Base Self-Intervention Technique with Increment and Decrement Voltage Conduction Method to Optimize the Renewable Energy Sources DC Output. 2016 UKSim-AMSS 18th International Conference on Computer Modelling and Simulation (UKSIM2016) April 6th - 8th, 2016 | Cambridge University, UK.

4. Ranjit Singh, Maysam Abbod, and W. Balachandran, A Design Scheme of Control/Optimization System for Hybrid Solar – Wind and Battery Energy Storages System. UPEC2016, September 6th - 9th, 2016 | University of Coimbra, Portugal.

CHAPTER 2

LITERATURE REVIEW

This chapter concentrates on studying the current and previously developed HRESs which are relevant to the scope of this research project development. Section 2.1 discusses an overview about the available Renewable Energy Sources (RESs) and Renewable Energy Technologies (RETs). Section 2.2 discusses about the types of HRESs structures. Section 2.3 discusses about the equivalent model of solar photovoltaic and wind energy generator. In Section 2.4, other basic relevant HRES's components that complete the HRES as a system is discussed.

In the Section 2.5, a review study which will concentrate on different methods and approaches to address the technical challenges such described in 1.3 is reviewed. The study in this section would help to access to the past research and contributions to improve renewable energy sources deliverability and HRES potentiality as a system. Therefore studying and reviewing the current and past research work by previous scholars helps to gain more information about the required relevant subjects.

2.1 OVERVIEW OF AVAILABLE RENEWABLE ENERGY SOURCES

Renewable energy is becoming an interesting topic around the world, but renewable energy is still not the main dominant energy generator. In addition, the rising cost of fossil fuels also has caused the cost of electricity generation increased. Other than that, the increasing electricity consumption in urban households have resulted inequality in the electricity supply. Looking at the issues concerning the conventional method of electricity generation, the power system and energy researchers brings to attention of substituting the conventional electricity generation to using the renewable energy sources for electricity generation such as in [11 - 14]. In the case to reduce the dependency on fossil fuels for electricity generation, renewable energy system which is based on the renewable energy sources is gaining popularity around the world. Renewable energy sources is said will not deplete and have the ability to replenish themselves for continuous usage [15]. Therefore, Table 2.1 summarises and explains the advantages and disadvantages of the available renewable energy sources.

Table 2.1: Types of available renewable energy sources advantages and disadvantages [15] [16]

Types of Energy	Source	Advantages	Disadvantages
Solar	Sun – The light is captured using to produce electricity.	Infinite energy supply potentiality. Each individual can install own electricity generator for supply.	Solar panels are too costly to manufacture and implement.
Wind	Wind turbines attached with the wind energy generator to produce electricity.	Individually installed but integrated together as operational wise as wind farm. Infinite energy supply potentiality.	Too costly in terms of manufacturing and implementing the wind form concept. Objection from local people – On-shore wind farms would destroy the countryside environment.
Tidal	Turbines are moved using the tide wave. Metal based barrage is built and placed into the sea. The water is forced through the gaps for electricity generation. In future underwater turbines are possible	Ideal for ASEAN countries and for island countries such as UK, Ireland, Iceland. Ability to generate a lot of potential electricity energy. Electricity output can double via	Barrage construction is very costly. Objected by some environmentalist groups – concern have negative impact on wildlife.

	for installation.	integrating tidal barrage, also would help to prevent flooding.	
Wave	The in and out seawater movement of a cavity on the shore help to compress the trapped air to drive the turbine.	Can be ideally installed in an island country. Ideal for small operation in a local area compare with national scale operation.	Developing and constructing the farm can be very costly. Probably opposed by the local residents or environmentalist groups.
Geothermal	The natural heat from the earth or any volcanic regions can be used as energy source. Steam is used to heat or as power for turbines movement to generate electricity.	Can be an infinite type of energy supply. Countries such as New Zealand and Iceland successfully the energy as source of demand.	Can be costly to set up and only can be operated in volcanic activity areas. Probability the geothermal and volcanic activity goes passive, letting the power station inactive. Proper handling of underground elements is carefully required.
Hydrological or Hydroelectric Power (HEP) Energy	One of the traditional energy harnessing methods from stream such as rivers, lakes	Water is reserved while energy is being supplied.	Expensive to build the system. Probability of causing flood is

	and dams.		always there. Big dam have ecological impact on the environment.
Biomass	Organic material - Decomposition of plant and animal waste. Can be burn to produce energy such as heat or sometimes electricity.	One of the cheapest and always available sources of energy. Biomass in long run can be replaced as a sustainable energy source.	Pollution to the environment and atmospheric during burning. Can be only said renewable energy if chopped plants are replanted.
Wood	Centuries used method from fall trees, are burn to produce heat and light.	Always available and cheapest energy source. Fall trees are advised to be replaced for long-term and sustainable energy source.	When burning cause pollution to environment and atmosphere, including greenhouse gas effect. If fallen trees not replanted then wood is not a renewable source.

Availability of numerous types of renewable energy sources has exploited the RETs. RETs is define as technology to provide energy that utilises one or more renewable energy sources, that way it will not deplete the available Earth's natural sources [17]. RETs have been used to exploit the available renewable energy sources with the potentiality to provide the increasing energy demand among the community in a sustainable operation. The decentralisation of renewable energy sources using the RETs has allowed the sources to be matched for continuous energy sustainability.

The efficient and effective use of any kind of renewable energy sources requires some kind technology. Therefore, RETs can be used to provide a sustainable energy from the available renewable energy sources, such in Table 2.1. Subsequently, understanding the required RETs for a potential renewable energy source is an important aspect. In that case, Table 2.2 presents the renewable energy sources corresponding RETs for sustainable energy.

Table 2.2: Renewable energy sources and corresponding RETs

<table>
<tr><td>Renewable energy sources</td><td colspan="5">Renewable energy technology</td></tr>
<tr><td rowspan="5">Solar / Sun</td><td colspan="5">Solar Panels/Photovoltaic (PV)</td></tr>
<tr><td colspan="5">Concentrating Solar Power (CSP)</td></tr>
<tr><td>Linear Concentrator Systems</td><td colspan="2">Dish/Engines System</td><td colspan="2">Power Towers</td></tr>
<tr><td colspan="5">Solar Hot Water</td></tr>
<tr><td colspan="5">Solar Ventilation Preheating (SVP) Systems</td></tr>
<tr><td>Wind</td><td colspan="5">Wind Turbine (WT)</td></tr>
<tr><td rowspan="2"></td><td>Horizontal Axis Turbines</td><td colspan="4">Vertical Axis Turbines</td></tr>
<tr><td></td><td colspan="2">Darrieus turbine</td><td colspan="2">Savonius turbine</td></tr>
<tr><td>Tidal</td><td>Tidal Dam, or Barrage</td><td>Tidal Lagoons</td><td>Underwater Tidal Turbines</td><td>Tidal Fences</td></tr>
<tr><td>Wave</td><td>Floats, Buoys, or Pitching devices</td><td>Oscillating Water Column (OWC)</td><td colspan="2">Tapered Channel or Over Topping Device</td></tr>
<tr><td>Geothermal</td><td>Geothermal Electricity Production</td><td>Geothermal Direct Use</td><td colspan="2">Geothermal Heat Pumps</td></tr>
<tr><td rowspan="2">Hydrological</td><td colspan="5">Hydroelectric Power (HEP) Energy</td></tr>
<tr><td colspan="3">Hydroelectric Power or Hydropower</td><td colspan="2">Pumped Storage Plant</td></tr>
<tr><td>Biomass</td><td colspan="3">High-Efficiency Gasification Systems</td><td colspan="2">Combustion</td></tr>
</table>

Table 2.2 includes a list of available renewable energy sources and its matching RETs that mean to allow modern type of energy services and ways to generate electricity. Most importantly also, RETs are always developed to address the balance of the energy demand [18].

2.2 HYBRID RENEWABLE ENERGY SYSTEM STRUCTURES

The rapid growth and development of renewable energy technologies for power generation, distribution and utilisation have explored the potentiality in the renewable energy sources. Also, the rapid growth in the new technology invention in the industrialisation has helped to reduce the supply – demand gap particularly in the electricity sector [19]. Above all, the supply – demand is expected to continue to rise exponentially unless the new technology inventions can be utilised for power generation. In general, deploying the new technology inventions with the renewable energy sources would therefore develop mature HRESs. Therefore, before any new technology is developed fundamental structure of HRESs is important to be understood. In particular, HRES is mainly categories into three types, which are DC Coupled-Systems, AC Coupled-System and Hybrid Coupled-Systems. Thus, in the next section a review of DC Coupled-Systems, AC Coupled-Systems and Hybrid Coupled-Systems structure is briefly discussed.

2.2.1 DC COUPLED-SYSTEMS

DC coupled-systems are systems that are entirely built-up based on the passive electricity generation sources [20]. These systems are all connected to the main DC linked bus before it get down to the grid system [21]. This kind of systems can be precisely described as the DC electricity generated from the DC generation sources are through the charge controller and stored into the battery storage [22]. The battery storages are connected to an inverter that able to convert the DC electricity to AC electricity for home utilisation [23]. A DC Coupled-System as shown in Figure 2.1 illustrates the most basic system that has a charge controller that potentially harvests all the energy from the installed renewable energy sources. The output of the charge controller is either bi-directionally connected to BESS or to the DC loads. The harvested electricity energy is stored into BESS for off-grid used when it is required [23].

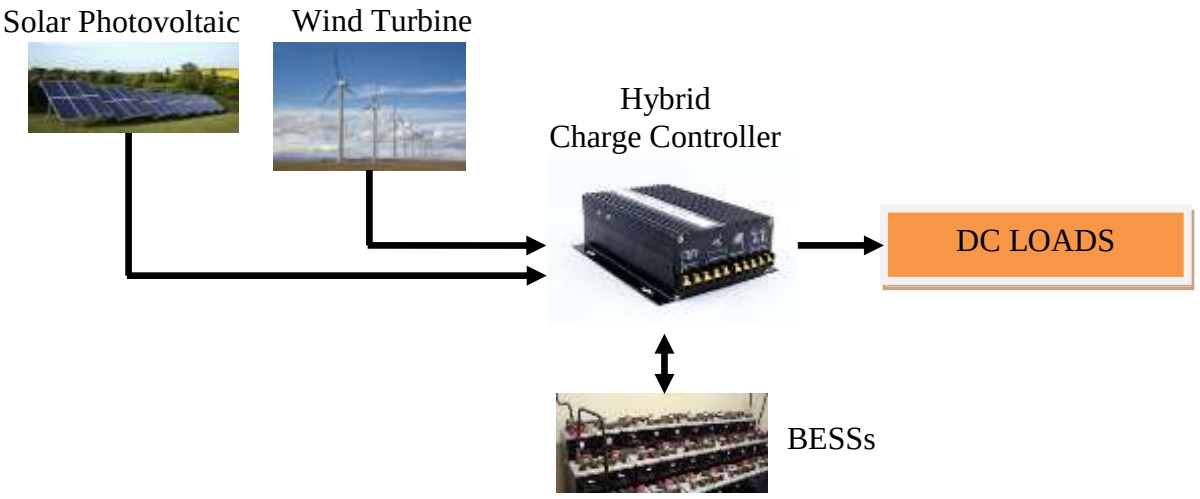

Figure 2.1: Diagram of Hybrid PV – Wind with BESS powering DC loads

2.2.2 AC COUPLED-SYSTEMS

AC Coupled-Systems are systems that usually connects the entirely loads to an AC bus line [24]. The architecture of an AC Coupled-System is entirely different compare with the DC Coupled-System. An AC Coupled-System is always connected to grid-tie inverter [23] as shown in Figure 2.2. The AC Coupled-System can be categories into TWO operations: 1) normal AC operation and 2) critical AC operation. Describing the normal AC operation system, the AC grid-tie inverter system will allow the system to operate alongside with the main power from the renewable energy sources and also maintain the grid-inverter tie to charge the BESS [25]. Furthermore, the critical AC operation or main power blackout period only allows the grid-tie inverter to operate from the BESS to support the main system.

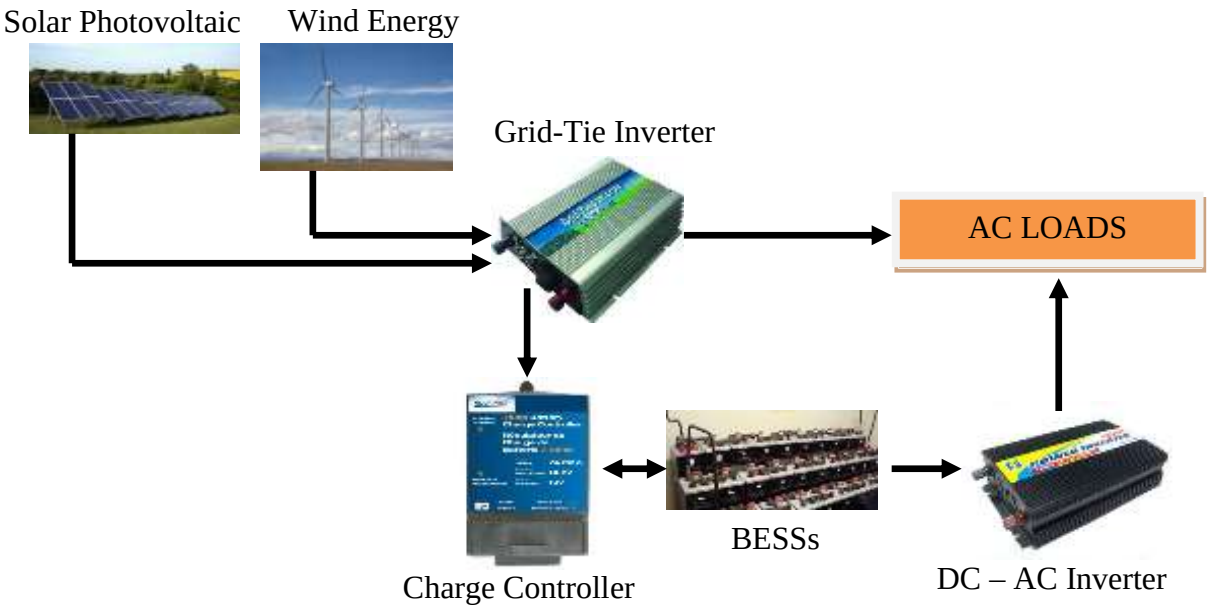

Figure 2.2: Diagram of AC electricity generation system with battery storages powering AC loads

2.2.3 HYBRID COUPLED-SYSTEMS

Hybrid Coupled-Systems shown in Figure 2.3 are incorporated of several types of fossil-fuelled electricity power generation plants and with the available renewable energy sources. All of these electricity generation components are usually connected to one major control system which enables the control system to perform at the optimum quality [26]. Now days, Hybrid Coupled-Systems are gaining interest for electricity generation at remote locations [27], [28]. Describing the Hybrid Coupled-System, the generated DC electricity is used to supply to the DC loads and excessive generated electricity source is stored into the battery storages for off-mode period utilisation. When the stored electricity power is fully utilised, the system power will be switched to the generator set.

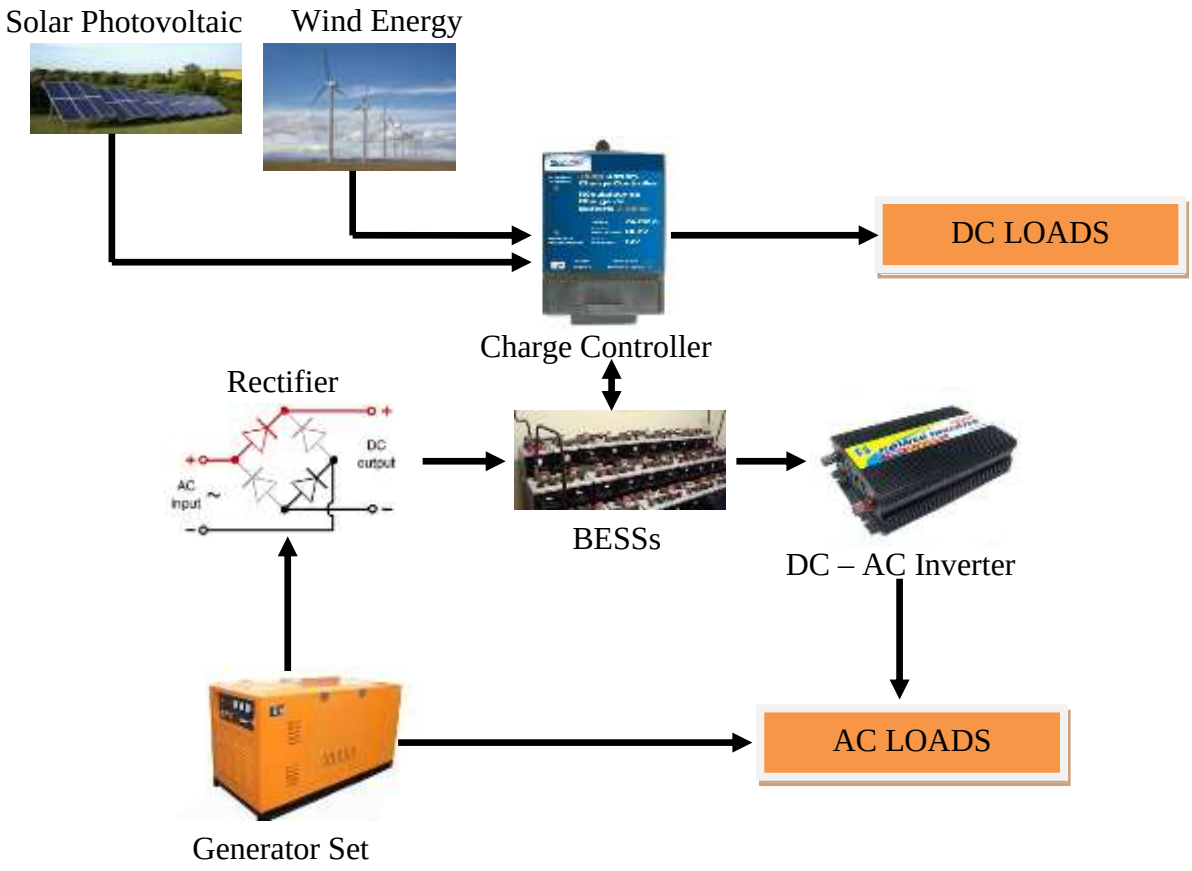

Figure 2.3: Diagram of hybrid electricity generation system with BESS powering DC loads and inverter powering AC loads

Generally, there are three types of HRES structures which can integrate different types of renewable energy sources. DC Coupled-System structure is only connected to DC bus line and renewable energy sources are integrated to DC bus line with proper power electronic system integration [29]. The DC Coupled-System is the simplest scheme to synchronise the renewable energy sources. The major drawback of DC Coupled-System is when the inverter fails, the overall system is unable to deliver the power supply [30]. This drawback can be possibly overcome with parallelisation of some low range inverter connection with the AC power [29]. The integration of AC Coupled-System structure has the fundamental of the DC Coupled-System, except all the loads are connected directly to the AC bus line [24]. As shown in Figure 2.2, the AC Coupled-System combines the BESS and BESS-less inverter into a single grid tied or off-grid tied structure. The Hybrid Coupled-System structure is formed based on

the DC – AC Coupled System. All the DC type of energy sources are connected to the DC bus lines via the DC to DC Converters, whist, bus lines are connected to the BESS. Meanwhile the AC energy source is connected to the BESS via the rectifier to charge the BESS for the DC loads. At the same time the AC source will supply energy to the connected AC loads.

2.3 COMPONENT DESCRIPTION

2.3.1 PHOTOVOLTAIC EQUIVALENT CELL DESCRIPTION

Solar energy is produced from the sun, therefore the incident of sun light falling onto the solar panels is converted into usable electricity energy by solar energy harvesting method and process [31]. To achieve the fundamental understanding of solar arrays operation the equivalent circuit of single-diode model in Figure 2.4 is used to explain the solar energy harvesting process.

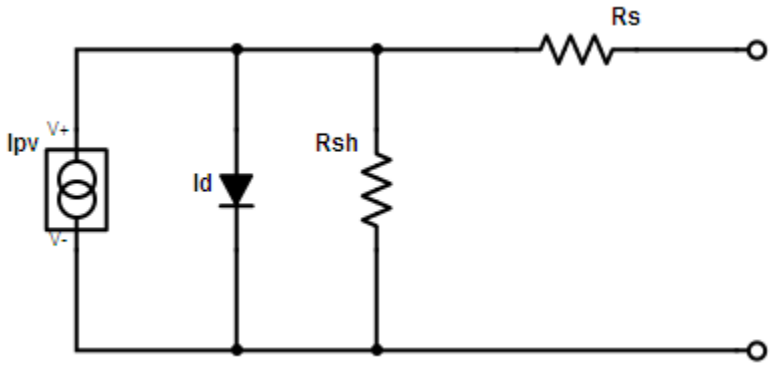

Figure 2.4: Single-Diode model for equivalent single solar cell [32 - 33]

The single-diode model shown in Figure 2.4 is the ideal identical circuit for a single solar cell. An ideal configuration is connecting the current source in parallel with a single-diode. The electronic circuit shown in Figure 2.4 describing the electrical operation of a solar cell while using a single diode and two resistors [34].

The equivalent electronic circuit model can be defined as in Equations (2.1) and (2.2).

$$I \equiv I_{PV} - I_0\left[\exp\left(\frac{V + IR_S}{aV_t}\right) - 1\right] - \frac{V + IR_s}{R_{sh}} \tag{2.1}$$

$$V_T = n\frac{kT}{q} \tag{2.2}$$

where,

I_{pv} = Constant current source produced by photocurrent,

I_0 = Diode to block the reserve saturation current,

R_s = Series resistor that takes into account losses in cell solders bonds, interconnect junction box, etc,

R_{sh} = Shunt resistor that takes into account the current leakage through the high conductivity shunts across the p-n junction,

a = Ideality factor that takes into account the deviation of the diodes from the Shockley diffusion theory,

V_T = Thermal voltage of the diode and depends on the charge of the electron,

q = Boltzmann constant, (1.3807 x 10^{-23} joule s per kelvin)

k = Number of cells in series,

T = Temperature (Kelvin)

The equivalent electronic circuit shown in Figure 2.4 is describing Direct Current (DC) static behaviour of a solar cell. Basically this model consists of a current source, as well as with a PN junction diode and a shunt resistor, (R_{sh}) [35] connected in parallel with a series resistor, (R_s) [36]. R_s parameter is important to be connected in series to reduce short circuit current of the solar cell and also the maximum power output [37]. The R_s ideally should be zero ohms [37]. The R_{sh} is connected in parallel to correspond to the edges surface leakage loss of the solar cell [37]. The R_{sh} as well should be infinite [37].

If a load is connected in series to the R_s resistor, in parallel with the R_{sh} resistor while the solar cell is illuminated, then the total current calculated in Equation (2.3) becomes;

$$I = I_s\left(e^{\frac{qV}{kT}} - 1\right) - I_L \tag{2.3}$$

where,

I_s = Current due to diode saturation

I_L = Current due to optical generation

Figure 2.5 illustrate the solar cell efficiency characteristics, several factors are used to measure the efficiency of a solar cell, such as the maximum power point $(P_{\max})$, the energy conversion efficiency (η), and Fill Factor (FF). The maximum power point $(P_{\max})$ which is at the point $V_{mp} : I_{mp}$ produces the maximum current $(I_{\max})$ and maximum voltage $(V_{\max})$ which relatively generates the maximum power output from the solar cell at the point $V_{mp} : I_{mp}$.

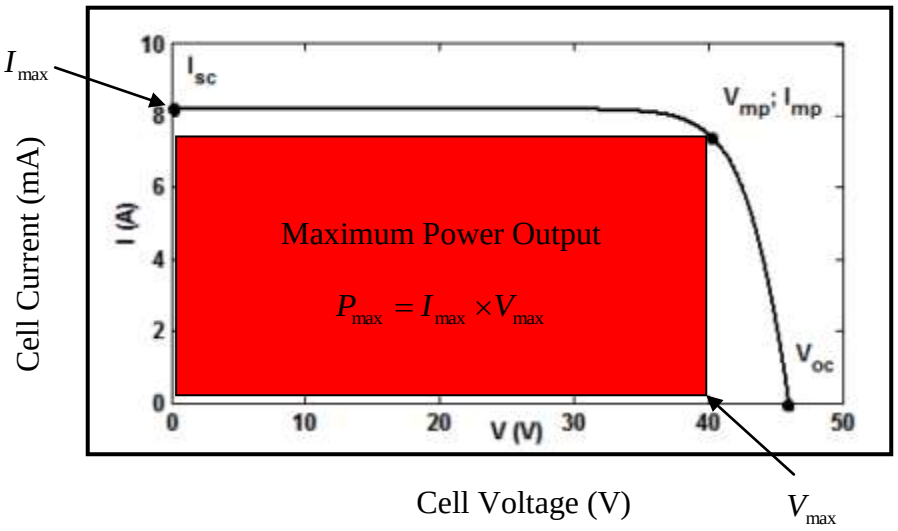

Figure 2.5: I-V curve characteristics for solar cell [34]

2.3.2 WIND TURBINE SYSTEM DESCRIPTION

The movement of air in the atmosphere produce kinetic energy and kinetic energy can be converted into wind energy using wind turbines [38]. While the height, blade length and generating capacity can be varies but the basic design is always the same. A typical wind turbine system as shown in Figure 2.6 is composed of a tower, rotor blades, yaw mechanism, wind speed and direction monitor and gear box [39 - 40].

The tower is usually used to fit the wind turbine system, apparently the tower is often forgotten as an essential part of the wind turbine system. The tower is used to uplift the rotor blades above the ground, surrounding obstacles such as buildings and trees to increase the wind turbines power output. Uplifting the wind turbine system will increase the clean unhindered air flows which are stronger, less destructive and more reliable especially during the low wind speeds.

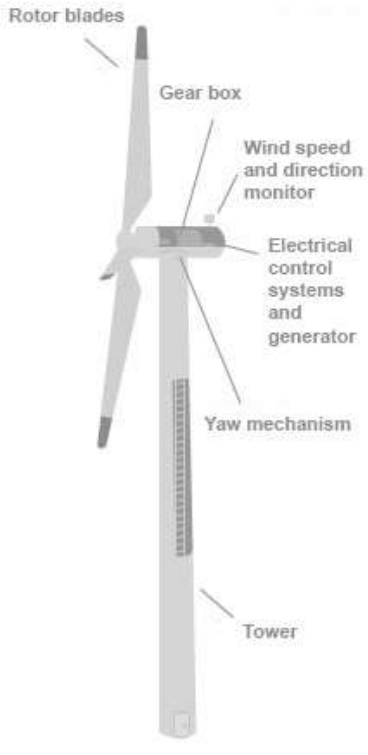

Figure 2.6: Typical major wind turbine structure [39] [41]

Rotor blades are one of the key components in the wind turbine system. The wind fall on the blades force the rotor to turn for energy production. This will help the mechanical rotor to capture the wind energy and drive the generator for power production.

Generator in the wind turbine is used to generate electricity to the grip supply. Figure 2.7 shows the typical asynchronous generator used in the Danish Wind Turbines in 1999 [42]. Wind turbine usually used asynchronous type of generator which also is known as induction generator or double-fed generator. Asynchronous generator is used because it can be used as a generator as well as a motor too. The asynchronous type of generator is used in the wind turbine because it is capable to rotate the rotor at a lower speed compare to synchronous type of generator. Also this asynchronous type generator speed can be exceed by integrating external source such as a diesel motor or wind turbine rotor blades.

Figure 2.7: Typical asynchronous generator for Danish wind turbine [42]

With the knowledge that wind turbine operates by converting the kinetic energy produced by the wind into rotational kinetic energy in the turbine and then into the electrical energy that is potential supplied to the grid network transmission. The wind speed is the main factor that allows the kinetic energy is converted into a usable energy. Thus, to calculate the amount of power that can be produced by the sweep area of the turbine, speed of the turbine and the turbine power rating is necessary to calculate.

2.3.2.1 TURBINE SWEEP AREA

Sweep area of a wind turbine relates to the amount of power output as shown in Figure 2.8, the sweep area measures the created circle by the blades whenever the air is through the blades. The larger the diameter of the blades, more power can be extracted from the wind. The sweep area is calculated using the formula in Equation (2.4).

$$\text{Area Swept by the Blades} = \pi r^2 \tag{2.4}$$

where

π = 3.14159 (pi)

r = radius is equal to the length of the one of the blade.

2.3.2.2 TIP SPEED RATIO

Tip Speed Ratio (TSR) [43] is also an extremely important aspect relating to the power production in wind turbine. It is also can be define as the ratio between the wind speed and the speed of the tips of the blades [44]. The wind hits the tip of the blades, rotor will rotate and if the rotor is at slow speed, too much of wind is getting pass through the blades undisturbed, thus giving zero power or very minimal power production [43 - 44]. Adversely, when the rotor turns too quickly, the blades will produce a resistance such as a large hard wall against the wind that is trying to spin the blades [43 - 44]. This condition will cause the blades to create turbulence as the blades rotate too fast through the blowing wind. Hence, before the TSR can be calculated, the duration that takes the rotor to complete a resolution is important to be calculated. This can be easily calculated if the Revolutions per Minute (RPM) can be determined, thus divide the RPM with 60 seconds and the result will be the duration for the rotor to complete a resolution. There are few means to measure the speed of blade rotation of a wind turbine, one of the most cheapest means is using the basic cycle computer. Cycle computer by itself can operate as a RPM sensor, but some modification is required to use the cycle computer as RPM sensor. Article [45] can be referred and explains the procedure to use the cycle computer to measure the RPM of a wind turbine. Figure 2.9 shows the magnet and sensor placement to measure the RPM for a wind turbine.

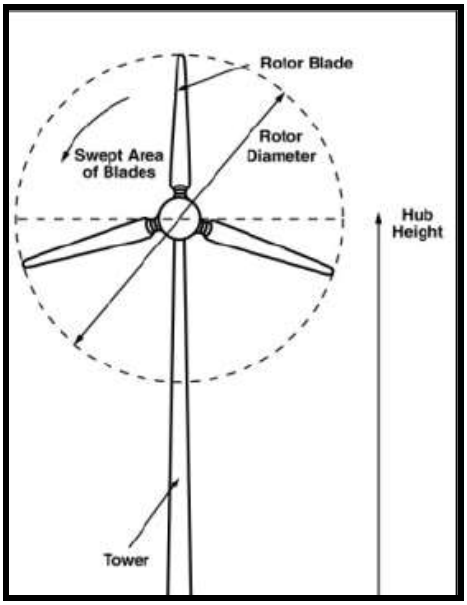

Figure 2.8: Measuring sweep area of wind turbine

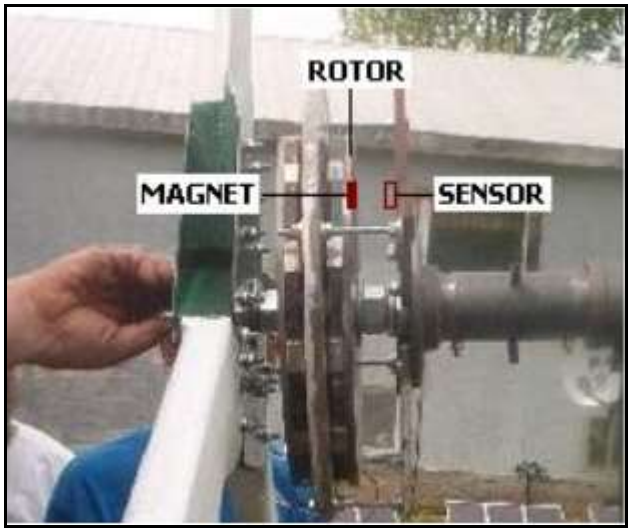

Figure 2.9: Placement of magnet and sensor to measure RPM [45]

The TSR can be defined as shown in Equation (2.5);

$$\text{TSR } (\lambda) = \frac{\text{Tip Speed of Blade}}{\text{Wind Speed}} \equiv \frac{v}{V} \equiv \frac{\omega r}{V} \tag{2.5}$$

where

$$V = \text{Wind speed area (m/sec)}$$

$v = \omega r = \text{Rotor tip speed (m/sec)}$

$r = \text{Rotor blade (m)}$

$\omega = 2\pi f \text{ Angular velocity (rad/sec)}$

$f = \text{Rotational frequency (Hz)}, (\sec^{-1})$

Wind speed area formula at the blades tip can be derived as shown in Equation (2.6);

$$\text{Wind Speed Area (Blades Tip)} = V = \frac{2\pi r}{T(\text{Time})} \tag{2.6}$$

where

pi = π = 3.142

Radius, r = rotor blade (m)

Time, T = rotation time (seconds)

As mentioned earlier, the TSR is an important element to maximise the power output and improve the efficiency of the wind turbine. Once all measurements have been made, the maximum power in can be calculated using equation (2.7) [46].

$$P = \frac{1}{2} \times \rho \times A \times V^3 \tag{2.7}$$

where

P = Power (Watts)

p = Air Density (about 1.225 kg/m^3 at sea level)

A = Swept Area of Blades (m^2)

V = Velocity of the wind (m/s)

2.4 OTHER RELEVANT HRES SYSTEM COMPONENTS

As discussed in section 2.2, HRES can be structured to be DC Coupled-System, AC Coupled-System and Hybrid Coupled-System. Continuing the background study it is also important to study or understand the other component of each HRES structured system. Therefore, this section will briefly discuss the other components of HRES such as Hybrid Charge Controller (HCC), Grid-Tied Inverter, DC – DC Converter, BESS, DC – AC Inverter and Rectifier. Although all of these components are used as plug and play system but it is essential to understand their functionality for respective individual type of HRES.

2.4.1 CHARGE CONTROLLER

Charge controller usually plays a central role of a HRES. A HCC is capable of controlling the switching ON or OFF of any supply connected to it and control the BESS charging and discharging as well as when the renewable energy sources are available [47]. Also, as the voltage and current from the [48] renewable energy sources fluctuates, the charge controller is used to regulate the charge that is supplied to charge the battery in order to avoid damaging the battery as well as protects from overcharging condition [49 - 50]. In addition to that, the charge controller also helps to protect against the reverse current back to the solar panel [48]. Even though this reverse current could only cause a minor damage but it is necessary to prevent and can easily be prevented [51]. Despite that, most of the charge controllers also have the ability to sense low-voltage supplied from the battery [52], this function in the charge controller prevents the battery from completely being discharged as well as damaged.

In [53] is mentioned that hybrid typed charge controller is used to complete the energy production, storing and consumption. Also, is used to convert the unstable AC and DC output from the renewable energy sources to a stable output for load supply and also battery storage. Besides that, the charge controller function is also to ensure a proper voltage and current for battery storages charging [54 - 55]. The voltage and current is monitored to avoid damaging the BESS. Therefore, the charge controller plays a very important role in HRES.

2.4.2 CHARGE CONTROLLER OPERATION

a) SOLAR CHARGE CONTROLLER

Figure 2.10 shows the basic circuit schematic of basic charge controller using Integrated Circuit (IC) TL431 shunt regulator. The IC TL431 is used to compare between the internal voltage and external voltage. The internal voltage reference is fairly precise at 2.5 volt that will be used to compare against an external voltage. Whenever the reference input voltage exceeds 2.5 volt, the output of the NPN transistor and the T1 power transistor also will turn ON. Thus, deviating small amount of output current from the panels towards the Light Emitting Diodes (LEDs). The resistors R1 and R2 are designed to detect the exceed battery voltage at approximately 14.2 volt. If an exact charge voltage adjustment is required, a parallel resistor to resistors R1 and R2 would be able to ease this adjustment. This is known as voltage 'shunting'. Shunting is regulating the panel, hence shunting the battery voltage that exceeds a certain threshold values. The voltage 'shunting' in this charge controller can be used to power all the 10 LEDs that are connected in parallel. Each LED consumes of 15mA and total of 150 mA is required to power all the 10 LEDs. Lastly, the D1 diode is known as low-drop Schottky diode. This diode is used to prevent the battery from over discharging during the unavailability of solar energy or at night.

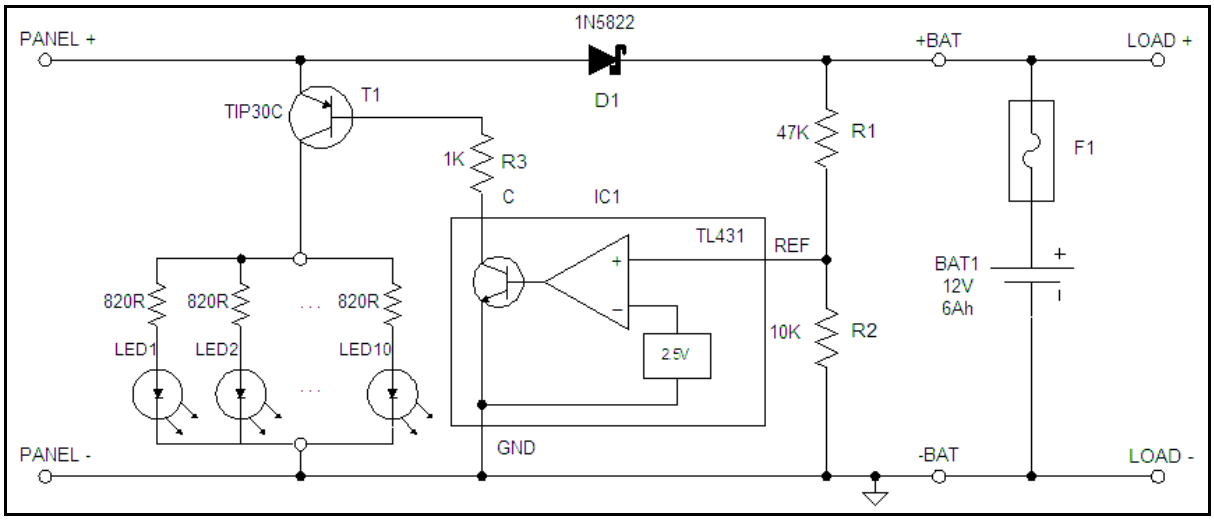

Figure 2.10: Circuit schematic of basic charge controller [56]

b) WIND TURBINE CHARGE CONTROLLER

The charge controller used in the wind turbine usually intended to divert the excessive power to a dump load, when the battery storage is fully charged [57]. When switching off the DL, over voltage that is still available needs to dissipate the excessive energy somewhere. Hence, the excessive dump load can be also diverted to a heater to prevent hammering noise over-speeding of the wind turbine and prevent the over-heating of the over-voltage in the wiring. Also, limiting the high power output during high wind condition, especially to avoid surcharging its rotor, power train produced by mechanical movement, as well as the electrical generator which will lead to great type of failure.

A simple charge controller that can be used for wind turbine and solar application is shown in Figure 2.11. The circuit shown in Figure 2.11 is suitable for 12 Volts and 24 Volts operation systems. This charge controller consists of TL-084 OP-AMP, automotive spotlight relay and easily available of other components. The designed circuit also can be used to disconnect the low voltage battery status to prevent the battery from fully discharged. Two Variable Resistors (VRs) are used to control the switching low and high voltages. A relay is used to turn on when the battery voltage exceed the high voltage setting. The relay will turn off only when the applied voltage falls under the low voltage setting. A conventional wind turbine and solar uses 12 Volts battery capacity for charging process, the high VR is set at maximum 15 Volts and the low VR is set at minimum 12 Volts. Both of the sources are connected to the battery through a normally closed contact. When the battery voltage is charged at 15 Volts, the controller energises the wind turbine relay contact from normally closed to normally open, whilst deviating the exceed energy as dump load. When the battery's voltage reduces to 12 Volts as it is set by the low VR, the relay is released and reconnecting the source to charge the battery. Two LEDs are used as power indicator and the other as relay energised indicator. The relay energised indicator is also known Dump Load (DL) indicator instead of connecting to battery.

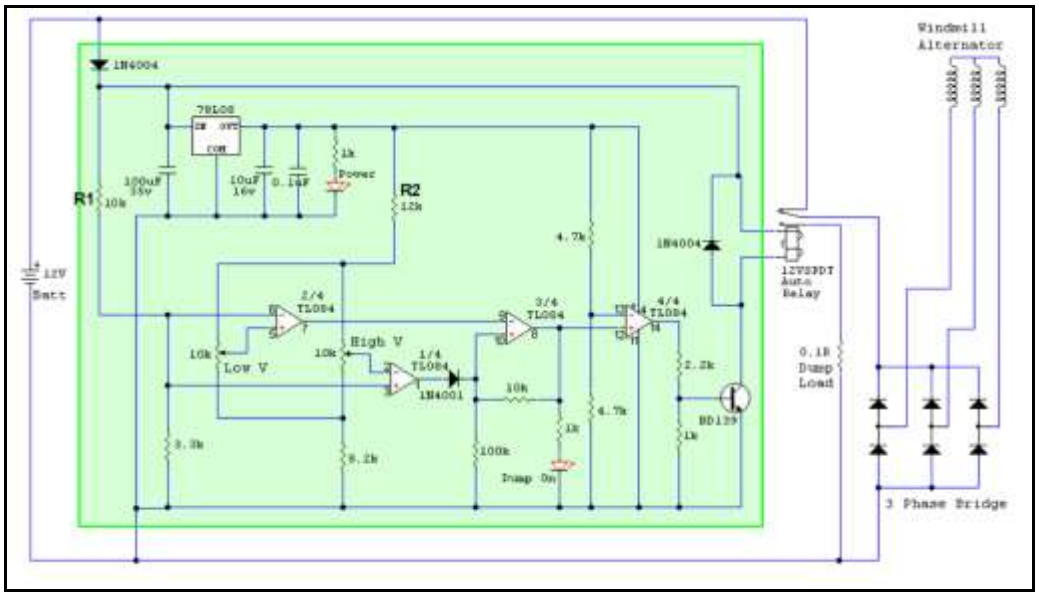

Figure 2.11: Simple charge controller for wind turbine and solar applications [58]

2.4.3 BATTERY ENERGY STORAGE SYSTEM

The application of renewable energy sources for electricity generation and distribution has seen a huge potential. Renewable energy sources such as solar and wind increased installation also has spurred the interest of BESS [59] due to their intermittent nature behaviour [60][48]. The intermittent behaviour has caused the power from either the solar or wind to fluctuate, therefore, the large power produced by the systems will cause stability damage on the power system in terms of the voltage and frequency [60]. To provide stability and effectiveness on the power system, BESS has been deployed into the solar and wind power system for power smoothing [61][51], levelling the high fluctuation of active-power [59], charging when excessive energy is available for storing and discharging when energy is required [48]. In [48][52][62] is mentioned that BESS provides high promise due to the high density and capacity to store energy and provide smoothing behaviours when fluctuation occurs in the active-power delivery. Thus, BESS importance can be summarised as voltage stabiliser.

2.5 TECHNICAL REVIEWS

Whenever the HRES is discussed, methods or approaches used to conduct the energy management strategy will arise to efficiently utilise the produced energy. This requirement is not only required by the non-grid connected hybrid renewable energy system but also required

by the grid connected HRES. The role of energy management strategy is to ensure the continuity of power source supply to the connected load and optimise the utilisation of the power source from the renewable energy sources as primary power delivery. To increase the HRES controllability and operability for the harvested energy and stored energy, the energy management strategy for HRES needs to adopt a central controller and the controller is programmed to supervise, coordinate, manage and control the HRES to optimise the available resources without depending on the grid network. Therefore, this section discusses about the methods or approaches applied to increase the controllability and operability of the renewable energy sources or the BESS through the energy management strategy for the HRES.

For the purpose of understanding the energy management strategy methods or approaches, an extensive review of research work by current and previous scholars is conducted. The energy management strategies that are presented in Figure 2.12 can be categorised into standalone, grid-connected HRES and SCADA. Generally, standalone power system is not connected to any grid network and usually installed in rural areas where grid transmission lines are not reachable. Whereby, grid and SCADA power system based is integrated with grid network and are usually operated based on smart distribution and control system.

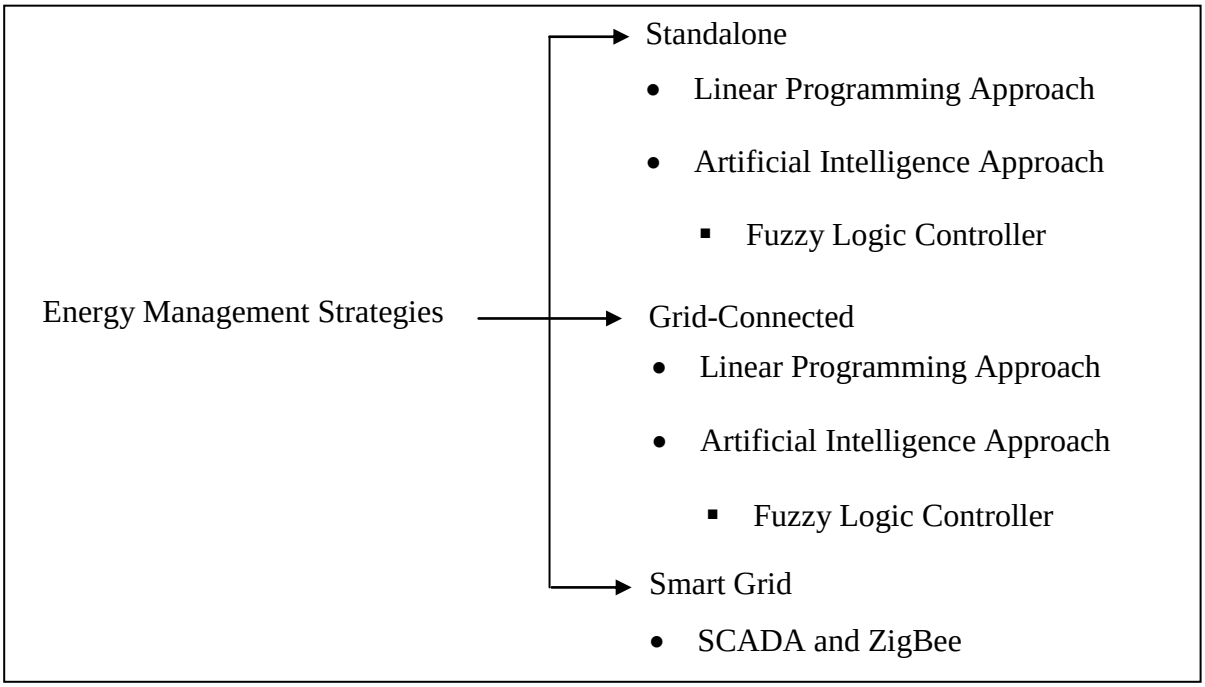

Figure 2.12: Energy management review scope [63]

In the first section, types of energy management strategy that are adopted for standalone HRES are reviewed. According to Figure 2.12, standalone HRES adopts linear programming approach and artificial intelligence approach to strategies and manage the energy delivery efficiently. The following sections will present the energy management strategies review based on these two approaches.

2.5.1 STANDALONE HRES – LINEAR PROGRAMMING APPROACH

The study conducted by Dursun and Kilic in [64] has reviewed the operation of three established energy management strategies for a standalone HRES which is solar photovoltaic (PV)/wind/Fuel Cells (FC). In this standalone HRES, PV and wind renewable energy sources designated as primary power source supply, whereas FC component is installed as a backup energy source. The energy management strategy adopted in this research focuses on the energy produced by the PV and wind renewable energy sources and State of Charge (SoC) of the battery storage. MATLAB Simulink based control algorithm is adopted as a consideration to measure the battery SoC. When the battery storage is fully charged, the excessive energy from the PV and wind renewable energy sources are directed to the FC component which is aimed to avoid damaging the battery storage. There are three strategies applied to manage the

power from the PV and wind renewable energy sources. They are explained as in the following:

- Strategy 1 – Battery SoC is between the positive limits, PV and wind renewable energy sources produce excessive energy then the battery storage discharges and the excessive energy is directed to power the electrolyser. On the contrary, when the battery storage is under its minimum SoC and no excess energy is available from PV and wind renewable energy source then the FC supplies the energy to the load and at the same time charges the battery storage.

- Strategy 2 – Battery SoC is between a positive limit and additional energy is unavailable from the PV and wind renewable energy sources, then the FC will not operate. During this condition, the battery storage will be discharged. However, if the battery storage SoC is below the limit then FC will charge the battery storage.

- Strategy 3 – Battery SoC is between a positive limit, PV and wind renewable energy sources produce surplus energy then the electrolyser will operate and battery storage will be charged. On the contrary, when the battery storage SoC is below the limits or excess energy from the PV and wind renewable energy sources are unavailable then FC component will operate and battery storage will be discharged.

In comparison, developed algorithm using strategy 3 seems to produce significant outputs for the battery storage efficiency, while measuring the battery storage efficiency rating at 85% [64]. The strategy 3 developed algorithms ensure that the available excessive energy from the PV and wind renewable energy sources is directed to the electrolyser, therefore protect the battery storage from being damage.

A power management control strategy for standalone PV and battery storage system is discussed by Liao and Ruan in [65]. The power management control intelligently controls the suitable operation of DC to DC Converter uni-directionally and bi-directionally according to different conditions or solar and battery storage. In addition to that, power management control is strategies to ensure coordination, operation and behaviour at high efficiency. A 500 watt prototype PV system is developed to validate the proposed power management strategy and the presented experiment results in [65] presents the operational of the proposed strategy.

Ismail and Moghavveni [66] proposed a simulation work to perform the energy management strategy to achieve the energy equalisation. The proposed energy management strategy optimised the sizing to achieve the minimum cost of energy of the hybrid system, at the same time assisting the demand load.

In a similar research conducted by Ismail and Moghavveni in [67], a simulation program is developed to execute the energy management strategy. It is focused to prioritise the PV and battery storage system to power the load, at any situation when the PV and battery SoC is at the least level, diesel generator is used as backup power supply to the load and for battery charging. The employed control strategies have successfully demonstrated the energy flow among the load and battery storage at each hour even though weather condition is vary. In another energy management strategy proposed by Nfah and Ngundam in [68], which focuses to perform the energy analysis. In fact the research prioritises the energy produced by the wind turbines and excessive energy is stored into the battery storage. Diesel generator is installed but the access is limited to only whenever the battery storage has reached its minimum SoC. Dahmane el at. [69], developed an intelligent algorithm provide control for the renewable energy generator (PV and wind) as primary power source supply and a backup diesel generator. The proposed algorithm prioritise the PV to operate at the maximum power while being assisted with maximum power point tracking algorithm to flow the power source as supply to the load. Whilst, the wind system operate as an assistive to the PV system in case when the PV system has shortage of power. Diesel generator is integrated to assist the increasing load demand supply and concurrently charge the battery storage when the PV and wind renewable energy sources are unavailable and battery storage have reach its minimum SoC.

Behzadi and Niasati in [70] proposed a PV/battery/FC/hydrogen tank based hybrid system. The proposed system sizing and performance analysis is performed using the Genetic Algorithm (GA) and HOGA application [63]. Three energy management strategies were used in this research work. Firstly, the amount of excessive energy is measured, if the amount is positive then the excess amount is flowed into the battery storages till its SoC is full. On the contrary, the FC will be connected to the load and will remain till the hydrogen's pressure is above the critical value, otherwise load is connected to the battery storage. The second strategy the hydrogen pressure level is checked regardless the minimum battery storage SoC.

The last strategy measures the minimum power of produced by each component, once this information is gathered then the amount of power flow to each storage device is decided. Dash and Bajpai in [71] adopted the similar approach in their research work.

Similar research work by Nasri el at. [72] proposed hybrid energy system which operate autonomously which is integrated with hydrogen and ultra-capacitor as energy storage is introduced. The load is the primary component which is connected to receive all of the energy from the PV system, in case if there is any excessive energy then it is used to generate hydrogen till it is full. Then, the excessive energy is shifted to charge the ultra-capacitor and will be shut down by the PV system when it is fully charged.

2.5.2 STANDALONE HRES – ARTIFICIAL INTELLIGENCE APPROACH

A study conducted in [63] explained that the artificial intelligence approach is also adopted to perform the energy management strategy. Artificial intelligence such as GA, Differential Evolution (DE), Neural Network (NN), Fuzzy Logic (FL), and neuro-fuzzy are used to develop the algorithm to perform the energy management strategy. Thus, this section will review some of the artificial intelligence approaches that are integrated to perform energy management strategy.

Abedi and Alimardani in [73] proposed the hybrid power system which consists of various sources and battery storage units are control to determine the optimum power management strategy. The sources such as PV and wind are given the priority to dispatch the energy to the load, while other connected sources priority is undefined, except to maximise the power management strategy controlling strategy. The aim to optimise the power management strategy control assisted to reduce the overall cost of the system [73]. Operational wise, the excessive energy produced by the renewable energy resources are directed to charge based on the sharing basis. The sizing algorithm is integrated in the power management optimisation process to the overall system costing, load demand, fuel consumption usage is considered when unpredictable nature condition occurs. The energy management strategy also adopts the DE algorithm and FL to optimise the nonlinear multi-objective drawbacks of the hybrid power system. In order to efficiently exploit the power from the renewable energy sources the tilting of the PV and wind turbine tower height are important to be calculated. The results are

compared to show the proposed energy management strategy performances for the hybrid power system.

The research conducted by Barley and Winn in [74] proposed the development of the predictive energy management strategy which assumed the future load demand information and the condition of the standalone wind/diesel/battery hybrid power system resources. The predictive energy management strategy in this research is used as a benchmark against some non-predictive hybrid power system for energy dispatching. A theoretical and experimental analysis of a standalone hybrid power system comprising PV/Wind/Battery is developed in [75]. Energy management strategy is integrated to manage the energy flow direction among the available sources, load and battery storage system. This is to ensure it is an unchanged and secure operation. In order to satisfy the sharing balance among the resources, a fast and slow control loops are proposed to achieve the energy conversion process and energy management strategy. The experimental results of the overall system showed that the system performed effectively for the objective. Model predictive control is applied into a power management and analysis for an off-grid system which operation is based on the weather estimation. The off-grid system is integrated with PV/FC/Battery and applied control strategy is to fully optimise the available renewable energy sources. The results show the proposed model manage to reduce the fossil fuel utilisation while increase the renewable energy source utilisation while still maintaining the comfortablity.

Khan et al. [76] present a energy management system that deploys the multi-agent distributed generation system. PV/wind/micro-hydro power/diesel/battery energy resources are integrated to develop the hybrid power system and load is connected at the output. The aim of the distributed energy management system is to manage individual energy sources and the load system. The non-cooperative game theory was adopted to achieve multi-agent system coordination in this proposed hybrid power system. The proposed scheme highly performed under different circumstances and showed effective control strategy. Brka et al. [77] developed a lab scale energy system that perform a predictive power management strategy control on the PV/wind/FC/Battery hybrid power system. To achieve the real-time prediction the NN was adopted to forecast the availability of the renewable energy sources and loads prior to implement the energy management strategy.

Upadhyay and Sharma [78] adopts three separate energy management strategies to size a hybrid power system. The three different energy management strategies are cycle charging strategy, peak shaving strategy, and load following strategy. The analysed hybrid power system is formed of renewable energy sources, diesel generator, and battery storage. The hybrid power system sizing was conducted using the following optimisation techniques Particle Swarm Optimisation (PSO), GA, and biogeography based optimisation. The results show that the cycle charging strategy performed effectively to manage the available energy.

Palma-Behnke et al. [79] proposed and developed NN approach is adopted into the energy management strategy for a microgrid based system containing PV/wind/diesel/battery. Data reference based from the real location is used when testing the hybrid power system. The energy management strategy helps to reduce the system operational costing while fulfilling the load demand. The hybrid power system performed the power balance when the system operational is conducted. Hatti and Tioursi in [80] proposed NN based Quasi-Newton algorithm which is incorporated into the proposed and developed controller. The dynamic NN is used to control the FC and the results proofs the system competence in terms of stabilisation, control and error tracking identification.

2.5.3 GRID-CONNECTED HRES – LINEAR PROGRAMMING APPROACH

Blasques and Pinho [81] have proposed a management model for a case study at demand-side in Brazil and is consolidated into a metering system. The presented model's aim was to have utilisation restriction on the grid based power source compared to the energy available from the renewable energy source. The objective is to consume the availability energy from the renewable energy source, and has the objective to prevent the lack of energy stored in the battery, at the same time utilise the diesel generator whenever the renewable energy supply low power source.

Rani et al. [82] proposed and developed a grid-connected PV system integrated with battery storages to supply the power source to the DC loads without causing any interruption. Thus, power management strategy is required to coordinate the power flow and balance sharing among these devices. The power management strategy adopts the battery voltages monitoring operation to generate signal for mode selection for the bidirectional converter (idling-

conducting mode – rectifier/inverter). The presented experimental results verified all the different modes of control strategy that is adopted for different loads.

Battistelli et al. [83] proposes a modelled and configuration of small electric energy systems which is integrated in the energy management strategy. The energy output from multiple generating units and the input/output from the charging stations or the grid networks were accessed. The proposed model aims to minimise the system operating cost. Karami et al. in [84] proposed a grid-connected hybrid power system which is composed with Proton Exchange Membrane Fuel Cell (PEMFC), PV, battery and supercapacitor. Generating sources are stressed to produce maximum power through Maximum Power Point Tracker (MPPT). The produced output voltage is regulated using the type III compensator - buck converter. A controller was developed to perform the energy management strategy on the following: uninterrupted power source supply, consistence operation of the multiple sources, re-storage of the utilised energy in the storage, disconnecting the FC for case zero load, and flowing any excessive energy to the grid network. The presented results show that 16 different conditions were simulated and the grid role is validated too.

Finn and Fitzpatrick [85] proposes and analyses the potentiality of implementing a price-based electricity utilisation for industries which is generated by the wind turbines that are connected to the same grid network which are used by the industries. Through this approach the electricity demand can be shift to the usage of wind turbines whenever the wind generation is high. Indirectly, the industries financially save the utility billing cost because operational task is conducted during low-price period. To execute this idea, the electricity supplier needs to forward the actual electricity pricing to the industries, so that they can decide and manage their demand accordingly to the tariff provided. It shows that 10% reduction was achieved in average unit price and 5.8% electricity generation increases through wind turbine system.

Pascual et al. [86] proposed a residential microgrid energy management strategy which is composed with PV/Wind/Battery. The hybrid power system is connected to the main grid to compensate any imbalance energy occurrence at any time. The control strategies estimate the power in/out from each renewable generation component to manage a smooth energy flow.

Comodi et al. [87] proposed a sized grid-connected PV plant which is also comprises of a Micro Gas Turbine (MGT). Two energy management strategies were used to ensure an hourly

estimation of electricity that actually can be generated by the power plants. The energy management strategies manage to resolve the unpredictability of PV plant generator and reduced the utilisation of fossil fuelled for electricity generation.

Kim et al. [88] conduct an economic feasibility study on the hybrid power system comprises of PV/wind/battery/converter. HOMER software was used to simulate and execute the economic feasibility study, in the meantime the configuration of energy management strategy was followed. According to the energy management strategy, renewable energy sources were handled as primary power sources. The grid network is utilised only when the renewable energy sources are unable to supply any power source. This study presented the grid-connected hybrid power system economic feasibility while decreasing the electricity price. Similar research was conducted in [89 - 92] which uses the HOMER to optimise the grid-connected hybrid power system and adopts the energy management strategy into the proposed hybrid systems.

2.5.4 GRID-CONNECTED HRES – ARTIFICIAL INTELLIGENCE APPROACH

Quanyuan et al. [93] proposed two layer energy management strategy model which are the scheduling later and dispatching layer. The scheduling layer is responsible to determine the economic operation based on the estimated data, while the dispatching layer provide the energy flow control to the respective units. The proposed energy management strategy also study on the deficit that occurs between the estimated and real-time data, this information is process to allow the system to compensate the insufficient energy from the available energy in the scheduling layer. The suggested model is tested in grid-connected and standalone hybrid power system, it is connected to the grid to maximise the renewable energy revenues, while reduce the dependency on the grid-connected system as well as increasing the utilisation of the source from renewable energy. Bahmani-Firouzi and Azizipanah-Abarghooee [94] suggest that a strong evolutionary algorithm is required to optimise the hybrid power system operation. Hence, an evolutionary technique which is to improve the improved bat algorithm was developed to counteractively strategies and allows the inexpensive dispatches. The proposed algorithm is developed to optimise the battery storage sizing in a grid-connected hybrid power system. Low voltage grid-connected system was used to evaluate the performances of the

proposed approach, thus the results show the developed approach manage to reduce the charging pr discharging frequency of the battery storage system and improve the durability.

2.5.5 ENERGY MANAGEMENT SYSTEM – SMART GRID – RENEWABLE ENERGY SOURCES

Smart grid is developed to intelligently transmit and consume the power source supply. The system needs a reliable and secure energy source that is not entirely dependable on the fossil fuels. Therefore, smart grid is a essential goal of many countries and adopting the renewable energy sources into their grid network falls under this goal [95]. Smart grid systems are integrated with smart meters, intelligent sensors, bidirectional two-way information sharing among the energy sources and consumers availability. The availability provides the system with an ability to successfully achieve and manage the energy deliverability to the consumers while consumers having the right to make decision. Even though many researchers have been carried out in the field of smart grid but there are still a lot of challenges to explore when the renewable energy sources are integrated.

To ensure the smooth and effective deployment of renewable energy sources into smart grid system, an efficient energy management strategy in smart grid should be given a serious consideration. Successive energy management strategies always are dependable on the requirements from all the connected sources and alleviate the interconnectivity between various resources. Smart grid is facilitated to reduce the energy costing at the customers' side and creating a reliable control, supervision and coordination helps to optimise the electricity generation distribution from various sources for various applications. The SCADA and ZigBee are two supervisory systems are used in smart grid to ensure a reliable energy source flowing.

Dumitru and Gligor [96] present the design and implementation a decision-making management system to provide the managing role and the availability of energy to the customers. Software was developed and integrated into the SCADA system to manage and supervise the received data for effective generation and transmission at recipient of command. In a similar study, Batista et al. [97] proposes ZigBee technology which is based on open source tool for a comprehensive test field. This approach monitors the photovoltaic, wind energy systems and energy management strategy for buildings and homes. Monitoring the energy sources and systems for optimisation and metering are the main function in this smart

grid development. The presented results demonstrated all of the techniques at the device. Al-Ali et al. [98] designed, implement and test an energy of an embedded system which is integrated with photovoltaic and battery storage into a smart home system. To manage and control the produced energy flow to the smart homes system an energy management strategy was proposed. The energy management strategy adopted for this system schedule and arranges the energy flow during the peak and off-peak hours. According to the results, the scheduling and arranging the energy flow during the peak and off-peak hours was successfully achieve. In addition to that, 33% of utility bill costing was saved due to the integration of renewable energy sources and energy management strategy.

2.6 SUMMARY

A summary of energy management strategies and approaches adopted to manage and control the energy flow in both standalone and grid-connected hybrid power systems were conducted in sections 2.5.1 – 2.5.5. The reviews are focused on the methods and approached used to develop an efficient energy management strategy for standalone and grid-connected hybrid power systems which integrates multiple renewable energy sources and grid-connected system. The reviewed work from various scholars' show that effective and efficient optimisations of the energy flow from the energy sources to the customers are the main concern to be achieved. Each energy management strategy reviewed also explains that it has its own objective to achieve to produce its overall system performances. Furthermore, the development of hybrid power system is not only focusing on the energy management strategy but integrating the renewable energy sources to reduce the utility bill costing which indirectly benefits the customers.

Looking at the objectives and benefits of integrating energy management strategies for hybrid power systems, this research proposed linear programming to design, develop, implement and construct a real-time DC HRES hardware system. The aim and objectives of the real-time DC HRES hardware system is explained in Chapter 1. Microcontroller PIC16F877A is used as a centralised controller to supervise, coordinate, manage and control the solar-wind renewable energy sources and BESS for charging or discharging. In order to optimise the controller operation as an energy manager such as supervision, coordination, managing and controlling, continuous dynamic decision making algorithm is developed using the embedded software

application which is incorporated into the microcontroller PIC16F877A, Having said that, the proposed real-time DC HRES hardware system development is divided into three stages, which in each stage the process of developing the real-time DC HRES hardware system is explained in the following chapters.

CHAPTER 3

MATLAB-SIMULINK MODELLING OF REAL-TIME DC HRES HARDWARE SYSTEM

This chapter presents the modelling and simulation of real-time DC HRES hardware system using the MATLAB Simulink/ Stateflow software. Therefore, in presenting the modelling and simulation of HRES, a model of real-time DC HRES hardware system is presented, which composed the voltage based self-intervention and decision-making controllers to ensure effective organisation between all system's components. The voltage based self-intervention designed using the Simulink library is to sense and measures the output voltage changes at the renewable energy sources and BESS SoC changes. The BESS is composed of BATT A STORAGE and BATT B STORAGE. The decision-making controllers, integrated with the condition decision-making algorithm, are designed and developed using the Stateflow tool in the Simulink library. The algorithm is designed to effectively supervise, manage, organise and coordinate all the real-time DC HRES hardware system's modelled components. In addition, the implementation of the condition decision-making algorithm also provide the capability to the real-time DC HRES hardware system to switch to the grid network if real-time DC HRES hardware system is not able to supply any source of power supply. Real-time DC HRES hardware system also is integrated with DC to DC BC to step-up the 7-12 Volt output voltages from the renewable energy sources for either load supply or BESS charging. The implementation of DC to DC BC would be good to help the energy transfer, therefore the core energy can be properly managed and control for load supply or BESS charging. DC to AC inverter implementation at the load input is to step-up the DC input voltages to an AC output voltage as power source for the connected load. The primary input source for the DC to AC inverter is from the renewable energy sources and is switch to BESS source when the availability of renewable energy sources are insufficient. To be able to understand the real-time DC HRES hardware system, the following presents the methodology design and

development of real-time DC HRES hardware system in MATLAB Simulink/Stateflow software.

3.1 REAL-TIME DC HRES HARDWARE SYSTEM DESIGNED MODEL

In sensing, switching, control application and system design, modelling and simulation is essential to effectively optimise the switching and control process via the efficient sensing to enhance the system operations. In this chapter, the methodology of the designed real-time DC HRES hardware system simulation model is described. The real-time DC HRES hardware system modelling and simulation is implemented using the Simulink and SimPowerSystem from the MATLAB software. The block diagram in Figure 3.1 is an illustration of the modelled real-time DC HRES hardware system in MATLAB Simulink/Stateflow software.

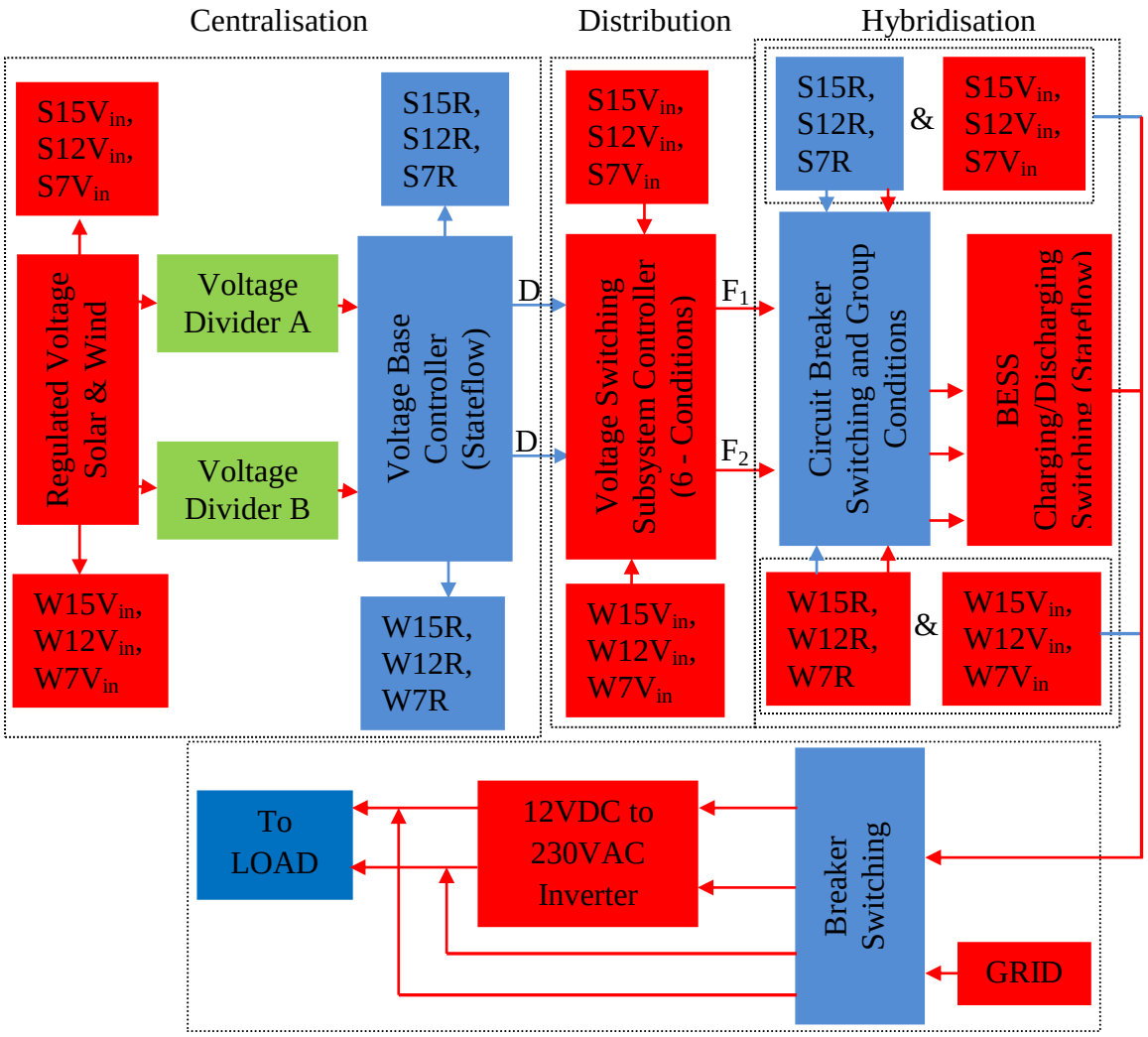

Figure 3.1: Block diagram of the modelled real-time DC HRES hardware system

The control structure of the designed real-time DC HRES hardware system in Figure 3.1 is classified into centralisation, distribution and hybridisation control paradigms. In all the three control paradigms, the renewable energy sources are connected to a single controller, which will determine the efficiency and optimum operation of all the corresponding subsystems. Brief descriptions of all the three control paradigms are discussed in the following section.

3.1.1 CENTRALISATION CONTROL PARADIGM

The centralisation controls paradigm sense and measures the regulated output voltages from all the available renewable energy sources and sends an activation control signal to the centralised controller. The voltage based controller which acts to make decision based on the regulated output voltages condition is shown in Figure 3.1. The objective to have the voltage based controller is to optimise the use of various renewable energy source output voltages for load supply and BESS charging.

The voltage base controller sense and measures the amount of regulated output voltages from the renewable energy sources and send an activation control signal to the next corresponding subsystem unit. The advantage of this control paradigm is to allow the real-time DC HRES to receive all the information from the voltage based controller.

3.1.2 DISTRIBUTION CONTROL PADADIGM

The distribution control paradigm receives the activation control signal from the voltage based controller and corresponds to activate the respective renewable energy sources connected to the voltage switching subsystem controller, as shown in Figure 3.1. The voltage switching subsystem controller communicates with the circuit breaker switching and group conditions controller to make the specific condition to switch on based on the received activation control signal from the voltage based controller. With this controllability, the controllers computational is greatly utilised and allows an effective renewable energy sources condition management and greatly optimise each renewable energy source’s output.

3.1.3 HYBRIDISATION CONTROL PARADIGM

The hybridisation control paradigm is composed of the centralisation and distribution control paradigms to manage all the corresponding subsystem of the real-time DC HRES hardware

system efficiently and effectively. The renewable energy sources are conditionally group as a unit in a subsystem. The circuit breaker switching and group conditions are used within the subsystem to effectively manage and coordinate the output voltages from the renewable energy sources to the connected load or BESS charging.

The hybridisation control paradigm is termed to control the framework at multilevel operation as shown in Figure 3.1. At the system operational level, the hybridisation control paradigm performs much decision-making and actually control each of the subsystems based on each subsystem's objective. This explained two-ways communication is necessary between each different subsystem in order to execute each made decision.

This section provides the description of the control paradigms used for the real-time DC HRES hardware system to perform and operate the system at its optimal ability. A detailed technical description of each subsystem of real-time DC HRES hardware system is presented in the following sections.

3.2 MODELING VOLTAGE BASED SELF – INTERVENTION – SIMULINK

The block diagram shown in Figure 3.2 presents the voltage based self-intervention which is used to perform the self-intervention among the renewable energy sources and centrally control the renewable energy sources for effective management and optimisation. In this case, solar-wind renewable energy sources are selected due to their huge popularity. The solar-wind renewable energy sources are used as primary power source supply while BESS is used as secondary power source supply.

The output voltages from solar-wind renewable energy sources are connected to the inputs of the HCC. The HCC regulates and stabilises the voltages from solar-wind renewable energy sources before sending into the PV voltage divider and WT voltage divider. The Analogue to Digital Conversion (ADC) converts the solar-wind renewable energy sources analogue voltage to digital voltage. This digital voltage value is send to the voltage based controller to perform voltage based self-intervention between the solar-wind renewable energy sources using continuous dynamic decision-making algorithm**.**

The renewable energy centralisation concept shown in Figure 3.2 consists of two voltage based self-intervention, two ADCs and a voltage based controller, which is designed using the MATLAB Simulink/Stateflow software. The Simulink/Stateflow based design models of each unit are presented and explained in the following.

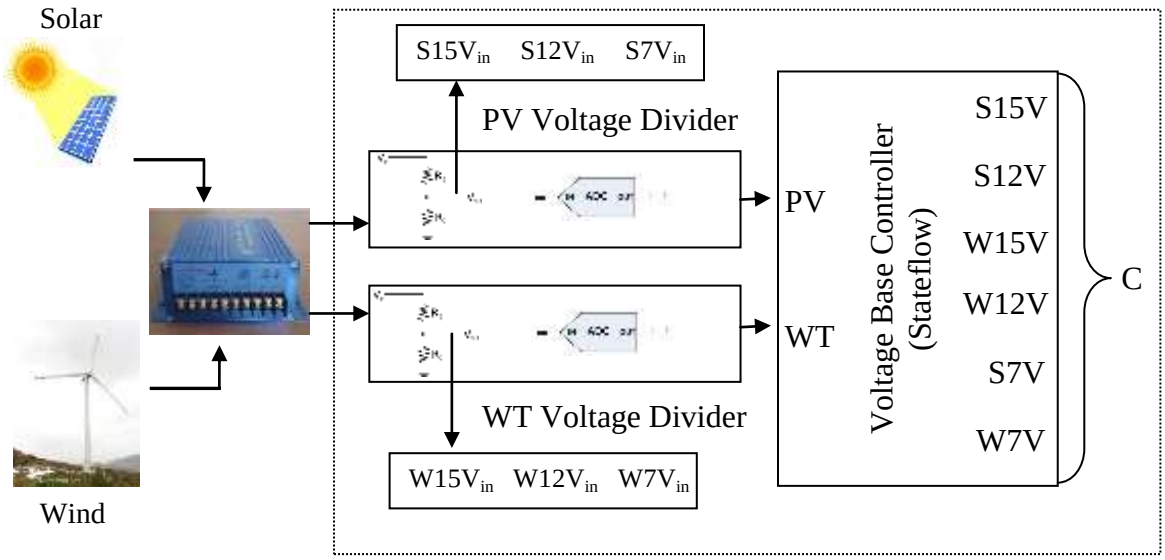

Figure 3.2: Block diagram of renewable energy sources centralization for real-time DC HRES hardware system model

3.3 VOLTAGE BASED SELF-INTERVENTION – SIMULINK DESIGN

The Simulink voltage based self-intervention designed model is shown in Figure 3.3, which is based on the voltage divider concept. The voltage based self-intervention is used to sense and measure the increment or decrement of regulated output voltages from solar-wind renewable energy sources. Referring to Figure 3.2, there are two voltage based self-intervention subsystems used to perform the self-intervention aspect between the solar-wind renewable energy sources. Therefore, in order to understand the operation, the following will explain the configuration and setup of voltage based self-intervention for voltage sensing and measurement during voltage increment or decrement.

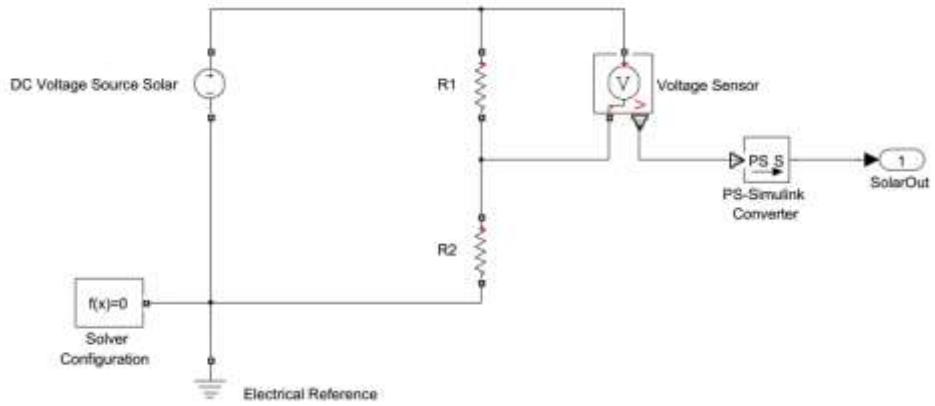

Figure 3.3: Simulink design of voltage based self-intervention

Let's assume voltage source (V_s) of solar renewable energy source is constant and equal to 17.5 Volt, Resistor 1 (R_1) = 10 kΩ, Resistor 2 (R_2) = 1.5 kΩ, therefore the voltage at R_1 needs to be calculated as an output voltage.

Hence,

$$\text{Voltage at Resistor 1 } (V_{R1}) = \left(\frac{R_1}{R_1 + R_2}\right) V_S \tag{3.1}$$

$$= \left(\frac{10\,\text{k}\Omega}{10\,\text{k}\Omega + 1.5\,\text{k}\Omega}\right) \times 17.5 \text{ Volt}$$

$$= 15 \text{ Volt}$$

The regulated output voltage from solar renewable energy source, which is also known as V_{R1} output voltage is sensed and measured between 7~15 Volt. The configuration shown in Figure 3.3 and Equation (3.1) is also used to calculate the regulated output voltage from wind renewable energy source. Sensing and measuring changes of the regulated output voltages from solar-wind renewable energy sources are important to perform the self-intervention, effectively manage and optimise the regulated output voltages as power source supply for the connected AC load or for BESS charging process. Therefore, before explaining the self-intervention process, the regulated output voltages from solar-wind renewable energy sources are quantified into three sections. Table 3.1 shows the quantification of regulated output

voltages from solar-wind renewable energy sources. The conditions presented in Table 3.1 are used to design and developed the voltage based controller shown in Figure 3.2.

Table 3.1: Solar-wind renewable energy sources analogue and digital voltages quantification

No.	Sources	Conditions (Analogue Voltage)	Conditions (Digital Voltage)
1.	PV	12 Volt < PV ≤ 15 Volt	1404 < PV ≤ 1755
	WT	12 Volt < WT ≤ 15 Volt	1404 < WT ≤ 1755
2.	PV	7 Volt < PV ≤ 12 Volt	819 < PV ≤ 1404
	WT	7 Volt < WT ≤ 12 Volt	819 < WT ≤ 1404
3.	PV	0 Volt < PV ≤ 7 Volt	0 < PV ≤ 819
	WT	0 Volt < WT ≤ 7 Volt	0 < WT ≤ 819

Prior to that, produced analogue output voltages from the solar-wind renewable energy sources are converted into digital voltage reading. The digital voltages are used to develop the continuous dynamic decision-making algorithm for voltage based condition controller.

The following presents the analogue output voltage to digital voltage conversion and calculation. The conversion and calculation results are recorded in Table 3.1.

Hence,

$$\frac{\text{Resolution}}{\text{Voltage Range}} = \frac{\text{Digital Output Voltage}}{\text{Measured Analogue Voltage}} \tag{3.2}$$

Therefore, Equation (3.2) is used to calculate the digital voltage for 15 Volt, 12 Volt and 7 Volt analogue voltages.

In conclusion, the digital voltage is used to develop continuous dynamic decision-making algorithm for the voltage based controller. The continuous dynamic decision-making algorithm which is incorporated in the voltage based controller will generate an activation control signal to perform self-intervention on the solar-wind renewable energy sources.

3.4 MODELLING VOLTAGE SWITCHING SUBSYSTEM CONTROLLER – MATLAB SIMULINK/STATEFLOW

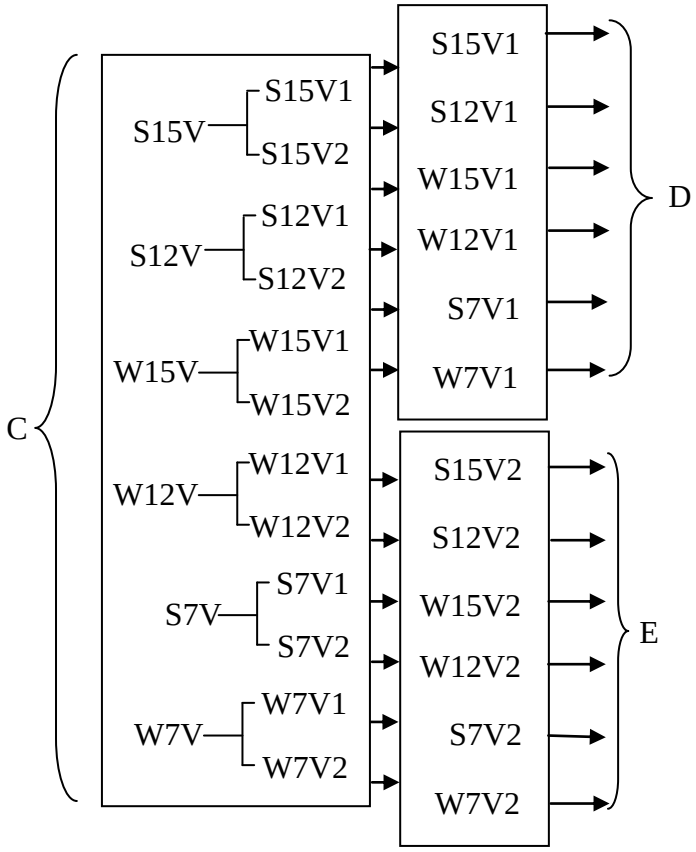

Figure 3.4: Block diagram of input – output connectivity

The input and output ports block diagram shown in Figure 3.4 is located inside the voltage based controller. The input and output ports are used to connect the HIGH activation signal output from voltage based controller to the voltage switching control subsystem. As shown in Figure 3.2, the voltage based controller produces HIGH activated signals or LOW signals at C, which is based on the amount of sensed and measured input voltage at the voltage based self-intervention. Therefore, the input ports (C) shown in Figure 3.4 are connected to the output ports (C) shown in Figure 3.2. Each HIGH activated signal or LOW signal produced by

voltage based controller is divided into two output signals (D and E), each to control the voltage switching subsystem controller (D) and circuit breaker switching and group conditions (E). This section explains about the use of the output signals in group E as control signals for voltage switching subsystem controller and coordinating the regulated output voltages from solar-wind renewable energy sources to the circuit breaker switching and group conditions.

The input-output ports subsystem in Figure 3.4 is performing as governing unit that provides an effective control of real-time DC – HRES hardware system for optimum management and operation. The voltage switching subsystem controller shown in Figure 3.5 illustrates the optimum management and operability of solar-wind renewable energy sources. The relays are used as control switches between the individual regulated output voltages to perform the self-intervention between solar-wind renewable energy sources. The voltage switching subsystem controller in Figure 3.5 shows six different types of configurations setup for the regulated output voltages from solar-wind renewable energy sources. The six different configurations setups are identified as the possible configuration when both or when only one of the renewable energy sources is available during solar-wind renewable energy sources operation.

An important consideration that is required when designing the voltage switching subsystem controller shown in Figure 3.5 is, not to let the other configured pairs to switch ON while one configured pair is switched ON. Therefore, Figure 3.5 presents the internal design of the voltage switching subsystem controller which is used to coordinate and manage the regulated output voltages from solar-wind renewable energy sources into circuit breaker switching and group conditions. The voltage switching subsystem controller is integrated with six different configurations which allows the real-time DC HRES hardware system to effectively manage the system inputs for efficient output coordination.

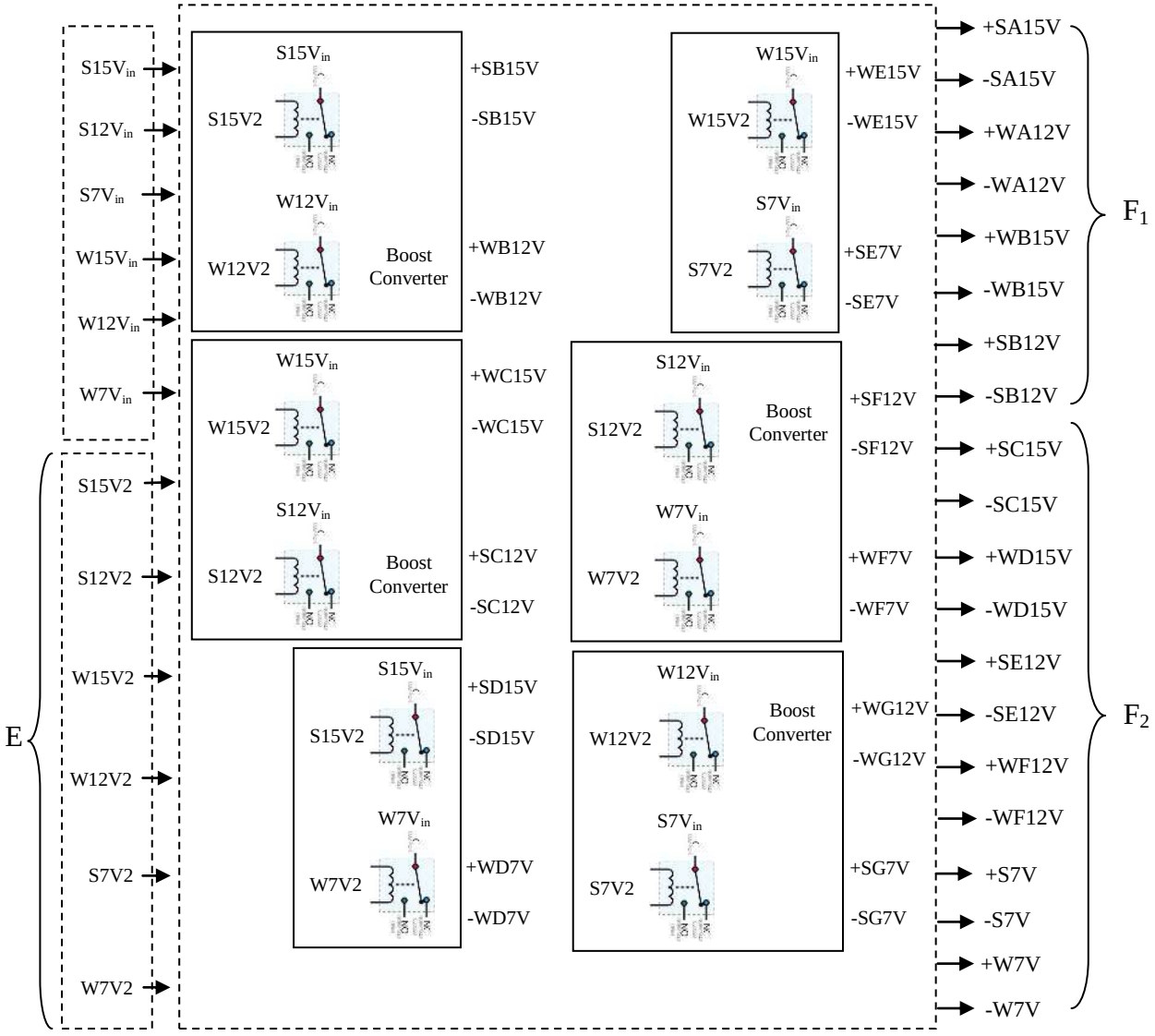

Figure 3.5: Block diagram of voltage switching subsystem controller

To further understand the configuration and setup of voltage switching subsystem controller, Figure 3.6 presents the configuration and setup for one of the designed units in the voltage switching subsystem controller.

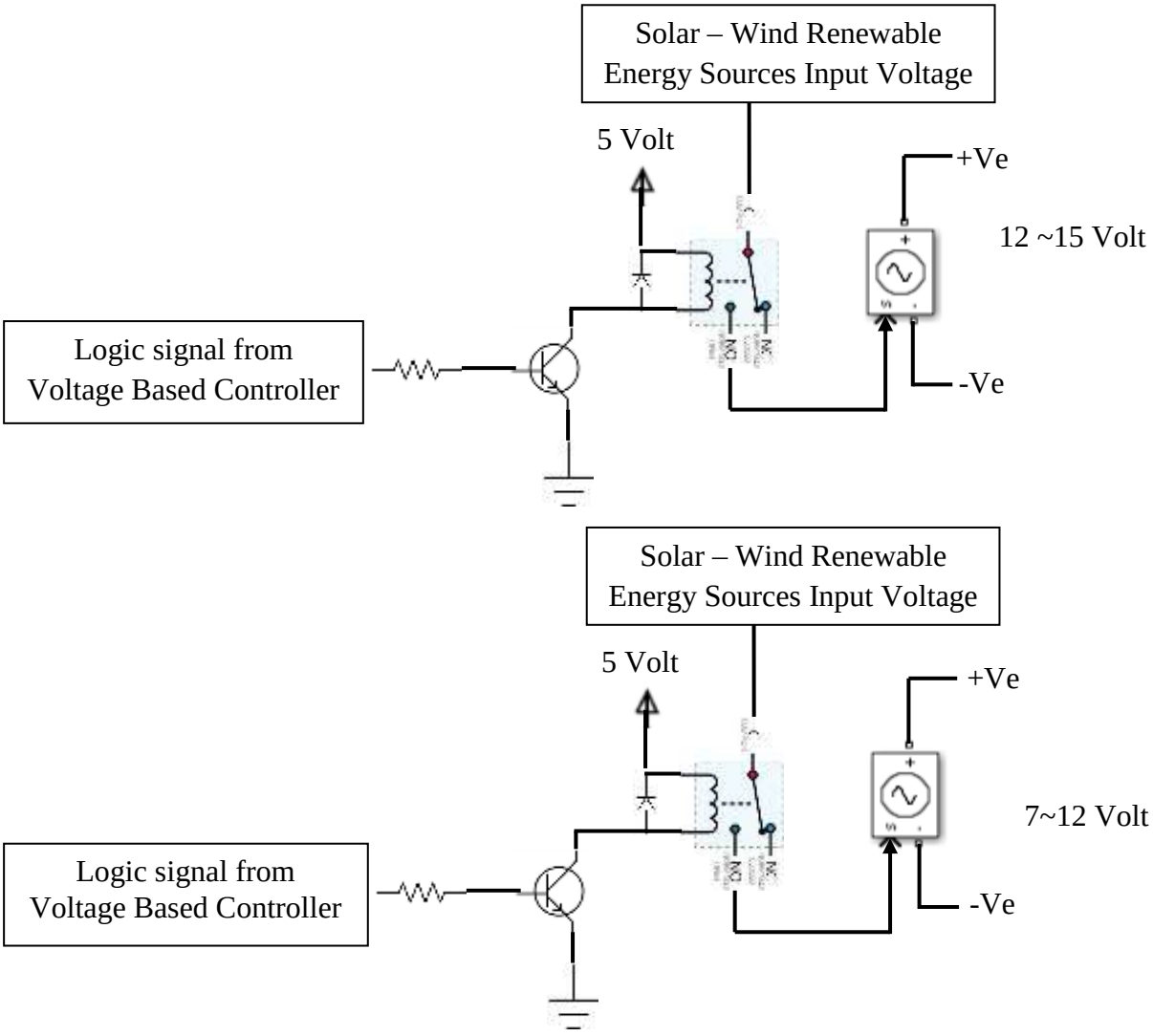

Figure 3.6: Block diagram of relay switching for voltage output

The activation signal from voltage based controller is used to control the relay switching when it is required. Therefore, when solar-wind renewable energy sources produce 15 Volt DC, voltage based controller produces a HIGH activated signal to NPN transistor's base, which energises the relay coil. Then, relay is switched from Normally Closed (NC) to Normally Open (NO). This connects the 15 Volt DC at Common (C) to the NO. This configuration is not only applied for 15 Volt regulated output voltages from solar-wind renewable energy sources but also other voltage combination as presented in Table 3.2.

Table 3.2: Voltage combination for relay switching

Conditions	Voltage based Controller Output	Analogue Input Voltage	Connectivity	
1	S15V1	12~15 Volt	F1	+SA15V
				-SA15V
	W15V1	12~15 Volt	F1	+WA15V
				-WA15V
2	S12V1	7~12 Volt	F1	+SB12V
				-SB12V
	W12V1	7~12 Volt	F1	+WA12V
				-WA12V
3	S15V1	12~15 Volt	F1	+SA15V
				-SA15V
	W12V1	7~12 Volt	F1	+WA12V
				-WA12V
4	W15V1	12~15 Volt	F1	+WA15V
				-WA15V
	S12V1	7~12 Volt	F1	+SB12V
				-SB12V

3.5 MODELING CIRCUIT BREAKER SWITCHING AND GROUP CONDITIONS – MATLAB SIMULINK/STATEFLOW

The primary aim of this section is to develop the circuit breaker switching and group conditions using Simulink/Stateflow tool in MATLAB software. The digital voltage presented in Table 3.1 is used to achieve the effectiveness, management and optimum operation of self-intervention of solar-wind renewable energy sources. The circuit breaker switching and group conditions presented in Figure 3.7 is a method used to combine the voltages from different sources to coordinate the power source supply to the respective connected AC load and BESS for charging, if required. Therefore, flowchart in Figure 3.7 depicts the methodology of circuit

breaker switching and group conditions, which performances are based on the voltage combination presented in the Table 3.2.

Figure 3.7 presents nine different conditions, which allow solar-wind renewable energy sources to supply the voltage power source to either to the connected AC load or BESS for charging process, if required. In the following, each presented condition in Table 3.2 is further explained.

Condition 1: PV = 12~15 Volt and WT = 12~15 Volt

According to Table 3.2, when the regulated output voltages from solar-wind renewable energy sources are 12~15 Volt, voltage based controller produces a HIGH activated signal for S15V1 and W15V1 into the 2 – inputs AND gate shown in Figure 3.8. When S15V1 and W15V1 outputs HIGH activated signals, then the output from 2 – inputs AND gate is also equal to HIGH. This HIGH activated signal is send into the circuit breaker as an external control signal (X). Then, +SA15V and –SA15V output voltage is connected to the respective +Ve_Inv and –Ve_Inv ports. The +WB15V and –WB15V output voltage is connected to the respective +Ve_Bat and –Ve_Bat ports.

Condition 2: PV = 7~12 Volt and WT = 7~12 Volt

According to Table 3.2, when the regulated output voltages from solar-wind renewable energy sources are 7~12 Volt, voltage based controller produces a HIGH activated signal for S12V1 and W12V1 into the 2 – inputs AND gate shown in Figure 3.8. When S12V1 and W12V1 outputs HIGH activated signals, then the output from 2 – inputs AND gate is also equal to HIGH. This HIGH activated signal is send into the circuit breaker as an external control signal (X). Then, +SA12V and –SA12V output voltage is stepped-up using DC to DC BC before sending the output voltage to +Ve_Inv and –Ve_Inv ports. The +WB15V and –WB15V output voltage is stepped-up using DC to DC BC before sending the output voltage to +Ve_Bat and –Ve_Bat ports.

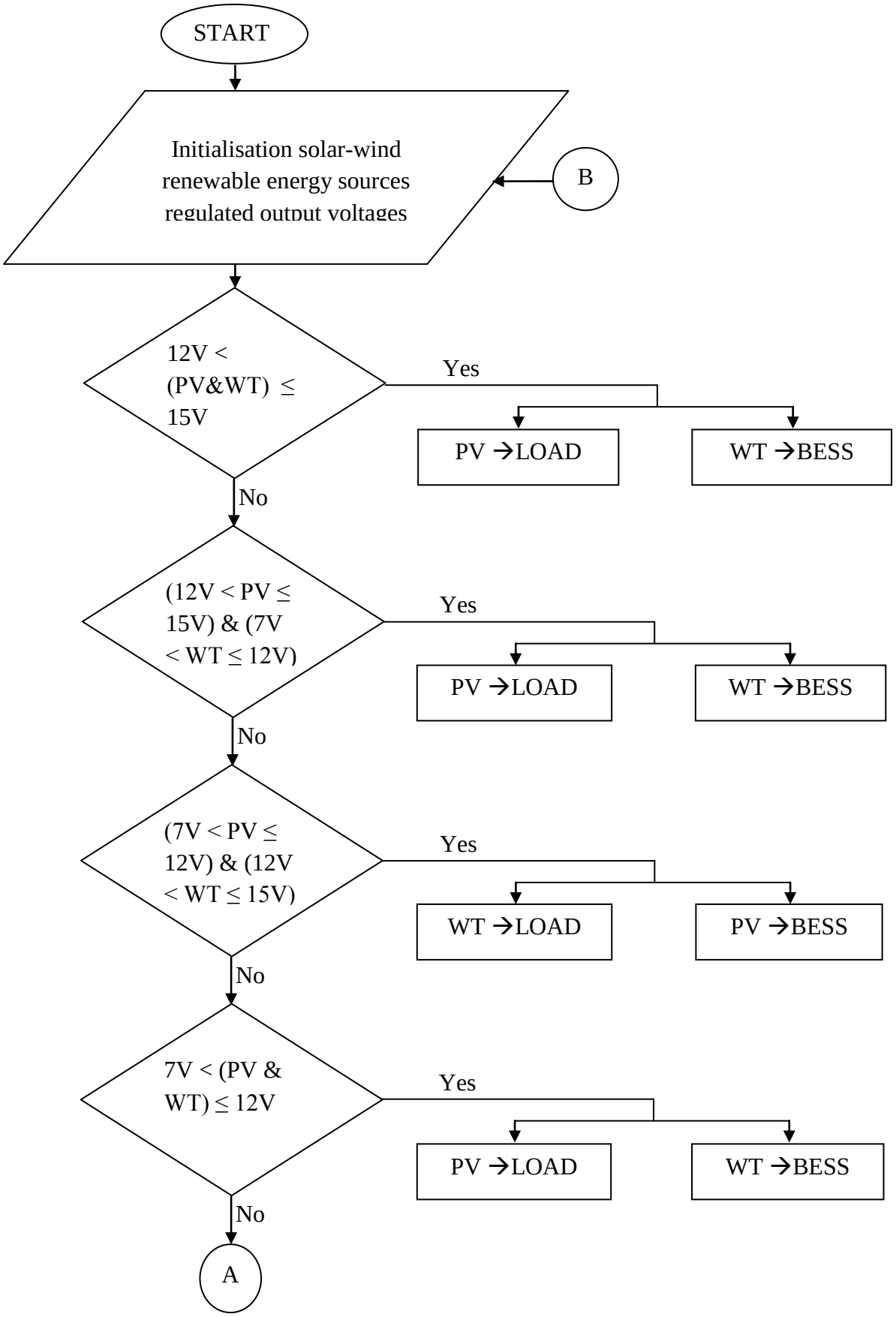
START
Initialisation solar-wind renewable energy sources regulated output voltages
B
12V < (PV&WT) ≤ 15V
Yes
PV →LOAD
WT →BESS
No
(12V < PV ≤ 15V) & (7V < WT ≤ 12V)
Yes
PV →LOAD
WT →BESS
No
(7V < PV ≤ 12V) & (12V < WT ≤ 15V)
Yes
WT →LOAD
PV →BESS
No
7V < (PV & WT) ≤ 12V
Yes
PV →LOAD
WT →BESS
No
A

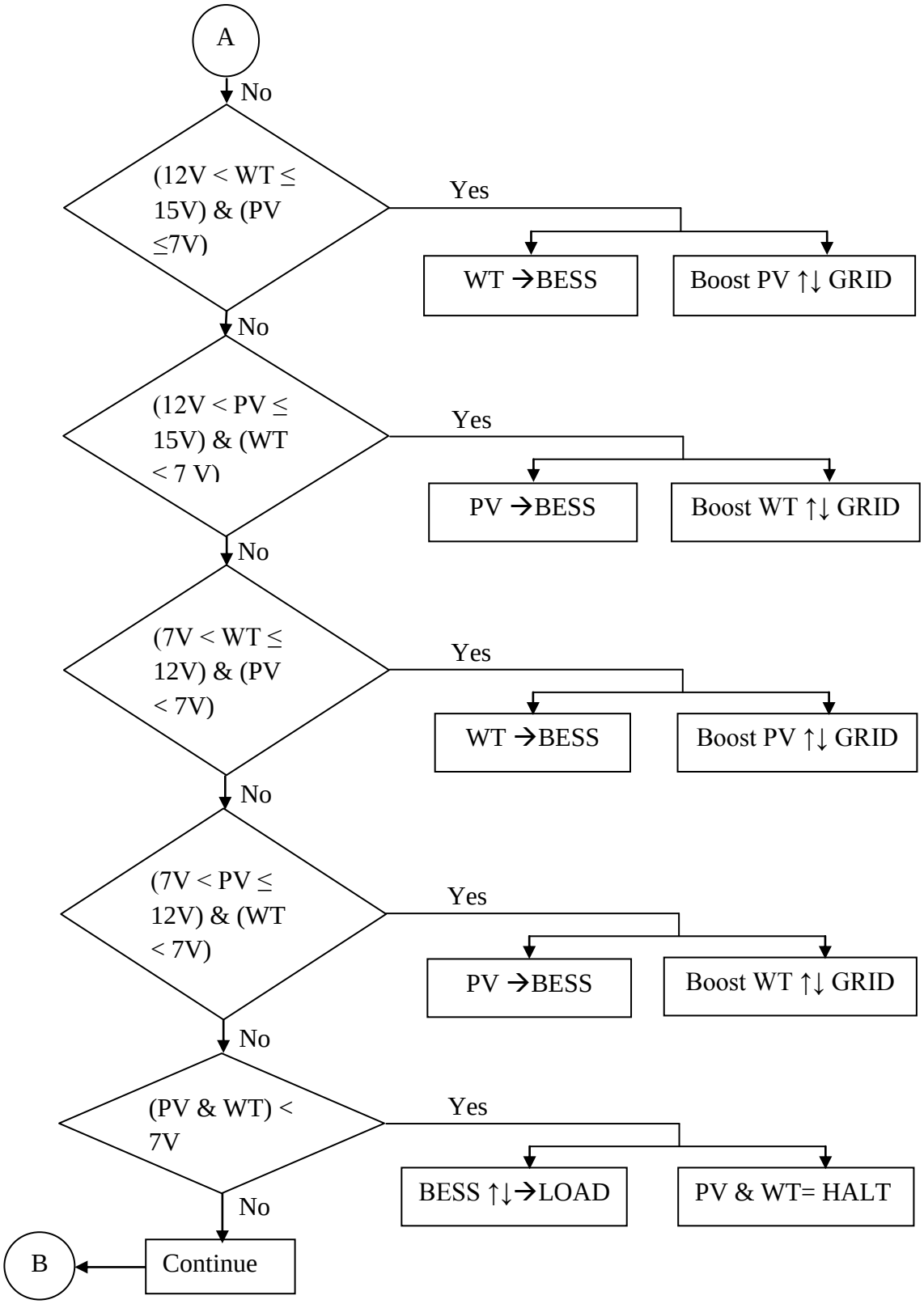

Figure 3.7: Circuit breaker switching and group conditions

Condition 3: PV = 12~15 Volt and WT = 7~12 Volt

According to Table 3.2, when the regulated output voltages from PV = 12~15 Volt and WT = 7~12 Volt, voltage based controller produces a HIGH activated signal for S15V1 and W12V1 into the 2 – inputs AND gate shown in Figure 3.8. When S15V1 and W12V1 outputs HIGH activated signals, then the output from 2 – inputs AND gate is also equal to HIGH. This HIGH activated signal is send into the circuit breaker as an external control signal (X). Then, +SA15V and –SA15V output voltage is connected to the respective +Ve_Inv and –Ve_Inv ports. The +WA12V and –WA12V output voltage is stepped-up using DC to DC BC before sending the output voltage to +Ve_Bat and –Ve_Bat ports.

Condition 4: WT = 12~15 Volt and PV = 7~12 Volt

According to Table 3.2, when the regulated output voltages from WT = 12~15 Volt and PV = 7~12 Volt, voltage based controller produces a HIGH activated signal for W15V1 and S12V1 into the 2 – inputs AND gate shown in Figure 3.8. When W15V1 and S12V1 outputs HIGH activated signals, then the output from 2 – inputs AND gate is also equal to HIGH. This HIGH activated signal is send into the circuit breaker as an external control signal (X). Then, +WB15V and –WB15V output voltage is connected to the respective +Ve_Inv and –Ve_Inv ports. The +SB12V and –SB12V output voltage is stepped-up using DC to DC BC before sending the output voltage to +Ve_Bat and –Ve_Bat ports.

Summarizing the four conditions of regulated output voltages from solar-wind renewable energy sources presented are in Table 3.2. It is understood that each pair in the configuration only will operate when the HIGH activated signals received from voltage based controller matches the condition’s configuration presented in Table 3.2

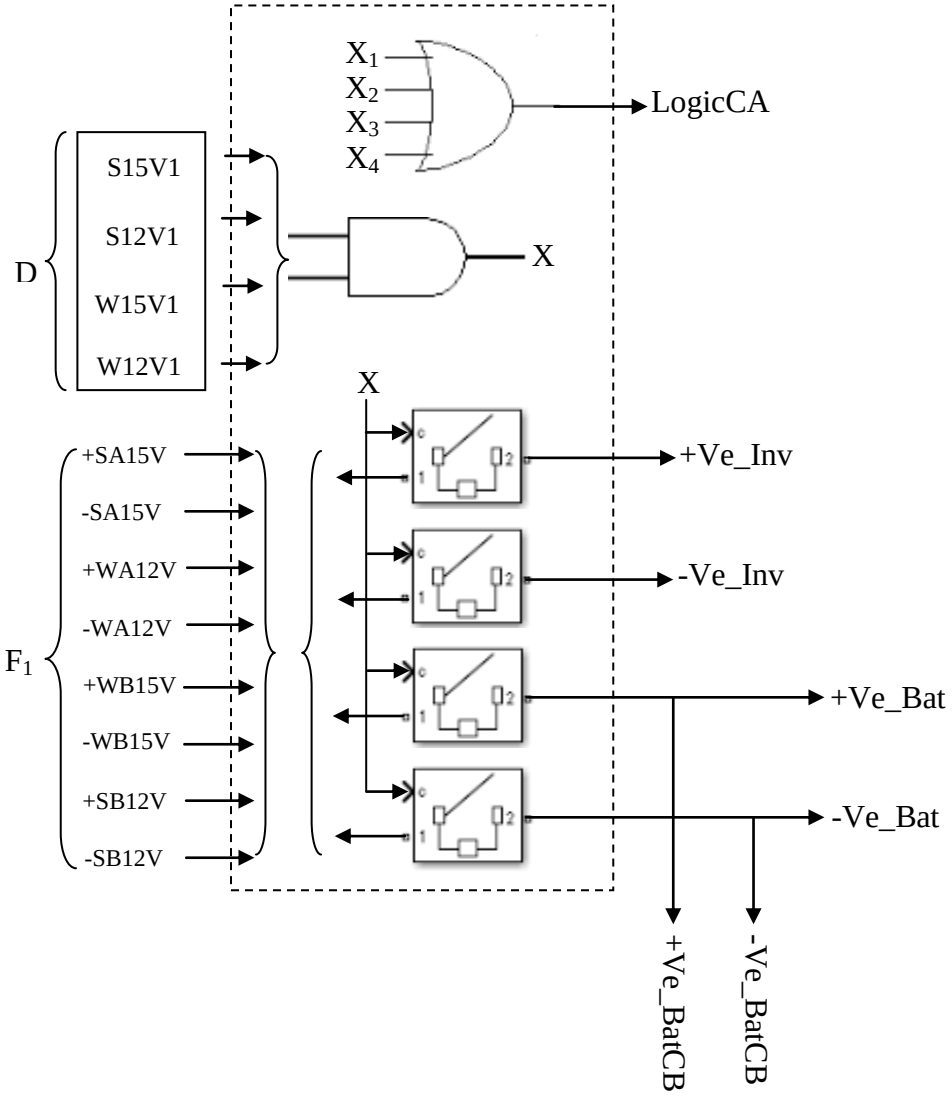

Figure 3.8: Block diagram of circuit breaker switching and group conditions configuration and setup

Despite the presented conditions in Table 3.2, there are five others conditions for the regulated output voltages from solar-wind renewable energy sources presented in Table 3.3. These conditions are mainly only based on single renewable energy source availability and used only to perform BESS charging process. The circuit breaker switching and group condition shown in Figure 3.9 is configured to operate only one regulated output voltage from renewable energy source. In the following, each presented condition in Table 3.3 is further explained.

Table 3.3: Solar-wind renewable energy sources pairing

Condition	Voltage based Controller Output	Analogue Input Voltage	Connectivity	
5	S15V1	12~15 Volt	F2	+SC15V
				-SC15V
	W7V1	0~7 Volt	F2	+W7V
				-W7V
6	W15V1	12~15 Volt	F2	+WD15V
				-WD15V
	S7V1	0~7 Volt	F2	+S7V
				-S7V
7	S12V1	7~12 Volt	F2	+SE12V
				-SE12V
	W7V1	0~7 Volt	F2	+W7V
				-W7V
8	W12V1	7~12 Volt	F2	+WF12V
				-WF12V
	S7V1	0~7 Volt	F2	+S7V
				-S7V
9	S7V1	0~7 Volt	F2	+S7V
				-S7V
	W7V1	0~7 Volt	F2	+W7V
				-W7V

Condition 5: PV = 12~15 Volt and WT = 0~7 Volt

According to Table 3.3, when the regulated output voltages from PV = 12~15 Volt and WT = 0~7 Volt, voltage based controller produces a HIGH activated signal for S15V1 and W7V1 into the 2 – inputs AND gate as shown in Figure 3.9. When, S15V1 and W7V1 activated signals are HIGH, then the output from 2 – inputs AND gate is also equal to HIGH. This HIGH activated signal is send into the circuit breaker as an external control signal (X). Then, +SC15V and –SC15V output voltage is connected to the respective +Ve_BatCB and -Ve_BatCB ports. The +W7V and –W7V output voltage is connected to the respective GROUND ports.

Condition 6: WT = 12~15 Volt and PV = 0~7 Volt

According to Table 3.3, when the regulated output voltages from WT = 12~15 Volt and PV = 0~7 Volt, voltage based controller produces a HIGH activated signal for W15V1 and S7V1 into the 2 – inputs AND gate as shown in Figure 3.9. When W15V1 and S7V1 outputs HIGH activated signals, then the output from 2 – inputs AND gate is also equal to HIGH. This HIGH activated signal is send into the circuit breaker as an external control signal (X). Then, +WD15V and –WD15V output voltage is connected to the respective +Ve_BatCB and -Ve_BatCB ports. The +S7V and –S7V output voltage is connected to the respective GROUND ports.

Condition 7: PV = 7~12 Volt and WT = 0~7 Volt

According to Table 3.3, when the regulated output voltages from PV = 7~12 Volt and WT = 0~7 Volt, voltage based controller produces a HIGH activated signal for S12V1 and W7V1 into the 2 – inputs AND gate as shown in Figure 3.9. When S12V1 and W7V1 outputs HIGH activated signals, then the output from 2 – inputs AND gate is equal to HIGH. This HIGH activated signal is send into the circuit breaker as an external control signal (X). Then, +SE12V and –SE12V output voltage is stepped-up using DC to DC BC before sending the output voltage to the respective +Ve_BatCB and -Ve_BatCB ports. The +W7V and –W7V output voltage is connected to the respective GROUND ports.

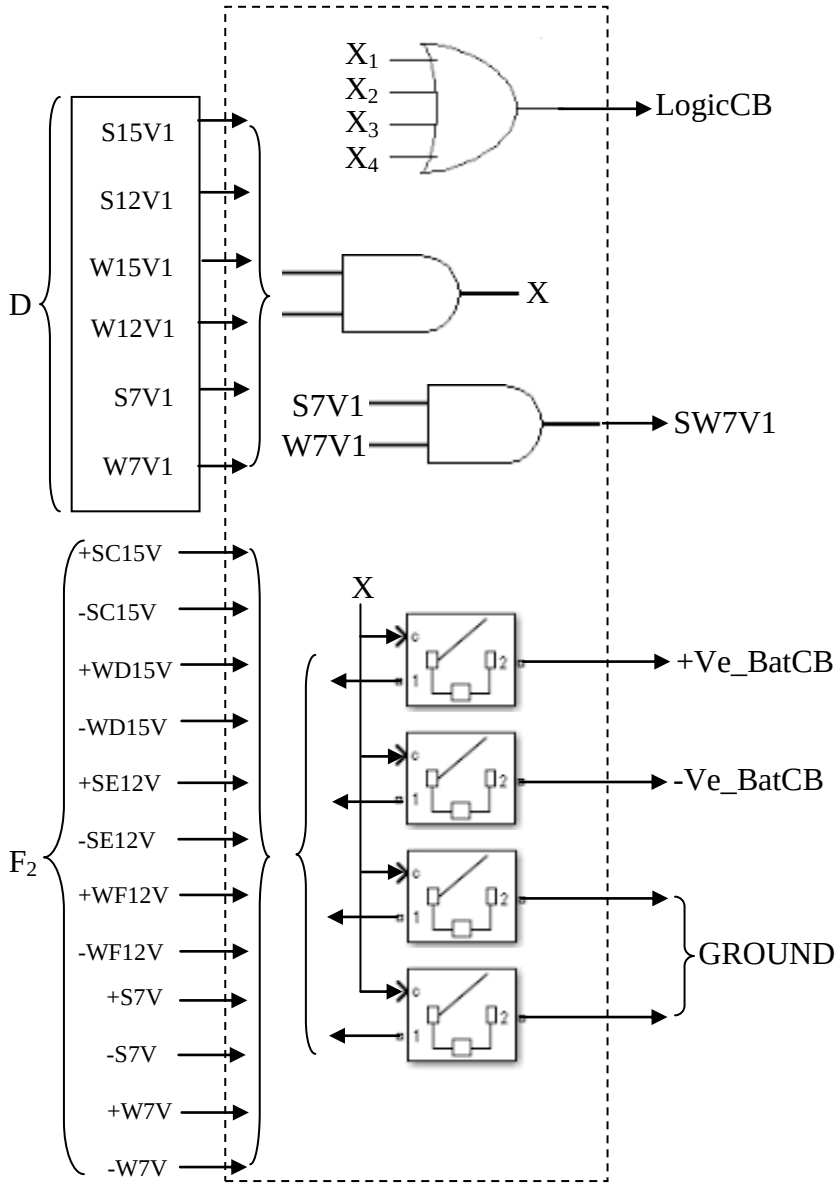

Figure 3.9: Block diagram circuit breaker switching control setup

Condition 8: WT = 7~12 Volt and PV = 0~7 Volt

According to Table 3.3, when the regulated output voltages from WT = 7~12 Volt and PV = 0~7 Volt, voltage based controller produces a HIGH activated signal for W12V1 and S7V1 into the 2 – inputs AND gate in the Figure 3.9. When W12V1 and S7V1 outputs HIGH activated signals, then the output from 2 – inputs AND gate is also equal to HIGH. This HIGH activated signal is send into the circuit breaker as an external control signal (X). Then, +WF12V and –WF12V output voltage is stepped-up using the DC to DC BC before sensing

the output voltage to the respective +Ve_BatCB and -Ve_BatCB ports. The +S7V and –S7V output voltage is connected to the respective GROUND ports.

Condition 9: PV = 0~7 Volt and WT = 0~7 Volt

According to Figure 3.7, when the regulated output voltages from PV = 0~7 Volt and WT = 0~7 Volt, voltage based controller produces a HIGH activated signal for S7V1 and W7V1 into the 2 – inputs AND gate in the Figure 3.9. When S7V1 and W7V1 outputs HIGH activated signals, then the output from 2 – inputs AND gate is also equal to HIGH. This HIGH activated signal is send into the circuit breaker as an external control signal (X). The HIGH external control signal (X) signal is send into the BESS charging/discharging switching controller to inform the BESS that solar-wind renewable energy sources are currently not available to produce any regulated output voltages. Therefore, the connected AC load is switched to the BESS for power source supply.

Summarizing the five conditions for the regulated output voltages from solar–wind renewable energy sources, it is understood that only one pair in the configuration is operating when the HIGH activated signals from the voltage based controller matches the configuration condition presented in Table 3.3. In these configurations, when one of the renewable energy sources is able to supply the output voltage, this voltage is used to charge the BESS, which is used as secondary power source supply during the unavailability of solar-wind renewable energy sources to produce output voltage.

3.6 MODELING BESS CHARGING/DISCHARGING SWITCHING ALGORITHM - STATEFLOW

This section aims to provide a description for the developed BESS charging/discharging switching algorithm using the Simulink/Stateflow toolbox in MATLAB software. The BESS charging/discharging switching algorithm is designed to provide a strategic charging/discharging management and control when the BESS is being charged or discharged. It is important to understand the methodology of BESS charging/discharging switching algorithm, therefore, Figure 3.10 illustrates the methodology of BESS charging/discharging switching algorithm.

The BESS charging/discharging switching algorithm is designed to collect the BESS SoC information during charging or discharging process. When the BATT A STORAGE SoC and BATT B STORAGE SoC is equal or less than 40%, BESS charging/discharging switching algorithm outputs a HIGH activated signal to stop the discharging process and starts charging the BATT A STORAGE.

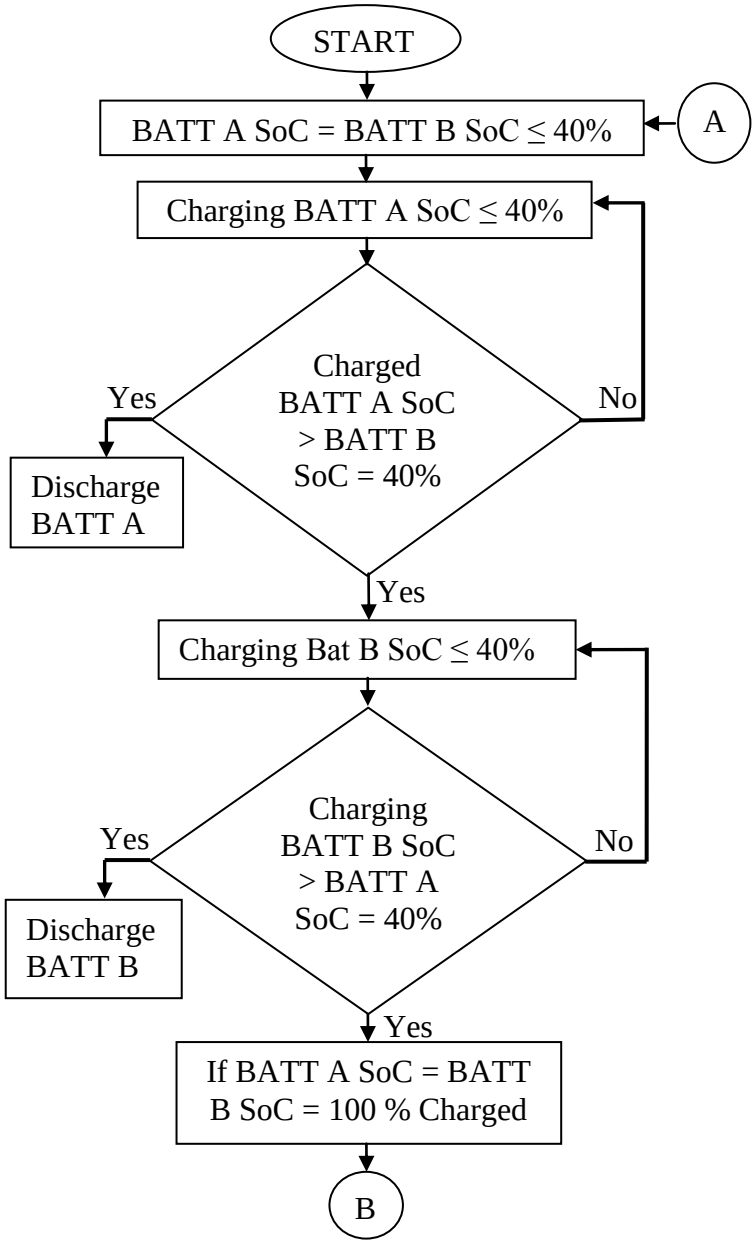

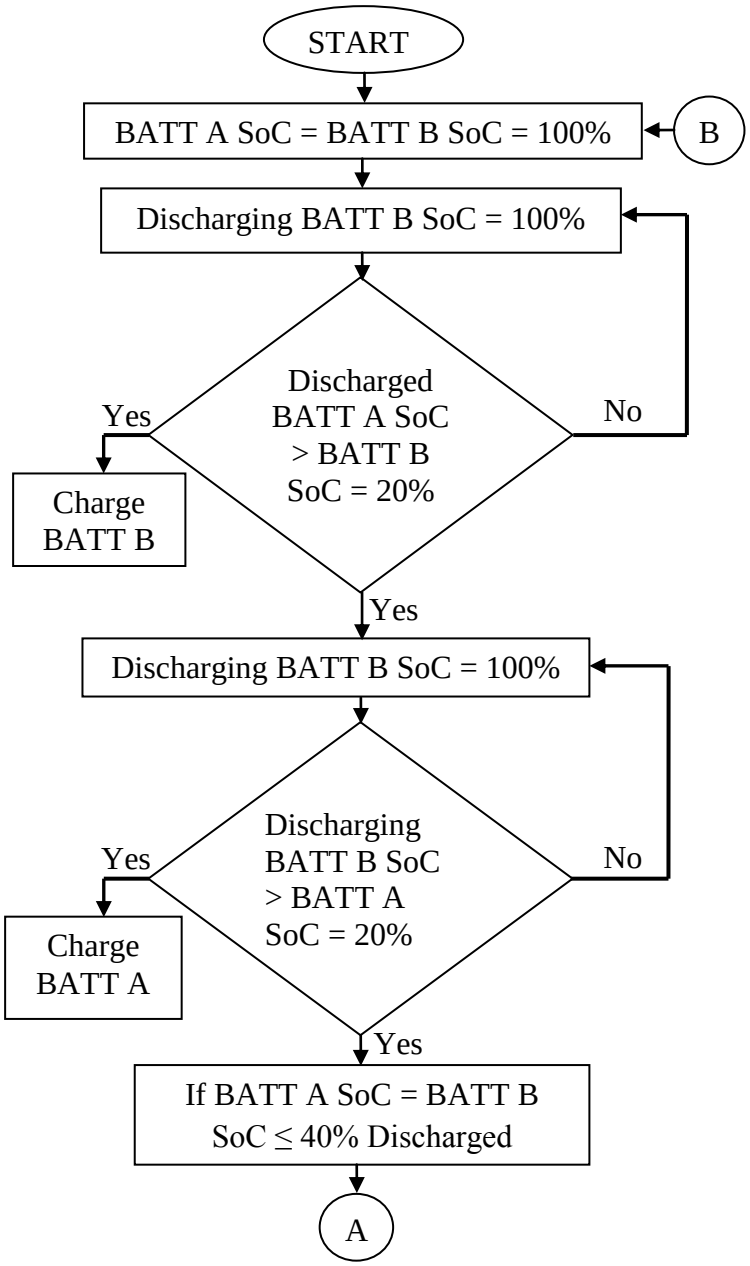

Figure 3.10: Methodology of BESS charging/discharging switching – Stateflow

Referring to Figure 3.10, BATT A STORAGE is priorities for charging process. When BATT A STORAGE SoC is charged 40% compared with BATT B STORAGE SoC, then charging process is switched to BATT B STORAGE and BATT A STORAGE is stop charging. The BATT A STORAGE is connected to the AC load for discharging, if required. When BATT A STORAGE SoC and BATT B STORAGE SoC is equal to 100%, then BESS is stop charging and ready for any potential discharging process.

During the discharging process, BATT B STORAGE is priorities to perform discharging process. BATT B STORAGE is discharged at the rate of 20% and when BATT B STORAGE SoC is equal or less than 20% compared with BATT A STORAGE SoC then the discharging is switched to BATT A STORAGE. The discharging process is alternately continued till BATT A STORAGE SoC and BATT B STORAGE SoC reaches at 40%, and then discharging BESS is halted.

As an overall performance for Figures 3 and 3.10, whenever a renewable energy source in Figure 3.7 is switched to the BESS, the BESS SoC status will be sensed and measured for charging process, if required. Otherwise, the charging process is not required and the charging/discharging switching circuitry is deactivated.

The BESS charging/discharging switching algorithm (Stateflow) and circuit breaker switching control diagram is shown in Figure 3.11. The BESS charging process is further explained with reference to Figures 3.8 and 3.9. Referring to Figure 3.11, LogicCA is the output signal from Figure 3.8. The LogicCA will only output HIGH activated signal when any one of the condition in Figure 3.8 is operating. When LogicCA outputs a HIGH activated signal, it also means that one of the renewable energy sources is connected to the AC load and the other one is connected to BESS for charging process, if required. LogicCB is the output signal from Figure 3.9. LogicCB will only output a HIGH activated signal when LogicCA outputs a LOW signal. When LogicCB output HIGH activated signal, it means that only one renewable energy source is producing output voltage as power source supply. This output voltage is used only to perform BESS charging process, if required.

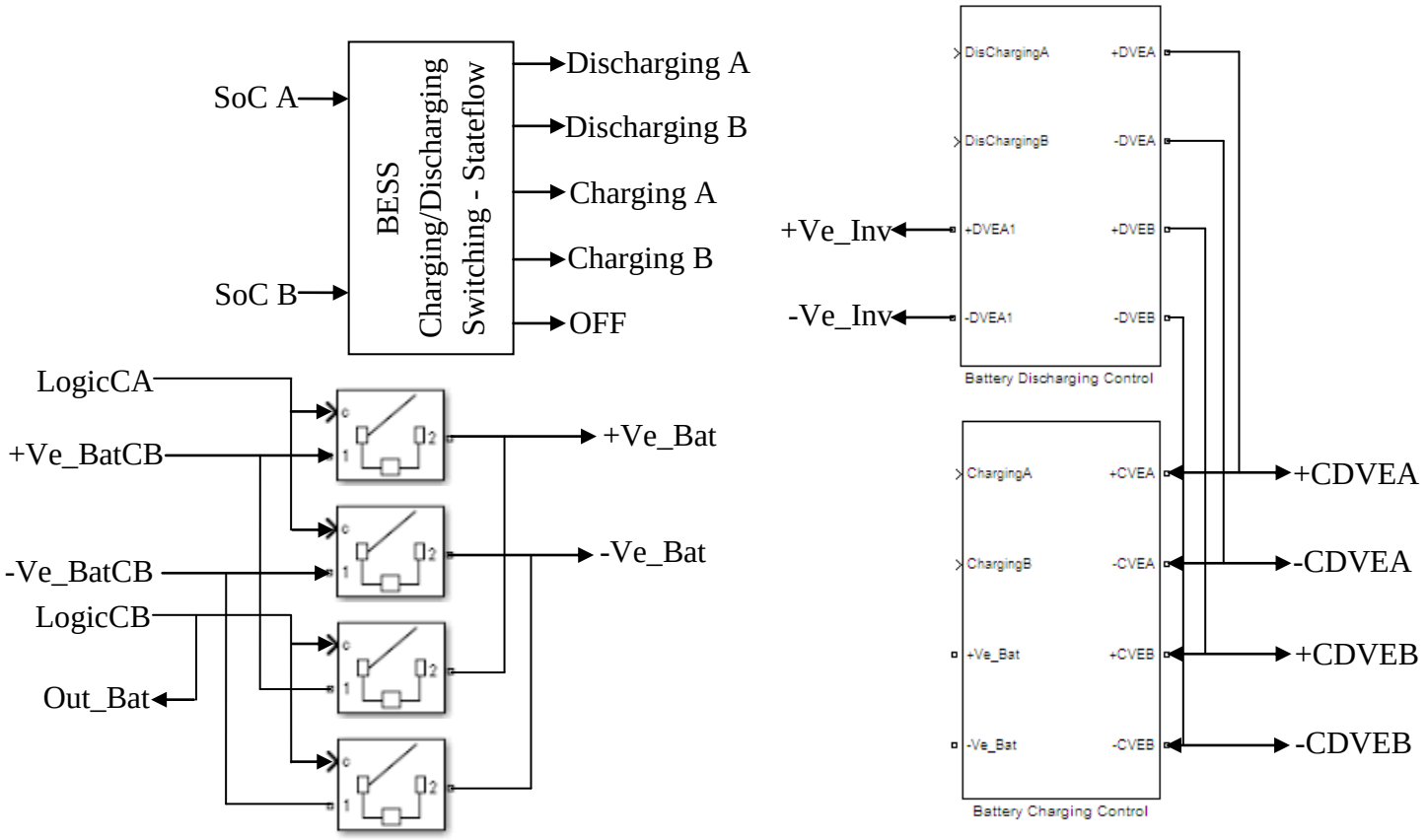

Figure 3.11: BESS charging/discharging switching algorithm (Stateflow) and circuit breaker switching control

The +Ve_Bat and –Ve_Bat output ports of the circuit breaker is connected to +Ve_Bat and –Ve_Bat input ports of the battery charging control (Stateflow). Hence, BESS charging process will start accordingly as it is depicted in Figure 3.11 methodology.

The BESS discharging process is only activated when the BESS charging/discharging switching algorithm receives a LOW signal from LogicCA and a HIGH activated signal from LogicCB. When LogicCB is at HIGH activated signal, the HIGH activated signal is send to BAT input of the breaker switching as shown in Figure 3.12. The HIGH activated signal into the BAT will trigger the external control signal of circuit breaker to go HIGH to allow battery discharging process to start. The +Ve_OInv and –Ve_OInv output ports is connected to the inputs of DC to AC Inverter. This process is switched OFF when BESS charging/discharging switching algorithm outputs a LOW signal at the OFF port as shown in Figure 3.11, which indicates BESS SoCs are less than 40% and requires charging.

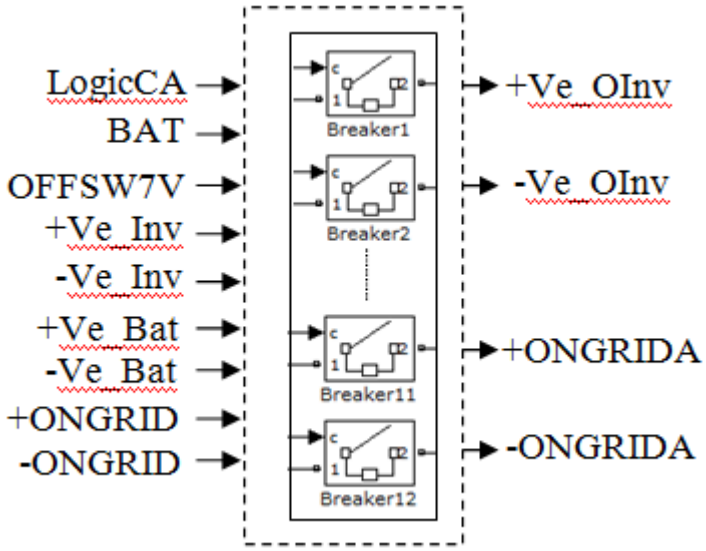

Figure 3.12: Simulink block of Breaker Switching

For condition when LogicCA and OFF outputs a LOW signal, solar-wind renewable energy sources and BESS is unable to supply any power source to the connected AC load. Therefore, S7V1 and W7V1 from voltage based controller and OFF from BESS charging/discharging switching algorithm will a output HIGH activated signal through the 2 – inputs AND gate. This HIGH activated signal is send to the OFFSW7V port at the breaker switching as shown in

Figure 3.12 to switch ON the grid network support connection for the connected AC load. Thus, +ONGRIDA and –ONGRIDA output ports are connected in parallel to the output ports of the DC to AC Inverter, which supplies power source from the grid network to the connected AC load.

3.7 MODELING DC TO DC BOOST CONVERTER

Referring to Figure 3.5, 12 Volt DC is stepped-up using DC to DC BC. Therefore, a DC to DC BC model is designed in MATLAB Simulink/Stateflow software is shown in Figure 3.13. The DC to DC BC is used to step-up the 7~12 Volt regulated output voltages from solar-wind renewable energy sources to a desired output voltage to utilise and optimise the power delivery via the real-time DC – HRES hardware system. The following are the configurations of DC to DC BC model.

DC to DC BC:

Minimum Voltage input, (V_{inmin}) = 7 Volt

Maximum Voltage input (V_{inmax}) = 12 Volt

Inductor = 1 mH

Diode Forward Voltage (V_{df}) = 0.8 Volt

Capacitor =6 µF

Period (sec) = 50 µs

Duty Cycle (D) = 35%

Switching Period (S) = T_s

Frequency, $(f) = \frac{1}{T} = \frac{1}{50us} = 20$ kHz

$V_{outmax} = \frac{V_{inmax}}{1-D} = \frac{12}{1-35\%} = \frac{12}{0.65} = 18.46$ Volt

$$V_{outmax} = 18.46 - V_{df} = 17.66 \text{ Volt}$$

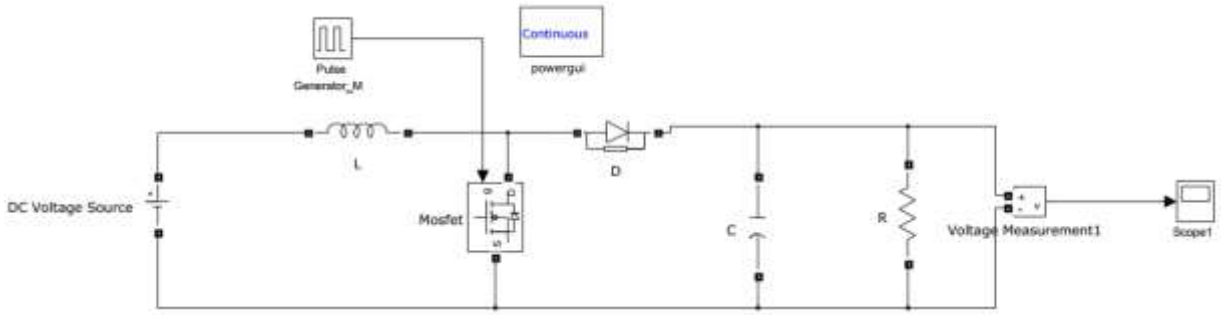

Figure 3.13: Simulink model design of DC to DC BC

3.8 MODELING DC TO AC INVERTER

DC to AC Inverter is an electronic device that is used to produce the main AC voltage from a low voltage DC energy sources, such as from battery, regulated output voltages from solar-wind renewable energy sources and many more. Therefore, this characteristic makes the DC to AC Inverter to be very suitable during the need to use the AC power equipment or appliances. The model depicted in Figure 3.14 shows the designed DC to AC Inverter using MATLAB Simulink blocks.

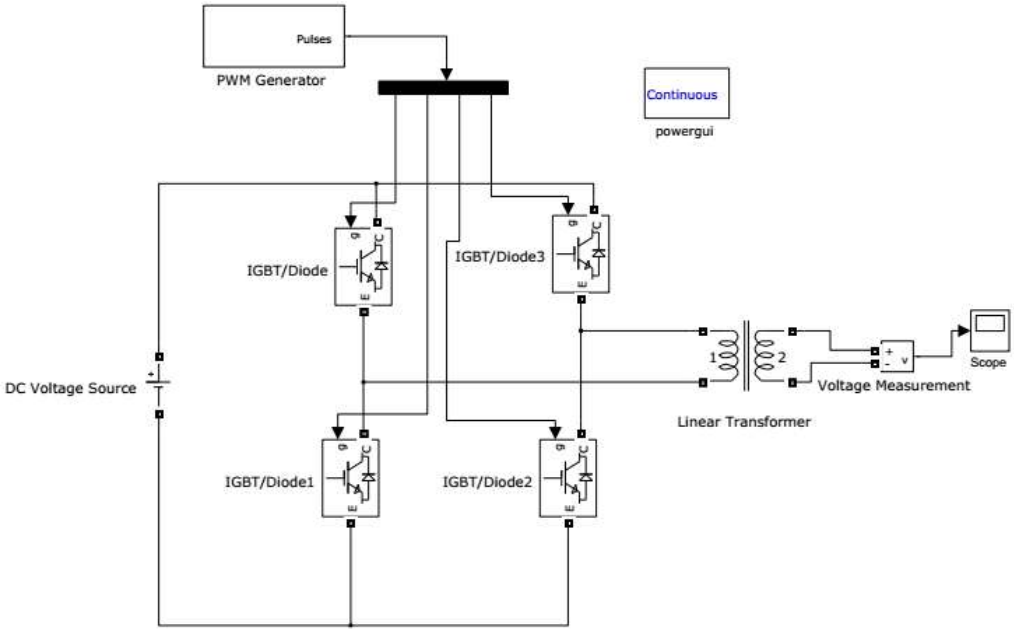

Figure 3.14: Simulink model design of DC to AC Inverter

3.9 REAL-TIME DC HRES HARDWARE SYSTEM MODELLING OVERVIEW

After completed designing the methodology for each subsystem for real-time DC HRES hardware system in MATLAB Simulink/Stateflow software, all the modelled subsystems are connected together to demonstrate the system's aim and objectives. The following section presents the system's results, analysis and validation of the designed subsystem for the modelled real-time DC HRES hardware system.

3.10 REAL-TIME DC HRES HARDWARE SYSTEM MODEL SIMULATION RESULTS

This section discusses about the real-time DC HRES hardware system model's simulation results. The results presented in this section are analysed and validates the real-time DC HRES hardware system overall performances. Besides that, these results are used as a fundamental benchmark to analyse and validate the development, integration, implementation and construction of real-time DC HRES hardware system.

3.10.1 CONDITION A: PV = 12~15 Volt and WT = 12~15 Volt - DC HRES MODEL SIMULATION

The sensed and measured regulated output voltages from solar-wind renewable energy sources are shown in Figures 3.15 (a) and (b). Referring to Figure 3.2, voltage based controller will output a HIGH activated signals at S15V port when PV15 = 1 and at W15V port when WT15 = 1.

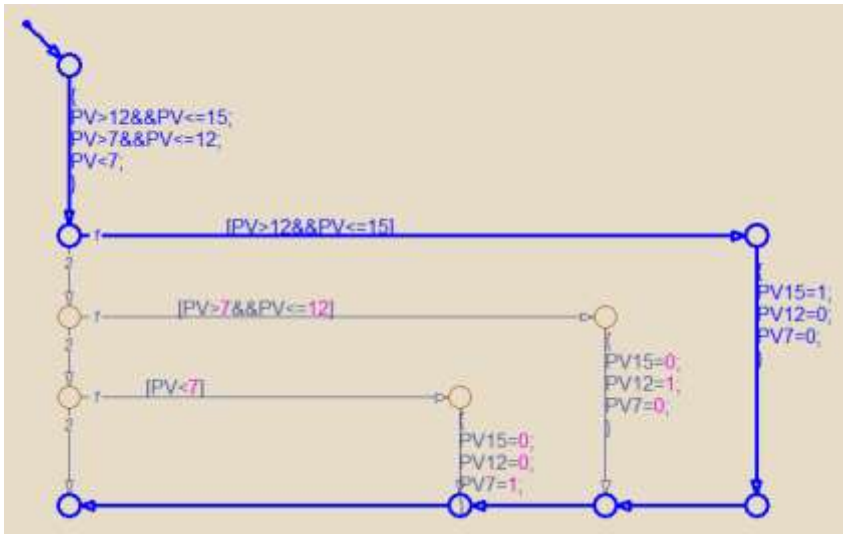

(a)

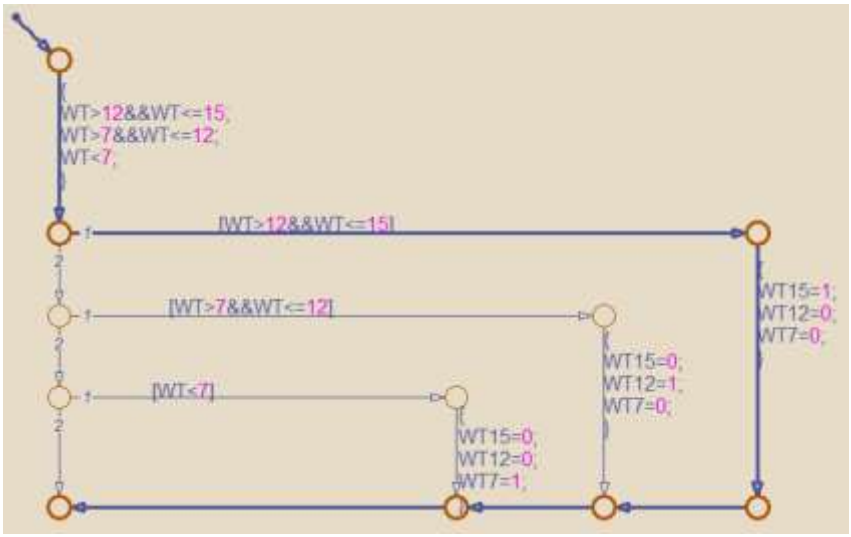

(b)

Figure 3.15: Solar-wind renewable energy source regulated output voltages – voltage based controller (Stateflow)

Referring to Figure 3.4, when S15V2 and W15V2 receives a HIGH activated signals at the voltage switching subsystem controller as shown in Figure 3.5, the connected relays are switched ON. Hence, 15 Volt voltages is output at SA15V and WA15V ports and the results are presented in Figure 3.16.

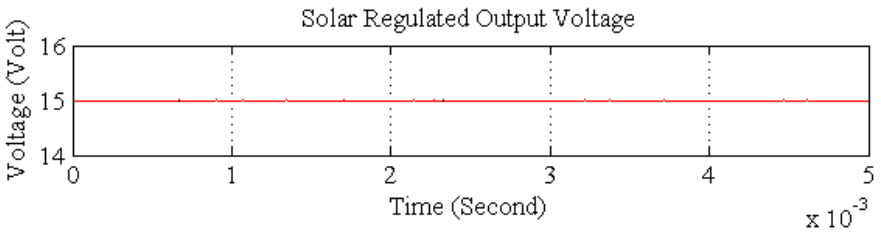

(a)

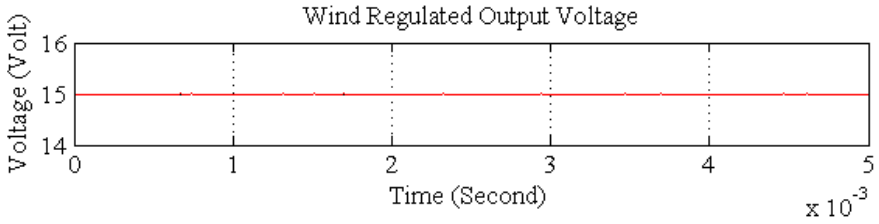

(b)

Figure 3.16: Solar-wind renewable energy sources regulated output voltages

Therefore, SA15V and WB15V are output voltages at Ve_Inv ports as power source for the connected AC load and Ve_Bat ports for BESS charging as shown in Figure 3.8. The 12~15 Volt solar regulated output voltage at Ve_Inv ports is used as input to the DC to AC inverter as shown in Figure 3.14 and the output result is presented in Figure 3.17. The 230 VAC output voltages shown in Figure 3.17 are used as power source to supply the connected AC load. The 12~15 Volt wind regulated output voltage at Ve_Bat ports is used to charge the BESS.

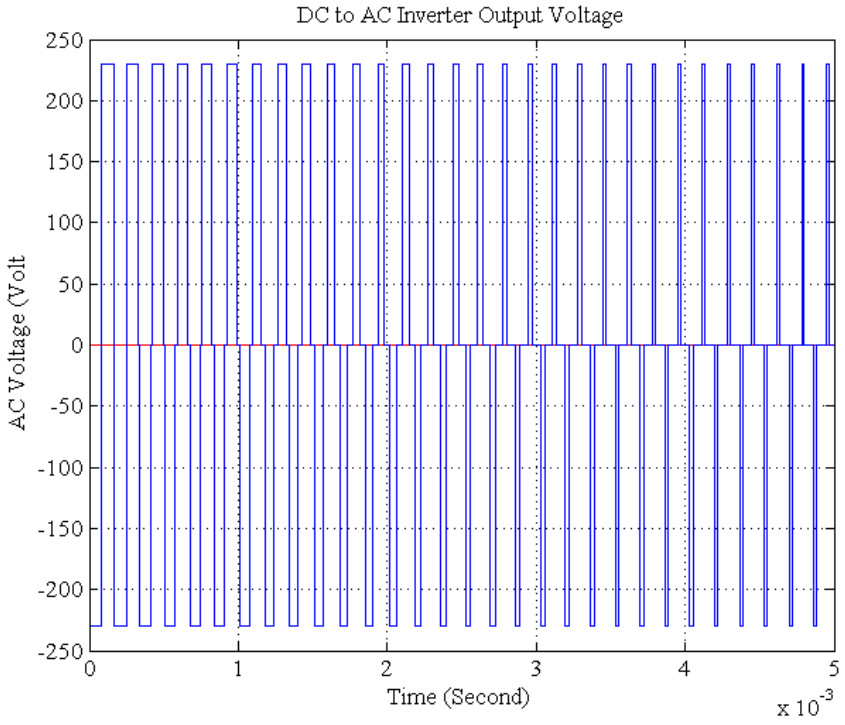

Figure 3.17: DC to AC Inverter output voltage

3.10.1.1 BESS MODEL SIMULATION OUTPUT

This section discusses about the BESS SoC, Current and Voltage status. Section (a) presents the results for BATT A STORAGE SoC = 100% and BATT B STORAGE SoC = 100%. Section (b) presents the results for BATT A STORAGE SoC = 100% and BATT B STORAGE SoC = 80%. Section (c) presents the results for BATT A STORAGE SoC = 80% and BATT B STORAGE SoC = 100%.

(a) BATT A and BATT B STORAGES SoC = 100%

The BESS charging/discharging switching algorithm is shown in Figure 3.18. As shown, when BATT A and BATT B STORAGES SoC are equal to 100% as shown in Figure 3.19 then BATT B STORAGE is connected to the AC load for discharging process. But, in this case the BATT B STORAGE is not discharging because there is power source available from the regulated output voltage from solar renewable energy source supplying to the connected AC load. This is verified due to low current measured shown in Figure 3.20.

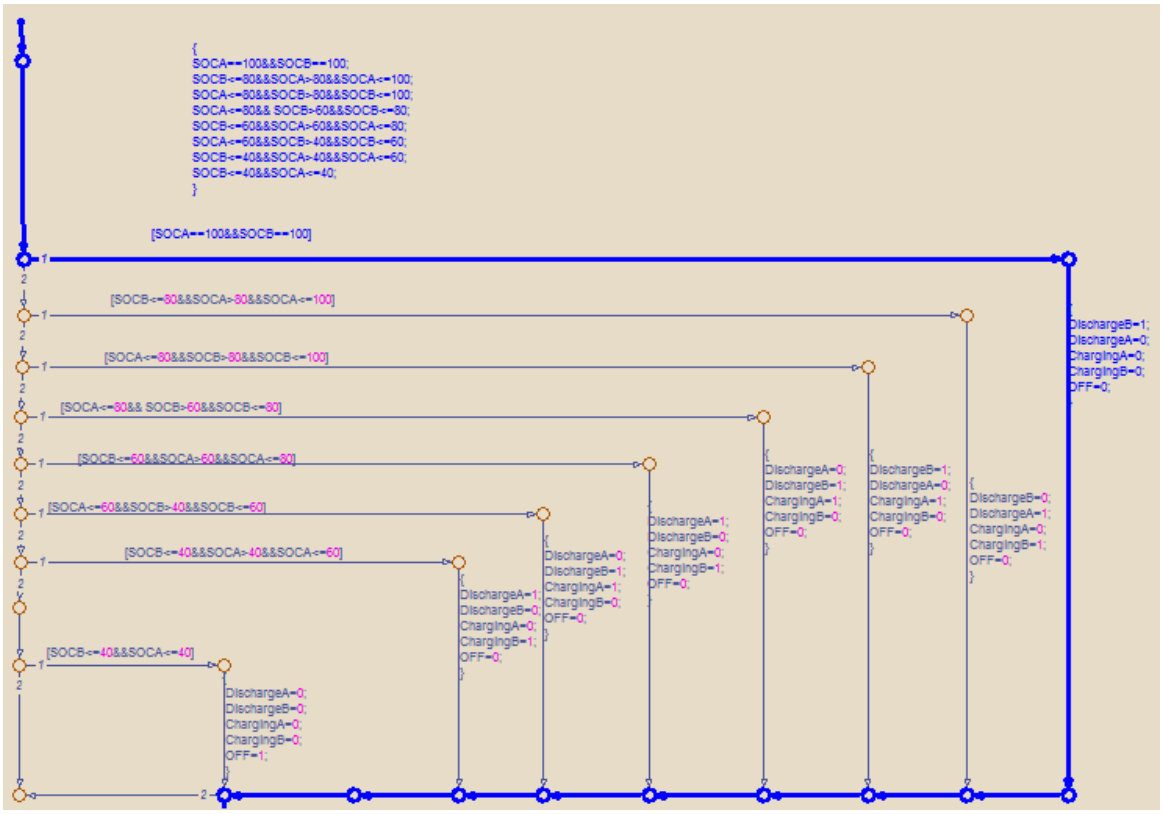

Figure 3.18: Charging/Discharging – SoC base controller (Stateflow)

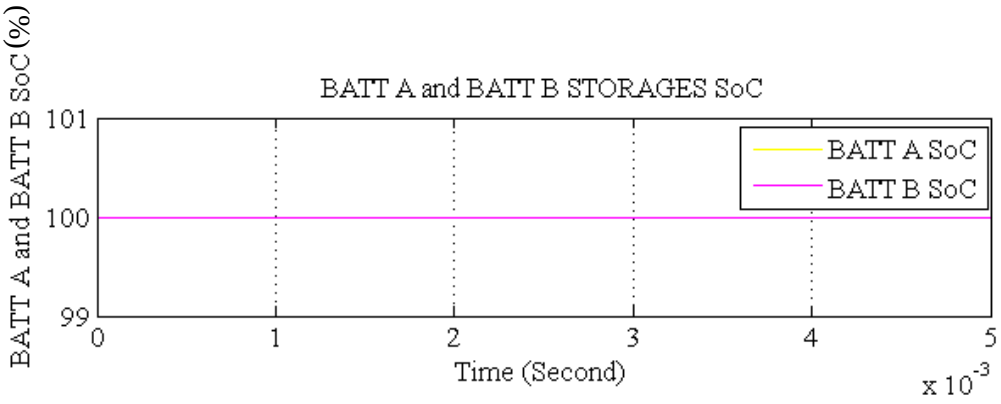

Figure 3.19: BATT A and BATT B STORAGES SoC

The BATT A and BATT B STORAGES current and voltage status is shown in Figures 3.20 and 3.21. When BATT A and BATT B STORAGES are fully charged as shown in Figure 3.21, the current is always low. This condition occurs due to source regulated current is raised at the voltage terminal above the upper charge voltage limit, which shows the current drops due to saturation. This indicates that BATT A or BATT B STORAGES are not supplying any power source to the connected AC load.

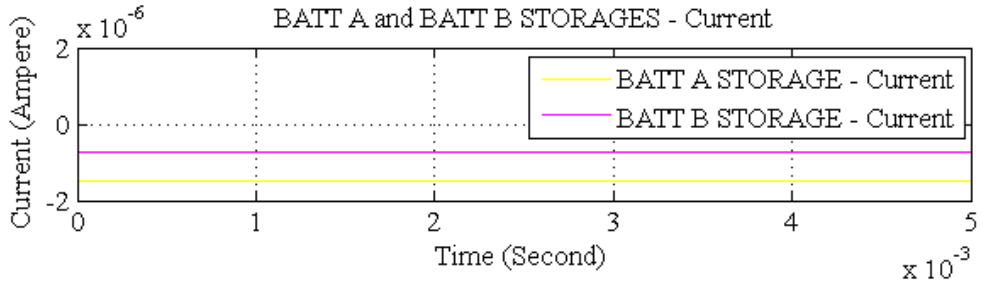

Figure 3.20: BATT A and BATT B STORAGES – Current

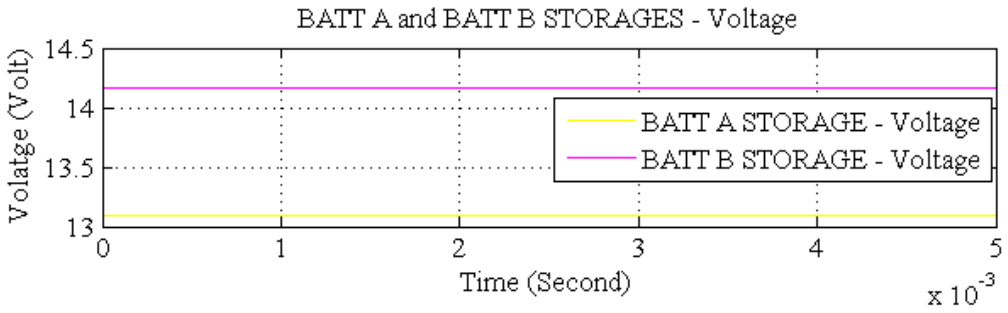

Figure 3.21: BATT A and BATT B STORAGES – Voltage

(b) BATT A STORAGES SoC = 100% and BATT B STORAGE SoC = 80%

The BESS charging/discharging switching algorithm shown in Figure 3.22 is indicating that BATT A STORAGE is connected to discharge the stored energy to the connected AC load and BATT B STORAGE is connected for charging process. As shown in Figure 3.23, BATT A STORAGE SoC is equal to 100% and BATT B STORAGE SoC is equal to 80%.

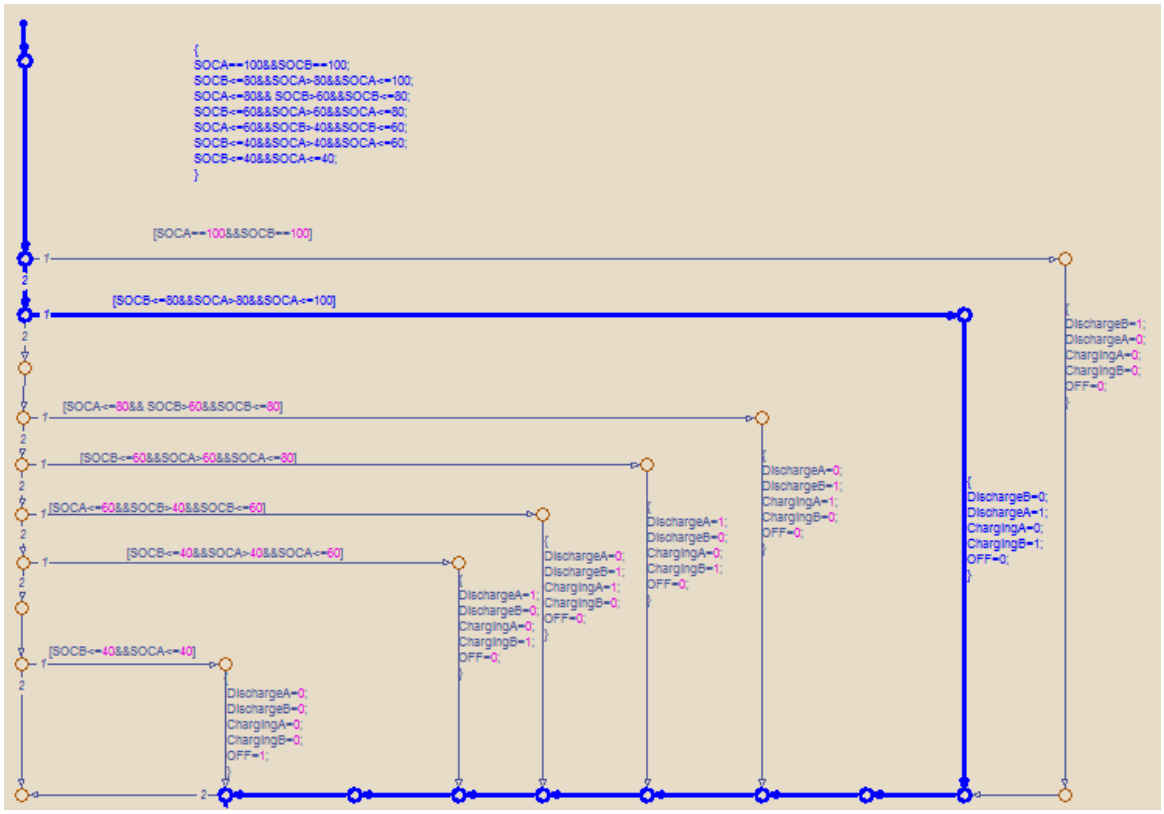

Figure 3.22: Charging/Discharging – SoC base controller (Stateflow)

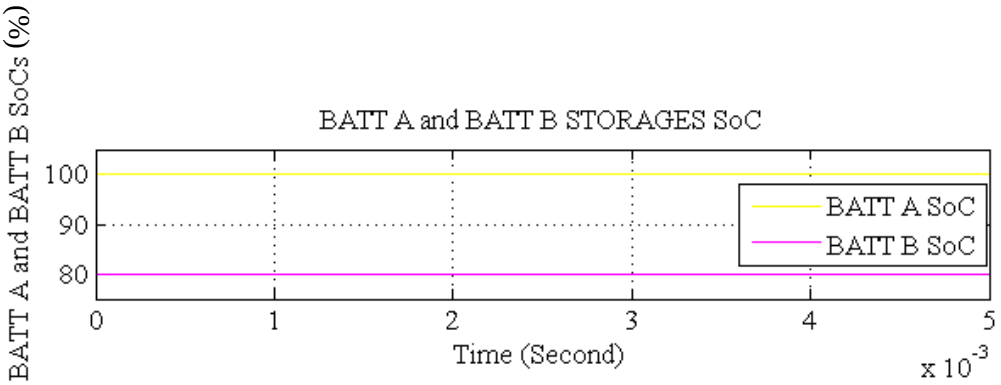

Figure 3.23: BATT A and BATT B STORAGES SoC

The BATT A and BATT B STORAGES current and voltage status are shown in Figures 3.24 and 3.25. When BATT A STORAGE is fully charged as shown in Figure 3.23, BATT A STORAGE current remain low and BATT B STORAGE current drops below the actual current reading as shown in Figure 3.24 to perform the charging process. The measure current

in this stage is known as pre-charge current [99 - 100]. The applied pre-charge current is usually very low [101] and is applied as part of the charging start sequence for a system [99]. The current will slowly increase once the battery voltage increases. The BATT B STORAGE voltage in Figure 3.25 shows the voltage of BATT B STORAGE is below the fully charged voltage status. Therefore, this indicates BATT B STORAGE has been discharged and is being charge to increase the BATT B STORAGE SoC.

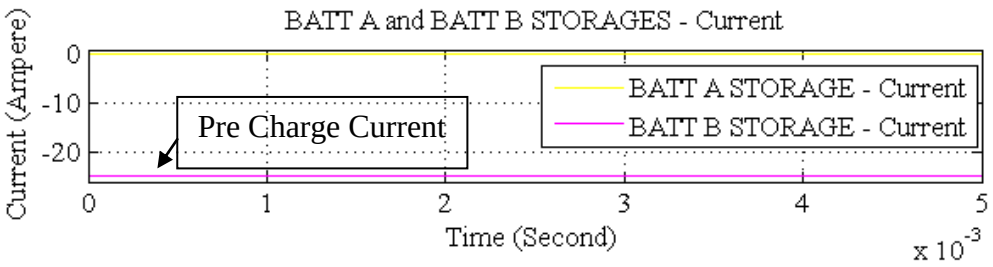

Figure 3.24: BATT A and BATT B STORAGES – Current

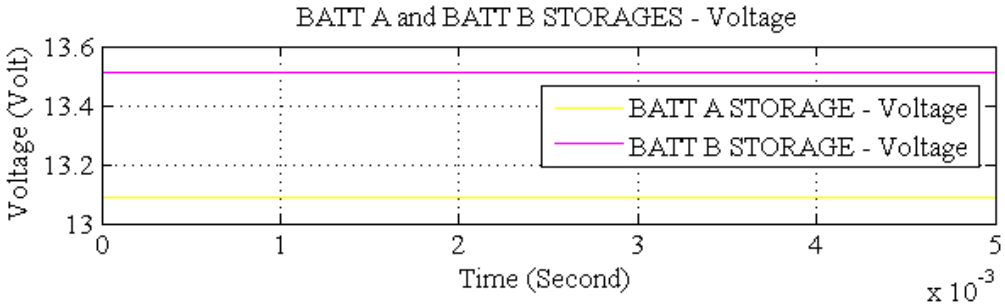

Figure 3.25: BATT A and BATT B STORAGES – Voltage

(c) BATT A STORAGE SoC = 80% and BATT B STORAGE SoC = 100%

The BESS charging/discharging switching algorithm shown in Figure 3.26 indicates BATT A STORAGE is connected for charging and BATT B STORAGE is connected to discharge the stored energy to the connected AC load. As shown in Figure 3.27, BATT A STORAGE SoC is equal to 80% and BATT B STORAGE SoC is equal to 100%.

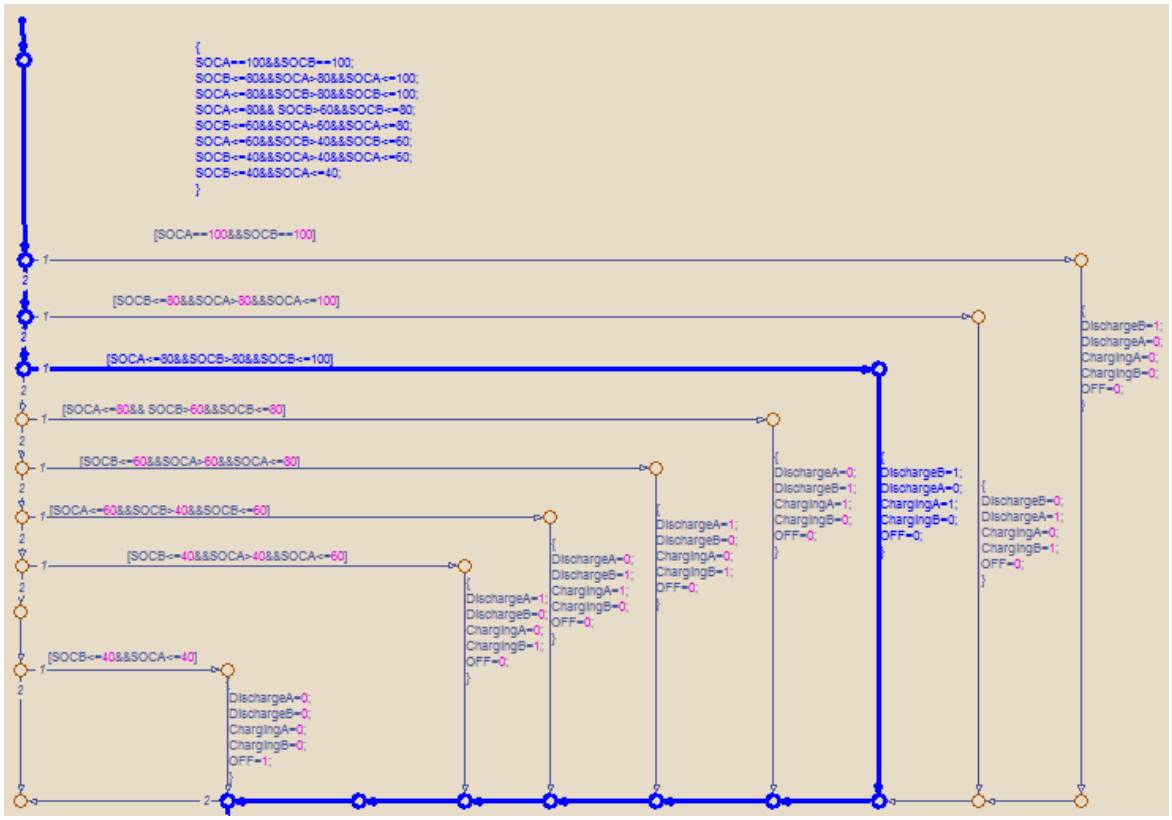

Figure 3.26: Charging/Discharging – SoC base controller (Stateflow)

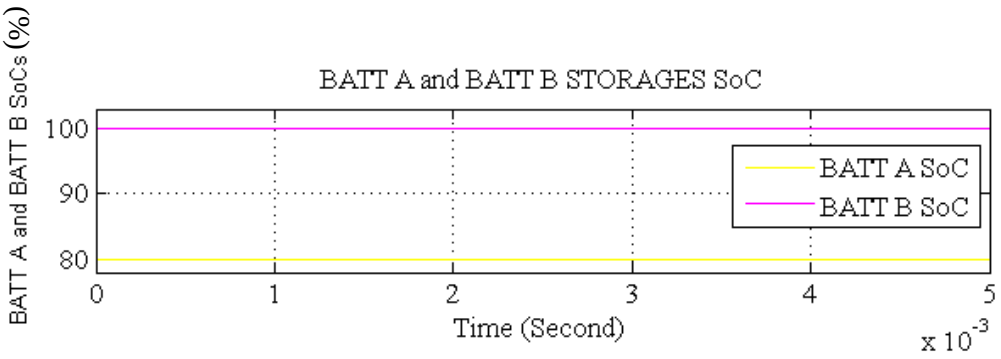

Figure 3.27: BATT A and BATT B STORAGES SoC

The BATT A and BATT B STORAGES current and voltage status are shown in Figures 3.28 and 3.29. When BATT A STORAGE starts charging, the charging current drops below the actual current reading as shown in Figure 3.28 and BATT A STORAGE voltage is not equal to fully charged voltage. As it is explained earlier, the very low charging current is known as pre-charge current [85]. This very low current is applied as part of the charging start sequence

for a system . The charging current will improve once the battery voltage increases. While, BATT B STORAGE did not discharge and the current remain at 0 Ampere due to no AC load is connected to perform discharging and BATT B STORAGE voltage remains fully charged as shown in Figures 3.28 and 3.29.

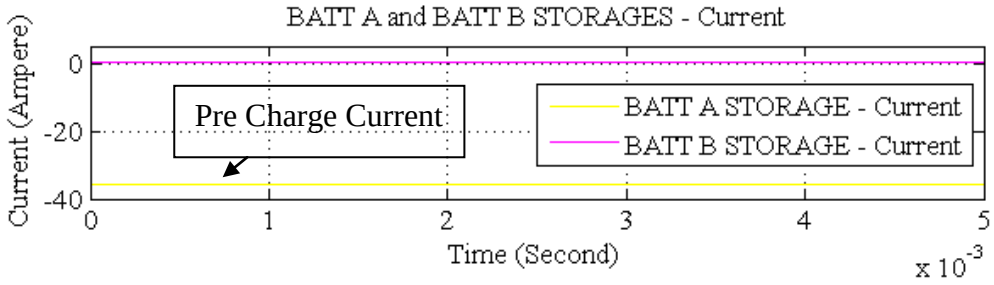

Figure 3.28: BATT A and BATT B STORAGES – Current

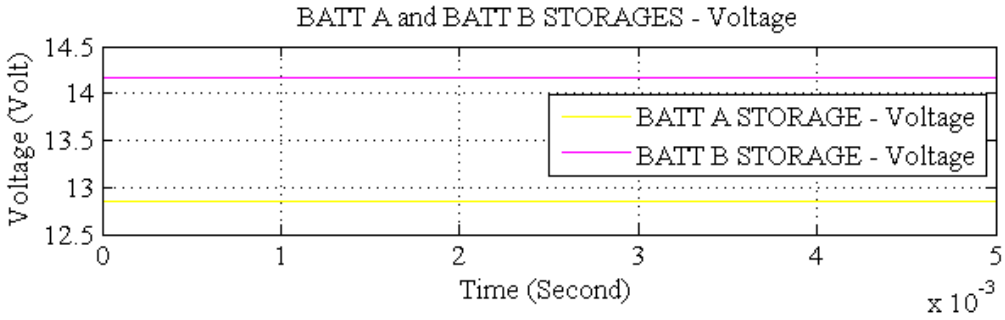

Figure 3.29: BATT A and BATT B STORAGES – Voltage

3.10.2 CONDITION C: PV = 12~15 Volt and WT = 7~12 Volt - DC HRES MODEL SIMULATION

The control signals for the regulated output voltages from solar-wind renewable energy sources are shown in Figures 3.30 (a) and (b). Referring to Figure 3.2, voltage based controller outputs a HIGH activated signals at S15V port when PV15 = 1 and at W12V port when WT12 = 1.

Referring to Figure 3.4, when S15V2 and W12V2 HIGH activated signals are received at voltage switching subsystem controller as shown in Figure 3.5, the connected relays are

switched ON. Hence, 12~15 Volt voltage is output at SA15V and WA12V ports and the results are presented in Figure 3.31.

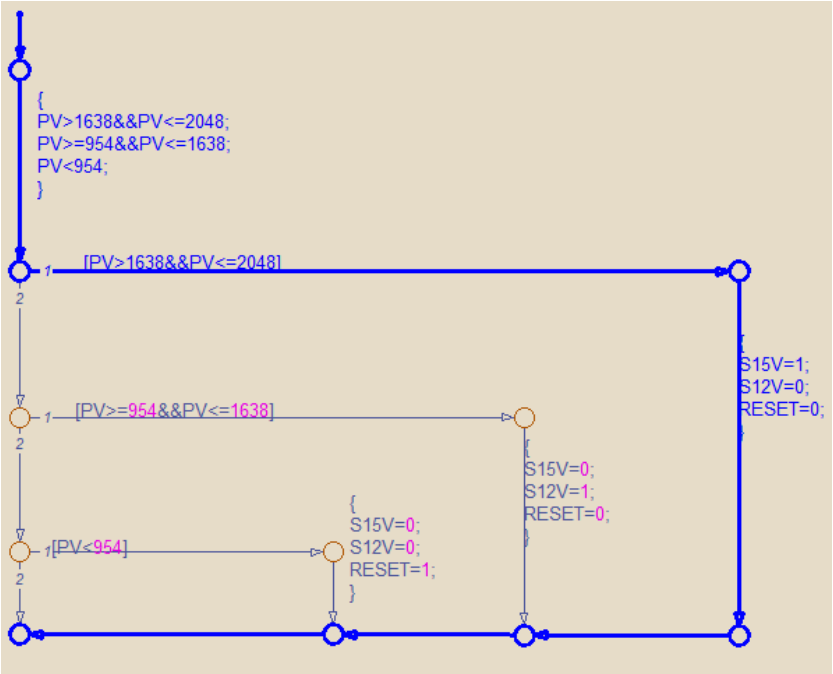

(a)

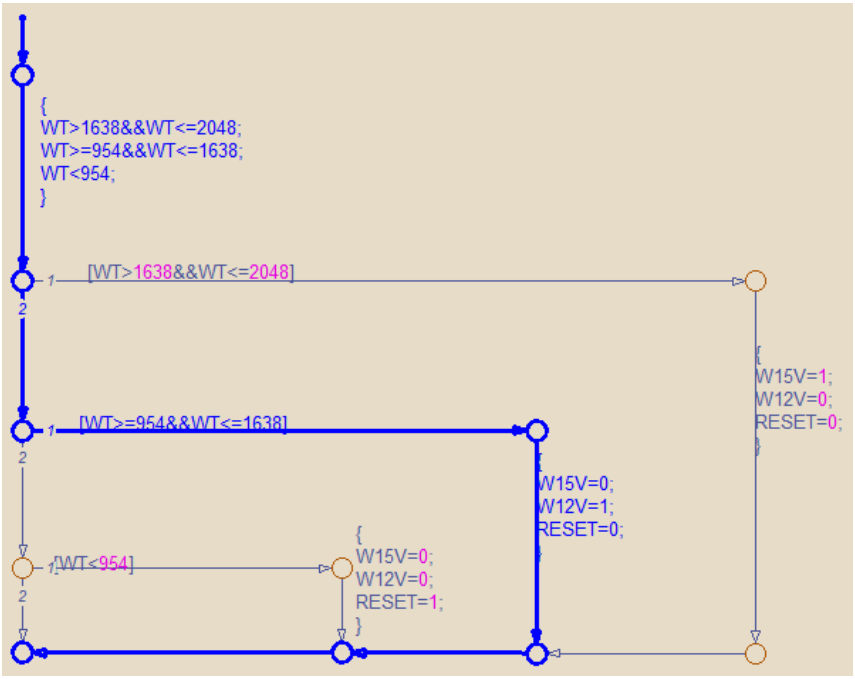

(b)

Figure 3.30: Solar-wind renewable energy source output voltages – voltage based controller (Stateflow)

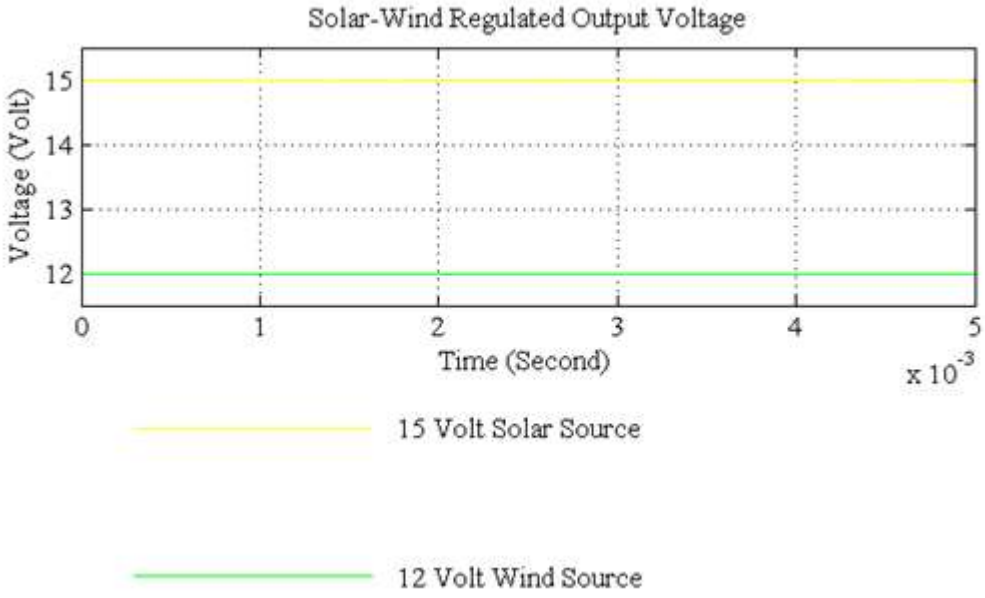

Figure 3.31: Solar-wind renewable energy sources regulated output voltages

The 12~15 Volt solar regulated output voltage at Ve_Inv ports is used as input to the DC to AC inverter as shown in Figure 3.14 and the output result is presented in Figure 3.17. The 7~12 Volt wind regulated output voltage at Ve_Bat ports is used to charge the BESS, if required. Before that, 7~12 Volt regulated output voltage from wind renewable energy source is input into DC to DC BC is shown in Figure 3.13 and the result is presented in Figure 3.32. Analysing the result presented in Figure 3.32, 7~12 Volt from wind renewable energy source is boosted to 15.5 Volt for BESS charging, if required.

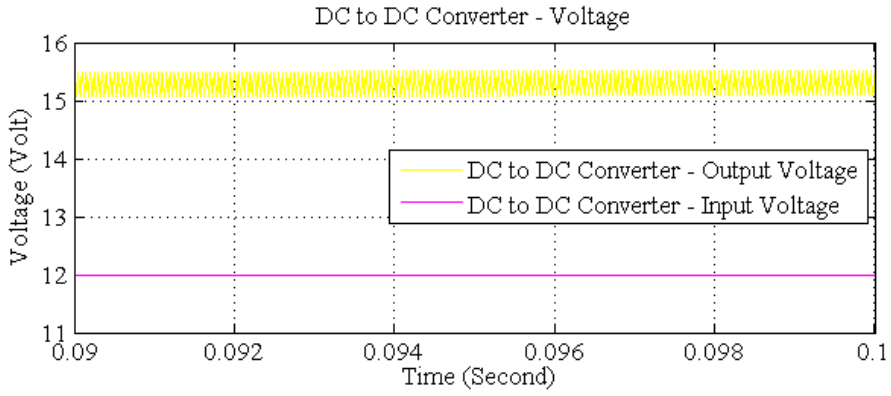

Figure 3.32: DC to DC Converter input-output voltage

3.11 SIMULATION RESULTS OVERVIEW

Section 3.10 presents the results to analyse and validate the design of real-time DC HRES hardware system modelled in MATLAB Simulink/Stateflow. The presented results in Figures 3.15 and 3.16 show the results for voltage based controller and voltage based self-intervention. The presented results show the voltage based controller have successfully manage to sense and measure the voltages at voltage based self-intervention. The presented results in Figure 3.17 shows the 12~15 Volt solar renewable energy source is stepped-up and converted into an AC voltage for the connected AC load. Looking at that, voltage switching subsystem controller have also successfully demonstrated to manage and coordinate the voltage combination presented in Tables 3.2 and 3.3 into the circuit breaker switching and group conditions. This also is verified by looking at the presented results for DC to AC Inverter or DC to DC BC for BESS charging process.

Section 3.10.1.1 discusses about the presented results for BATT A and BATT B STORAGES charging/discharging process. The BESS charging/discharging switching algorithm results are shown in Figures 3.18, 3.22 and 3.26 presents BATT A and BATT B STORAGES status. The BESS charging/discharging switching algorithm have successfully sensed and measured the SoC changes between BESS to perform the charging/discharging process among BATT A and BATT B STORAGES.

The DC to DC BC result is presented in Figure 3.32 shows the presented DC to DC BC model in Figure 3.10 have successfully performed the objective to step-up the 7~12 Volt regulated output voltages from solar-wind renewable energy sources for BATT A and BATT B STORAGES charging process.

3.12 SUMMARY

The modelled real-time DC HRES hardware system using MATLAB Simulink/Stateflow software was analysed and validated through to verify the described operation and functionality. The recorded results from the simulation of modelled real-time DC HRES hardware system is used as a fundamental study to develop, integrate, implement and construct the real-time DC HRES hardware system using PROTEUS software. Therefore, Chapter 4 presents the design and development of real-time DC HRES hardware system using

the PROTEUS software. Therefore, Chapter 4 presents the electronic circuits designs, developments and the circuit simulation results as well.

CHAPTER 4

DESIGN AND DEVELOPMENT METHODOLOGY FOR HARDWARE SYSTEM SIMULATION: PROTEUS SOFTWARE

In Chapter 4, PROTEUS software is used to design, develop and model the real-time DC HRES hardware system. The modelled system and methodology in MATLAB Simulink/Stateflow software is used as a fundamental work to design, develop and model the real-time DC HRES hardware system using the PROTEUS software. PROTEUS software is an electronic circuits, microcontroller/microprocessor circuit based design and simulation, Printed Circuit Board (PCB) which also known as ARES PCB layout, Virtual System Modelling (VSM) a popular embedded software for microcontroller and hardware design and development [102 - 104]. These characteristics of PROTEUS software serve the perfect platform for development, integration implementation and construction of the real-time DC HRES hardware system. Despite PROTEUS software advantage of its capability for electronic circuits design, development and modelling, it is not an easy task to design, develop and model the real-time DC HRES hardware system. Hardware system integration, implementation and construction in real-time requires a lot of studies such as circuits and component rating. For this reason, a component level mathematical calculation is necessary to design and develop the hardware circuitry. Then, the circuits are designed and modelled using the PROTEUS software before the development, integration, implementation and construction of real-time DC HRES hardware system. Before the real-time DC HRES hardware system implementation and construction, circuits performances and behaviours are simulated and analysed using the PROTEUS software. Hence, each subsystem designed is simulated in

PROTEUS software to understand the performances prior to the implementation and construction of real-time DC HRES hardware system. Also, the simulation results for the real-time DC HRES hardware system are captured and presented in this chapter. These results of the real-time DC HRES hardware system are important to be analysed before the real-time DC HRES hardware implementation and construction process, which is discussed in Chapter 6.

Other interesting features of PROTEUS software is that its capability to incorporate with embedded software. There are many kinds of embedded software available, PCWH CCS C Compiler is used to write the embedded software application for the microcontroller PIC16F877A and is incorporated with PROTEUS software to simulate the real-time DC HRES hardware system. Chapter 5 will further discuss the developed embedded software application for microcontroller PIC16F877A.

4.1 DC HRES SCHEMATIC SYSTEM DESIGN – DESCRIPTION

In order to design, develop, integrate, implement and construct the real-time DC HRES hardware system, electronic circuits modelling and simulation demonstration is an important aspect to consider before fully constructs the real-time DC HRES hardware system. Therefore, this chapter presents the hardware subsystem's circuits that are designed using PROTEUS software for the real-time DC HRES hardware system. Figure 4.1 show the real-time DC HRES hardware system circuitries, which composed the voltage based self-intervention (voltage divider), relay switching and control, microcontroller PIC16F877A, oscillator, and Master Clear Unit (MCLR). The BESS-GRID connection/LOAD relay switching is shown in Figure 4.2. The voltage based self-intervention subsystems are connected to the respective ADC channels, the regulated output voltages from solar-wind renewable energy sources are connected to the input relay switching and control, the microcontroller PIC16F877A acts as the Central Processing Unit (CPU) for real-time DC HRES hardware system, the oscillator unit provides clock signal to synchronise all the subsystems to work together and the MCLR unit is known as external reset which is used to reset the microcontroller PIC16F877A back to its start program. The BESS-GRID connection/LOAD relay switching subsystem is connected to the microcontroller PIC16F877A to perform the output function for the real-time DC HRES hardware system. Therefore, to further understand about all the subsystems of real-time DC

HRES hardware system, the following sections will elaborate further about the mathematical calculation and the technicality of each subsystem.

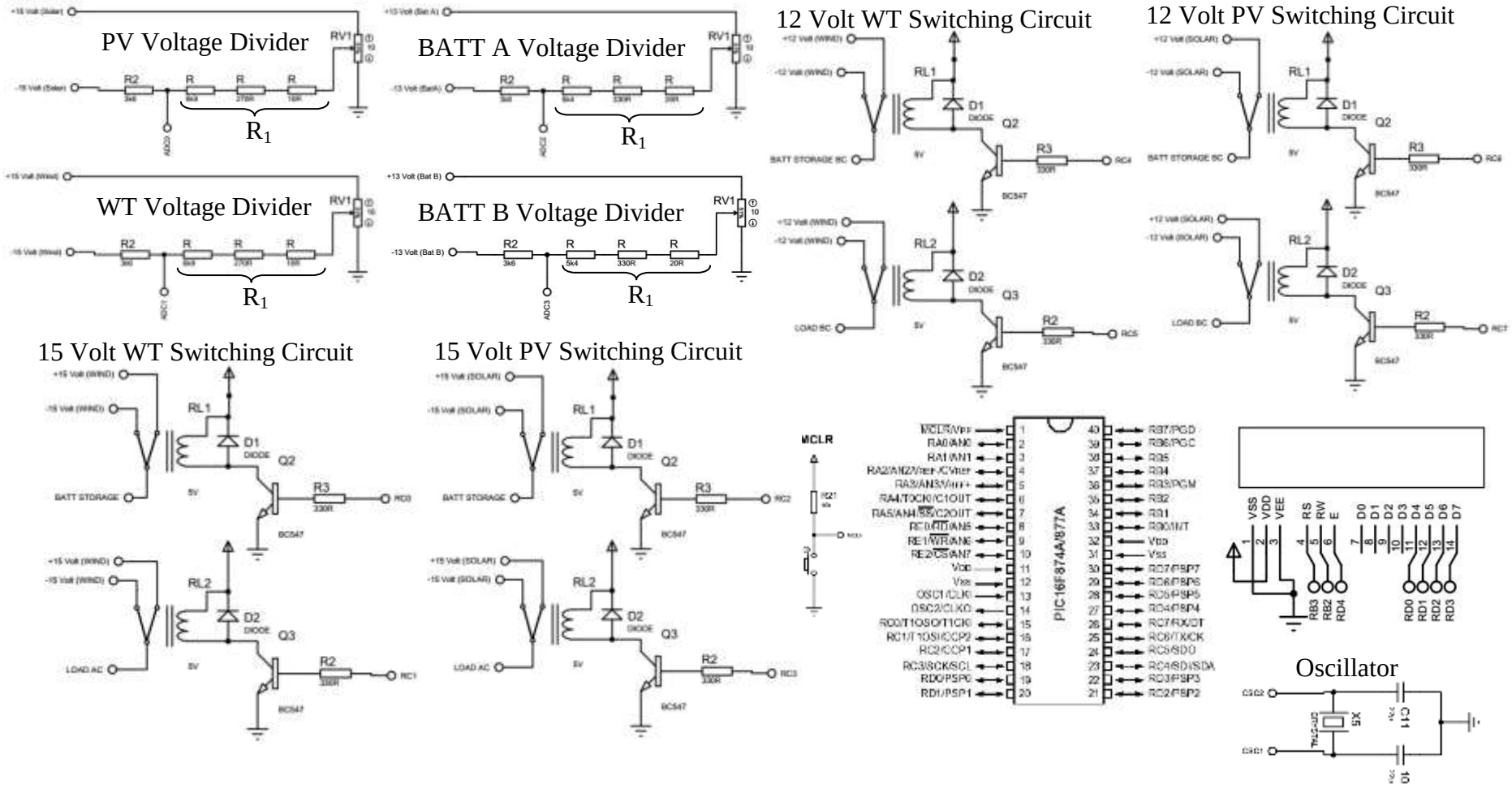

Figure 4.1: DC HRES schematic circuits design (voltage divider and relay switching and control module)

BATT A Charging Switching Circuit (15 Volt)

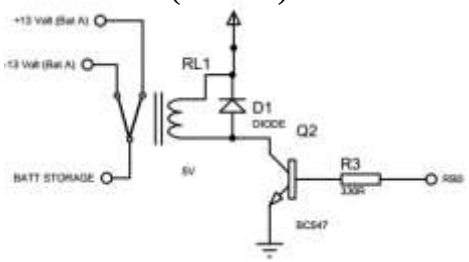

BATT A Discharging Switching Circuit (15 Volt)

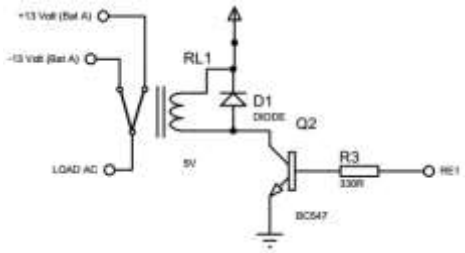

BATT A BC Charging Switching Circuit (12 Volt)

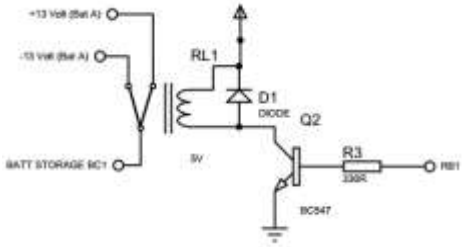

BATT B Charging Switching Circuit (15 Volt)

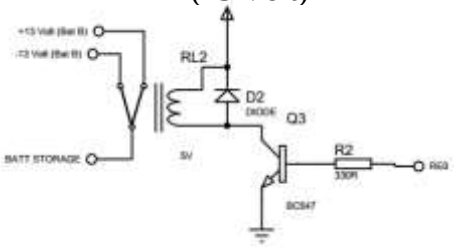

BATT B Discharging Switching Circuit (15 Volt)

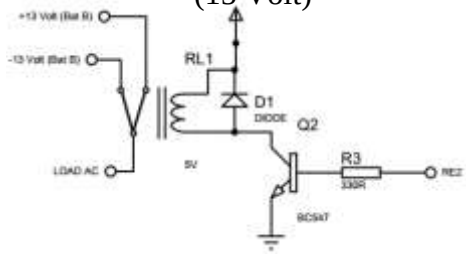

BATT B BC Charging Switching Circuit (12 Volt)

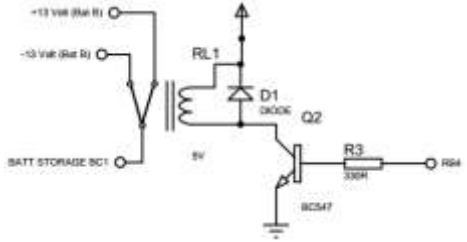

BATT A Discharging Switching Circuit (13 Volt)

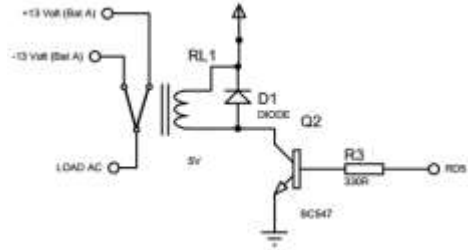

BATT B Discharging Switching Circuit (13 Volt)

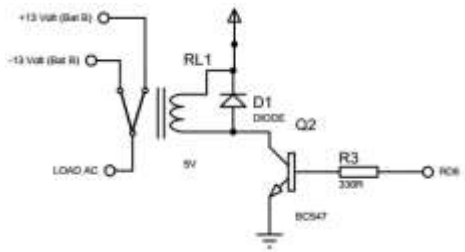

GRID Connection/LOAD Switching Circuit

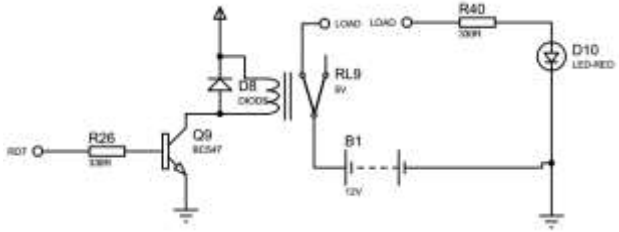

Figure 4.2: DC HRES schematic circuitry design (BESS-GRID connection/LOAD relay switching)

4.2 DESIGN AND SIMULATION OF VOLTAGE BASED SELF-INTERVENTION

This section discusses about the design, development and simulation of voltage based self-intervention using PROTEUS software. As mentioned in section 3.2.1 the concept of voltage divider is adapted to sense and measure the increment or decrement of the regulated output voltages from solar-wind renewable energy sources. Hence, mathematical calculation for each component in the design and development of voltage based self-intervention circuitry are presented in this section.

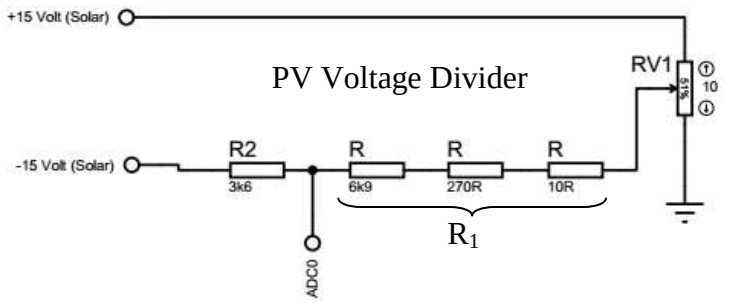

(a)

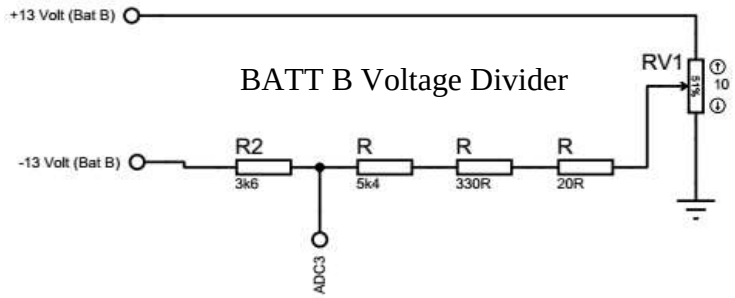

(b)

Figure 4.3: Configuration and setup of voltage based self-intervention

The configuration and setup for voltage based self-intervention for sensing and measuring the voltage increment or decrement is shown in Figure 4.3. The configuration and setup shown in Figure 4.2(a) is used to sense and measure the regulated output voltages from solar-wind renewable energy sources. A 15 Volt regulated output voltage is used as an input voltage to the voltage based self-intervention. The voltage based self-intervention is composed of 6.9 kΩ, 270 Ω, 10 Ω for resistor one (R_1) and 3.6 kΩ for resistor two (R_2) as shown in Figure 4.3.

The R_2 resistor is used as a reference voltage to output a 5 Volt voltage at the respective ADC channels (ADC0 and ADC1).

As mentioned, ADC only sense and measure a 5 Volt reference voltage for solar-wind renewable energy sources, therefore, the mathematical calculation for ADC sensing and measuring is presented in the following.

Let voltage source ($V_s = V_{solar\text{-}wind}$) = 15 Volt, R_1 = 6.9 kΩ and R_2 = 3.6 kΩ and ADC voltage (V_{adc}) is determined using Equation (4.1).

$$V_{adc} = \frac{R_2}{R_1 + R_2} \times V_s \tag{4.1}$$

$$= \frac{3.6\,k\Omega}{7.18\,k\Omega + 3.6\,k\Omega} \times 15\,Volt$$

$$= \frac{54000}{10780}$$

$$= 5 \text{ Volt}$$

Referring to the mathematical calculation, configuration and setup for voltage based self-intervention is shown in Figure 4.3 (a), the ADCs will output a maximum of 5 Volt.

The configuration and setup in Figure 4.3(b) is used for the BESS voltage sensing and measurement. The BESS 13 Volt reference voltage is used as an input voltage to the voltage based self-intervention setup. The voltage based self-intervention setup is composed of 5.4 kΩ, 330 Ω, 20 Ω for resistor one (R_1) and 3.6 kΩ for resistor two (R_2) as shown in Figure 4.3. The R_2 resistor is used as a reference voltage to output a 5 Volt voltage at the respective ADC channels (ADC2 and ADC3).

As mentioned, ADC only sense and measure a 5 Volt reference voltage for each BESS unit, therefore, the mathematical calculation for ADC sensing and measuring is presented in the following:

Let voltage source (V_{BESS}) = 13 Volt, R_1 = 5.75 kΩ and R_2 = 3.6 kΩ and the ADC voltage (V_{adc}) is determined using Equation (4.1).

$$V_{adc} = \frac{3.6\,k\Omega}{5.75\,k\Omega + 3.6\,k\Omega} \times 13\,Volt$$

$$= \frac{46800}{9350}$$

$$= 5\ Volt$$

The voltage based self-intervention individual connections to the respective ADC channels at microcontroller PIC16F877A is presented in Table 4.1. The mathematical calculation for the ADCs input voltage shows that each ADC only can sense and measure a maximum of 5 Volt regardless of any amount of input voltage at the voltage based self-intervention. For this reason, a voltage relationship between solar-wind renewable energy source and BESS input voltages and the ADC's input voltages are discussed in the following section.

Table 4.1: Voltage based self-intervention ADC connectivity to the microcontroller PIC16F877A

Voltage based Self-Intervention (Voltage Divider)	ADC at microcontroller PIC16F877A
PV Voltage Divider	ADC0 (Port RA0)
WT Voltage Divider	ADC1 (Port RA2)
BATT A Voltage Divider	ADC2 (Port RA3)
BATT B Voltage Divider	ADC3 (Port RA5)

4.2.1 INPUT VOLTAGE PROPORTION EQUIVALENCY

In order to understand solar-wind renewable energy sources and BESS output voltages proportion equivalency at ADC's inputs, a detail mathematical relationship is discussed between the microcontroller PIC16F877A ADC voltage ($V_{pic\text{-}ADC}$) and solar-wind renewable energy sources regulated output voltages ($V_{PV\text{-}WT}$) and BESS output voltages ($V_{BATT\ A\text{-}BATT\ B}$) in the following..

Referring to the voltage proportion equivalency mathematical calculation for the microcontroller PIC16F877A ADC, Figure 4.4 presents the voltage proportion equivalence between regulated output voltages from solar-wind renewable energy sources and microcontroller PIC16F877A ADC's input voltage.

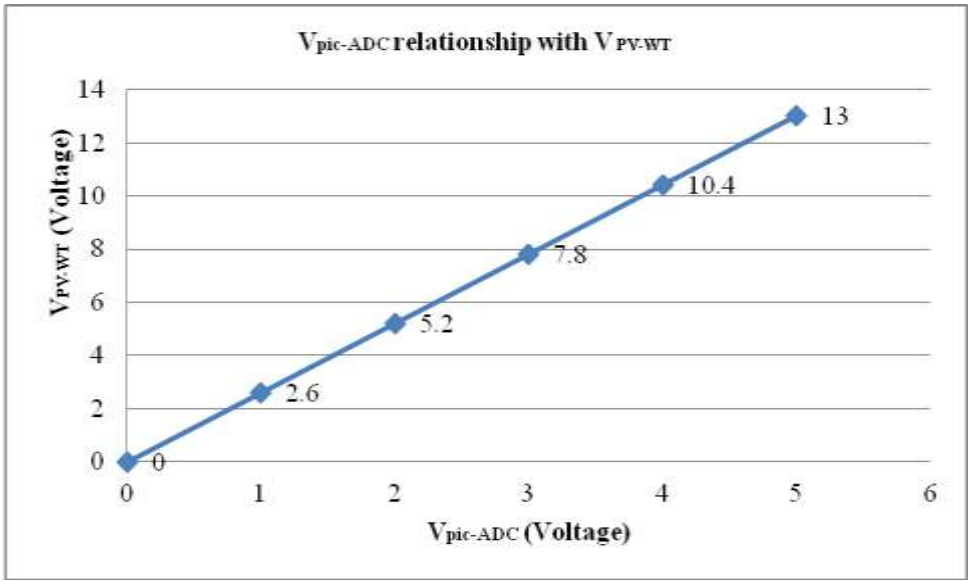

Figure 4.4: Voltage proportion equivalency between regulated output voltages from solar-wind renewable energy sources and microcontroller PIC16F877A ADC's input voltage

The microcontroller PIC16F877A have 10 bits resolution in an ADC, therefore each ADC is equal to $2^{10} = 1024$ bits (0 – 1023).

Hence, input voltage per bit for solar-wind renewable energy sources are calculated using Equation (4.2).

$$\text{Input Voltage/bit} = \frac{V_{\text{PV-WT}}}{1024\,\text{bits}} \tag{4.2}$$

$$= \frac{15\,\text{Volt}}{1024\,\text{bits}}$$

$$= 0.0146\,\text{Volt/bit}$$

Thus, each bit of voltage increment or decrement for regulated output voltages from solar-wind renewable energy sources are equivalent to 0.0146 Volt/bit. The 0.0146 Volt/bit is not the input voltage to the microcontroller PIC16F877A ADC for sensing and measuring the increment or decrement voltage at the input of the voltage based self-intervention subsystems. To calculate the input voltage at the microcontroller PIC16F877A ADC channels (ADC0 and ADC1), the total number of resolution bits is required for every 3 Volt of voltage increment or decrement for the regulated output voltages from solar-wind renewable energy sources.

Hence, the total number of resolution bits required for every 3 Volt of voltage increment or decrement for the regulated output voltages from solar-wind renewable energy sources is calculated using Equation (4.3).

$$\text{Total Number of resolution bits} = \frac{3\,\text{Volt}\,(V_{PV-WT})}{\text{Input Voltage/bit}} \tag{4.3}$$

$$= \frac{3\,\text{Volt}\,(V_{PV-WT})}{0.0146}$$

$$= 205\,\text{bits}$$

Thus, the 205 resolution bits represent the 3 Volt voltage increment or decrement for the regulated output voltage from solar-wind renewable energy sources. This 205 resolution bits is used to calculate the voltage per bit increment or decrement at the microcontroller PIC16F877A ADC channels.

Hence, per bit voltage increment or decrement at the microcontroller PIC16F877A ADC ($V_{pic-ADC}$) is calculated using Equation (4.4).

$$V_{pic-ADC} = \frac{1\,\text{Volt}_{pic}}{\text{Number of bits}} \tag{4.4}$$

$$= \frac{1\,\text{Volt}_{pic}}{205}$$

$$= 0.0049\,\text{Volt}$$

Thus, every 1-bit resolution voltage increment and decrement at microcontroller PIC16F877A ADC is equal to 0.0049 Volt. Therefore, each bit voltage increases or decreases by 0.0049 Volt at the microcontroller PIC16F877A ADC during voltage based self-intervention operation.

The mathematical calculation presents the input voltage proportion equivalency at the microcontroller PIC16F877A ADC for the regulated output voltages for solar-wind renewable energy sources. Therefore, in the following the voltage proportion equivalency at the microcontroller PIC16F877A for BESS output voltages is presented.

Referring to the voltage proportion equivalency mathematical calculation for BESS output voltages, Figure 4.5 presents the voltage proportion equivalence between BESS output voltages and microcontroller PIC16F877A ADC's input voltage.

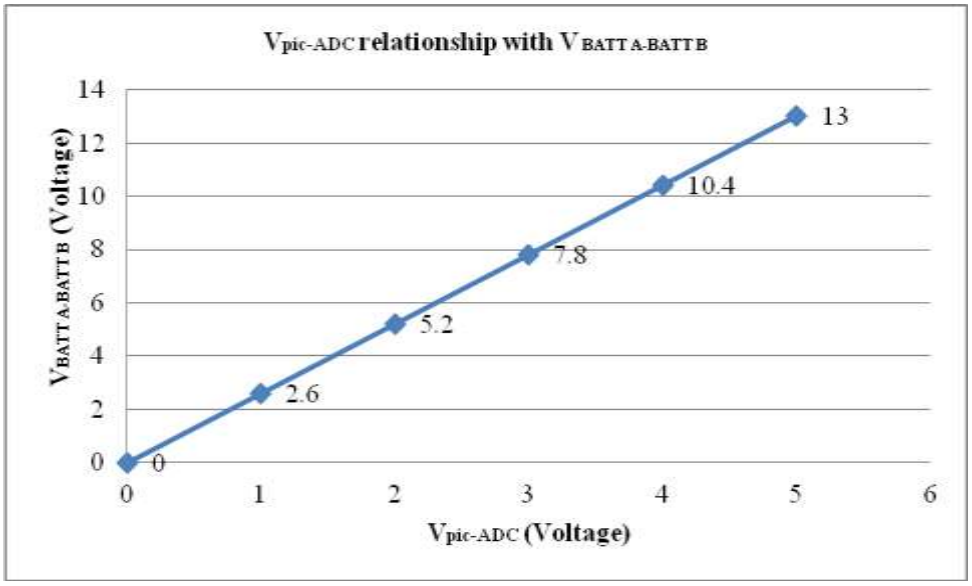

Figure 4.5: Voltage proportion equivalency between BESS output voltages and microcontroller PIC16F877A ADC's input voltage

Hence, input voltage per bit for BESS output voltages is calculated using Equation (4.5).

$$\text{Input Voltage/bit} = \frac{V_{BATT\,A\,-\,BATT\,B}}{1024\,\text{bits}} \tag{4.5}$$

$$= \frac{13\,\text{Volt}}{1024\,\text{bits}}$$

$$= 0.0127\,\text{Volt/bit}$$

Thus, each bit voltage increment or decrement for BESS output voltages is equivalent to 0.0127 Volt/bit. The 0.0127 Volt/bit is not the input voltage to the microcontroller PIC16F877A ADC for sensing and measuring but the increment or decrement voltage is at the input of the voltage based self-intervention subsystems. To calculate the input voltage at the microcontroller PIC16F877A ADC channels (ADC2 and ADC3), the total number of resolution bits is required for every 2.6 Volt of voltage increment or decrement for BESS output voltages.

Hence, the total number of resolution bits required for every 2.6 Volt of voltage increment or decrement for BESS output voltages is calculated using Equation (4.6).

$$\text{Total Number of resolution bits} = \frac{2.6\,\text{Volt}\,(V_{\text{BATT A}-\text{BATT B}})}{\text{Input Voltage/bit}} \tag{4.6}$$

$$= \frac{2.6\,\text{Volt}\,(V_{\text{BATT A}-\text{BATT B}})}{0.0127}$$

$$= 205\,\text{bits}$$

Thus, the 205 resolution bits represent the 2.6 Volt voltage increment or decrement for BESS output voltages. This 205 resolution bits is used to calculate the voltage per bit increment or decrement at the microcontroller PIC16F877A ADC channels.

Hence, per bit voltage increment or decrement at the microcontroller PIC16F877A ADC ($V_{\text{pic-ADC}}$) is calculated using Equation (4.7).

$$V_{\text{pic}-\text{ADC}} = \frac{1\,\text{Volt}_{\text{pic}}}{\text{Total Number of resolution bits}} \tag{4.7}$$

$$= \frac{1\,\text{Volt}_{\text{pic}}}{205}$$

$$= 0.0049\,\text{Volt}$$

Thus, every 1-bit resolution voltage increment or decrement at microcontroller PIC16F877A ADC is every equal to 0.0049 Volt. Therefore, each bit voltage increase or decrease is by 0.0049 Volt at microcontroller PIC16F877A ADC during voltage based self-intervention sensing and measurement operation.

The mathematical calculation presents the input voltage proportion equivalency at the microcontroller PIC16F877A for BESS output voltages.

It is important to understand the voltage proportion equivalency at microcontroller PIC16F877A for the regulated output voltages from solar-wind renewable energy sources and BESS output voltages because the voltage proportion equivalency helps the microcontroller PIC16F877A to understand the instance or immediate status of the regulated output voltages fro solar-wind renewable energy sources and output voltages from BESS. Also, the voltage proportion equivalency mathematical calculation is used as a fundamental study to develop the continuous dynamic decision-making algorithm using embedded software application for microcontroller PIC16F877A. With that, the development of the continuous dynamic decision-making algorithm is explained in Chapter 5. For this reason, the next section further elaborates on the design, development and simulation of relay switching and control modules as shown in Figure 4.1.

4.3 DESIGN AND SIMULATION RELAY SWITCHING AND CONTROL MODULE

The relay switching and control modules are used to perform the self-intervention between the regulated output voltages from solar-wind renewable energy sources, which is the primary power source supply to the connected AC load. Referring to Figure 4.1, relay switching and control modules controls two different sources regulated output voltages from solar-wind renewable energy sources. There is a total of seventeen relay switching and control modules,

eight of these modules are connected to receive the regulated output voltages from solar-wind renewable energy sources, the other eight modules are connected to BESS to perform the charging/discharging process and the one only is connected to the GRID connection/LOAD switching circuit. All of the relay switching and control modules are controlled by a HIGH activated signal from microcontroller PIC16F877A. Prior to the understanding the operation and functionality of the relay switching and control module in section 4.3.3, it is important to understand the part 1 of technical explanation discussed in section 4.3.2.

4.3.1 RELAY SWITCHING AND CONTROL TECHNICAL EXPLANATION

A single relay switching and control module is consists of a 5 Volt relay, a diode, BC547 NPN transistor and a 330 Ω resistor as shown in Figure 4.6. The relay switching and control module switching ON is controlled by a HIGH activated signal from microcontroller PIC16F877A. The HIGH activated signal from microcontroller PIC16F877A is usually equivalent to 5 Volt.

The schematic design of relay switching and control modules is shown in Figure 4.6. Initially, all the relay switching and control modules are connected to NO port, which is in OFF state.

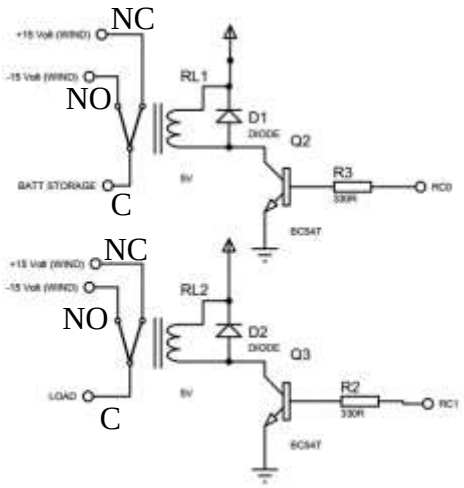

Figure 4.6: Voltage relay switching and control module

The relay switching and control module is switched ON only when the resistor's input port receives a HIGH activated signal from microcontroller PIC16F877A. Therefore, the HIGH activated signal is send to the NPN transistor's base for switching control. The NPN transistor is used to amplify the input current from microcontroller PIC16F877A. The current is

amplified so that the relay coil is energised and the relay contact is switched to NC, which is the ON state.

Referring to the SONGLE 5 Volt relay, the relay coil requires 0.35 Watt or 0.45 Watt power and 0.18~0.23 Ampere (Amps) current to energise the coil for the relay to switch. Therefore, using the relay coil power and current information, the required current to energise the relay coil is calculated mathematically. Equation (4.8) is used to obtain the load resistor, (R_L) the value of the relay coil, which is also known as load resistor.

$$P = \frac{I}{R_L}$$

$$R_L = \frac{I}{P} \tag{4.8}$$

$$R_L = \frac{10\,A}{0.35\,W \text{ or } 0.45\,W}$$

$$= 29\,\Omega \text{ or } 22\,\Omega$$

The R_L refers to the relay load, now the load current, (I_L) is calculated using Equation (4.9).

$$I_L = \frac{V_S}{R_L} \tag{4.9}$$

$$I_L = \frac{5\,V}{278\,\Omega \text{ or } 222\,\Omega}$$

$$= 18\,mA \text{ or } 23\,mA$$

To energise the relay coil the transistor collector current, (I_C) must be higher than the load current. Thus, the minimum current gain, $(h_{FE})$of NPN transistor must be five times larger than the ratio of the load current so that maximum load current is supplied to the voltage relay switching and control circuit. Equation (4.10) is used to obtain the minimum current gain of the BC547 NPN transistor.

$$h_{FE} > 5 \text{ x } \frac{\text{Load Current, } I_L}{\text{Maximum Input Current}} \tag{4.10}$$

$$h_{FE}(\text{min}) > 5 \text{ x} \frac{18\text{m A or } 23\,\text{mA}}{0.5\,\text{A}}$$

$$h_{FE}(\text{min}) > 0.23 \text{ or } 0.18$$

Referring to NPN BC547 transistor, BC547 NPN transistor has 100mA of maximum collector current and 110 of h_{FE} (min). The BC547 NPN transistor is used to energise the relay coil. A base resistor, (R_B) is connected in series with the BC547 NPN transistor's base in order to limit the current flowing into the transistor. This is important to avoid any damage on the transistor. Therefore, in the following the appropriate resistor value is calculated using Equation (4.11).

$$R_B = \frac{V_C \times h_{FE}}{5 \times I_L} \tag{4.11}$$

$$= \frac{5\,\text{Volt}\,(0.23 \text{ or } 0.18)}{5\,(0.023\,\text{A or } 0.018\,\text{A})}$$

$$= 10\ \Omega$$

Therefore, the minimum value for the base resistor is equal to 10 Ω.

In conclusion, mathematical calculation for relay switching and control module is used to design the schematic circuits in PROTEUS software in Chapter 6 and is used as fundamental information to suitably construct the real-time DC HRES hardware system.

4.3.2 OPERATION AND FUNCTIONALITY OF RELAY SWITCHING AND CONTROL

This section further explains about the operation and functionality of relay switching and control modules corresponding to voltage based self-intervention and microcontroller PIC16F877A. As mentioned in section 4.3, there are eight relay switching and control

modules connected to regulated output voltages from solar-wind renewable energy sources and the other eight relay switching and control modules are connected to perform the BESS charging/discharging process. Although all of the relay switching and control modules are connected to microcontroller PIC16F877A input or output ports but each still operates individually based on the received HIGH activated signal from the continuous dynamic decision-making algorithm. Each of the relay switching and control modules is connected as an output port at the microcontroller PIC16F877A. The connectivity of each relay switching and control module corresponding to microcontroller PIC16F877A is indicated in Table 4.2.

Table 4.2: Relay switching and control module connectivity to microcontroller PIC16F877A ports and output

Tasks.	Subsystem Unit	Port at Microcontroller PIC16F877A	Connectivity (Output)
1.	15 Volt WT Switching Circuit	RC0	BATT STORAGE
		RC1	LOAD AC
	15 Volt PV Switching Circuit	RC2	BATT STORAGE
		RC3	LOAD AC
2.	12 Volt WT Switching Circuit	RC4	BATT STORAGE BC
		RC5	LOAD BC
	12 Volt PV Switching Circuit	RC6	BATT STORAGE BC
		RC7	LOAD BC
3.	BATT A Charging Switching Circuit (15 Volt)	RB0	BATT STORAGE
	BATT A Discharging Switching Circuit (15 Volt)	RE1	LOAD AC
	BATT B Charging Switching Circuit (15 Volt)	RE0	BATT STORAGE

	BATT B Discharging Switching Circuit (15 Volt)	RE2	LOAD AC
4.	BATT A BC Charging Switching Circuit (12 Volt)	RB1	BATT STORAGE BC1
	BATT A Discharging Switching Circuit (13 Volt)	RD5	LOAD AC
	BATT B BC Charging Switching Circuit (12 Volt)	RB4	BATT STORAGE BC1
	BATT B Discharging Switching Circuit (13 Volt)	RD6	LOAD AC
5.	MCLR	MCLR	RESET
6.	Oscillator	OSC1	OSC1
		OSC2	OSC2
7.	GRID Connection / LOAD Switching Circuit	RD7	GRID / LOAD

The operation and functionality of each subsystem are explained accordingly based on the tasks in Table 4.2. Task 1 explains the condition when the regulated output voltages for solar-wind renewable energy sources are between 12~15 Volt. There are four relay switching and control modules, which are individually connected at RC0, RC1, RC2 and RC3 ports at microcontroller PIC16F877A. The RC0 and RC2 ports are connected to control the relay switching and control modules that connect to the BESS (BATT STORAGES). While, RC1 and RC3 ports are connected to control the relay switching and control modules that connects to DC to AC Inverter (LOAD AC).

Task 2 explains the condition when the regulated output voltages from solar-wind renewable energy sources are between 7~12 Volt. There are four relay switching and control modules, which are individually connected at RC4, RC5, RC6 and RC7 ports at microcontroller PIC16F877A. The RC3 and RC6 ports are connected to control the relay switching and control modules that connects the DC to DC BC to step-up the 7~12 Volt before supplying to BESS (BATT STORAGE BC) for charging process. While, the RC5 and RC7 ports are connected to control the relay switching and control modules that connects the DC to DC BC (LOAD BC) to step-up the 7~12 Volt from the BESS before supplying the stepped-up voltage to DC to AC Inverter (LOAD AC).

Task 3 explains the condition for BESS charging or discharging when the regulated output voltages from solar-wind renewable energy sources are between 12~15 Volt. There are four relay switching and control modules, which are individually connected at RB0, RE1, RE2 and RE3 ports at microcontroller PIC16F877A. The RB0 and RE2 ports are connected to control the relay switching and control modules that connect the BESS (BATT STORAGE) for charging process. While, RE1 and RE3 ports are connected to control relay switching and control modules that connects to DC to AC Inverter (LOAD AC).

Task 4 explains the condition for BESS charging or discharging when the regulated output voltages from solar-wind renewable energy sources are between 7~12 Volt. There are four relay switching and control modules, which are individually connected at RB1, RD6, RB4 and RD5 ports at microcontroller PIC16F877A. The RB1 and RB4 ports are connected to control the relay switching and control modules that connect the DC to DC BC (BATT STORAGE BC) for BESS charging process. While, RD6 and RD5 ports are connected to control relay switching and control modules that connects to DC to DC BC (LOAD BC) for voltage step-up before supplying the stepped-up voltage to DC to AC Inverter (LOAD AC).

Task 5 is the MCLR, which connects the MCLR port at the microcontroller PIC16F877A. The MCLR is an important unit to perform the system reset function.

Task 6 is the oscillator, which connects the OSC1 and OSC2 ports at the microcontroller PIC16F877A. The oscillator is important to provide the timing to allow all the subsystems to operate synchronizing-ly during the overall system operation.

Task 7 is the last task which is the GRID connection/LOAD switching circuit. This task is activated when regulated output voltages from solar-wind renewable energy sources and BESS output voltages are not available. The GRID connection/LOAD switching circuit is connected at RD7 port at microcontroller PIC16F877A.

In conclusion, the operation and functionality of relay switching and control modules are equally important to supervise, coordinate, manage and control different tasks of the real-time DC HRES hardware system. Therefore, it is fundamentally important to understand the operation and functionality of each relay switching and control module before integrating, implementing and constructing the real-time DC HRES hardware system.

4.4 DESIGN AND SIMULATION DC TO DC BOOST CONVERTER

The DC to DC BC schematic diagram is shown in Figure 4.7. The DC to DC BC is used to step-up the 7~12 Volt regulated output voltages from solar-wind renewable energy sources and BESS output voltages.

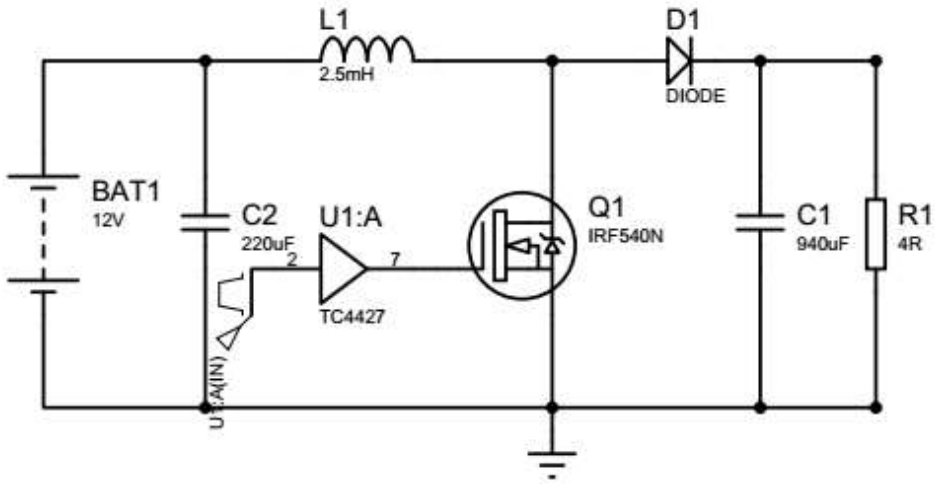

Figure 4.7: DC to DC BC schematic diagram

The voltage is stepped-up when available regulated output voltage is between 7~12 Volt. The DC to DC BC shown in Figure 4.7 is designed based on the following characteristics:

DC to DC BC characteristics:

Minimum Voltage input, (V_{inmin}) = 7 Volt

Maximum Voltage input, (V_{inmax}) = 12 Volt

Inductor = $2.5\,\text{mH}$

Diode Forward Voltage, (V_{df}) = 0.8 Volt

Capacitor = $220\,\text{uF}$

Period (sec) = $50\,\text{uS}$

Duty Cycle, D = 27%

Switching Period, S = T_s

Frequency, $(\text{f}) = \frac{1}{\text{T}}$

$$= \frac{1}{50\,\text{uS}}$$

$$= 20\,\text{kHz}$$

$$V_{outmax} = \frac{V_{inmax}}{1 - D}$$

$$= \frac{12}{1 - 27\%}$$

$$= \frac{12}{0.73} = 16.44 \text{ Volt}$$

$$= 16.44 - V_{df} = 15.64 \text{ Volt}$$

4.5 DESIGN AND SIMULATION DC TO AC INVERTER

The term inverter explains the about the low voltage DC conversion into high voltage AC voltage. The DC to AC inverter schematic circuit diagram using timer IC 555 is shown in Figure 4.8. The IC 555 timer is wired to operate as an astable multivibrator mode. This is one of the cheapest methods to develop an oscillator circuit to provide continuous pulses. The oscillation circuit frequency is controlled using the Resistor 1 (R_1), Resistor 2 (R_2) and Capacitor 1 (C_1). The diode IN4007 is used to obtain 50% duty cycle for the pulses from IC 555 and this reduces the inverter design complexity. The timer IC 555 output pulse is fed into the 2N2222 transistor's base. The 2N2222 transistor operates as a switch to allow the 12 Volt DC through into the transformer. Therefore, 12 Volt DC step-up transformer is integrated to produce 220 Volt AC at 50 Hz.

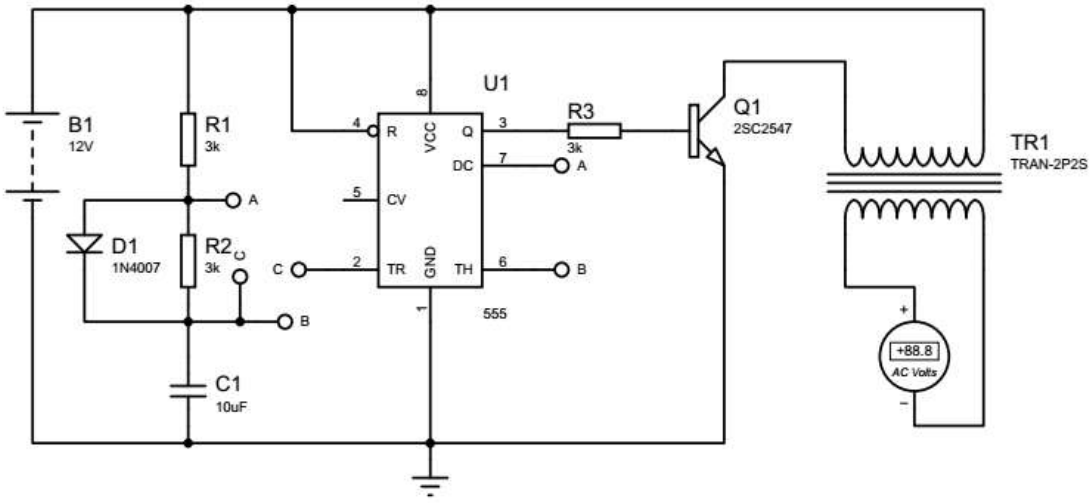

Figure 4.8: DC to AC inverter schematic diagram

After completing the design of each subsystem for real-time DC HDES hardware system using PROTEUS software, all the subsystems are connected to analyse and validate the designed system based on the developed methodology using Simulink/Stateflow MATLAB software. However, to demonstrate the system management, operation and functionality embedded software application is used to develop continuous dynamic decision-making algorithm that is supposed to be incorporated into the microcontroller PIC16F877A. Therefore, prior to

simulate the real-time DC HRES hardware system the embedded software application was development and is explained in Chapter 5. The PCWH CCS C Compiler embedded software application is used to develop the continuous dynamic decision-making algorithm to integrate and coordinate all the subsystems connected to microcontroller PIC16F877A. The continuous dynamic decision-making algorithm is developed to demonstrate all the mentioned conditions in Chapter 3 and operating tasks in Chapter 4. Therefore, continuous dynamic decision-making algorithm the further explanation is provided in Chapter 5.

However, the following section presents and discusses about the simulation results for the modelled electronic circuits for real-time DC HRES hardware system using PROTEUS software. Hence, selected conditions have been simulated and the captured results are further explained in terms of the individual modelled circuit operations and as well as results for the overall hardware system.

4.6 REAL-TIME DC HRES HARDWARE SYSTEM SIMULATION RESULTS – PROTEUS SOFTWARE

This section presents the design and simulation results for real-time DC HRES hardware system as shown in Figures 4.1 and 4.2 using PROTEUS software. To simulate the designed real-time DC HRES hardware system as shown in Figures 4.1 and 4.2 in real-time, the continuous dynamic decision-making algorithm is incorporated into microcontroller PIC16F877A. Hence, while designing the real-time DC HRES hardware system's electronic circuits, continuous dynamic decision-making algorithm were also developed simultaneously. However, this chapter will only present the real-time DC HRES hardware system electronic circuits simulation results. The electronic circuits simulation results are used to benchmark the developed real-time DC HRES hardware system which is discussed in Chapter 6. Also, while executing the electronic circuits simulation, the continuous dynamic decision-making algorithm is also improved so that the real-time DC HRES hardware system operates smoothly to perform supervision, coordination, management, controlling and optimise the sources as a complete system.

4.6.1 CONDITION A: PV = 12~15 Volt and WT = 12~15 Volt - DC HRES MODEL SIMULATION

The regulated output voltages from solar-wind renewable energy sources are shown in Figure 4.9. As shown in Figure 4.1, the PV and WT voltage dividers which are also known as voltage based self-intervention is used to sense and measure the regulated output voltages from solar-wind renewable energy sources. The regulated output voltages are sensed and measured to supervise and coordinate the power source supply to the connected DC to AC Inverter (LOAD AC) for the connected AC load or BESS charging process, if required. Also, the regulated output voltages are sensed and measured at the respective ADC0 and ADC1 channels at microcontroller PIC16F877A using the voltage proportion equivalency shown in Figure 4.4. Therefore, when the regulated output voltages at the PV and WT voltage based self-intervention is equal to 15 Volt then a 5 Volt is sensed and measured at ADC0 and ADC1 ports as shown in Figure 4.10.

Referring to Figure 4.1 and Table 4.2, Figure 4.9 shows RC1 and RC2 ports at microcontroller PIC16F877A is HIGH activated. When the 15 Volt PV (RC2) and 15 Volt WT (RC1) switching circuits receive a HIGH activated signal from microcontroller PIC16F877A, the connected relay coil is energised to switch from NC to NO. Therefore, a 15 Volt regulated output voltage from wind renewable energy source is connected to DC to AC Inverter (LOAD AC) as power source supply and a 15 Volt regulated output voltage from solar renewable energy source is connected to perform BESS (BATT STORAGE) charging process, if required. The HIGH activated signals at RC1 and RC2 ports are captured using the logic analyser is shown in Figure 4.11.

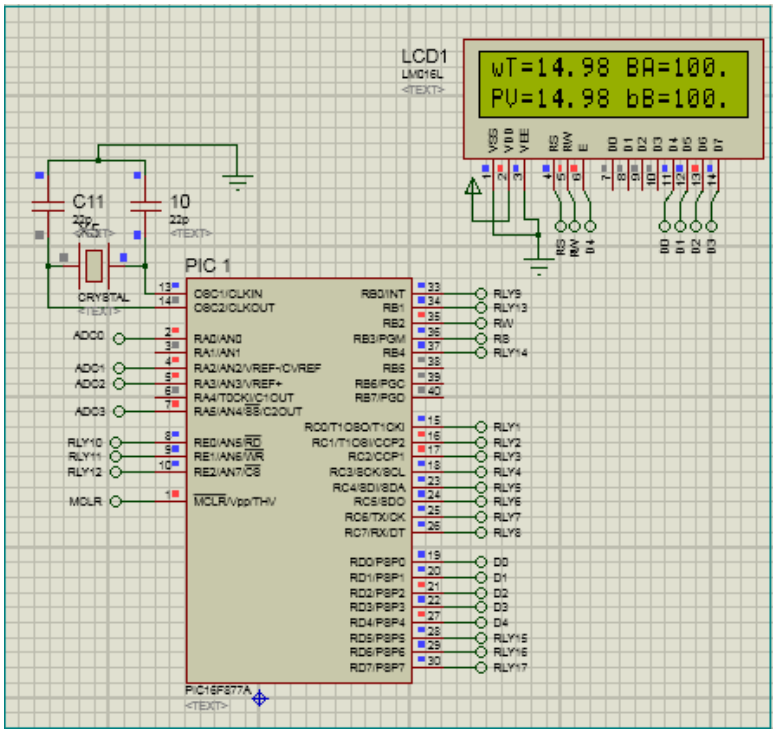

Figure 4.9: Microcontroller PIC16F877A – PORTS RC1 (RLY2) – RC2 (RLY3)

The Liquid Crystal Display (LCD) shown in Figure 4.9 indicates the connectivity of regulated output voltages from solar-wind renewable energy sources. The wT indicates the regulated output voltage from wind renewable energy source is connected to DC to AC Inverter (LOAD AC) as primary power source supply. Whilst, PV indicates the regulated output voltage from solar renewable energy source is connected to perform BESS (BATT STORAGE) charging process, if required.

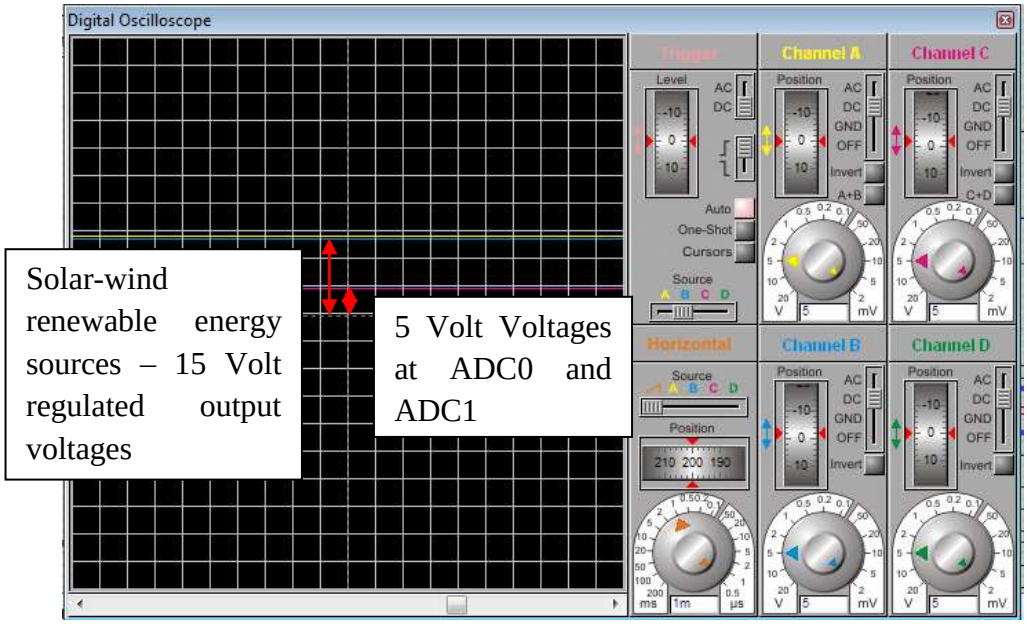

Figure 4.10: Solar-wind renewable energy sources regulated output voltages

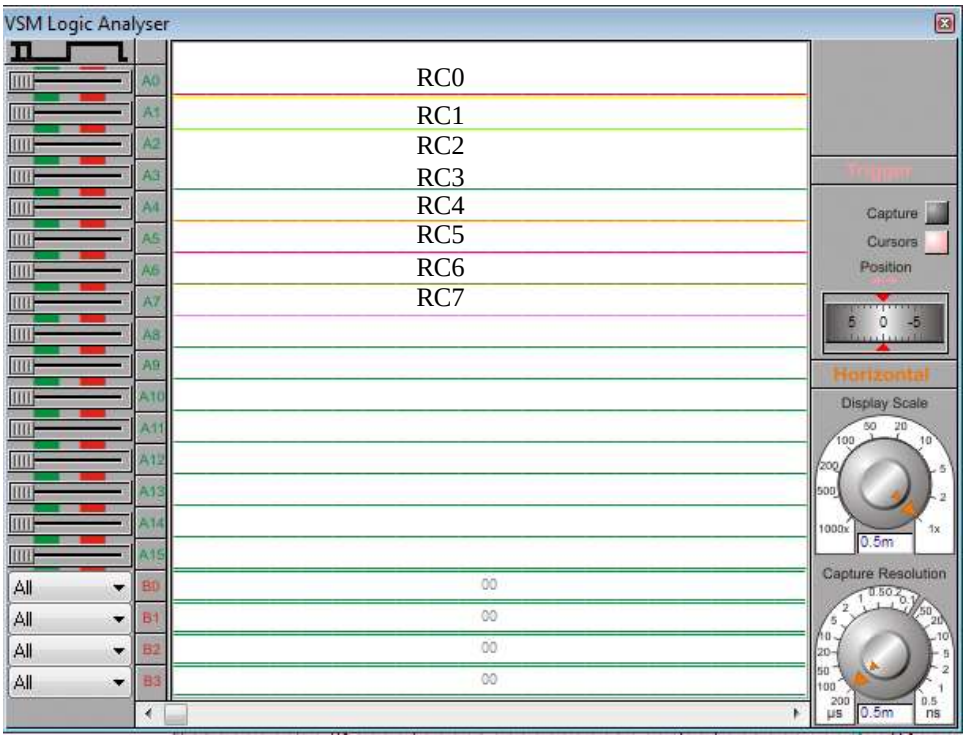

Figure 4.11: Logic analyser – HIGH activated signals at PORTS RC1 – RC2

The relay switching and control modules shown in Figure 4.12 is presenting the 15 Volt PV and WT switching circuits used to manage the voltage power source connectivity to the respective connected DC to AC Inverter (LOAD AC) for the connected AC load and performing BESS charging process, if required. Looking at 15 Volt WT switching circuit in Figures 4.1 and 4.12, the RLY2 port receives a HIGH activated signal from RC1 port at microcontroller PIC16F877A. Hence, the current from NPN transistor's base will energise the relay coil and switch the relay from NC to NO. Therefore, the 15 Volt regulated output voltage from wind renewable energy source is connected to DC to AC Inverter (LOAD AC) for the connected AC load. Whilst, referring to Figures 4.1 and 4.12 the RLY 3 port at 15 Volt PV switching circuit receives a HIGH activated signal from RC2 port of microcontroller PIC16F877A. Hence, the current from NPN transistor's base will energise the relay coil and switch the relay from NC to NO. Therefore, the 15 Volt regulated output voltage from solar renewable energy source is connected to perform BESS (BATT STORAGE) charging process, if required.

Referring to the 15 Volt WT switching circuit shown in Figure 4.12, the regulated output voltage from wind renewable energy source is connected to DC to AC Inverter (LOAD AC) for the connected AC load. Hence, the load port (common) at the relay is connected to the load port at DC to AC Inverter as shown in Figure 4.13. This connection completes the 15 Volt voltage step-up and conversion to 240 VAC for the connected AC load.

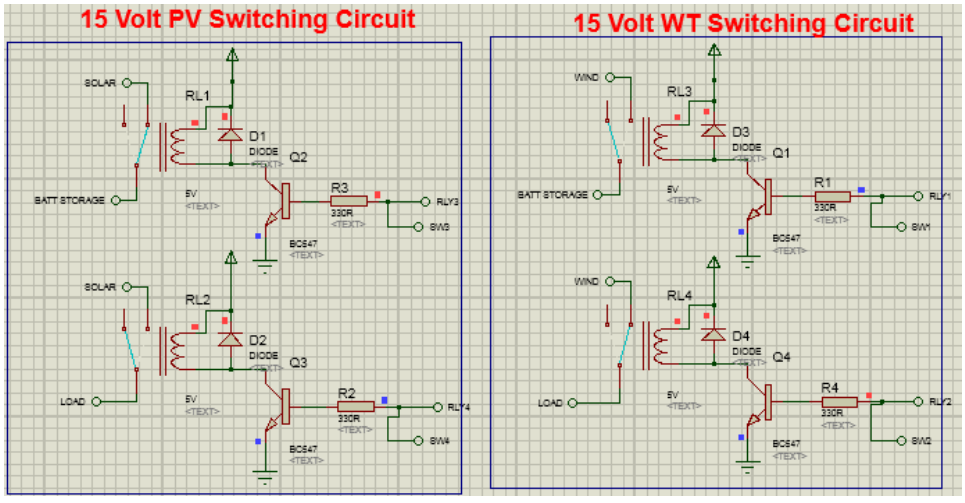

Figure 4.12: Relay switching and control module – PORTS RC1 (RLY2) – RC2 (RLY3)

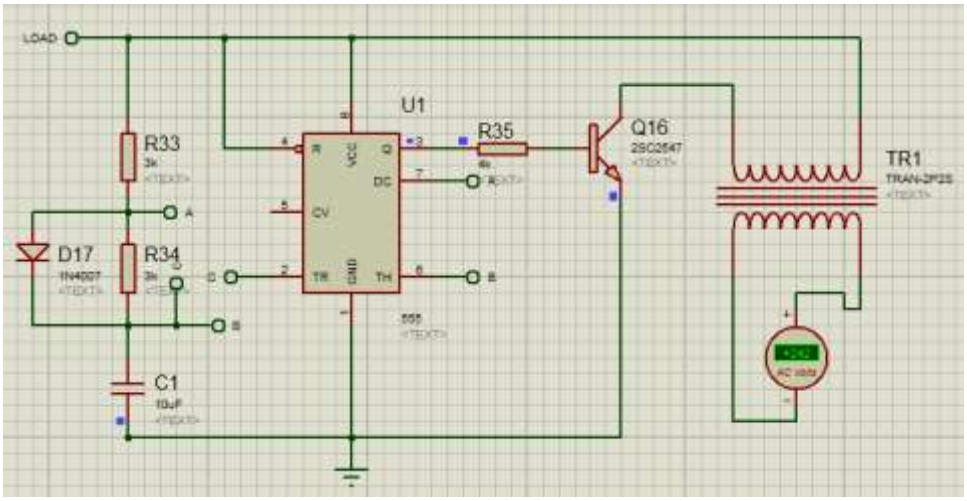

Figure 4.13: 15 VDC – 240 VAC – Inverter output

As shown in Figure 4.1, BATT A and BATT B voltage dividers which are also known as voltage based self-intervention is used to sense and measure the BESS output voltages. The output voltages are sensed and measured to continuously monitor the BESS SoC and voltage status. The BESS SoC and voltage status is sensed and measured at the respective ADC2 and ADC3 channels at microcontroller PIC16F877A using the voltage proportion equivalency shown in Figure 4.5.

This section discusses about the BESS SoC and voltage status. Section (a) presents the results for BATT A STORAGE and BATT B STORAGE SoCs = 100%. Section (b) presents the results for BATT A STORAGE SoC = 100% and BATT B STORAGE SoC = 80%. Section (c) presents the results for BATT A STORAGE SoC = 80% and BATT B STORAGE SoC = 100%.

(a) BATT A STORAGE and BATT B STORAGES SoC = 100%

The BATT A and BATT B STORAGES SoC status shown in Figure 4.10 are equal to 100%. The actual BESS voltages are also sensed and measured at the respective ADC2 and ADC3 ports are presented in Figure 4.14. Sensing and measuring the BESS voltages at the ADCs are important to coordinate and manage the BESS charging or discharging operation. Based on the BESS SoCs and voltage status, the BESS charging or discharging status is shown in Figure 4.9. The bB indicates BATT B STORAGE is connected for discharging at RE2 port and BA

indicates BATT A STORAGE is connected for charging at RB0 port at the microcontroller PIC16F877A.

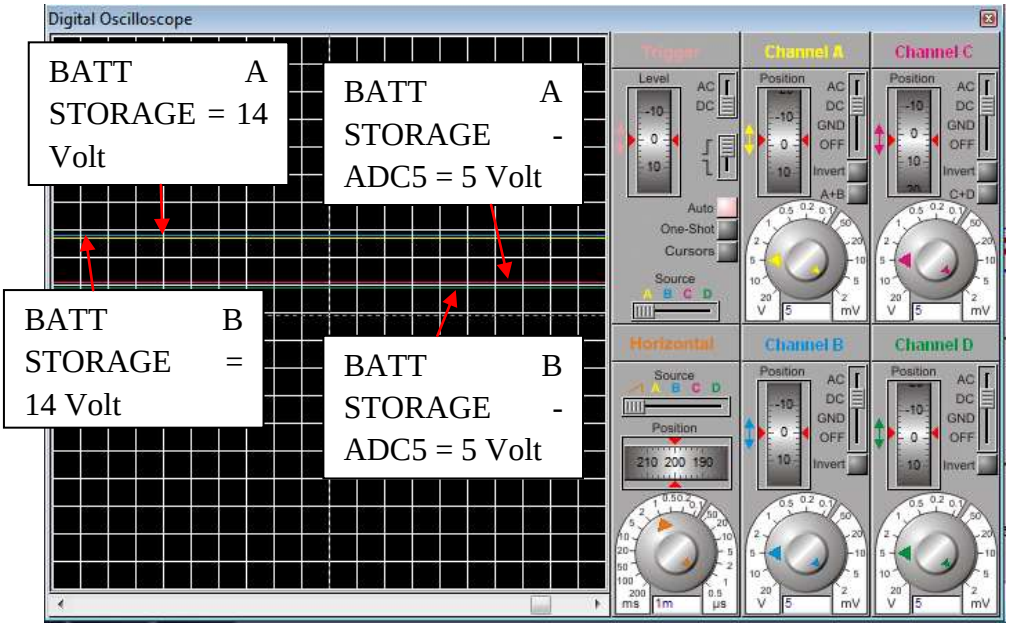

Figure 4.14: BESS STORAGES voltage and ADC status

According to Figure 4.15, none of the BESS is connected for charging or discharging due to the availability of regulated output voltages from solar-wind renewable energy sources which are the primary voltage source supply for the connected AC load. The logic analyser shown in Figure 4.16 presents the LOW signal at RB0 (RLY9) and RE2 (RLY12) ports. The microcontroller PIC16F877A output LOW signal at RB0 and RE2 ports because the BESS SoC is equal to 100% and according to Figure 4.12 the wind renewable energy source is connected to the AC load for power source supply.

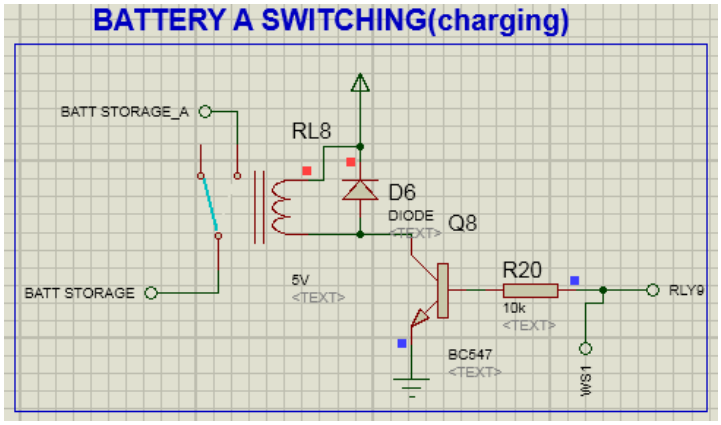

(a) Battery A Charging switching circuit

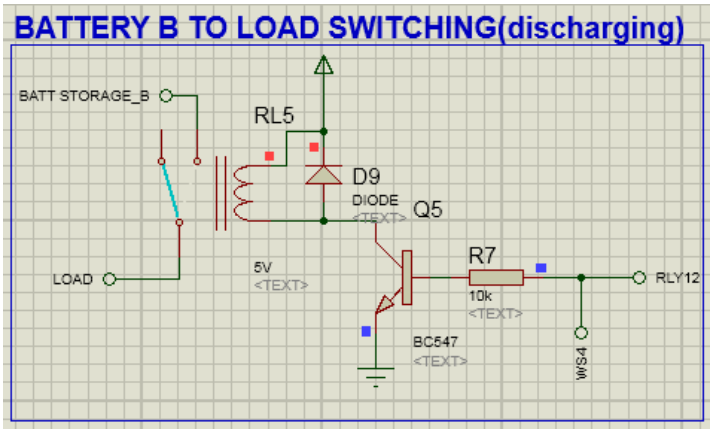

(b) Battery B to LOAD switching circuit (Discharging)

Figure 4.15: Charging/Discharging switching circuit - PORTS RB0 (RLY9) and RE2 (RLY12)

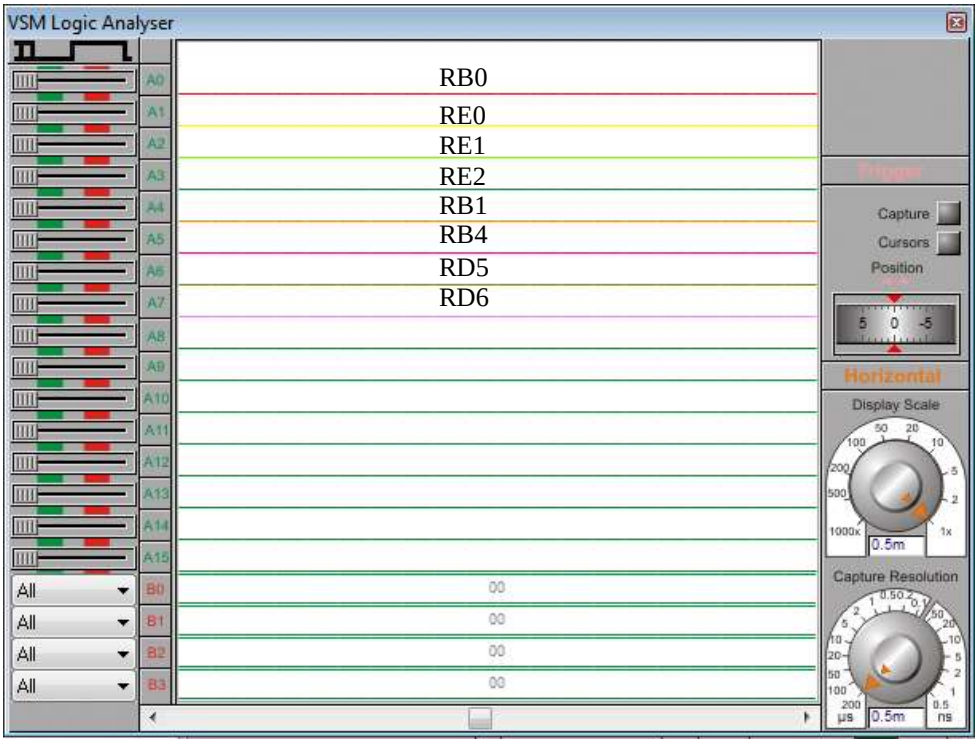

Figure 4.16: Logic analyser – LOW signal at PORTS RB0 and RE2

This section simulate a condition when the regulated output voltages from solar-wind renewable energy sources are between 12~15 Volt, BESS SoC is equal to 100% and BESS voltage is between 12~14 Volt. The presented simulation results in this section explained that the real-time DC HRES hardware system priorities the regulated output voltages from solar-wind renewable energy source as primary power source supply for the connected AC load and BESS charging process, if required.

(b) BATT A STORAGE SoC = 100% and BATT B STORAGE SoC = 80%

The BATT A STORAGE SoC and BATT B STORAGE SoC status are shown in Figure 4.17. The actual BESS output voltages are sensed and measured at the respective ADC2 and ADC3 channels is shown in Figure 4.18. According to Figure 4.17, BATT A STORAGE SoC is equal to 100% and BATT B STORAGE SoC have been discharged to 80% SoC. The bA indicates BATT A STORAGE is connected for discharging at RE1 port and BB indicates BATT B STORAGE is connected for charging at RE0 port at microcontroller PIC16F877A. The microcontroller PIC16F877A output a LOW signal at the RE1 port to deactivate the

BATT A STORAGE discharging and output a HIGH activated signal at RE0 port to activate the BATT B STORAGE charging. The regulated output voltage from solar renewable energy source is connected to charge BATT B STORAGE as shown in Figures 4.12 and 4.20(b).

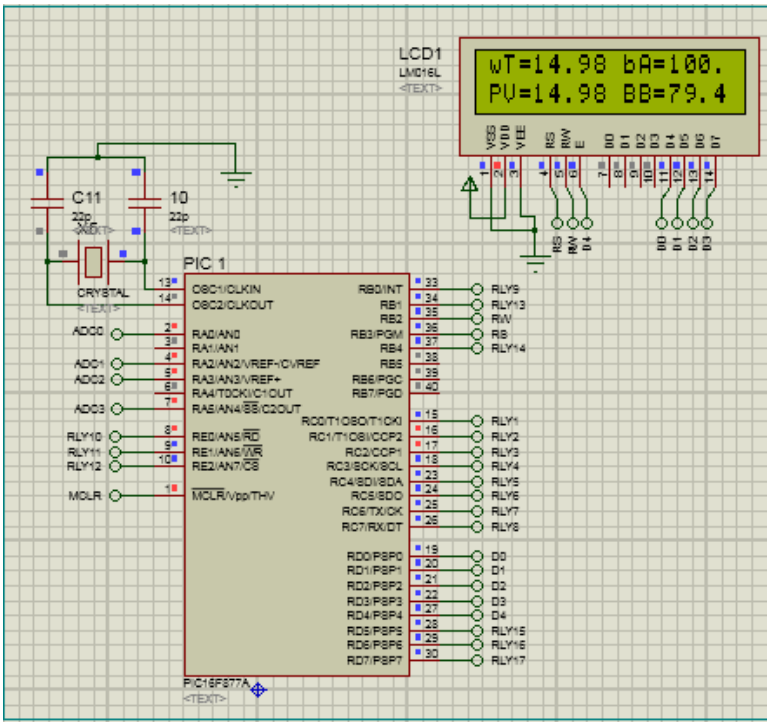

Figure 4.17: Microcontroller PIC16F877A – PORTS RE0 (RLY10) – RE1 (RLY11)

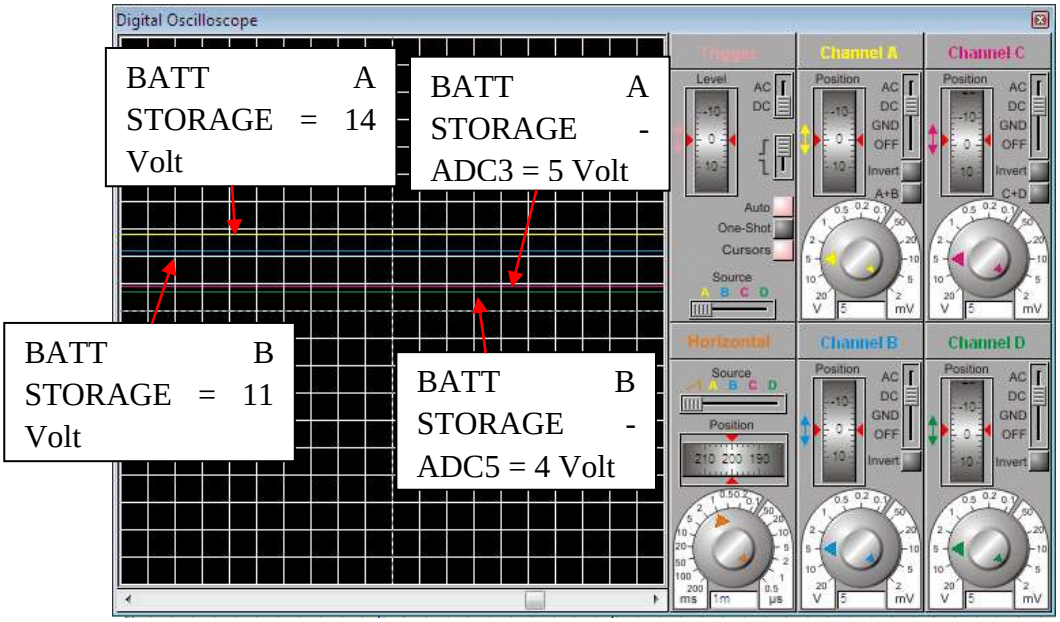

Figure 4.18: BESS voltage and ADC status

According to Figure 4.19, a LOW signal at RE0 port shows that BATT A discharging switching circuit (15 Volt) shown in Figure 4.20 (a) is deactivated to disallow BATT A STORAGE discharging process. This condition occurs because the continuous voltage sensing and measurement method which is performed using the voltage based self-intervention informs the microcontroller PIC16F877A that there is sufficient power source supply available from the renewable energy sources. Whereas, the HIGH activated signal at RE1 shows that the BATT B charging switching circuit (15 Volt) shown in Figure 4.20(b) is activated to charge BATT B STORAGE. The relay is switched ON from NC to NO. Therefore, the regulated output voltage from solar renewable energy source shown in Figure 4.12 is supplied to perform BATT B STORAGE charging process.

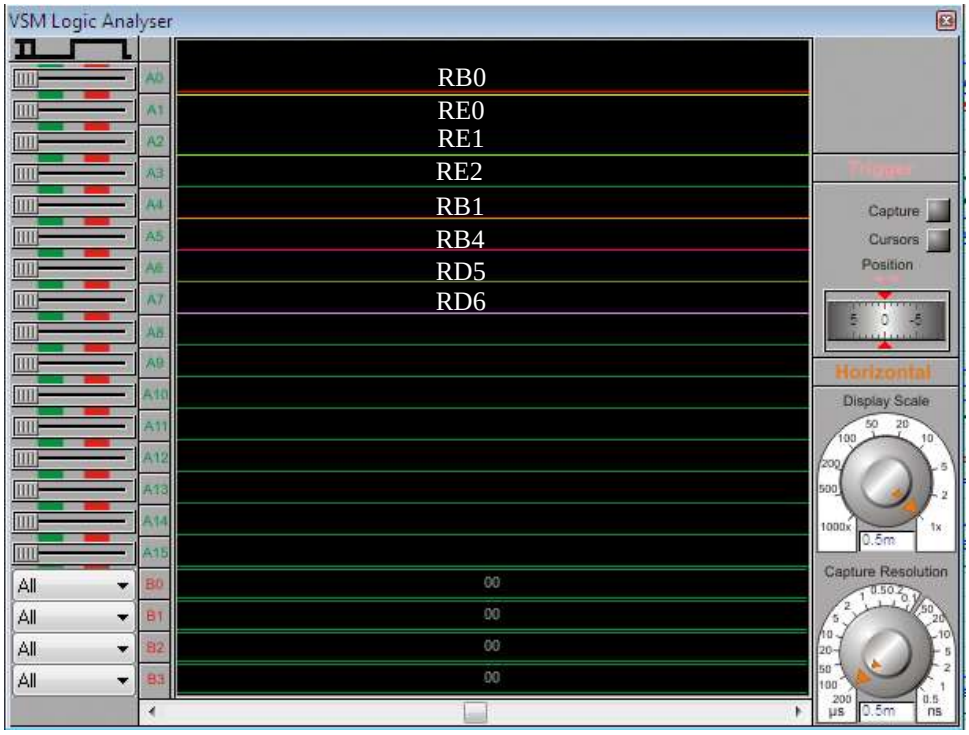

Figure 4.19: Logic analyser – HIGH activated signal at PORT RE0 and LOW signal at PORT RE1

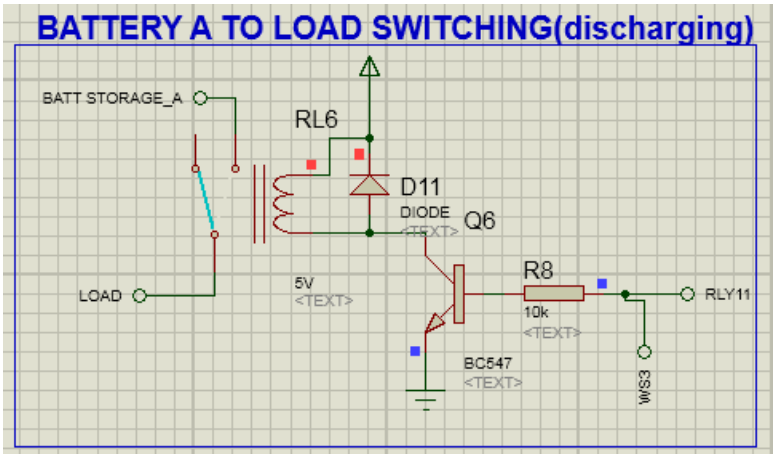

(a) Battery A to LOAD switching circuit (Discharging)

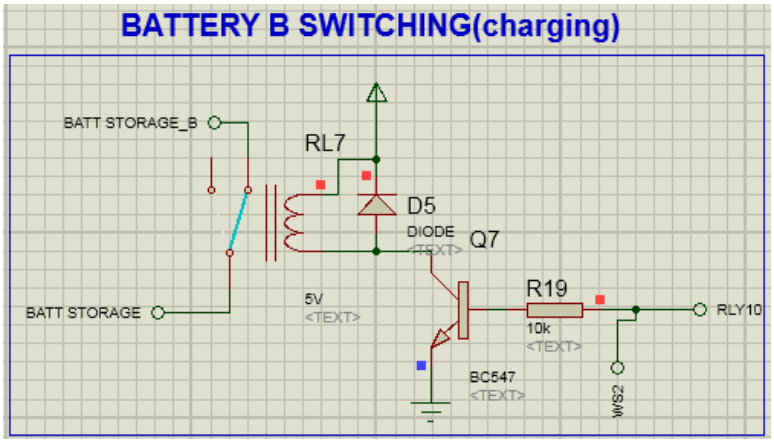

(b) Battery B Charging switching circuit

Figure 4.20: Charging/Discharging switching circuit - PORTS RE0 (RLY10) and RE1 (RLY11)

(c) BATT A STORAGE SoC = 80% and BATT B STORAGE SoC = 100%

The BATT A STORAGE SoC and BATT B STORAGE SoC status is shown in Figure 4.21. The actual BESS output voltages are sensed and measured at the respective ADC2 and ADC3 channels is shown in Figure 4.22. According to Figure 4.21, BATT A STORAGE has been discharged at 80% SoC and BATT B STORAGE is equal to 100%. The BA indicates BATT A STORAGE is connected for charging at RB0 port and bB indicates BATT B STORAGE is connected for discharging at RE2 port at microcontroller PIC16F877A. The microcontroller PIC16F877A output a HIGH activated signal at RB0 port to activate BATT A STORAGE for charging process and output a LOW signal to at RE2 to deactivate BATT B STORAGE discharging process. In this case, the regulated output voltage from solar renewable energy is connected to perform BATT A STORAGE charging process is shown in Figures 4.12 and 4.24(b).

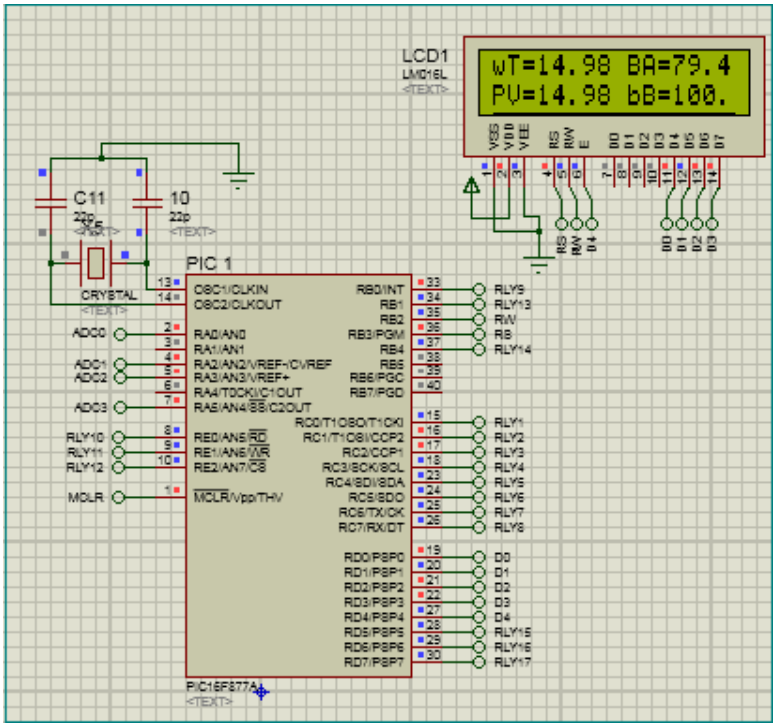

Figure 4.21: Microcontroller PIC16F877A – PORTS RB0 (RLY9) – RE2 (RLY12)

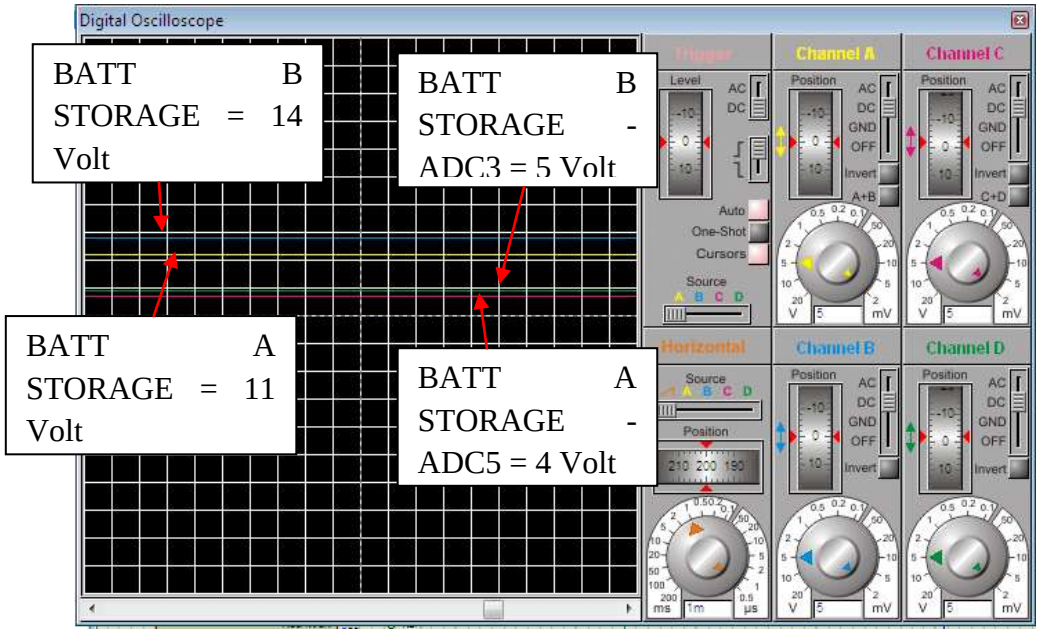

Figure 4.22: BESS STORAGES voltage and ADC status

According to Figure 4.23, a HIGH activated signal at RB0 port shows that BATT A charging switching circuit (15 Volt) shown in Figure 4.24(a) is activated to perform BATT A

STORAGE charging process. Therefore, the regulated output voltage from solar renewable energy source shown in Figure 4.12 is supplied to perform BATT A STORAGE charging process. The LOW signal at RE2 port shows that BATT B discharging switching circuit (15 Volt) shown in Figure 4.24(b) is deactivated to disallow BATT B STORAGE discharging process. In this case, the continuous voltage sensing and measurement method which is using the voltage based self-intervention informs the microcontroller PIC16F877A that there is sufficient power source supply available from the renewable energy sources for the connected AC load.

Figure 4.23: Logic analyser – HIGH activated signal at PORT RB0 and LOW signal at PORT RE2

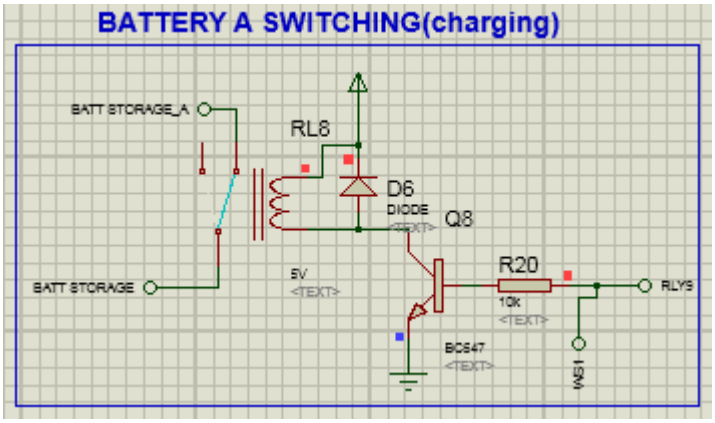

(a) Battery A Charging switching circuit

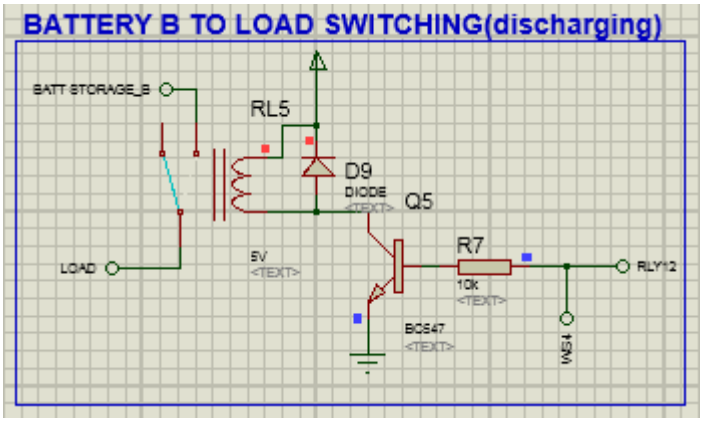

(b) Battery B to LOAD switching circuit (Discharging)

Figure 4.24: Charging/Discharging switching circuit - PORTS RB0 (RLY9) and RE2 (RLY12)

The section (b) and (c) simulates and discusses about charging or discharging condition for BESS. In this simulation, the charging or discharging switching circuits are simulated to analyse and validate the real-time DC HRES hardware system operation to perform charging or discharging on BESS. The presented simulation results explained that the real-time DC HRES hardware system have successfully able to coordinate, manage and control the charging or discharging process when it is required.

4.6.2 CONDITION B: PV = 12~15 Volt and WT = 7~12 Volt - DC HRES MODEL SIMULATION

This section discusses about the different regulated output voltages from solar-wind renewable energy sources for the connected AC load and BESS charging process. The regulated output voltages from solar-wind renewable energy sources are shown in Figure 4.25. Referring to Figure 4.1, PV and WT voltage based self-intervention are used to sense and measure the regulated output voltages from solar-wind renewable energy sources as shown in Figure 4.25. In this situation, solar renewable energy source outputs higher voltage compare to wind renewable energy source. Thus, the regulated output voltage from solar renewable energy source is used as primary power source supply for the connected AC load. The regulated output voltage from solar renewable energy source is connected to DC to AC Inverter for step-up and conversion process. On that contrary, wind renewable energy source is used to perform BESS charging, if required. Before the regulated output voltage from wind renewable energy source is used to charge the BESS, the voltage is stepped-up using DC to DC BC to a desired output voltage.

Referring to Figure 4.1 and Table 4.2, Figure 4.25 shows RC3 and RC4 ports at microcontroller PIC16F877A is HIGH activated. When the 15 Volt PV switching circuit is connected at RC3 port at microcontroller PIC16F877A receives a HIGH activated signal, then the connected relay coil is energised to switch from NC to NO. Thus, 12~15 Volt regulated output voltage from solar renewable energy source is connected to DC to AC Inverter (LOAD AC) as primary power source supply for the connected AC load. Whilst, the 12 Volt WT switching circuit is connected at RC4 at microcontroller PIC16F877A receives a HIGH activated signal, then the connected relay coil is energised to switch from NC to NO. Thus, 7~12 Volt regulated output voltage from wind renewable energy source is connected to DC to DC BC (BATT STORAGE BC) to perform BESS charging process operation, if required. The HIGH activated signals at RC3 and RC4 ports are captured using the logic analyser is shown in Figure 4.26.

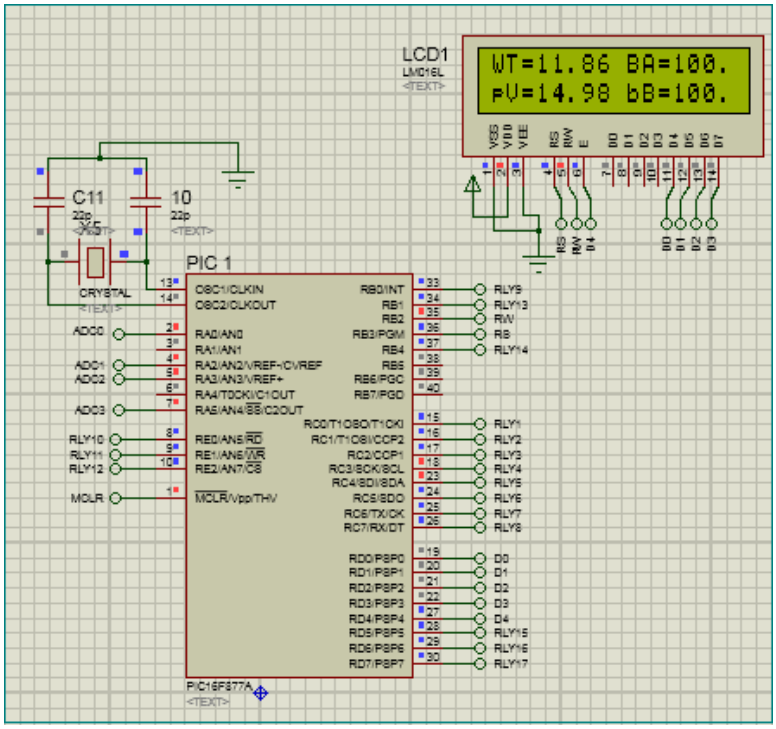

Figure 4.25: Microcontroller PIC16F877A – PORTS RC3 (RLY4) – RC4 (RLY5)

The LCD display in Figure 4.25 indicates the connectivity of the regulated output voltages from solar-wind renewable energy sources. The WT indicates the regulated output voltage from wind renewable energy source is connected to DC to DC BC (BATT STORAGE BC) to perform BESS charging process, if required. Whilst, pV indicates the regulated output voltage from solar renewable energy source is connected to DC to AC Inverter (LOAD AC) as power source supply for the connected AC load.

Referring to Figure 4.27(b), 7~12 Volt regulated output voltage from wind renewable energy source is connected to DC to DC BC (BATT STORAGE BC) when the relay is switched from NC to NO. Therefore, Figure 4.27 shows the 7~12 Volt regulated output voltage from wind renewable energy source is connected to DC to DC BC and 15 Volt output from the DC to DC BC is supplied to perform BESS charging, if required.

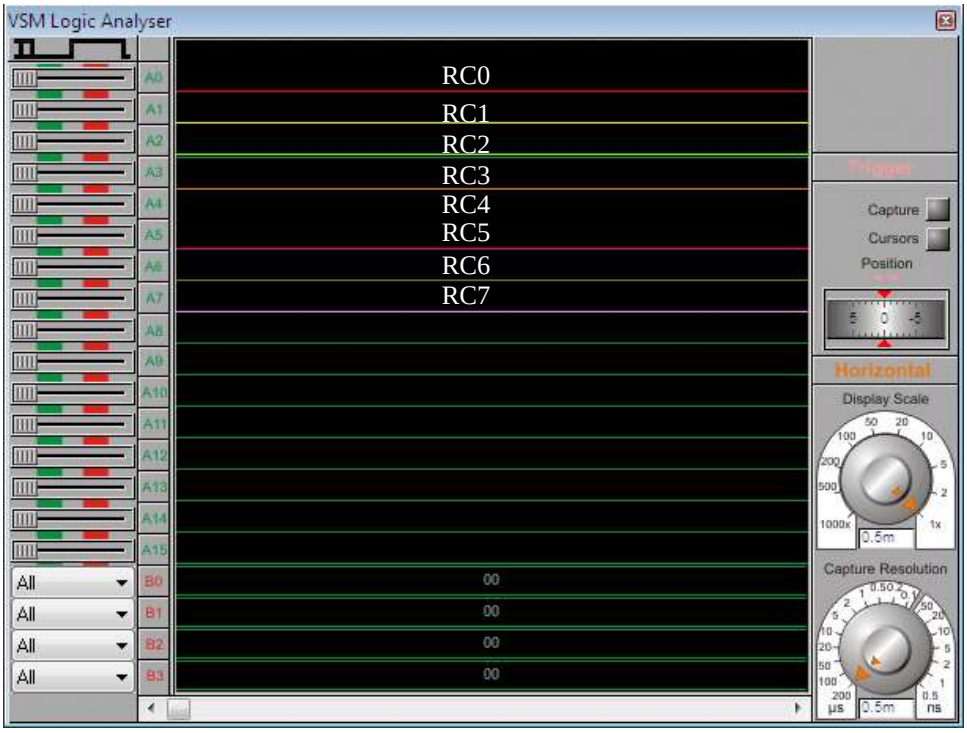

Figure 4.26: Logic analyser – HIGH activated signal at PORTS RC3 – RC4

The relay switching and control modules shown in Figure 4.27 is presenting the 15 Volt PV switching circuit and 12 Volt WT switching circuit. Both of these switching circuits are used to manage the voltage power source connectivity to the connected DC to AC Inverter (LOAD AC) for the connected AC load and to DC to DC BC (BATT STORAGE BC) to step-up the regulated output voltage to a desired output voltage to perform BESS charging process, if required. Looking at 15 Volt PV switching circuit and 12 Volt WT switching circuit in Figures 4.1 and 4.27(a), the RLY4 port receives a HIGH activated signal from RC3 port at microcontroller PIC16F877A. Hence, the current from NPN transistor's base will energise the relay coil and switch from NC to NO. Thus, the 15 Volt regulated output voltage from solar renewable energy source is connected to DC to AC Inverter (LOAD AC) for the connected AC load.

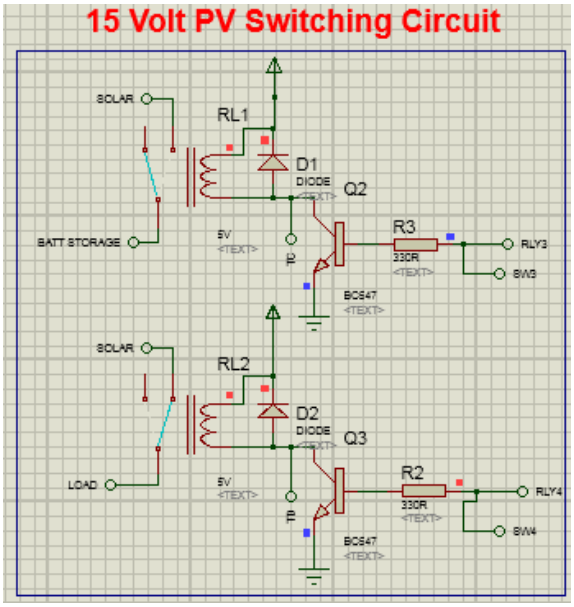

(a) 15 Volt PV switching circuit

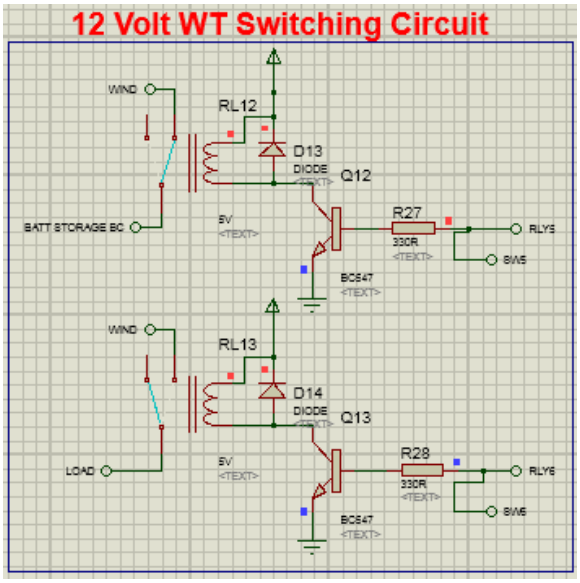

(b) 12 Volt WT switching circuit

Figure 4.27: Relay switching and control module – PORTS RC3 (RLY4) – RC4 (RLY5)

Whilst, referring to the Figures 4.1 and 4.27(b), RLY5 port at the 12 Volt WT switching circuit receives a HIGH activated signal from RC4 port at microcontroller PIC16F877A. Hence, the current from NPN transistor's base will energise the relay coil and switch from NC to NO. Thus, 7~12 Volt regulated output voltage from wind renewable energy source is

connected to DC to DC Converter (BATT STORAGE BC) for BESS charging process, if required.

Referring to Figure 4.27(b), 12 Volt regulated output voltage from wind renewable energy source is connected to DC to DC BC (BATT STORAGE BC) when the relay is switched from NC to NO. Therefore, Figure 4.28 shows the 12 Volt regulated output voltage from wind renewable energy source is send into DC to DC BC and a 15 Volt desired output voltage from DC to DC BC is achieved for BESS charging process, if required.

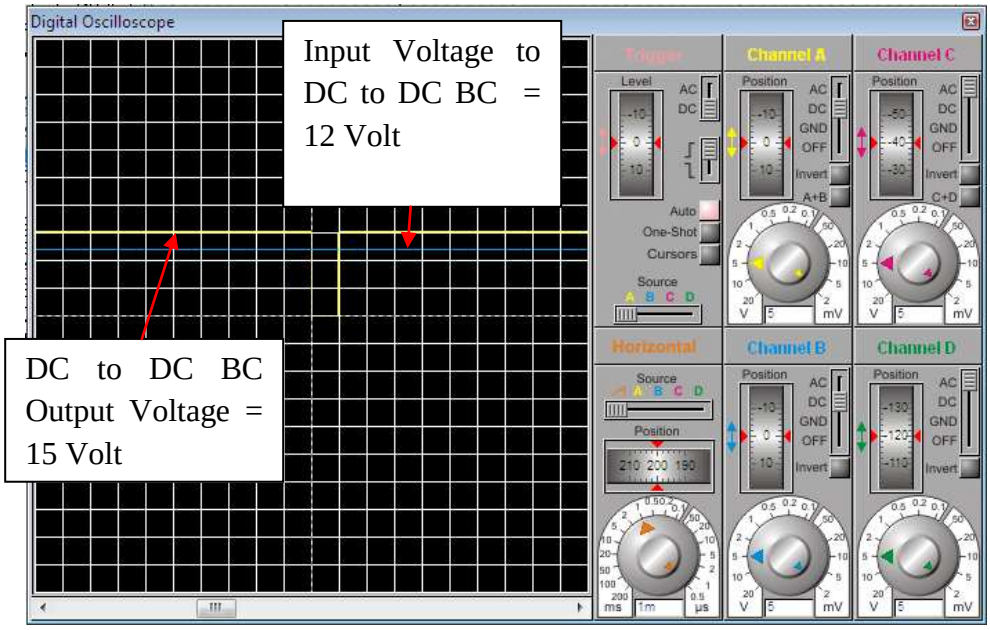

Figure 4.28: DC to DC BC output voltage

This section discusses about the self-intervention process of different regulated output voltages from solar-wind renewable energy sources. In earlier section, wind renewable energy source is used as power source supply to DC to AC Inverter for the connected AC load and regulated output voltage from solar renewable energy source is used to perform BESS charging, if required. On that contrary, in this section the voltage based self-intervention managed to perform self-intervention by selecting the regulated output voltage from solar renewable energy source for DC to AC Inverter for the connected AC load. Whereas, the regulated output voltage from wind renewable energy source is used for BESS charging process, if required. On the other hand, 7~12 Volt regulated output voltage from wind

renewable energy source is stepped-up using DC to DC BC to a desired output voltage. This voltage is used to perform BESS charging. The presented simulation results explained that the real-time DC HRES hardware system have successfully performed the self-intervention between solar-wind renewable energy sources. Also, the real-time DC HRES system have successfully coordinate the 7~12 Volt regulated output voltage to DC to DC BC for voltage step-up to a desired output voltage for BESS charging process.

4.6.3 CONDITION C: PV = 12~15 Volt and WT = 0~7 - DC HRES MODEL SIMULATION

This section discusses the circumstances of the availability of only one renewable energy source as power source supply. When this condition occurs, the only available renewable energy source is used only for BESS charging. At the same time, RD7 port at microcontroller PIC16F877A is HIGH activated as shown in Figure 4.29 to activate the GRID connection/LOAD switching circuit. This condition occurs when the BESS SoCs are equal or less than 40% and there is no power source being supplied to the connected AC load.The available regulated output voltages from solar-wind renewable energy sources are shown in Figure 4.29. Referring to Figure 4.1, PV and WT voltage based self-intervention are used to sense and measure the regulated output voltages from solar-wind renewable energy sources as shown in Figure 4.29. In this situation, the regulated output voltage from solar renewable energy source is between 12~15 Volt and the regulated output voltage from the wind renewable energy source is between 0~7 Volt. Thus, the regulated output voltage from solar renewable energy source is used to perform the BESS charging process, if required. Whilst, the 0~7 Volt regulated output voltage from wind renewable energy source is deactivated and not connected to perform any operation due to the low regulated output voltage.

Referring to Figure 4.2 and Table 4.2, Figure 4.29 shows RB0, RC2 and RD7 ports at microcontroller PIC16F877A is HIGH activated. When 15 Volt PV switching circuit connected at RC2 port at microcontroller PIC16F877A receives a HIGH activated signal, then the connected relay coil is energised and switched from NC to NO. Thus, 12~15 Volt regulated output voltage from solar renewable energy source is used to perform BESS charging, if required. Whilst, 12 Volt and 15 Volt WT switching circuit is deactivated because

of the low 0~7 Volt regulated output voltage from wind renewable energy source. The HIGH activated signals at RC2 and RB0 ports are captured using the logic analyser is shown in Figure 4.30.

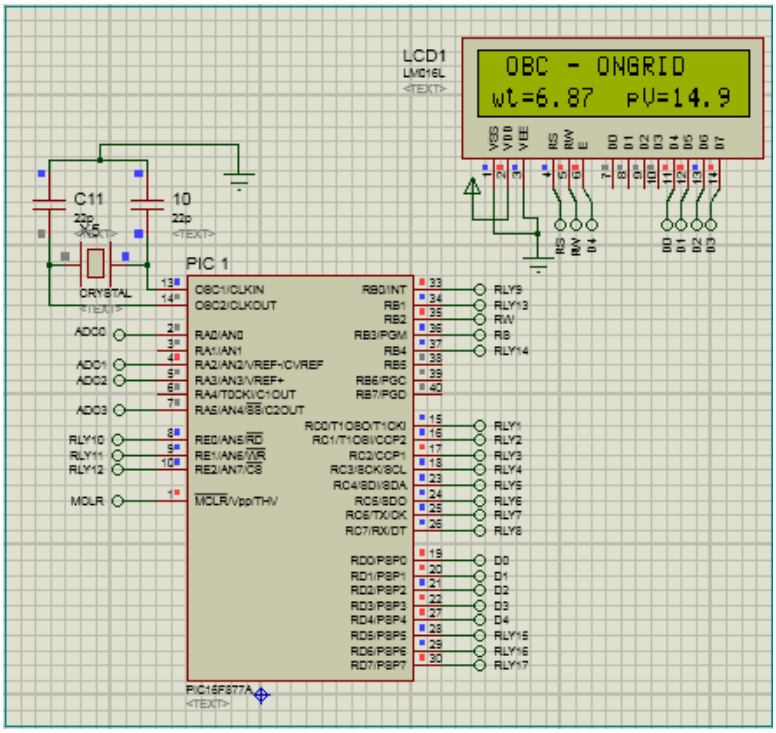

Figure 4.29: Microcontroller PIC16F877A – PORTS RB0 (RLY9) – RC2 (RLY3) - RD7 (RLY17)

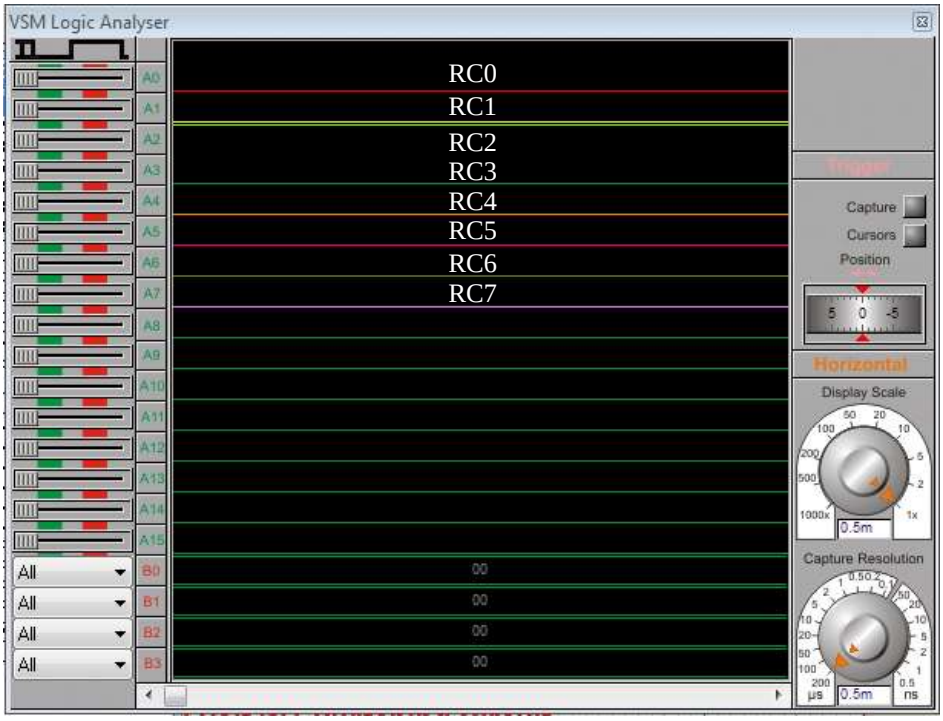

(a) HIGH activated port RC2

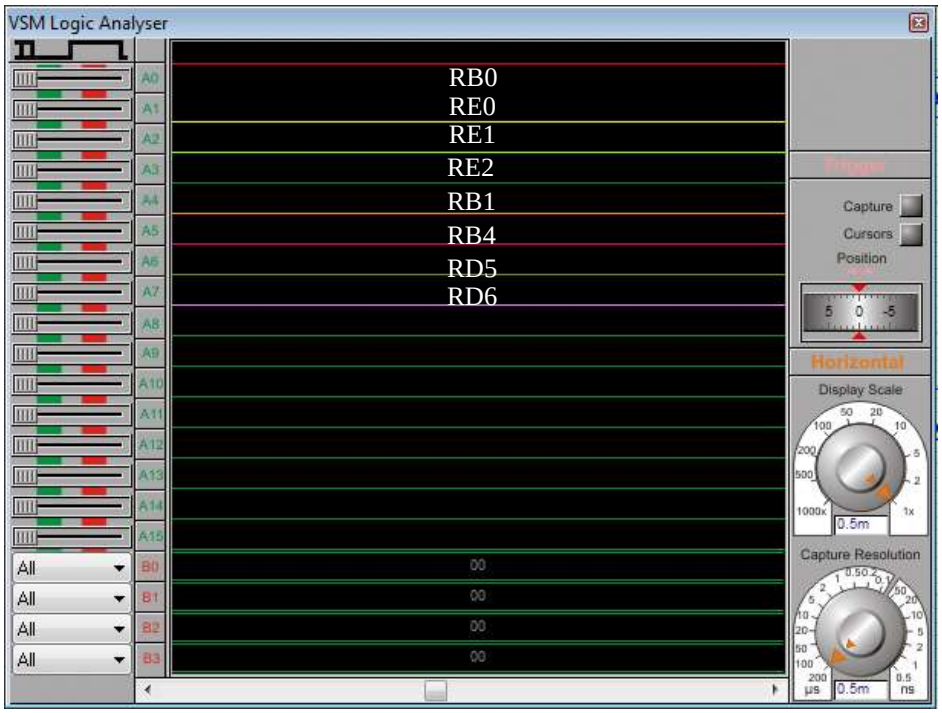

(b) HIGH activated port RB0

Figure 4.30: Logic analyser – HIGH activated signal at PORTS RB0 (RLY9) – RC2 (RLY3) - RD7 (RLY17)

The Only Battery Charging (OBC) ONGRID indicates that there is only one renewable energy source available to provide the power source. As mentioned earlier, the only regulated output voltage from solar renewable energy source is used to charge BESS, if required. Therefore, referring to Figure 4.2 and Table 4.2, Figure 4.31 shows 15 Volt PV switching circuit and BATT A charging switching circuit (15 Volt) is connected at RC2 and RB0 ports at microcontroller PIC16F877A receives a HIGH activated signal, then the connected relay coil is energised to switch from NC to NO. Thus, 12~15 Volt regulated output voltage from 15 Volt PV switching circuit is connected to BATT A charging switching circuit (15 Volt) to charge BATT A STORAGE.

Referring to Figure 4.2 and Table 4.2, Figure 4.29 shows RD7 port at microcontroller PIC16F877A is HIGH activated to activate GRID connection/LOAD relay switching circuit shown in Figure 4.33. The AC load is connected to GRID connection/LOAD switching circuit to receive the power source supply from the grid network.

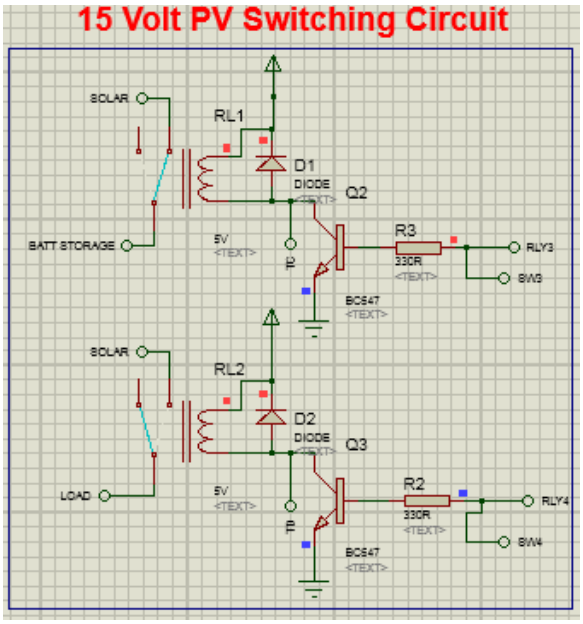

Figure 4.31: Relay switching and control module – PORT RC2 (RLY3)

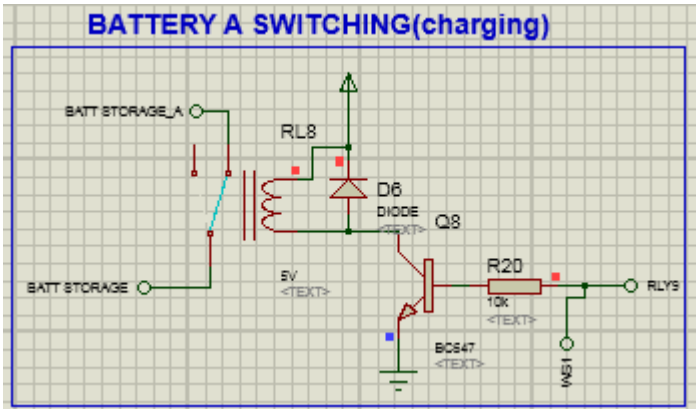

Figure 4.32: Charging/Discharging switching circuit - PORT RB0 (RLY9)

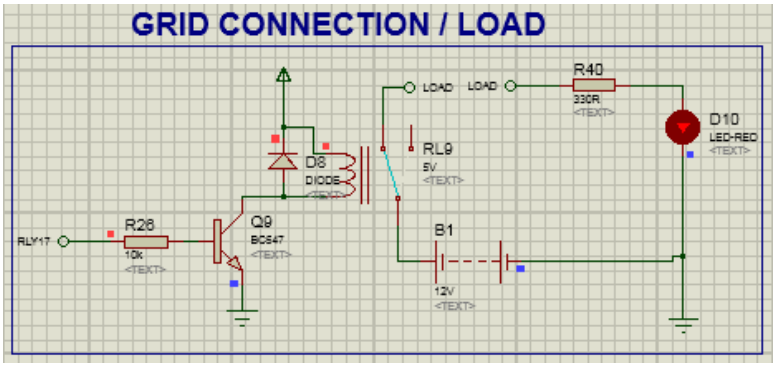

Figure 4.33: GRID connection/LOAD switching circuit – PORT RD7 (RLY17)

This section discusses about the availability of only one renewable energy source for BESS charging operation and the use of GRID connection/LOAD switching circuit as power source supply for the connected AC load. The presented results explain that real-time DC HRES hardware system has successfully performed self intervention between energy sources and GRID connection/LOAD switching circuit. Also, real-time DC HRES hardware system have successfully performed the sensing and measurement of the available BESS SoC before switching the relay to connect to the GRID connection/LOAD switching circuit for the connected AC load.

In the following sections, the charging or discharging process based on only one available renewable energy source is discussed. As shown in Figure 4.29, regulated output voltage is only available from solar renewable energy source. This regulated output voltage is only used

to charge BESS, if required. Referring to Figure 4.1, BATT A and BATT B voltage based self-intervention is used to sense and measure BESS SoC and voltages. The BESS SoC and voltages status are sensed and measured at the respective ADC2 and ADC3 channels at microcontroller PIC16F877A. The input voltage proportion equivalency shown in Figure 4.5 is used as reference to perform the voltage reading at the ADC channels. Thus, this section discusses about BESS SoC and voltage status. Section (a) presents the simulation for BATT A STORAGE and BATT B STORAGE SoCs = 40%. Section (b) presents the simulation for BATT A STORAGE SoC = 100% and BATT B STORAGE SoC = 80%. Section (c) presents the simulation for BATT A STORAGE SoC = 80% and BATT B STORAGE SoC = 100%.

(a) BATT A STORAGE SoC and BATT B STORAGE SoC ≤ 40%

The BATT A STORAGE and BATT B STORAGE SoCs and voltages status are shown in Figure 4.34. Referring to the LCD in Figure 4.29, the pV indicates the regulated output voltage from solar renewable energy source is used to charge BATT A STORAGE and BATT B STORAGE. Referring to Figure 4.1 and Table 4.2, Figure 4.29 shows RB0 and RC2 ports are HIGH activated. When RB0 (RLY9) and RC2 (RLY3) ports are HIGH activated, then the 15 Volt PV switching circuit shown in Figure 4.31 is connected to BATT A charging switching circuit. Thus, 12~15 Volt regulated output voltage from solar renewable energy source is supplied to charge the BATT A STORAGE.

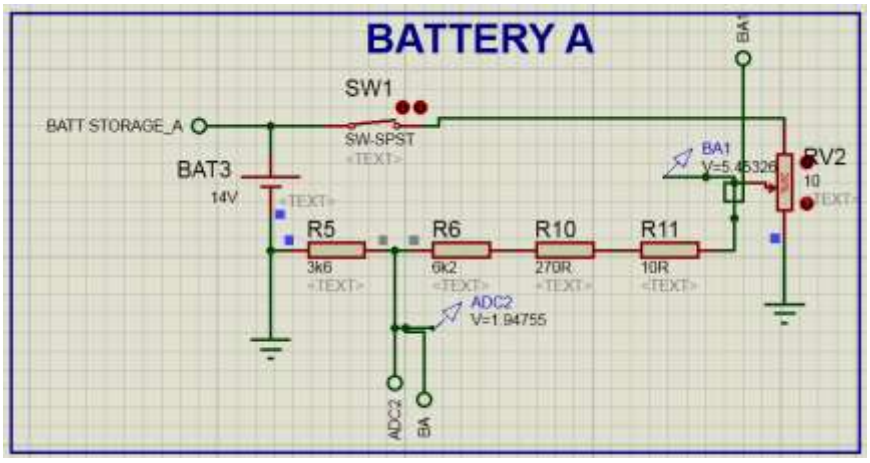

(a) Battery A sensing and measuring circuit

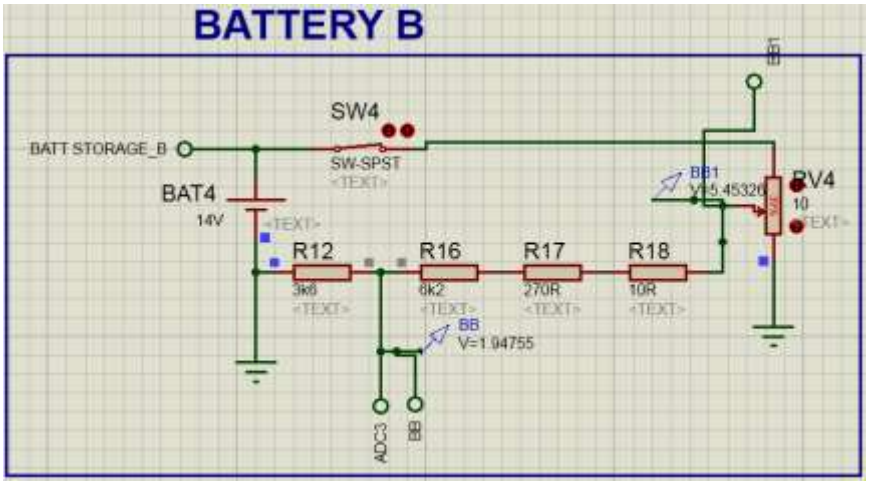

(b) Battery B sensing and measuring circuit

Figure 4.34: BATT A STORAGE and BATT B STORAGE SoCs and voltages status

This section explains the importance to manage and control the BESS charging when the BESS SoC is equal or less than 40%. The simulation results explain that the real-time DC HRES hardware system has successfully supervise and coordinate all the circuits and managed to priorities the BATT A STORAGE for charging.

(b) BATT A STORAGE =75% and BATT B STORAGE SoC = 45%

The regulated output voltages from solar-wind renewable sources are shown in Figure 4.35. Referring to the LCD in Figure 4.35, pV indicates the regulated output voltage from solar renewable energy source is used to charge BESS, if required. The BATT A STORAGE SoC and BATT B STORAGE voltages are shown in Figure 4.36. Referring to Figure 4.35, RC2 (RLY3), RE0 (RLY10) and RE1 (RLY11) ports are HIGH activated.

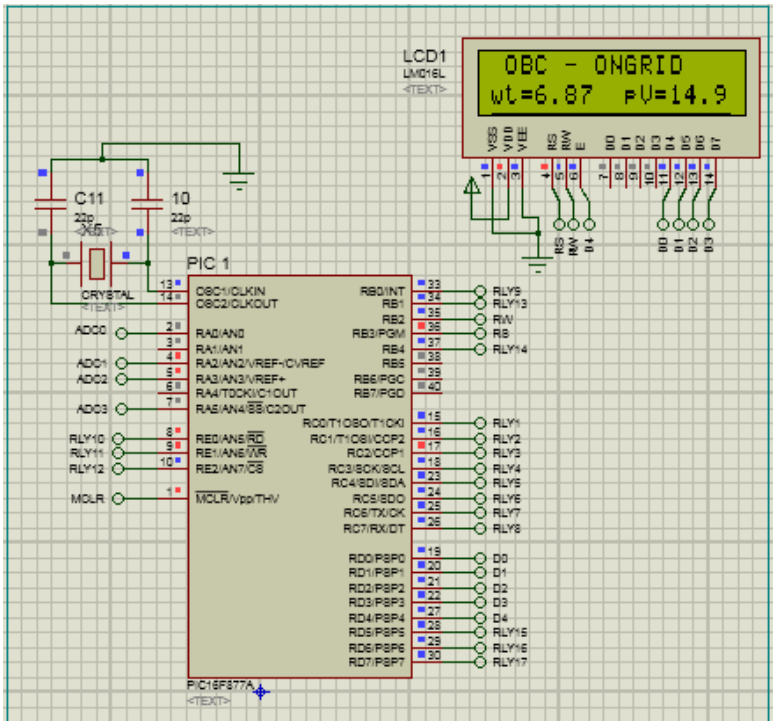

Figure 4.35: Microcontroller PIC16F877A – PORTS RC2 (RLY3) – RE0 (RLY10) – RE1 (RLY11)

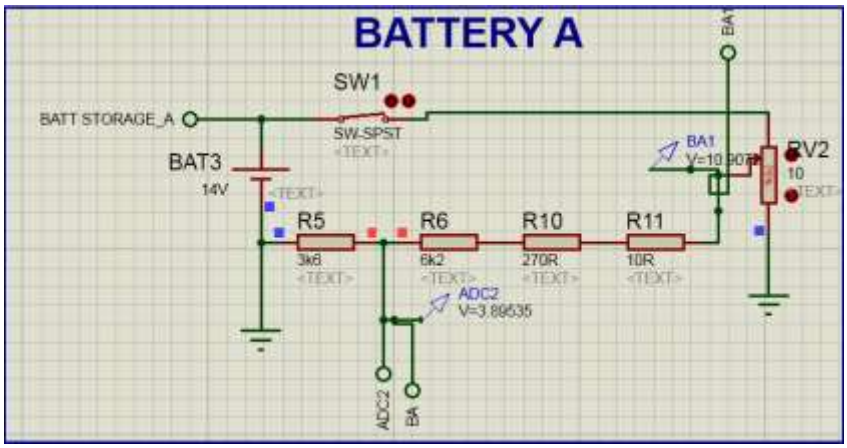

(a) Battery A sensing and measuring circuit

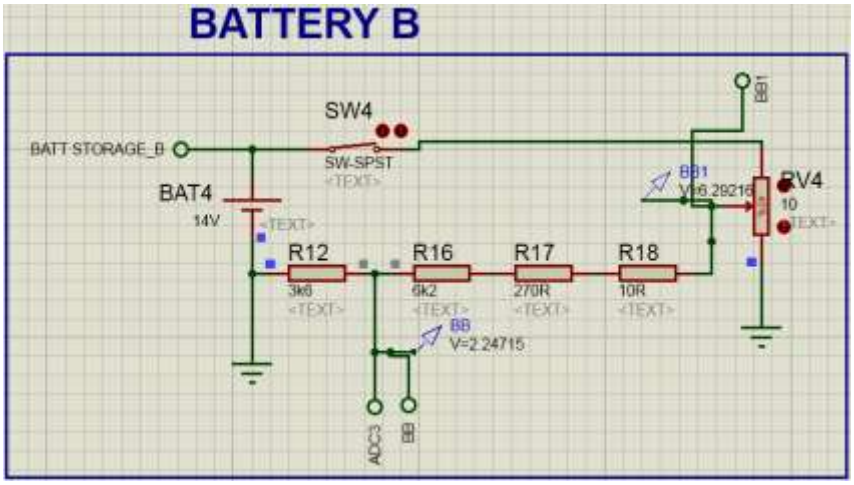

(b) Battery B sensing and measuring circuit

Figure 4.36: BATT A STORAGE and BATT B STORAGE SoCs and voltages status

The HIGH activated RC2, RE0 and RE1 ports at microcontroller PIC16F877A is captured using the logic analyser and is shown in Figure 4.37. When RC2 and RE0 ports are HIGH activated, then the 15 Volt PV switching circuit shown in Figure 4.38 is connected to BATT B charging switching circuit shown in Figure 4.39(b). Thus, allowing 12~15 Volt regulated output voltage from solar renewable energy source to charge BATT B STORAGE. At the same time, RE1 port at microcontroller PIC16F877A is also HIGH activated. When RE1 port is HIGH activated, then the BATT A discharging switching circuit (15 Volt) is activated. The relay coil is switched from NC to NO. Therefore, connecting power source from BATT A STORAGE to DC to AC Inverter (LOAD AC) for the connected AC load is shown in Figure 4.39(a). Also, RD1 port at microcontroller PIC16F877A is deactivated because of sufficient power source is available for AC load supply.

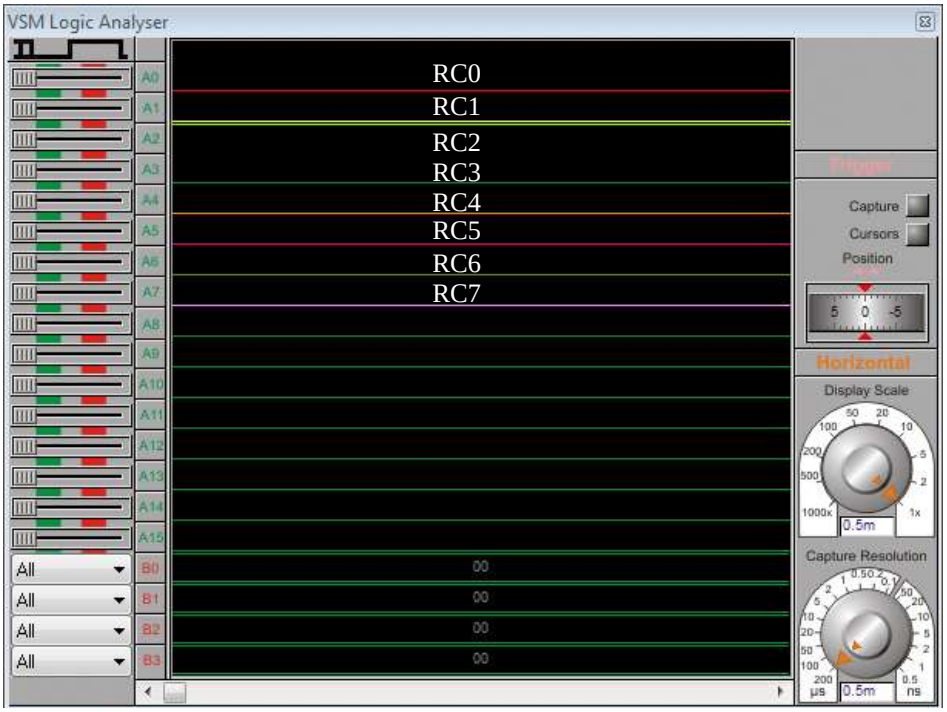

(a) HIGH activated port RC2

(b) High activated port RE1

Figure 4.37: Logic analyser – HIGH activated signal at PORTS RC0 (RLY3) – RE0 (RLY10) – RE1 (RLY11)

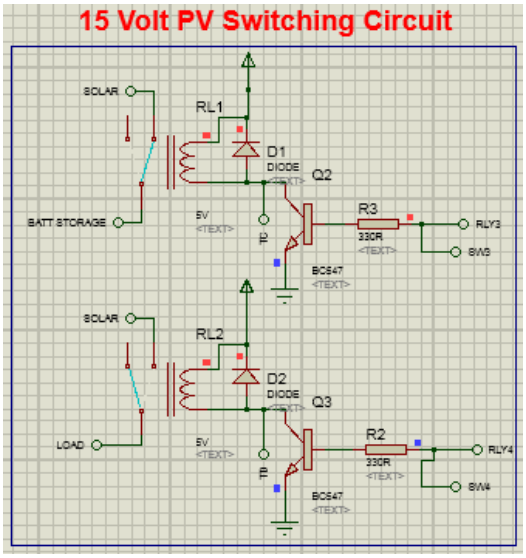

Figure 4.38: Relay switching and control module – PORT RC2 (RLY3)

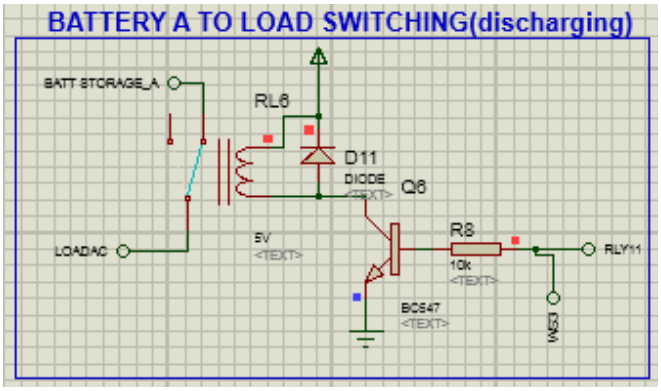

(a) Battery A LOAD switching circuit (Discharging)

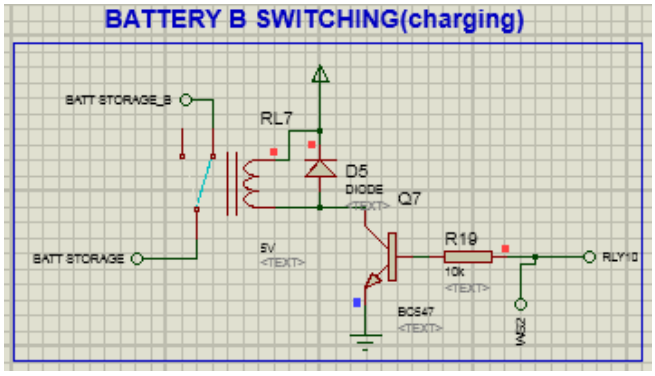

(b) Battery A Charging switching circuit

Figure 4.39: Charging/Discharging switching circuit - PORTS RE0 (RLY10) – RE1 (RLY11)

This section explains the importance to coordinate, manage and control the BESS charging or discharging when BESS SoC is more than 40%. The simulation results explain that real-time DC HRES hardware system has successfully supervised and coordinated the charging/discharging switching circuits for BESS charging or discharging purposes. Also, real-time DC HRES hardware system has successfully managed to priorities the stored energy for AC load supply.

(c) BATT A STORAGE SoC = 100% and BATT B STORAGE SoC = 100%

The regulated output voltages from solar-wind renewable sources are shown in Figure 4.40. Referring to the LCD in Figure 4.40, pV indicates the regulated output voltage from solar renewable energy source is used to charge the BESS. The sensed and measured BATT A STORAGE and BATT B STORAGE voltages are captured using the oscilloscope as shown in Figure 4.41. Referring to Figure 4.35, RC2 (RLY3) and RE3 (RLY12) ports are HIGH activated.

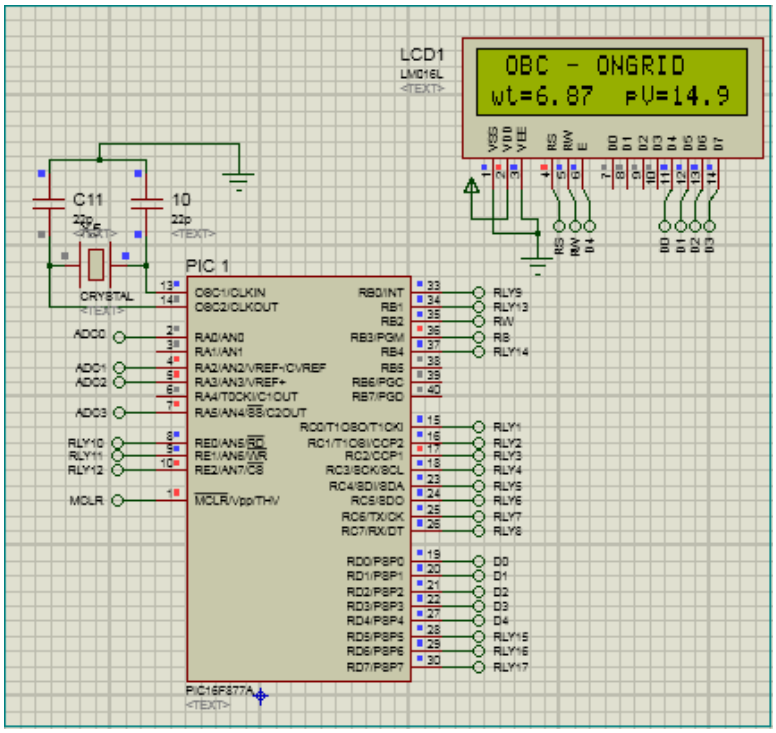

Figure 4.40: Microcontroller PIC16F877A – PORTS RC2 (RLY3) – RE3 (RLY12)

The sensed and measured BATT A STORAGE and BATT B STORAGE voltages shown in Figure 4.41 shows the BESS is fully charged at 14 Volt. Also, ADC2 and ADC3 channels sensed and measured the voltages status are shown in Figure 4.41.

Referring to Figure 4.2 and Table 4.2, Figures 4.40 and 4.42 shows the RE2 port at microcontroller is HIGH activated. When RE2 port is HIGH activated, RLY 12 connecting BATT B discharging switching circuit (15 Volt) is activated. Thus, 14 Volt from BATT B STORAGE is connected to DC to AC Inverter (LOAD AC) for AC load supply. The 14 Volt is stepped-up and converted into an AC voltage, the result is shown in Figure 4.43.

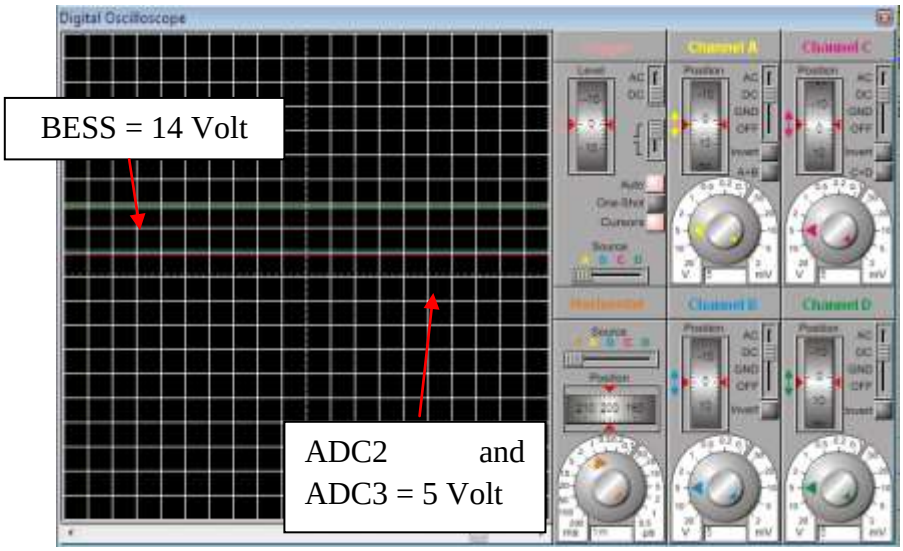

Figure 4.41: BESS voltages and ADC channels status

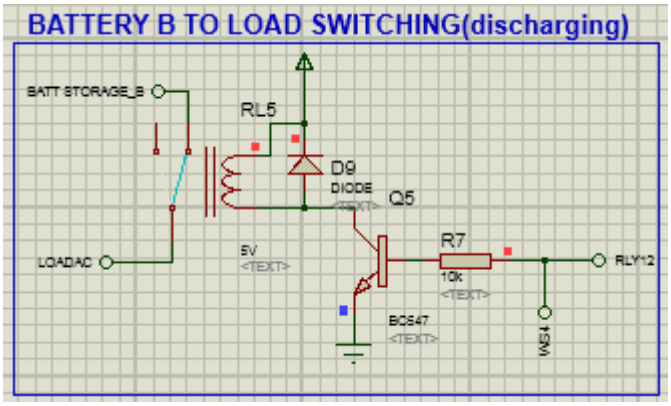

Figure 4.42: Charging/discharging switching circuit – PORT RE2 (RLY12)

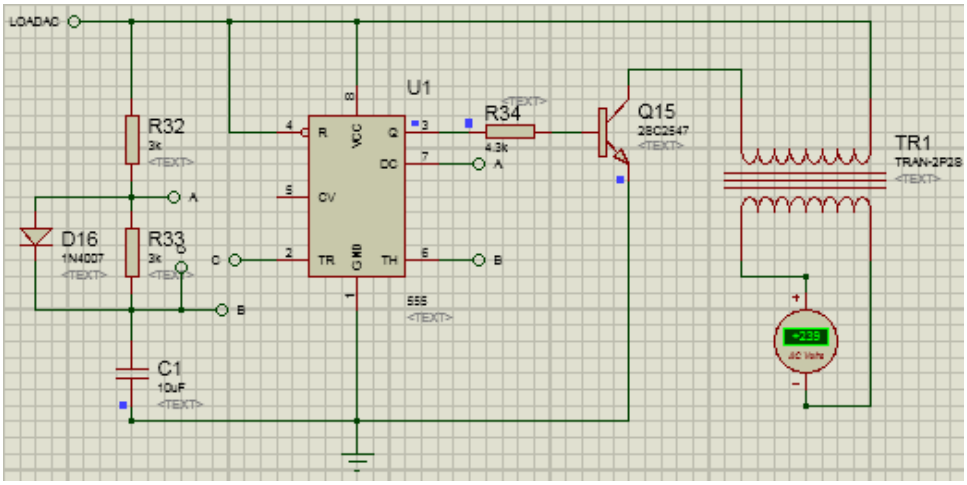

Figure 4.43: 15 VDC – 240 VAC – Inverter output

This section explains about the importance to manage and control the charging/discharging switching circuits when BESS SoCs are equal to 100%. The simulation results explain the real-time DC HRES hardware system has successfully managed to deactivate the charging switching circuit when BESS SoCs are 100%. Also, real-time DC HRES hardware system has successfully connect the discharging switching circuits to the DC to AC Inverter (LOAD AC) for AC load supply.

4.6.4 CONDITION D: WT = 7~12 Volt and PV = 0~7 - DC HRES MODEL SIMULATION

This section discusses about the availability of only one renewable energy source as power source supply. When this condition occurs, the only available regulated output voltage from renewable energy sources is stepped-up using DC to DC BC to charge BESS. At the same time, if BESS SoC status is equal or less than 40%, then GRID connection/LOAD switching circuit shown in Figure 4.2 is connected at RD7 port at microcontroller PIC16F877A is HIGH activated. Otherwise, GRID connection/LOAD switching circuit is LOW activated. The available regulated output voltage from the wind renewable energy source is shown in Figure 4.44. The regulated output voltage from wind renewable energy source is between 7~12 Volt and regulated output voltage from solar renewable energy source is between 0~7 Volt. Thus, the regulated output voltage from wind renewable energy source is stepped-up to a desired output voltage using DC to DC BC for BESS charging, if required. Whilst, the regulated

output voltage from solar renewable energy source is not connected to any source to perform any kind of operation due to the low regulated output voltage.

Referring to Figure 4.2 and Table 4.2, Figures 4.44 and 4.45 shows the RC4, and RD6 ports at microcontroller PIC16F877A is HIGH activated. When RC4 port is HIGH activated, 12 Volt WT switching circuit as shown in Figure 4.45 is activated. Thus, 7~12 Volt regulated output voltage from wind renewable energy source is connected to DC to DC BC (BATT STORAGE BC) as shown in Figure 4.46. Hence, 14 Volt stepped-up output voltages from DC to DC BC are used to charge BESS, if required. At the same time, RD6 port is HIGH activated HIGH. When RD6 port is HIGH activated, BATT B discharging switching circuit (13 Volt) shown in Figure 4.48 is activated. Thus, 14 Volt voltages from BATT B STORAGE are connected to DC to AC Inverter (LOAD AC) for AC load supply as shown in Figure 4.46.

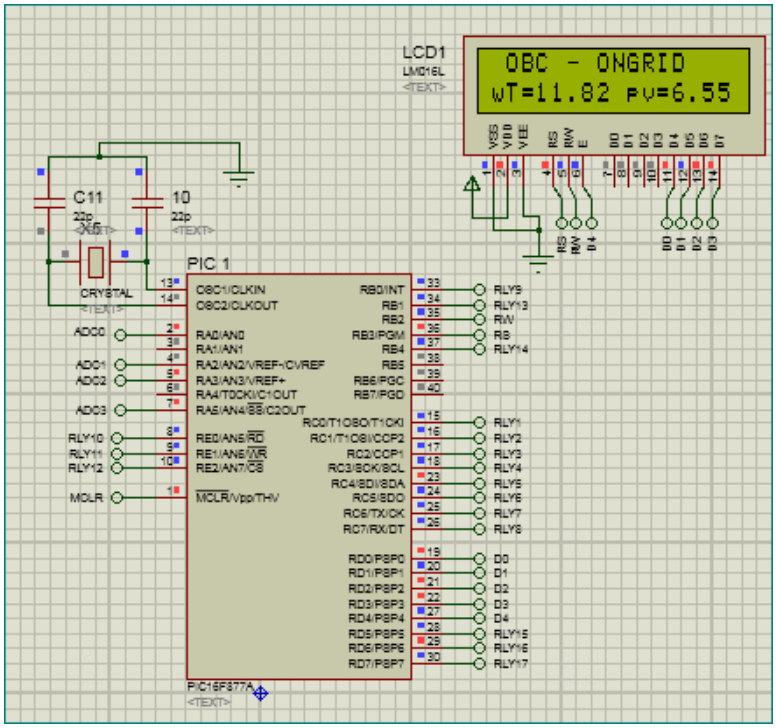

Figure 4.44: Microcontroller PIC16F877A – PORTS RC4 (RLY5)

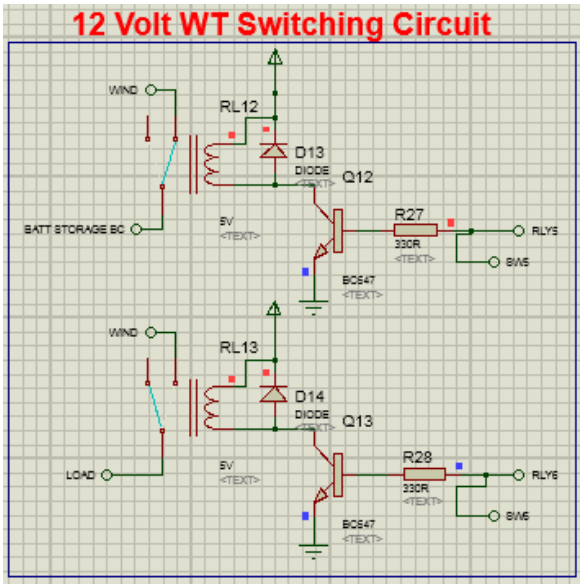

Figure 4.45: Relay switching and control module – PORT RC4 (RLY5)

Referring to Figure 4.44, none of BESS STORAGES are connected for charging process due to BESS STORAGES SoC is equal to 100% and BESS voltages are at 14 Volt as shown in Figure 4.47.

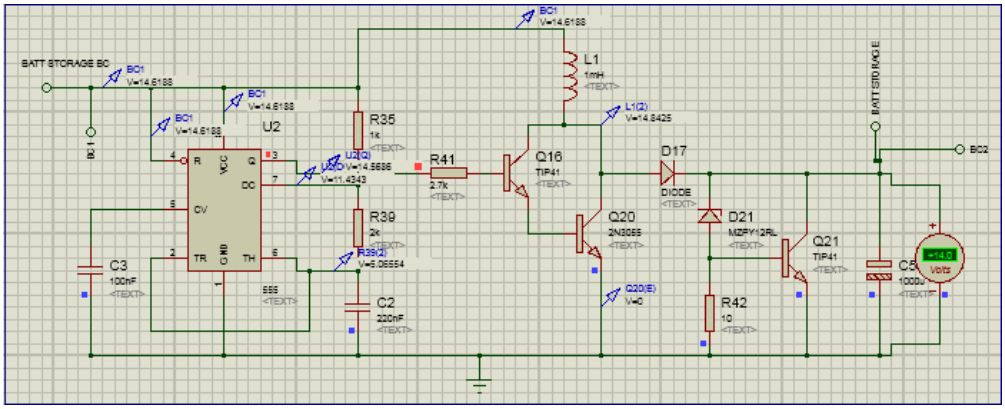

Figure 4.46: DC to DC BC output voltage

When BATT B discharging switching circuit (13 Volt) connected at RD6 (RLY16) as shown in Figure 4.48 is HIGH activated, BATT B STORAGE is supplying 14 Volt voltages to DC to AC Inverter (LOAD AC) for the connected AC load. The stepped-up and converted AC output voltage for the connected AC load is presented in Figure 4.49.

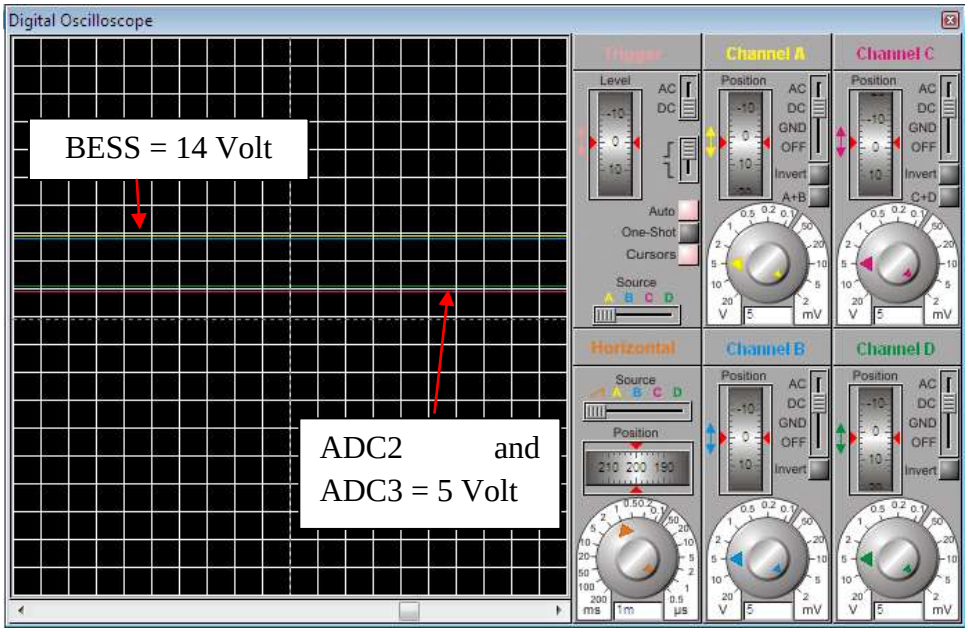

Figure 4.47: BESS STORAGES voltage and ADC channels status

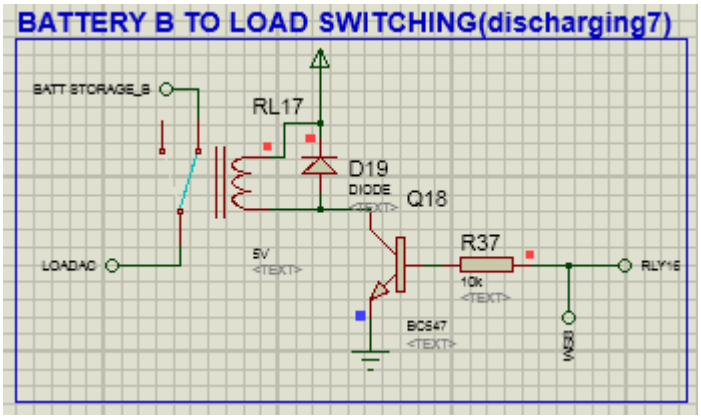

Figure 4.48: Relay switching and control module – PORT RD6 (RLY16)

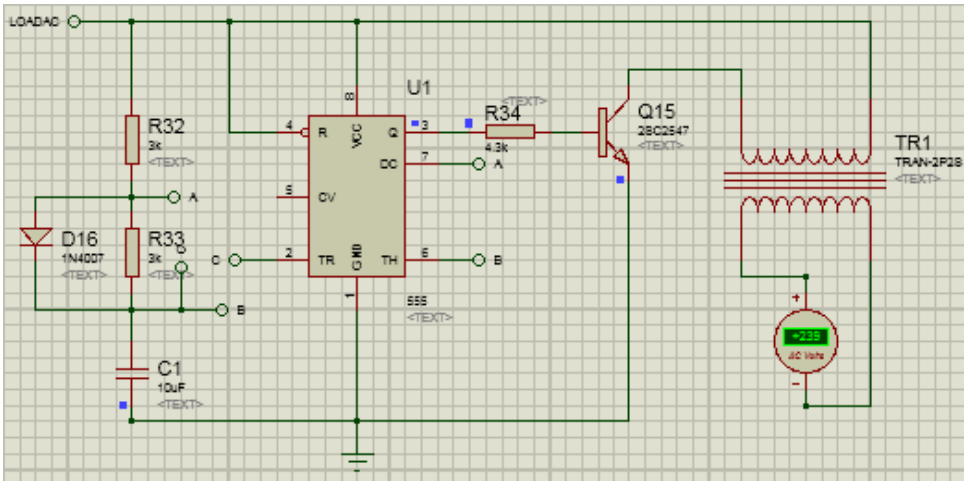

Figure 4.49: 15 VDC – 240 VAC – Inverter output

This section explains about stepping-up the 7~12 Volt regulated output voltage from renewable energy sources for BESS charging. The simulation results explained that the DC to DC BC has successfully managed to step-up the 7~12 Volt regulated output voltage to a desired output voltage. Also, real-time DC HRES hardware system have successfully able to step-up and convert the 7~12 Volt DC voltage from BESS STORAGES into an AC voltage for the connected AC load supply.

4.6.5 CONDITION E: PV = 0~7 Volt and WT = 0~7 Volt - DC HRES MODEL SIMULATION

Referring to Figure 4.50, the sensed and measured regulated output voltages from solar-wind renewable energy sources at PV and WT voltage based self-intervention are less than 7 Volt. Thus, referring to Figure 4.50, RC0 – RC7 ports assigned for solar-wind renewable energy sources are deactivated. Therefore, when there is no voltage source produced from solar-wind renewable energy sources, BESS will take over the task as the primary power source supply. Hence, BESS Discharging (DisCh) status shown in Figure 4.50 indicates the regulated output voltages from solar-wind renewable energy sources are less than 7 Volt and BESS is now the primary power source supply to the connected AC load.

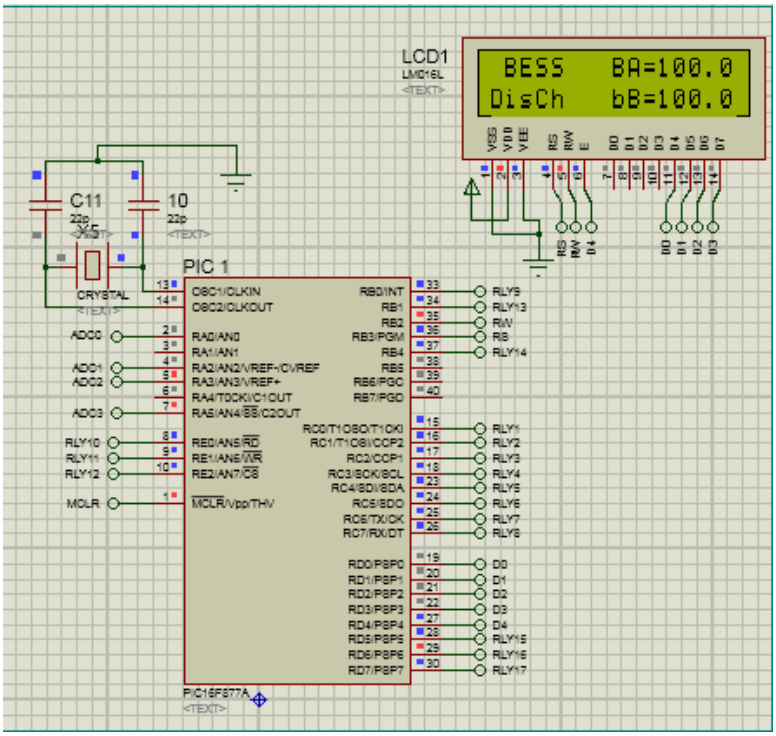

Figure 4.50: Microcontroller PIC16F877A – PORT RD6

(a) BATT A STORAGE SoC = 100% and BATT B STORAGE SoC = 100%

The BATT A STORAGE SoC and BATT B STORAGE SoC status is shown in Figure 4.50. The BA indicates BATT A STORAGE is not connected for charging and bB indicates BATT B STORAGE is connected for discharging at RD6 port at microcontroller PIC16F877A. The RD6 port HIGH activated signal captured using logic analyser is shown in Figure 4.51.

Before the power source is supplied to the connected AC load, voltage from BESS is stepped-up and converted into an AC voltage using DC to AC Inverter for the AC load. As shown in Figure 4.51, RD6 port at microcontroller PIC16F877A is HIGH activated. Referring to Figure 4.2 and Table 4.2, when RD6 port is HIGH activated, BATT B discharging switching circuit (13 Volt) shown in Figure 4.52 is HIGH activated. The relay is switched from NC to NO and connects the voltage from BATT B STORAGE to DC to AC Inverter (LOAD AC) for the connected AC load. Thus, the AC voltage output from the DC to AC Inverter for AC load is shown in Figure 4.53.

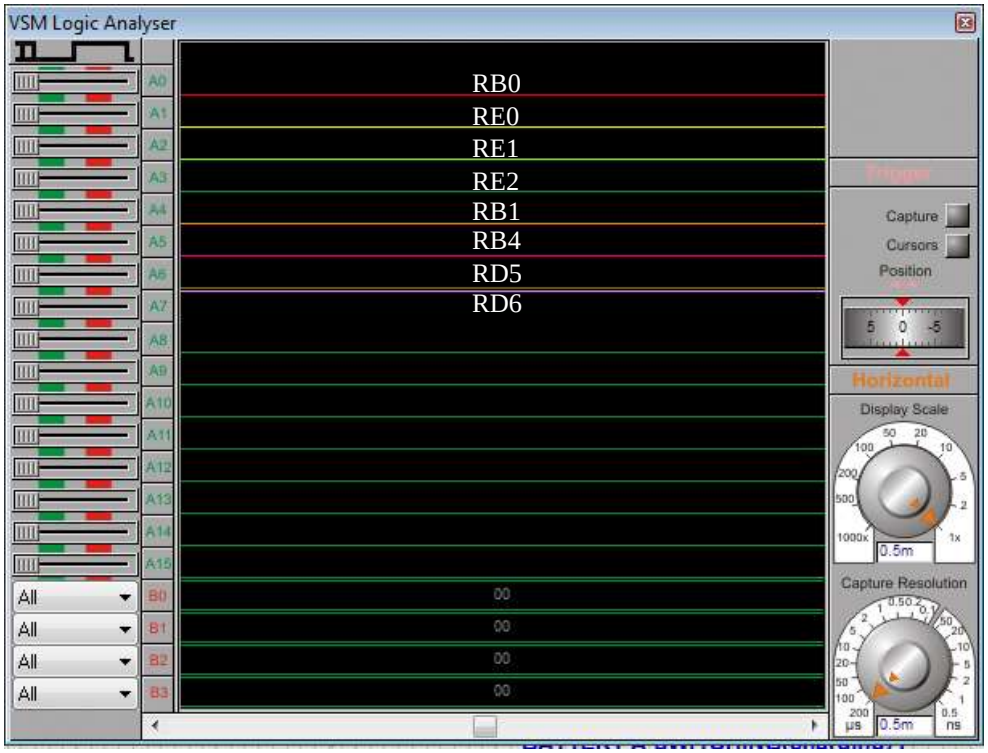

Figure 4.51: Logic analyser – HIGH activated signal at PORT RD6

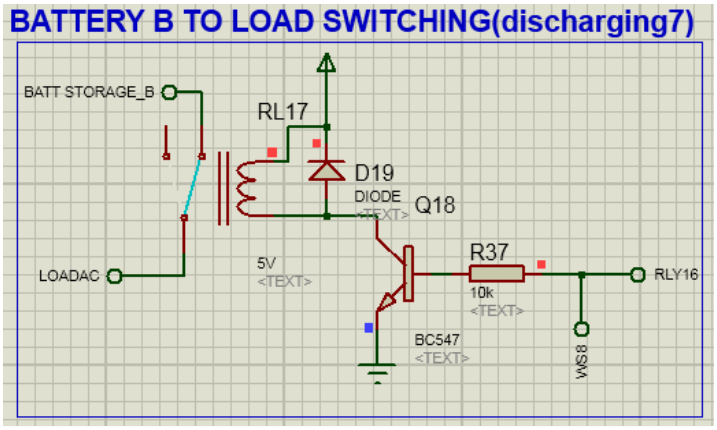

Figure 4.52: Charging/Discharging switching circuit - PORT RD6 (RLY16)

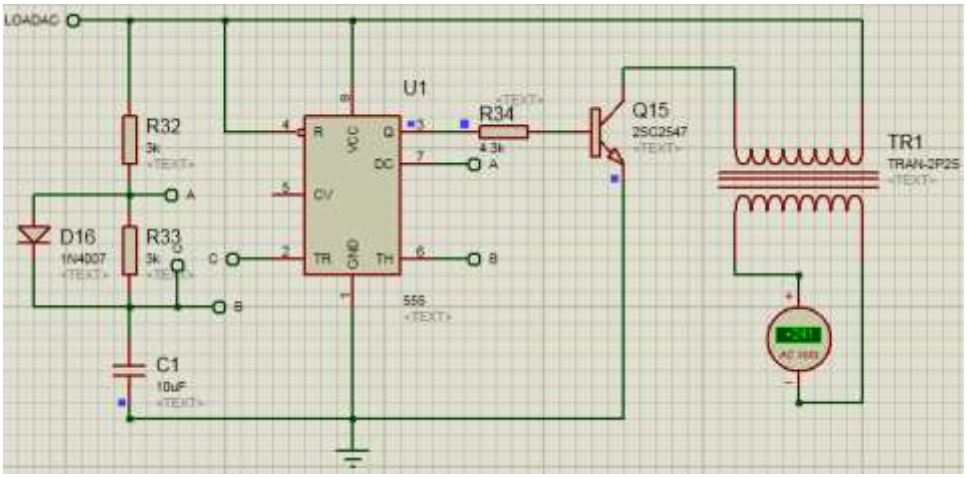

Figure 4.53: 15 VDC – 240 VAC – Inverter output

This section explains about the unavailability of the regulated output voltage from solar-wind renewable energy sources, BESS STORAGES are assigned as the primary power source supply for the connected AC load. The simulation results explained that the output voltages from BESS STORAGES are successfully stepped-up and converted into an AC voltage. Also, real-time DC HRES hardware system has successfully utilities the stored energy in BESS for AC load supply. Other than that, real-time DC HRES hardware system has successfully managed to coordinate the discharging process between BATT A STORAGE and BATT B STORAGE.

(b) BATT A STORAGE SoC = 100% and BATT B STORAGE SoC = 80%

The BATT A STORAGE SoC and BATT B STORAGE SoC status is shown in Figure 4.54. The bA indicates BATT A STORAGE is connected for discharging at RD5 port meanwhile BB indicates BATT B STORAGE is not connected for discharging at RD6 port of the microcontroller PIC16F877A. The HIGH activated signal captured using the logic analyser is shown in Figure 4.55 also shows that only RD5 port is activated.

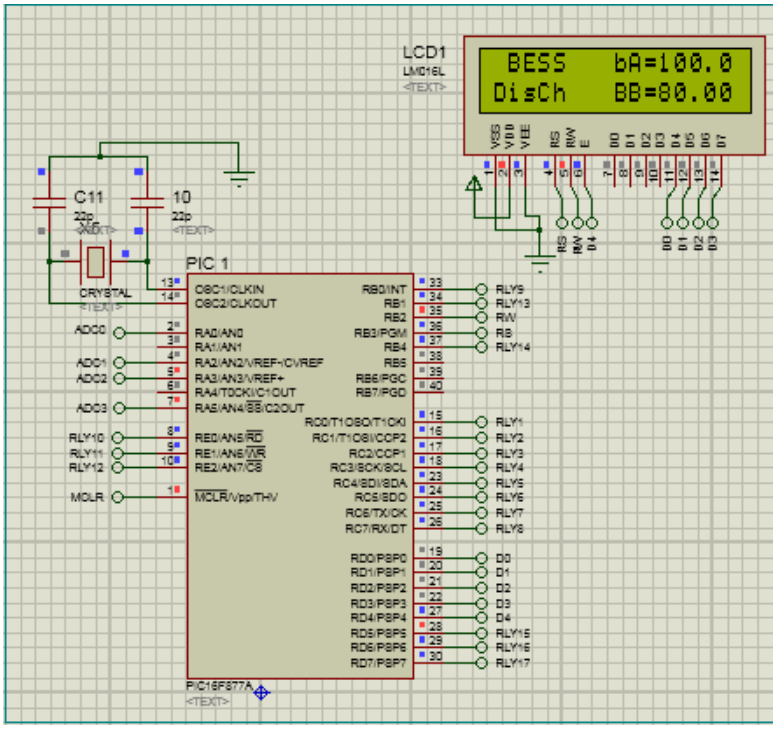

Figure 4.54: Microcontroller PIC16F877A – PORT RD5

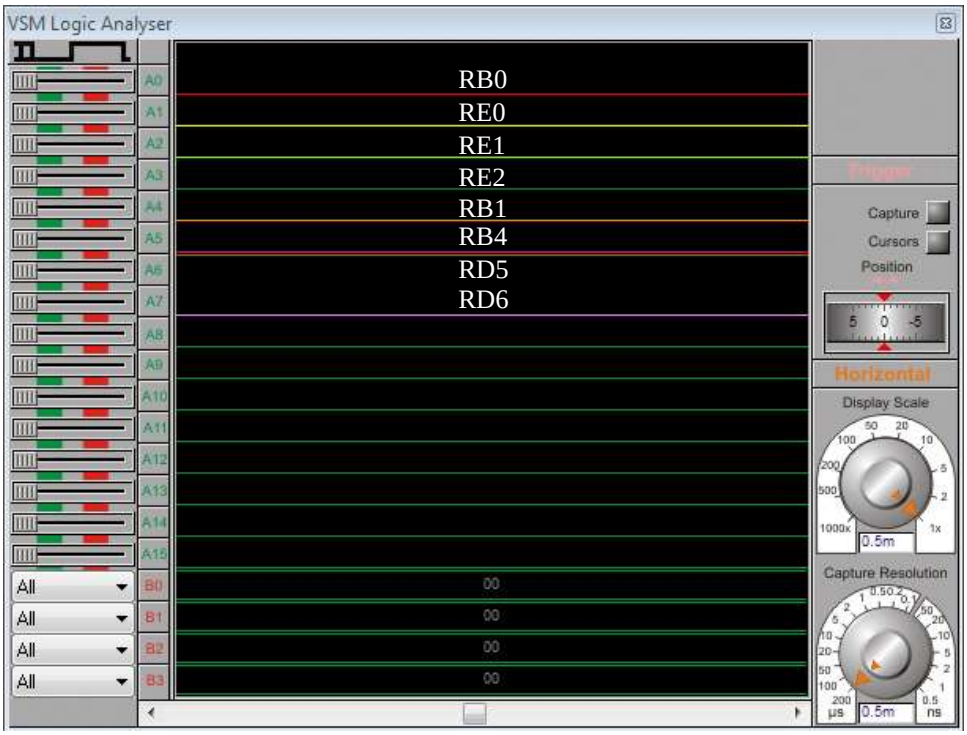

Figure 4.55: Logic analyser – HIGH activated signal at PORT RD5

When RD5 (RLY15) port is activated, then BATT A discharging switching circuit is connected to DC to AC Inverter (LOAD AC) as shown in Figure 4.56 for the connected AC load. Hence, the stepped-up and converted AC output voltage is shown in Figure 4.57.

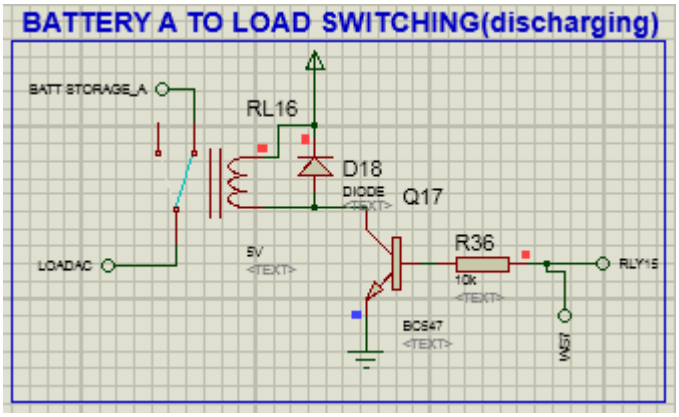

Figure 4.56: Charging/Discharging switching circuit - PORT RD5 (RLY15)

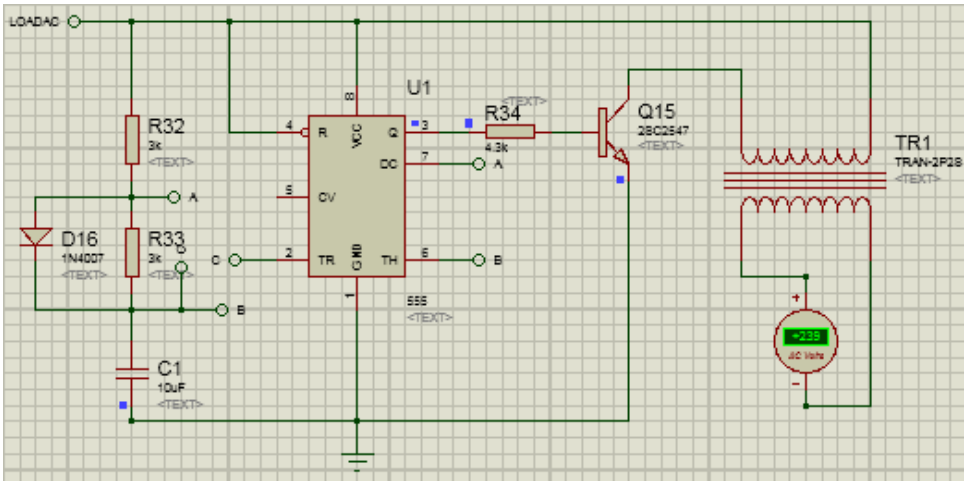

Figure 4.57: 15 VDC – 240 VAC – Inverter output

This section explains that the real-time DC HRES hardware system has successfully managed to coordinate the discharging process between BATT A STORAGE and BATT B STORAGE. Also, the stored energy is utilities successfully for AC load supply.

(c) BATT A STORAGE SoC = 60% and BATT B STORAGE SoC = 80%

The BATT A STORAGE SoC and BATT B STORAGE SoC status is shown in Figure 4.58. The BA indicates BATT A STORAGE is not connected for discharging at RD5 port and bB indicates BATT B STORAGE is connected for discharging at port RD6 at microcontroller PIC16F877A. The RD6 port HIGH activated signal captured using the logic analyser is shown in Figure 4.51.

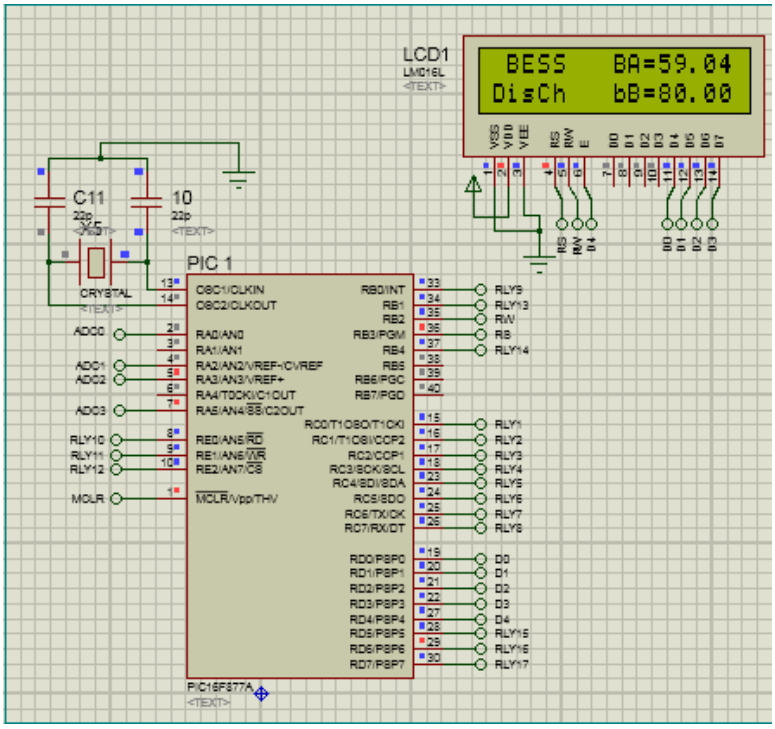

Figure 4.58: Microcontroller PIC16F877A – PORT RD6

(d) BATT A STORAGE SoC = 40% and BATT B STORAGE SoC = 40%

The BATT A STOARGE and BATT B STORAGE voltages status is shown in Figure 4.59. The wt and pv status indicates the BATT A STORAGE SoC and BATT B STORAGE SoC is equal or less than 40%. When the regulated output voltage from solar-wind renewable energy sources are between 0~7 Volt and BESS SoC are equal or less than 40% then real-time DC HRES hardware system is halted as shown in Figure 4.59.

When the halted condition occurs the real-time DC HRES hardware system will start system initialisation process. During the system initialisation process, PV and WT voltage based self-intervention circuits have to sense and measure 9 Volt regulated output voltage from solar-wind renewable energy sources. Then, the real-time DC HRES hardware system will start to operate as usual. When the real-time DC HRES hardware system is halted, then RD7 port connecting the GRID connection/LOAD switching circuit is HIGH activated. Thus, the AC load is switched to GRID connection/LOAD switching circuit for power source supply as shown in Figure 4.60.

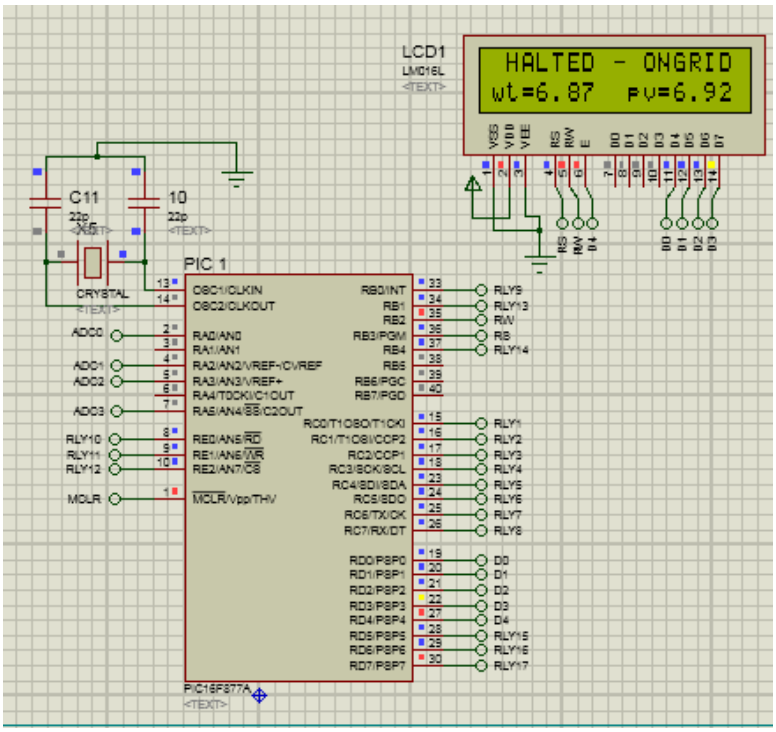

Figure 4.59: Microcontroller PIC16F877A – PORT RD7

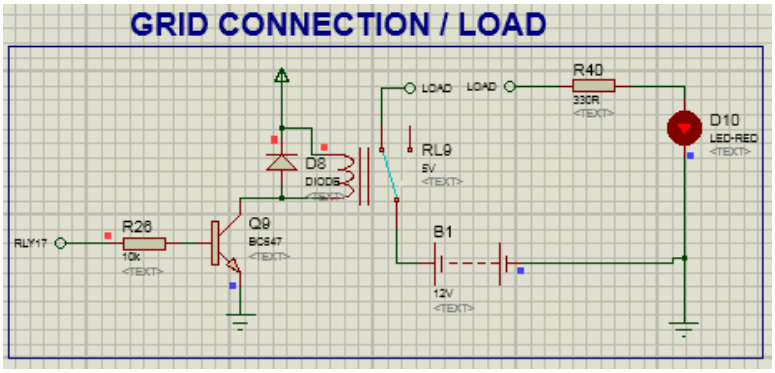

Figure 4.60: Grid connection/load switching circuit – PORT RD7 (RLY17)

This section explains that when there is no voltage source available from solar-wind renewable energy sources and BESS then the connected AC load is switched to grid network power source. Also, the simulation results show that real-time DC HRES hardware system has successfully managed to execute the task to switch to the grid network for power source when there is no source available.

4.7 SUMMARY

The modelling and simulation of real-time DC HRES hardware system circuitries using PROTEUS software is conducted to capture the results to analyse and validate the system operation and functionality as described in the research aim and objectives. The designed electronic circuits using PROTEUS software is used as reference to integrate, implement and construct the real-time DC HRES hardware system. These results are benchmarked with the results obtained from the testbed analysis conducted after the actual hardware system is implemented and constructed. Therefore, the testbed results, analysis and validation are presented in Chapter 6.

CHAPTER 5

EMBEDDED SOFTWARE APPLICATION ALGORITHM DEVELOPMENT – CCS C COMPILER

Chapter 4 describes about the design and development of real-time DC HRES hardware system using the PROTEUS software. The design and development of real-time DC HRES hardware system are composed of voltage based self-intervention, relay switching and control module and grid network or LOAD switching circuit subsystems. All of these subsystems are connected to microcontroller PIC16F877A for an effective supervision, coordination, management and controlling between all the subsystems. Hence, to effectively supervise, coordinate, manage and control all the subsystems using microcontroller PIC16F877A the algorithm developed using embedded software application is required to be incorporated into microcontroller PIC16F877A. Thus, Chapter 5 discusses about the continuous dynamic decision-making algorithm developed using PCWH CCS C Compiler embedded software application for implementation into microcontroller PIC16F877A. The continuous dynamic decision-making algorithm development is divided into four parts, which are the voltage based self-intervention, relay switching and control modules, BESS charging/discharging switching circuits and grid network or load switching circuit. Therefore, in the following section, each part of the continuous dynamic decision-making algorithm development is discussed and explained further.

5.1 VOLTAGE BASED SELF-INTERVENTION CONTINUOUS DYNAMIC DECISION- MAKING ALGORITHM

In order to perform the self-intervention between solar-wind renewable energy sources for energy management and optimisation using microcontroller PIC16F877A the embedded

software application algorithm is required. For energy output management and optimisation, microcontroller PIC16F877A can perform to achieve maximum system computational using the embedded software application. The PCWH CCS C Compiler embedded software application is used to develop the supervision, coordination, management and controlling instructions or functions for real-time DC HRES hardware system performances. The PCWH CCS C Compiler embedded software application is used as a platform to develop the continuous dynamic decision-making algorithm for the microcontroller PIC16F877A to interact with all the subsystems to perform the supervision, coordination, management and controlling as a real-time DC HRES hardware system.

The self-intervention between solar-wind renewable energy sources are performed based on the different conditions presented in Figure 5.1. According to Figure 5.1, each condition performs a task to manage and optimise the regulated output voltages from solar-wind renewable energy sources.

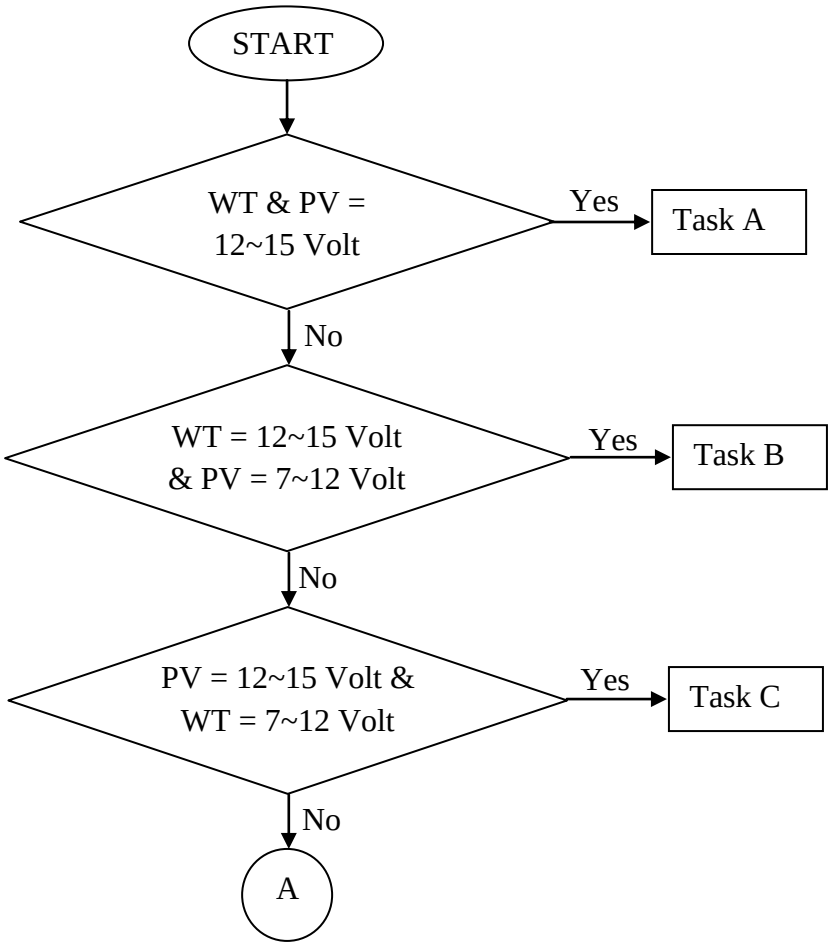

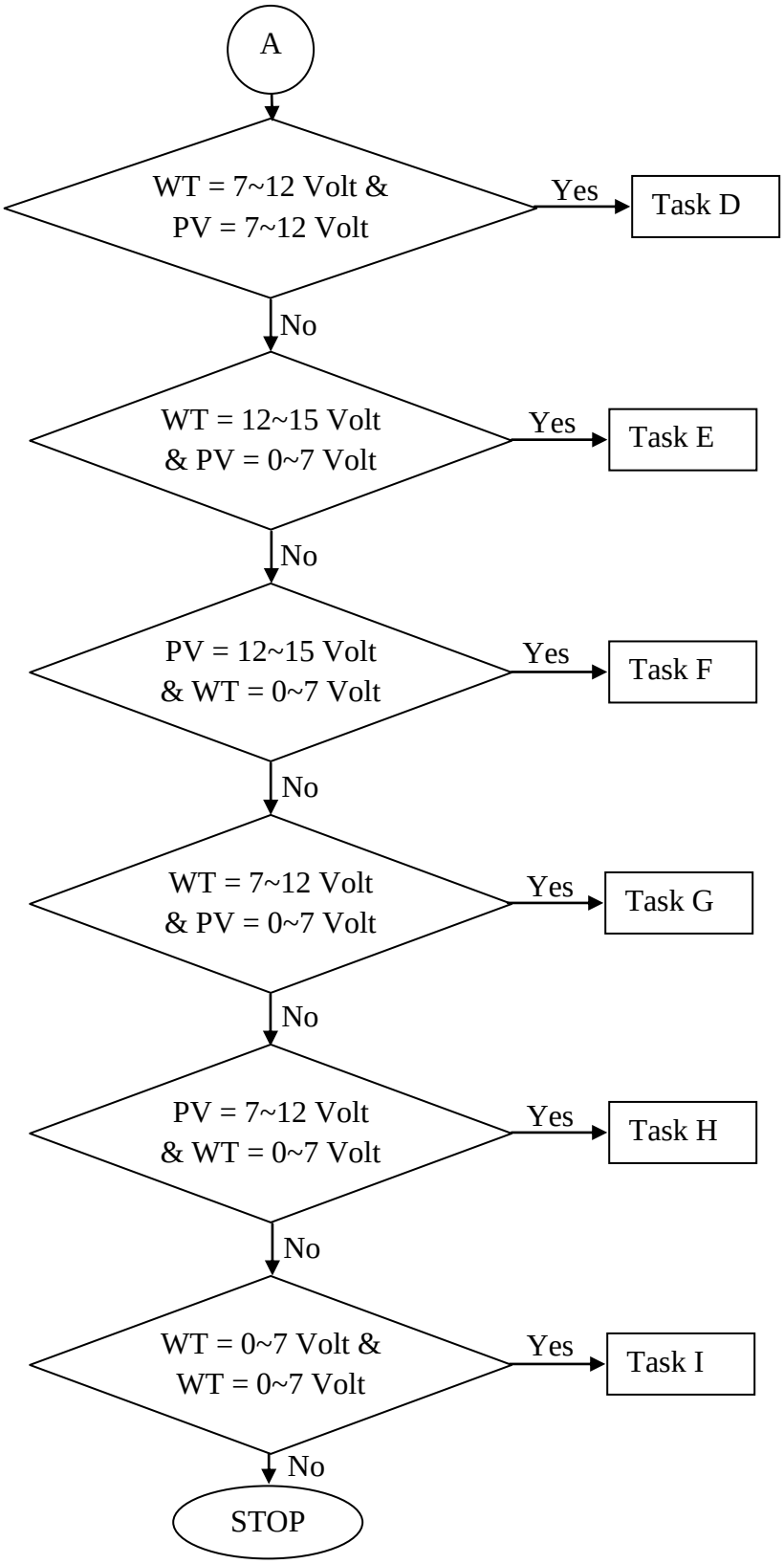

Figure 5.1: Voltage based self-intervention - embedded software application algorithm

Flow chart presented in Figure 5.1 describes about the operation of continuous dynamic decision-making algorithm to supervise coordinate, manage and control the real-time DC HRES hardware system using voltage based self-intervention. The continuous dynamic decision-making algorithm for real-time DC HRES hardware system consists of nine stages.

During the stage 1, the PV and WT regulated output voltages are between 12~15 Volt. Referring to Figure 4.1 in Chapter 4, when the PV voltage divider and WT voltage divider regulated output voltages are between 12~15 Volt then the ADC0 and ADC1 will sense and measure a voltage between 4~5 Volt reference voltages to execute task A.

The stage 2 have WT regulated output voltage between 12~15 Volt and PV regulated output voltage is between 7~12 Volt. Referring to Figure 4.1 in Chapter 4, when WT voltage divider regulated output voltage is between 12~15 Volt and PV voltage divider regulated output voltage is between 7~12 Volt then ADC0 will sense and measure a voltage between 4~5 Volt reference voltage and ADC1 will sense and measure a voltage between 2.33~4 Volt reference voltage to execute task B.

At stage 3, PV regulated output voltage is between 12~15 Volt and WT regulated output voltage is between 7~12 Volt. Referring to Figure 4.1 in Chapter 4, when PV voltage divider regulated output voltage is between 12~15 Volt and WT voltage divider regulated output voltage is between 7~12 Volt then ADC0 will sense and measure a voltage between 2.33~4 Volt reference voltage and ADC1 will sense and measure a voltage between 4~5 Volt reference voltage to execute task C.

At stage 4, WT and PV regulated output voltages are between 7~12 Volt. Referring to Figure 4.1 in Chapter 4, when WT voltage divider and PV voltage divider regulated output voltages are between 7~12 Volt, then ADC0 and ADC1 will sense and measure a voltage between 2.33~4 Volt reference voltages to execute task D.

During the stage 5, WT regulated output voltage is between 12~15 Volt and PV regulated output voltage is between 0~7 Volt. Referring to Figure 4.1 in Chapter 4, when WT voltage divider regulated output voltage is between 12~15 Volt and PV voltage divider regulated output voltage is between 0~7 Volt, then ADC0 will sense and measure a voltage between 4~5

Volt reference voltage and ADC1 will sense and measure a voltage between 0~2.33 Volt reference voltage to execute task E.

At stage 6, PV regulated output voltage is between 12~15 Volt and WT regulated output voltage is between 0~7 Volt. Referring to Figure 4.1 in Chapter 4, when PV voltage divider regulated output voltage is between 12~15 Volt and WT voltage divider regulated output voltage is between 0~7 Volt, then ADC0 will sense and measure a voltage between 0~2.33 Volt and ADC1 will sense and measure a voltage between 4~5 Volt reference voltage to execute task F.

During the stage 7, WT regulated output voltage is between 7~12 Volt and PV regulated output voltage is between 0~7 Volt. Referring to Figure 4.1 in Chapter 4, when WT voltage divider regulated output voltage is between7~12 Volt and PV voltage divider regulated output voltage is between 0~7 Volt, then ADC0 will sense and measure a voltage between 2.33~4 Volt reference voltage and ADC1 will sense and measure a voltage between 0~2.33 Volt reference voltage to execute task G.

During stage 8, PV regulated output voltage is between 7~12 Volt and WT regulated output voltage is between 0~7 Volt. Referring to Figure 4.1 in Chapter 4, when PV voltage divider regulated output voltage is between 7~12 Volt and WT voltage divider regulated output voltage is between 0~7 Volt, then ADC0 will sense and measure a voltage between 0~2.33 Volt reference voltage and ADC1 will sense and measure a voltage between 2.33~4 Volt reference voltage to execute task H.

At stage 9, WT and PV regulated output voltages are between 0~7 Volt. Referring to Figure 4.1 in Chapter 4, when WT voltage divider and PV voltage divider regulated output voltages are between 0~7 Volt, then output voltages from solar-wind renewable energy sources will be disconnected due to low voltage. At the same time, task I is executed.

At every stage, there is a specific task needs to be executed. Each task to be executed will receive a HIGH activated signal from microcontroller PIC16F877A for either switching ON or OFF the relay switching and control modules or charging/discharging switching circuit. The switching ON and OFF the relay switching and control modules will be either to supply the

power source to the connected AC load or to perform the charging/discharging process on the BESS. Hence, the following section discusses the relay switching and control modules execution base on each electronic circuit provided in Figure 4.1 and each task in Figure 5.1.

5.2 RELAY SWITCHING AND CONTROL MODULES – CONTINUOUS DYNAMIC DECISION-MAKING ALGORITHM

As mentioned in Chapter 4, the relay switching and control modules are used to perform the self-intervention between solar-wind renewable energy sources and BESS for charging or discharging. Nevertheless, the self-intervention can only be performed using the relay switching and control modules when a HIGH activated signal from microcontroller PIC16F877A is send to trigger the respective individual relay switching and control module. Hence, description and development of each task in Figure 5.1 using embedded software application for continuous dynamic decision-making algorithm is described and explained further. During the development of continuous dynamic decision-making algorithm, the operational instruction to perform the relay switching and control module that correspond to the received HIGH activated signal from microcontroller PIC16F877A is discussed.

Task A in Figure 5.1 is activated when WT and PV regulated output voltages are between 12~15 Volt. Therefore, referring to Figure 4.1 in Chapter 4 ports RC1 and RC2 at microcontroller PIC16F877A will send a HIGH activated signal to the NPN transistor's base to energise the relay coil. When the relay coil is energised, the relay will switch from NO to NC. Hence, 12~15 Volt regulated output voltage from WT switching circuit will supply the power source to DC to AC Inverter (LOAD AC). And, 12~15 Volt regulated output voltage from PV switching circuit will supply the power source to the BESS (BATT STORAGE).

Task B in Figure 5.1 is activated when WT regulated output voltage is between 12~15 Volt and PV regulated output voltage is between 7~12 Volt. Therefore, referring to Figure 4.1 in Chapter 4 ports RC1 and RC6 at microcontroller PIC16F877A will send a HIGH activated signal to the NPN transistor's base to energise the relay coil. When the relay coil is energised, the relay will switch from NO to NC. Hence, 12~15 Volt regulated output voltage from WT switching circuit will supply the power source to DC to AC Inverter (LOAD AC). And, 7~12

Volt regulated output voltage from PV switching circuit will supply the power source to DC to DC BC (BATT STORAGE BC).

Task C in Figure 5.1 is activated when PV regulated output voltage is between 12~15 Volt and WT regulated output voltage is between 7~12 Volt. Therefore, referring to Figure 4.1 in Chapter 4 ports RC3 and RC4 at microcontroller PIC16F877A will send a HIGH activated signal to the NPN transistor's base to energise the relay coil. When the relay coil is energised, the relay will switch from NO to NC. Hence, 12~15 Volt regulated output voltage from PV switching circuit will supply the power source to DC to AC Inverter (LOAD AC). And, 7~12 Volt regulated output voltage from WT switching circuit will supply the power source to DC to DC BC (BATT STORAGE BC).

Task D in Figure 5.1 is activated when the WT and PV regulated output voltage is between 7~12 Volt. Therefore, referring to Figure 4.1 in Chapter 4 ports RC5 and RC6 at microcontroller PIC16F877A will send a HIGH activated signal to the NPN transistor's base to energise the relay coil. When the relay coil is energised, the relay will switch from NO to NC. Hence, 7~12 regulated output voltages from the WT switching circuit and PV switching circuit will supply the power source to DC to DC BC (LOAD BC and BATT STORAGE) for the connected AC load and BESS charging process, if required.

Task E in Figure 5.1 is activated when WT regulated output voltage is between 12~15 Volt and PV regulated output voltage is between 0~7 Volt. Therefore, referring to Figure 4.1 in Chapter 4 port RC0 at microcontroller PIC16F877A will send a HIGH activated signal to the NPN transistor's base to energise the relay coil. When the relay coil is energised, the relay will switch from NO to NC. Hence, 12~15 Volt regulated output voltage from WT switching circuit will supply the power source to BESS (BATT STORAGE) for charging process, if required. Also, if BESS is less than 40% and is being charged, port RD7 at microcontroller PIC16F877A will also send a HIGH activated signal to switch the relay coil from NO to NC to turn on the grid network to supply the power source to the connected AC load.

Task F in Figure 5.1 is activated when the PV regulated output voltage is between 12~15 Volt and WT regulated output voltage is between 0~7 Volt. Therefore, referring to Figure 4.1 in Chapter 4 port RC2 at microcontroller PIC16F877A send a HIGH activated signal to the NPN

transistor's base to energise the relay coil. When the relay coil is energised, the relay will switch from NO to NC. Hence, 12~15 Volt regulated output voltage from PV switching circuit is supplied as power source to BESS (BATT STORAGE) for charging process, if required. Also, if BESS is less than 40% and is being charged, port RD7 at microcontroller PIC16F877A will send a HIGH activated signal to switch the relay coil from NO to NC to turn on the grid network for the connected AC load.

Task G in Figure 5.1 is activated when the WT regulated output voltage is between 7~12 Volt and PV regulated output voltage is between 0~7 Volt. Therefore, referring to Figure 4.1 in Chapter 4 port RC4 at microcontroller PIC16F877A will send a HIGH activated signal to the NPN transistor's base to energise the relay coil. When the relay coil is energised, the relay will switch from NO to NC. Hence, 7~12 Volt regulated output voltage from WT switching circuit will supply the power source to DC to DC BC (BATT STORAGE) for charging process, if required. Also, if BESS is less than 40% and is being charged, port RD7 at microcontroller PIC16F877A will send a HIGH activated signal to switch the relay coil from NO to NC to turn on the grid network for the connected AC load.

Task H in Figure 5.1 is activated when the PV regulated output voltage is between 7~12 Volt, and WT regulated output voltage is between 0~7 Volt. Therefore, referring to Figure 4.1 in Chapter 4 port RC6 at microcontroller PIC16F877A will send a HIGH activated signal to the NPN transistor's base to energise the relay coil. When the relay coil is energised, the relay will switch from NO to NC. Hence, 7~12 Volt regulated output voltage from PV switching circuit will supply the power source to DC to DC BC (BATT STORAGE) for charging process, if required. Also, if BESS is less than 40% and is being charged, port RD7 at microcontroller PIC16F877A will send a HIGH activated signal to switch the relay coil from NO to NC to turn on the grid network for the connected AC load.

Task I in Figure 5.1 is activated when the PV and WT regulated output voltage is between 0~7 Volt. In this case, BESS is given the priority to supply the power source to the connected AC LOAD only if the BESS SoC capacity is above 40%. Hence, referring to Figure 4.1 in Chapter 4 ports RD5, RD6, RE1 and RE2 at microcontroller PIC16F877A are connected to discharge BESS. When BESS SoC capacity is equal and above 90%, then port RE2 which connects the

BATT B discharging switching circuit is switched ON to supply the power source to the connected AC load. Otherwise, port RD6 will send a HIGH activated signal to allow the relay in BATT B discharging switching circuit to switch from NO to NC. In a different case, if BESS capacity is less than 40% then microcontroller PIC16F877A will not send a HIGH activated signal to any of the NPN transistor's base to energise the relay coil except for NPN transistor's base connected at port RD7. When the relay coil is energised, the relay is switched from NO to NC. During this condition, the connected load is solely dependent on the power supply from the grid network.

Concluding this section, tasks A to D shows that the real-time DC HRES hardware system efficiently operate when the solar-wind renewable energy sources are supplying the regulated output voltage as power source. During this period of operation either renewable energy sources supplying the power source is connected to the AC load or for BESS charging, if required. In spite of that, tasks E to H are the conditions when only one of the renewable energy sources is supplying the regulated output voltage as power source. In this situation, the available renewable energy source power source is only used to charge the BESS, if required. As mentioned in each condition description, when BESS is charging the AC load is connected to Grid network for power source. Task I is a condition when only BESS is available to supply the power source to the connected AC load, otherwise the load will be connected to the grid network. Therefore, this section discusses the continuous dynamic decision-making algorithm incorporation into the microcontroller PIC16F877A is divided into three stages and each stage effectively control, coordinate, manage and control the regulated output voltages from solar-wind renewable energy sources and BESS charging or discharging process. As each task have explained of its important for the development, integration, implementation and construction of real-time DC HRES hardware system, next section will explain further on BESS charging or discharging process.

5.3 BESS CHARGING/DISCHARGING – CONTINUOUS DYNAMIC DECISION-MAKING ALGORITHM

Reviewing Figure 4.1 in Chapter 4, the continuous dynamic decision-making algorithm is designed and developed to supervise, coordinate, manage and control each subsystem

effectively to operate the real-time DC HRES hardware system for energy management and system optimisation. Sections 5.1 and 5.2 explained the two important parts of real-time DC HRES hardware system which supervise, coordinate, manage and control the solar-wind renewable energy sources and BESS charging or discharging process. As the real-time DC HRES hardware system supervise, coordinate, manage and control the solar-wind renewable energy sources for supplying the power source to the connected AC load, it is also important to understand the BESS charging or discharging process base on the continuous dynamic decision-making algorithm. Hence, this section will explain the continuous dynamic decision-making algorithm embedded software application development for BESS charging or discharging process. The continuous dynamic decision-making algorithm development for the BESS charging or discharging is presented in Figures 5.2 and 5.3. The BESS discharging process is illustrated in Figure 5.2 and Figure 5.3 illustrates the BESS charging process. According to Figure 4.1, the charging or discharging switching circuits are divided into 12~15 Volt and 7~12 Volt.

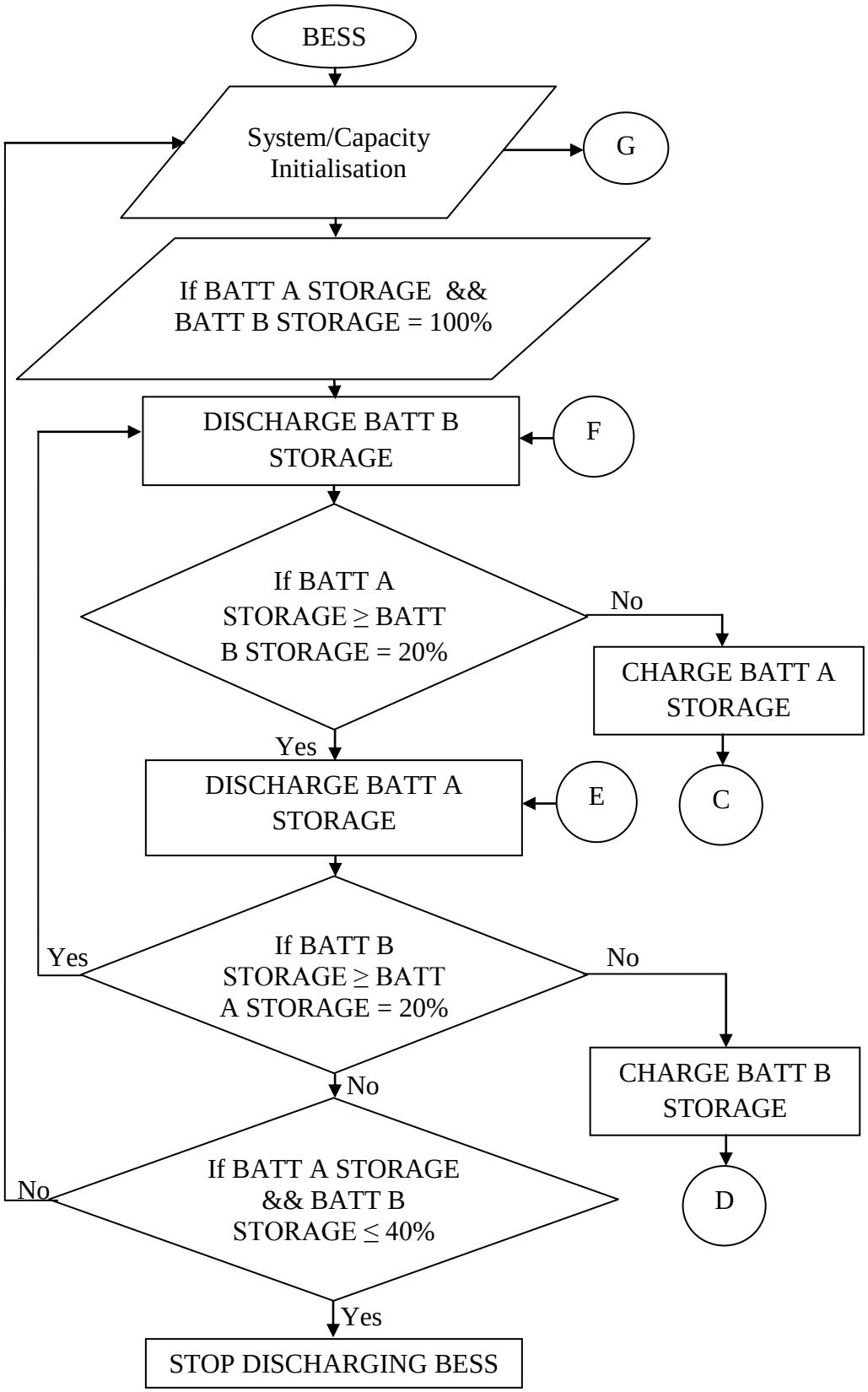

Figure 5.2: BESS discharging – continuous dynamic decision-making algorithm

5.3.1 BESS DISCHARGING – 13 Volt

This section explains about the BESS discharging process for 12~13 Volt regulated output voltage from BESS. Firstly, the continuous dynamic decision-making algorithm will always perform check and initialisation to sense and measure the BESS SoC. To sense and measure BESS voltage the batteries are respectively connected to the BATT A Voltage Divider and BATT B Voltage Divider. The BATT A Voltage Divider and BATT B Voltage Divider are known as voltage based self-intervention subsystem which acts to continuously sense and measure the voltage increment or decrement for each battery. Hence, the initialisation process is done to check the voltage information of each battery and this information is converted into the percentage of SoC. The SoC of each battery is determined using Equation (5.1).

$$\text{SoC} = \frac{\text{Actual Voltage}}{\text{Reference Voltage}} \times 100\% \tag{5.1}$$

where,

Actual Voltage = The measured voltage

Reference Voltage = System reference voltage

The battery information voltage is used to obtain the battery SoC during the battery charging or discharging process. This information is necessary to activate the charging or discharging switching circuit when it is required.

Looking at Figures 5.2 and 5.3, BESS SoC capacity initialisation process decides whether the BESS should be charging or discharging. The Figure 5.2 flow chart shows the capacity initialisation process that determines the BESS should be discharging when the BESS SoC is equal to 100%. The BATT B STORAGE is first discharged when both batteries SoC are equal to 100%. Referring to Figure 4.1, BATT B discharging switching circuit (13 Volt) is activated to start discharging BATT B STORAGE. When NPN transistor's base receives the HIGH activated signal from the microcontroller PIC16F877A, the relay coil is energised and the relay is switched from NO to NC. The +13 Volt from BATT B STORAGE is connected to the DC to AC Inverter (LOAD AC). The BATT B STORAGE is discharged 20% of its current

SoC, BATT B STORAGE discharging is stopped for charging process if there is regulated output voltage from solar-wind renewable energy sources. When BATT B STORAGE has stopped discharging, BATT A STORAGE is connected as power source supply to the connected AC load. Therefore, BATT A discharging switching circuit (13 Volt) is activated to start discharging BATT A STORAGE. The charging process between BATT A STORAGE and BATT B STORAGE is alternately continued if the regulated output voltages from solar-wind renewable energy sources is continuous available.

The discharging process between BATT A STORAGE and BATT B STORAGE continues till both of BESS SoC is equal or less than 40%. Once BESS SoC is equal or less than 40%, then the discharging process is stopped and at the same time, the continuous dynamic decision-making algorithm returns to system initialisation.

5.3.2 BESS DISCHARGING – 12 Volt

This section explains about the BESS discharging process for 12 Volt regulated output voltages from BESS. The continuous dynamic decision-making algorithm always performs checking and initialisation process to sense and measure the BESS SoC. When the sensed and measured voltage at the voltage based self-intervention is equal to or less than 12 Volt then the port RD5 at microcontroller PIC16F877A connecting BATT A Discharging Switching Circuit (12 Volt) and port RD6 at microcontroller PIC16F877A connecting BATT B Discharging Switching Circuit (12 Volt) is HIGH activated for BESS discharging process.

For discharging BESS during the battery voltage output equal or less than 12 Volt, BATT B STORAGE is first connected to discharge. Referring to Figure 4.1, BATT B discharging switching circuit (12 Volt) is HIGH activated to start discharging BATT B STORAGE. When the NPN transistor's base connected at port RD5 at microcontroller PIC16F877A receives HIGH activated signal, then the relay coil is energised and switch the relay from NO to NC. The +12 Volt from BATT B STORAGE is connected to DC to AC Inverter (LOAD AC). The BATT B STORAGE is discharged 20% of its current SoC, and then discharging BATT B STORAGE is stopped for charging if there is regulated output voltage from solar-wind renewable energy sources. When BATT B STORAGE stops discharging, BATT A STORAGE is connected as power source supply to the connected AC load. Therefore, the

BATT A discharging switching circuit (12 Volt) is HIGH activated to start discharging BATT A STORAGE. The charging process between the BATT A STORAGE and BATT B STORAGE is continued alternately if any regulated output voltages are available from the solar-wind renewable energy sources.

5.3.3 BESS CHARGING – 15 Volt

To start charging BESS, the continuous dynamic decision-making algorithm always perform the system or capacity initialisation. The system or capacity initialisation is an important task to check if there is any regulated output voltages available from solar-wind renewable energy sources. Therefore, if regulated output voltages are available from solar-wind renewable energy sources then BATT A Charging Switching Circuit (15 Volt) and BATT B Charging Switching Circuit (15 Volt) is alternately switched on to perform the BESS charging process.

Referring to Figure 5.3, if BATT A STORAGE and BATT B STORAGE is equal or less than 40%, then BATT A STORAGE is first charged upto 40% SoC and charging process is continued with BATT B STORAGE upto 40% SoC. When BATT A STORAGE starts charging the port RB0 at microcontroller PIC16F877A outputs a HIGH activated signal to BATT A Charging Switching Circuit (15 Volt). The HIGH activated signal is send to the NPN transistor's base, and then the relay coil is energised and switch the relay from NO to NC. When the BATT A STORAGE is charged upto 40% SoC then charging process is switched to BATT B Charging Switching Circuit (15 Volt). Thus, port RE0 at microcontroller PIC16F877A outputs a HIGH activated signal to the NPN transistor base. When the NPN transistor's base receives a HIGH activated signal, the relay coil is energised and switch the relay from NO to NC.

5.3.4 BESS CHARGING – 12 Volt

The process of charging BESS at 7~12 Volt regulated output voltage from solar-wind renewable energy sources have to be connected to DC to DC BC. The 7~12 Volt voltage is stepped-up to charge BESS. Therefore, for 7~12 Volt voltage, BATT A BC Charging Switching Circuit and BATT B BC Charging Switching Circuit is used to perform BESS charging as shown in Figure 4.1.

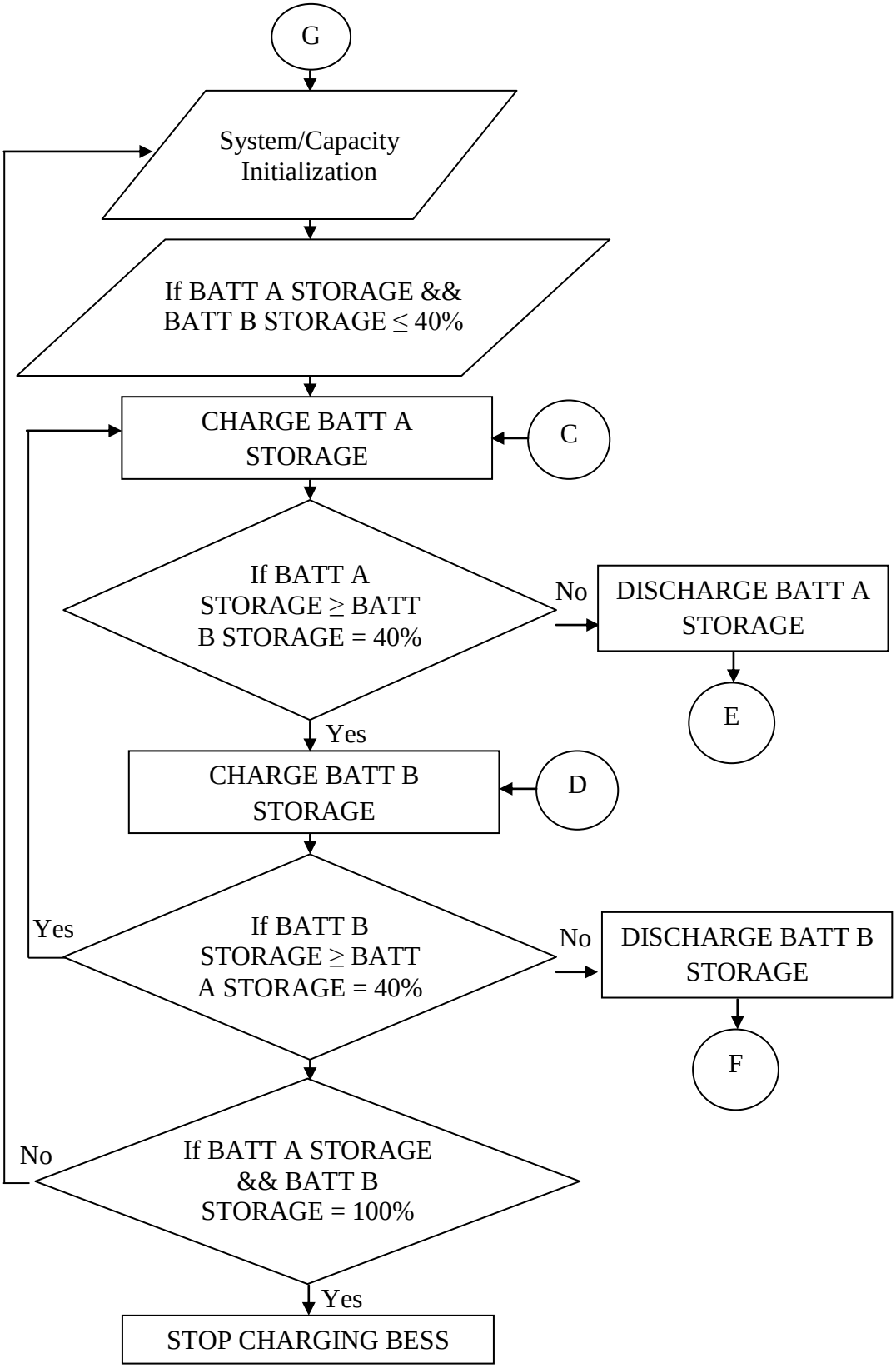

Figure 5.3: BESS charging – continuous dynamic decision-making algorithm

Referring to Figure 5.3, if BATT A STORAGE and BATT B STORAGE is equal or less than 40% then BATT A STORAGE is first charged up to 40% SoC and charging process is continued with BATT B STORAGE up to 40% SoC. Therefore, when BATT A STORAGE starts charging the port RB1 at microcontroller PIC16F877A outputs a HIGH activated signal to BATT A BC Charging Switching Circuit (12 Volt). The HIGH activated signal is send to the NPN transistor's base, and then the relay coil is energised and switch the relay from NO to NC. When BATT A STORAGE is charged up to 40% SoC then the charging process is switched to BATT B BC Charging Switching Circuit (12 Volt). Thus, port RB4 at microcontroller PIC16F877A outputs a HIGH activated signal to the NPN transistor's base. When NPN transistor base receives a HIGH activated signal, the relay coil is energised and switch the relay from NO to NC.

The charging process between BATT A STORAGE and BATT B STORAGE alternately continues till BESS SoC are equal to 100%. Once BESS SoC is equal to 100%, then charging process is stopped and at the same time, the continuous dynamic decision-making algorithm return to system or capacity initialisation.

5.4 SUMMARY

This chapter discusses about the continuous dynamic decision-making algorithm development for the microcontroller PIC16F877A using PCWH CCS C Compiler embedded software application. The development of continuous dynamic decision-making algorithm is divided into three stages. The stage 1 development is involving sensing and measuring the regulated output voltages at the PV voltage divider and WT voltage divider which is also known as voltage based self-intervention. At this stage also the regulated output voltages are converted into the digital voltage for the microcontroller PIC16F877A ADCs to perform the voltage based self-intervention between the solar-wind renewable energy sources. Stage 2 development is involving supervising and coordinating the PV and WT Switching Circuit switching based on the input voltage proportion equivalency presented in Figures 4.3 and 4.4. The PV or WT Switching Circuits switching are based on the HIGH activated signal from the microcontroller PIC16F877A which is send after a decision is made during the voltage sensing and measuring in stage 1. Therefore, the respective PV or WT Switching Circuits are switched

on to allow the real-time DC HRES hardware system to operate as discussed in tasks in Chapter 4. Stage 3 development is involving managing and controlling the power source switching to the AC load and BESS charging or discharging relays switching on. When stages 1 and 2 sends the desired outputs, the continuous dynamic decision-making algorithm makes a decision for either to connect the desired output to the connected AC load or BESS charging process. Also, when stages 1 and 2 are not active then the continuous dynamic decision-making algorithm is informed, and if stored energy in BESS is available, then the AC load is connected to the BESS for power source supply. Otherwise, the AC load is connected to the Grid network. The continuous dynamic decision-making algorithm is developed as an embedded software application for the microcontroller PIC16F877A. Therefore, the development process discussed in this chapter is a real implementation process into the microcontroller PIC16F877A. The analysis and results of continuous dynamic decision-making algorithm performances that correspond with the microcontroller PIC16F877A as real-time DC HRES hardware system are presented in Chapter 6.

CHAPTER 6

HARDWARE IMPLEMENTATION AND CONSTRUCTION – RESULTS, ANALYSIS, VALIDATION AND DISCUSSION

In Chapter 3 the simulation of the real-time DC HRES hardware system is conducted using the MATLAB Simulink/Stateflow software. Prior to the simulation, each subsystem is modelled to understand the components characteristic. Each subsystem is simulated to analyse and examine the subsystem simulation output results. The simulation output results examination is an important task to design the real-time DC HRES hardware system operational and functional methodology. As each model and simulation is described in Chapter 3, the presented simulation results in Chapter 3 which is based on the discussed methodology have successfully demonstrated the overall real-time DC HRES hardware system operation. Thus, the designed methodology using the MATLAB Simulink/Stateflow software is used as a fundamental methodology to construct the real-time DC HRES hardware system's electronic circuits for simulation in Chapter 4 using the PROTEUS software. The constructed electronic circuits are simulated using the PROTEUS software and the results are presented in Chapter 4. At the same time, to simulate the real-time DC HRES hardware system the microcontroller PIC16F877A need to be incorporated with an embedded software application. The embedded software application developed for the microcontroller PIC16F877A is described in Chapter 5. The development of the embedded software application for the real-time DC HRES hardware system operational and functionality is based on the fundamental and simulation methodology described in Chapters 3 and 4. Therefore, this chapter presents and explains the results of the real-time DC HRES hardware system that is constructed based on the presented

methodologies in Chapter 3, electronic circuits simulation in Chapter 4 and embedded software application in Chapter 5. The designed embedded software is included in the appendix for reference.

6.1 REAL-TIME DC HRES HARDWARE SYSTEM INTEGRATION

As the mathematical calculation, operation and functionality of all the subsystems are discussed and explained in Chapters 3 and 4, this section presents the integration, implementation and construction of the real-time DC HRES hardware system.

6.1.1 VOLTAGE BASED SELF-INTERVENTION (VOLTAGE DIVIDER)

The voltage based self-intervention hardware subsystem which is constructed based on the voltage divider concept is presented in Figure 6.1. The constructed hardware system is composed of four units of voltage based self-intervention for voltages sensing and measurement from the solar-wind renewable energy sources and BESS. As it is explained in Chapter 4, ADC0 and ADC2 is connected to sense and measure the regulated output voltages from the solar-wind renewable energy sources. Whereby, ADC3 and ADC5 are connected to sense and measure the voltages from the BESS (BATT A and BATT B STORAGES).

The configuration setup for the voltage based self-intervention hardware system explained in Chapters 3 and 4 is modelled and simulated using the MATLAB Simulink/Stateflow and PROTEUS electronic circuit software. The modelling and simulation results are presented in Chapters 3 and 4. Therefore, the presented results have successfully validated the modelling and simulation of all the subsystems, the methodology also can be used to implement and construct the real-time DC HRES hardware system.

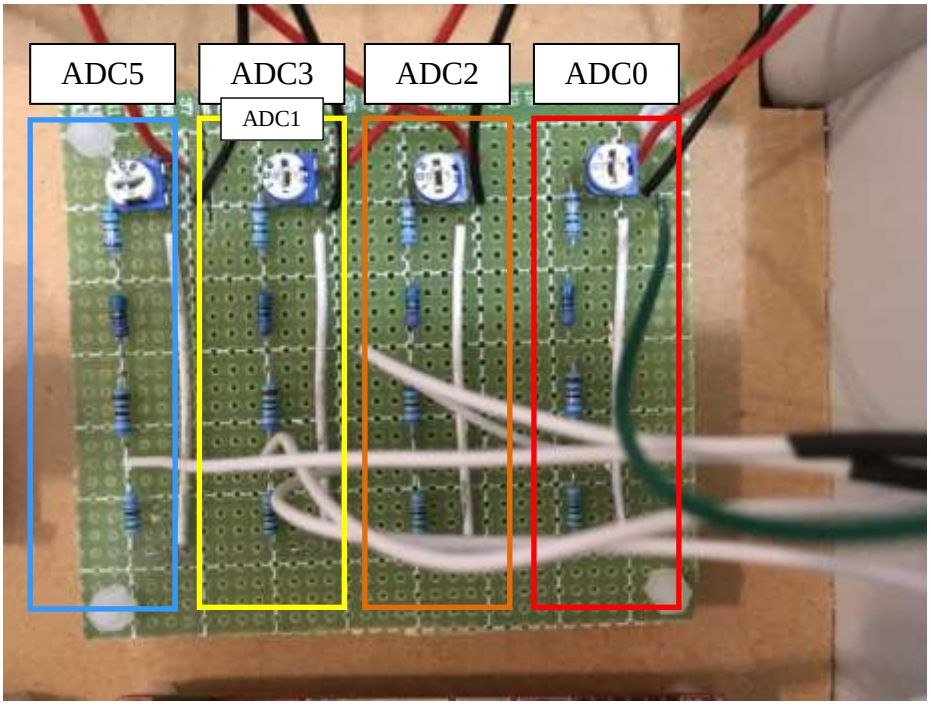

Figure 6.1: Voltage based self-intervention hardware subsystem

6.1.2 RELAY SWITCHING AND CONTROL MODULE – SOLAR-WIND RENEWABLE ENERGY SOURCES

The relay switching and control modules which are shown in Figure 6.2 are used to control different regulated output voltages from the solar-wind renewable energy sources. As it has been discussed in Chapters 3 and 4, Table 6.1 explains about the relay switching and control module connectivity for regulated output voltages from the solar-wind renewable energy sources.

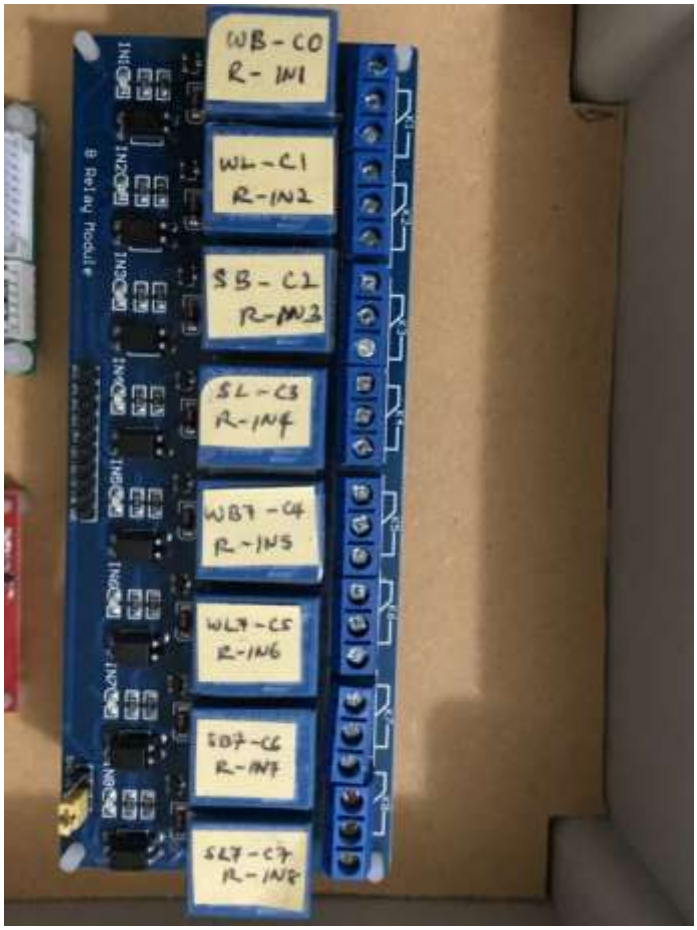

Figure 6.2: Relay switching and control module – solar-wind renewable energy sources

Looking at Table 6.1, each relay switching and control module is connected to a respective port at the microcontroller PIC16F877A. Referring to Table 6.1, overall there are eight relay switching and control modules connected to each respective port at microcontroller PIC16F877A.

Table 6.1: Relay switching and control modules connectivity – solar-wind renewable energy sources regulated output voltages

Regulated output voltages	Relay switching and control modules	Connectivity – Microcontroller PIC16F877A
12 Volt < WT ≤ 15 Volt	Wind BESS (WB)	PORT RC0
	Wind LOAD (WL)	PORT RC1
12 Volt < PV ≤ 15 Volt	Solar BESS (SB)	PORT RC2
	Solar LOAD (SL)	PORT RC3
7 Volt < WT ≤ 12 Volt	Wind BESS - 7 (WB7)	PORT RC4
	Wind LOAD - 7 (WL7)	PORT RC5
7 Volt < PV ≤ 12 Volt	Solar BESS - 7 (SB7)	PORT RC6
	Solar LOAD - 7 (SL7)	PORT RC7
240 VAC	GRID connection/LOAD switching circuit	PORT RD7

6.1.3 CHARGING/DISCHARGING SWITCHING CIRCUIT – BATT A STORAGE AND BATT B STORAGE

The charging/discharging switching circuits which are shown in Figure 6.2 is used to control different input and output voltages to or from BESS. As it has been discussed in Chapters 3 and 4, Table 6.2 explains about each charging/discharging switching circuit connectivity for the input and output voltages to or from BESS.

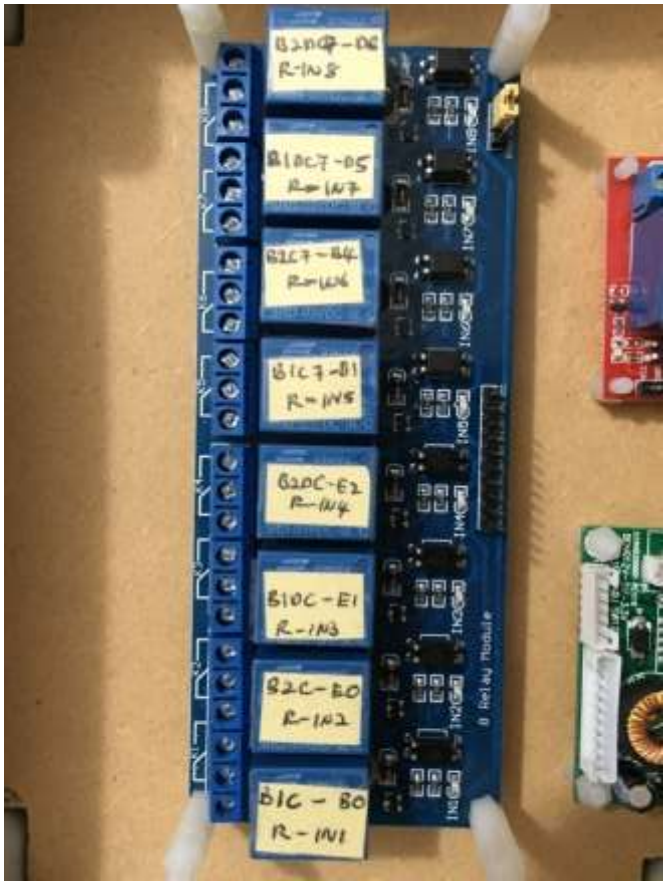

Figure 6.3: Charging/discharging switching circuit – BATT A STORAGE and BATT B STORAGE

Looking at Table 6.2, each charging/discharging switching circuit is connected to a respective port at the microcontroller PIC16F877A. Referring to Table 6.2, overall there are eight

charging/discharging switching circuits and each circuit is connected to a respective port at the microcontroller PIC16F877A.

Table 6.2: Charging/discharging switching circuits' connectivity – BATT A STORAGE and BATT B STORAGE

BESS	Charging/discharging switching circuit	Connectivity – Microcontroller PIC16F877A
BATT A STORAGE	BATT A STORAGE (B1C) - Charging	PORT RB0
	BATT A STORAGE (B1DC) - Discharging	PORT RE1
	BATT A STORAGE – 7 - (B1C7) - Charging	PORT RB1
	BATT A STORAGE – 7 - (B1DC7) - Discharging	PORT RD5
BATT B STORAGE	BATT B STORAGE (B2C) - Charging	PORT RE0
	BATT B STORAGE (B2DC) - Discharging	PORT RE2
	BATT B STORAGE – 7 - (B2C7) - Charging	PORT RB4
	BATT B STORAGE – 7 - (B2DC7) - Discharging	PORT RD6

The relay switching and control modules and charging/discharging switching circuits are arranged and integrated as shown in Figure 6.4. The top deck is referred to relay switching and control modules. While, lower deck is referred to the charging/discharging switching circuits.

Figure 6.4: Relay switching and control modules - charging/discharging switching circuits – integration

6.1.4 GRID CONNECTION/LOAD SWITCHING CIRCUIT

The grid connection/load switching circuit which is shown in Figure 6.5 is used as a switching mechanism to grid network. There are few conditions that are checked before the grid connection/load switching circuit is activated. The conditions are explained as in the following:

i. Only one renewable energy source regulated output voltage is available and BESS SoCs are equal or less than 40%.

ii. Both renewable energy sources regulated output voltages are not available and BESS SoCs are equal and below 40%.

When the microcontroller PIC16F877A detects either one or both of the the two conditions are activated, then the grid connection/load switching circuit which is connected at RD7 port of the microcontroller PIC16F877A will receive a HIGH signal to switch the relay from NC to NO. In other words, when condition (i) occurs the available regulated output voltage from any one of the renewable energy sources are used to charge the BESS, only if the BESS SoCs are equal or less than 40%. Otherwise, the BESS are the primary power source supply to the connected AC load. For the condition (ii), the connected AC load will fully dependent on the grid network for power source supply. In this sense, the connected AC load will be connected to the grid network till a reliable amount of voltage is available from either the renewable energy sources or the BESS STORAGES.

Figure 6.5: GRID connection/LOAD switching circuit

6.1.5 MICROCONTROLLER PIC16F877A SYSTEM DEVELOPMENT BOARD

The microcontroller PIC16F877A development board attached with LCD screen is shown in Figure 6.6. The LCD screen is used display the sensed and measured voltage values from the renewable energy sources and the BESS SoC values. The microcontroller PIC16F877A consists 33 input and output ports. Seventeen input and output ports are used to connect the relay switching and control modules shown in Figure 6.2, charging/discharging switching circuits shown in Figure 6.3 and grid connection/load switching circuit shown in Figure 6.5. The input and output ports that are used to construct the real-time DC HRES hardware system is shown in Tables 6.1 and 6.2.

Figure 6.6: Microcontroller PIC16F877A development board

6.1.6 OVERALL REAL-TIME DC HRES HARDWARE SYSTEM INTEGRATION, IMPLEMENTATION AND CONSTRUCTION

Real-time DC HRES hardware system integration, implementation and construction are presented in Figure 6.7. All the subsystems to construct the real-time DC HRES hardware system has been connected together to let the system to operate as a unit. The results of each

subsystem of the real-time DC HRES hardware system are recorded in Chapters 3 and 4 are used to analyse and validate the obtained results in Chapter 6.

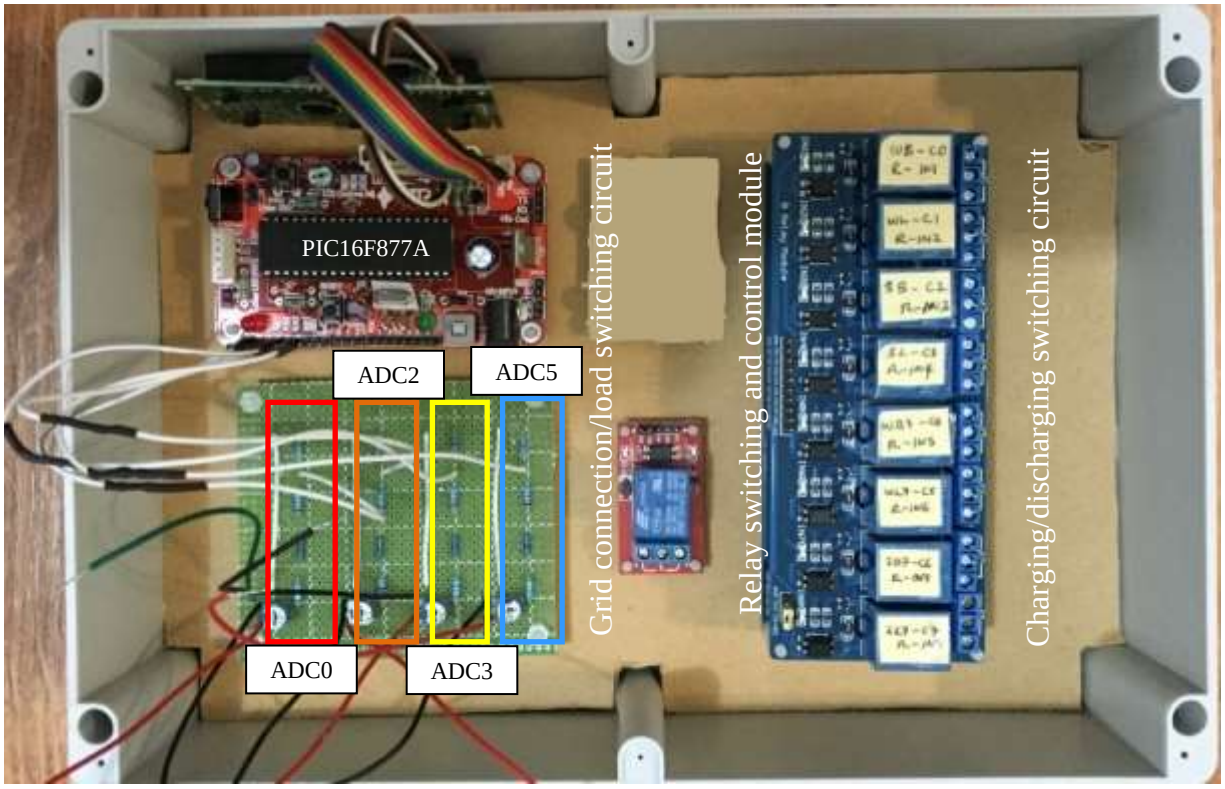

Figure 6.7: Overall real-time DC HRES hardware system integration, implementation and construction

6.2 REAL-TIME DC HRES HARDWARE SYSTEM RESULTS

This section presents and discusses the results obtained from the real-time DC HRES hardware system testing. Therefore, the obtained results are based on the conditions discussed in Chapters 3 and 4. The obtained results are analysed and validated based on the results obtained from the modelling and simulation in Chapters 3 and 4.

6.2.1 CONDITION A: PV = 12~15 Volt and WT = 12~15 Volt – REAL-TIME DC HRES HARDWARE SYSTEM

The sensed and measured solar-wind renewable energy sources regulated output voltages are shown in Figures 6.8 and 6.9. The LCD in Figure 6.8 show the BESS SoCs are at 99% and the

measured voltage reading is presented in Figure 6.10. As it is discussed in Chapter 4, wT status indicates the regulated output voltage from the wind renewable energy source is connected as a primary power source supply to the connected AC load. The PV status indicates the regulated output voltage from the solar renewable energy source is connected to charge the BESS, if required. The BA and BB indicate neither of the BESS is connected to perform the charging or discharging process. In this condition, the regulated output voltage from solar renewable energy source is being waste but this can be overcome with addition more BESS.

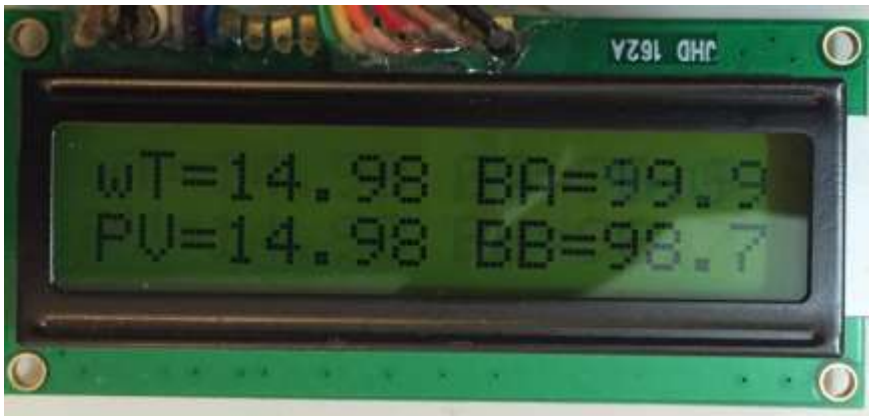

Figure 6.8: LCD reading – WT and PV = 12~15 Volt, BESS STORAGES SoC = 99%

The captured results using the logic analyser is shown in Figure 6.11 show that the channel 1 which is connected at RC1 port and channel 2 which is connected at RC2 port at the microcontroller PIC16F877A is HIGH activated. The HIGH activated at channel 1 show the regulated output voltage from the wind renewable energy source (wT) is directly connected to the DC to AC Inverter (LOAD AC) to produce an AC voltage for the connected AC load. Thus, relay WL – RC1 shown in Figure 6.12 is switched from NC to NO. Hence, the 12~15 Volt regulated output voltage from the wind renewable energy source is utilised as a primary power source supply for the connected AC load. The HIGH activated at channel 2 show the regulated output voltage from the solar renewable energy source (PV) is directly connected to charge the BESS, if required. Thus, relay SB – RC2 shown in Figure 6.12 is switched from NC to NO. Even though the SB – RC2 relay is switched from NC to NO as shown in Figure 6.12, the 12~15 Volt regulated output voltage from solar renewable energy source is not

connected to perform BESS charging. This can be observed through the LOW signal at channels 8 ~15 in Figure 6.11 and captured charging/discharging switching circuits status shown in Figure 6.13.

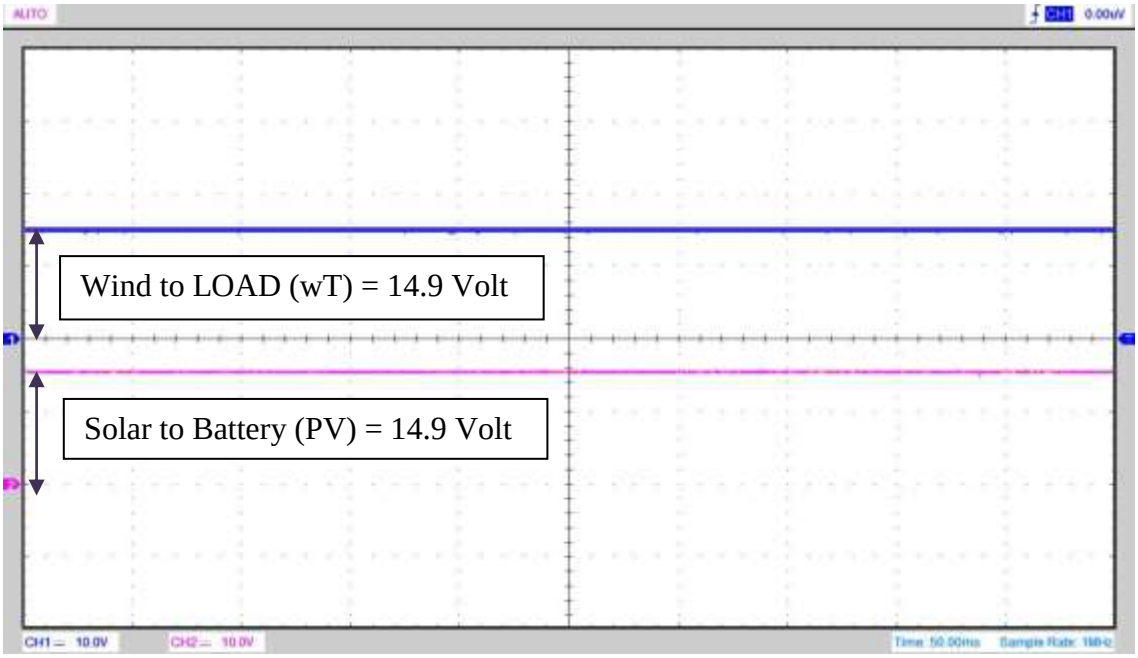

Figure 6.9: Oscilloscope voltage reading - WT and PV = 12~15 Volt

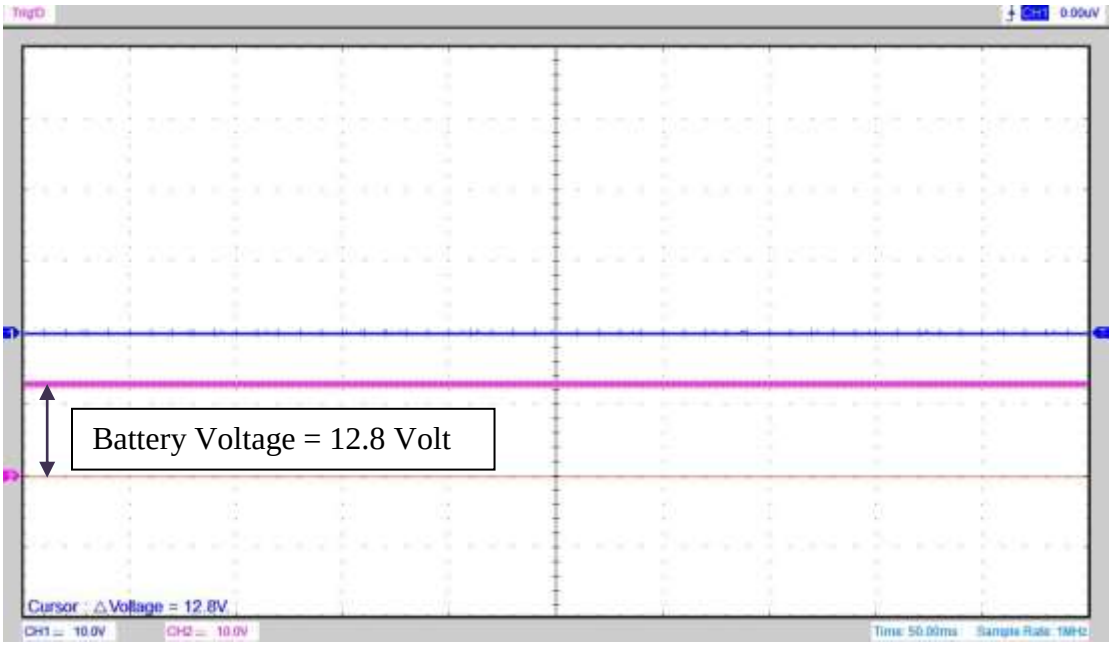

Figure 6.10: Oscilloscope voltage reading – BESS = 12.8 Volt

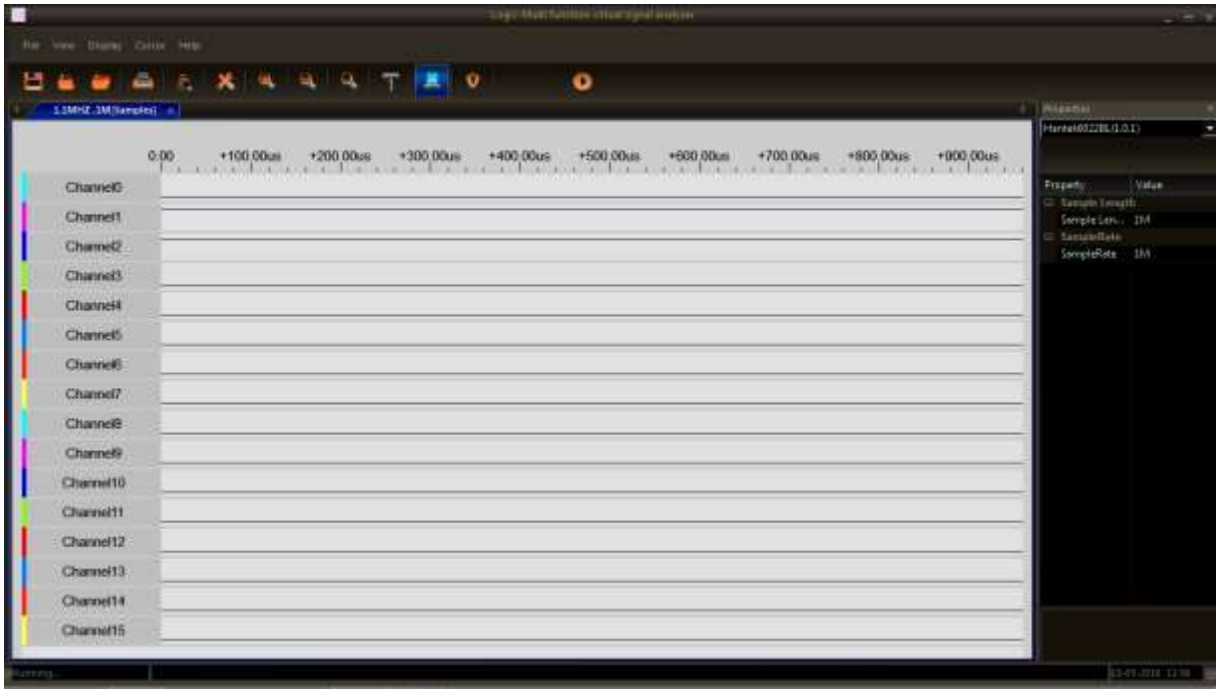

Figure 6.11: Logic analyser results (Channel 1 = wT – Relay IN2 and Channel 2 = PV – Relay IN3)

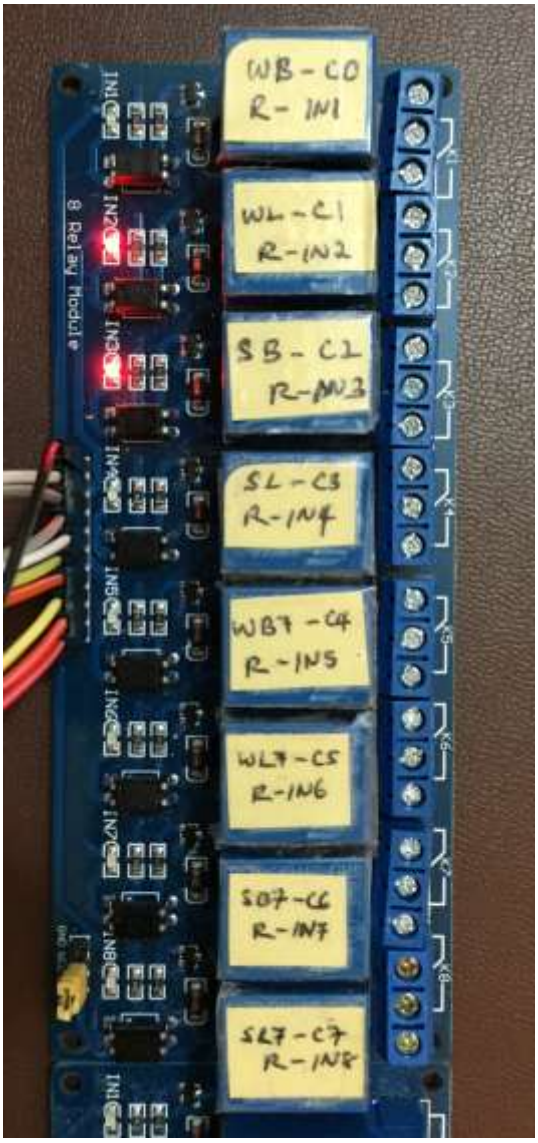

Figure 6.12: Relay switching and control modules – WL-RC1 and SB-RC2

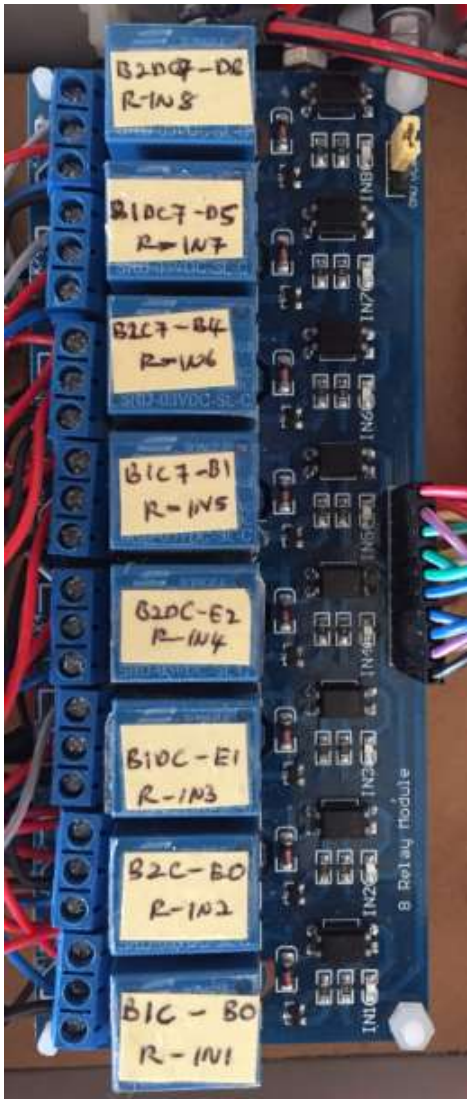

Figure 6.13: Charging/discharging switching circuits

Reviewing the obtained results, the voltage based self-intervention have successfully demonstrated the voltage sensing and measuring for the regulated output voltages from the solar-wind renewable energy sources. Also, the developed embedded software application incorporated into the microcontroller PIC16F877A has effectively perform the mathematical operation to sense and measure (a) the regulated output voltages from solar-wind renewable energy sources and (b) BESS SoC. In line with that also, the embedded software application incorporated into the microcontroller PIC16F877A have successfully demonstrated the coordination and switching of the respective relays based on the sensed and measured regulated output voltages amount. It show the real-time DC HRES hardware system priorities

the regulated output voltages from renewable energy sources as a power source supply for the connected AC load. This presented result in this section is validated with the obtained results in Chapter 4 section 4.6.1 (a).

(a) BATT A STORAGE SoC = 100% and BATT B STORAGE SoC = 80%

The sensed and measured solar-wind renewable energy sources regulated output voltages are shown in Figures 6.9 and 6.14. The LCD in Figure 6.14 also shows the BATT A STORAGE SoC is equal to 99% and BATT B STORAGE SoC is equal to 79%. The sensed and measured voltage reading is presented in Figure 6.10. As it is mentioned, wT and PV status shown in Figure 6.14 has been explained in the previous section. In this section the utilisation of PV for BESS charging process is discussed. As it is shown in Figure 6.14, bA indicates the BATT A STORAGE is connected to perform discharging process and BB indicates the BATT B STORAGE is connected to perform charging process. Based on the developed embedded software application incorporated in microcontroller PIC16F877A, when the BATT B STORAGE SoC is 20% equal or less than BATT A STORAGE SoC, then the 12~15 Volt regulated output voltage from the solar renewable energy source is connected to the BATT B STORAGE for charging process.

Figure 6.14: LCD reading – wT and PV = 12~15 Volt, BATT A STORAGE SoC = 99% and BATT B STORAGE SoC = 79%

Looking at Figure 6.15, channels 1 and 2 are HIGH activated and respectively are connected to the AC load as a primary power source supply and BESS for charging process, if required.

In this condition, the BATT B STORAGE SoC is 20% equal or less then BATT A STORAGE, hence, BATT B STORAGE is connected for charging process. Analysing Figure 6.15, channel 9 which is connected at RE0 port at the microcontroller PIC16F877A measure a HIGH activated signal. This indicates BATT B STORAGE (B2C) charging switching circuit is switched on to charge the battery. Thus, B2C-RE0 relay shown in Figure 6.16 is switched from NC to NO. Hence, the 12~15 Volt regulated output voltage from the solar renewable energy source is utilised to charge BATT B STORAGE as shown in Figure 6.17. According to Figure 6.16, BATT A STORAGE (B1DC) charging switching circuit is not switched ON because there is regulated output voltage available from the wind renewable energy source which is connected to the load as power source supply.

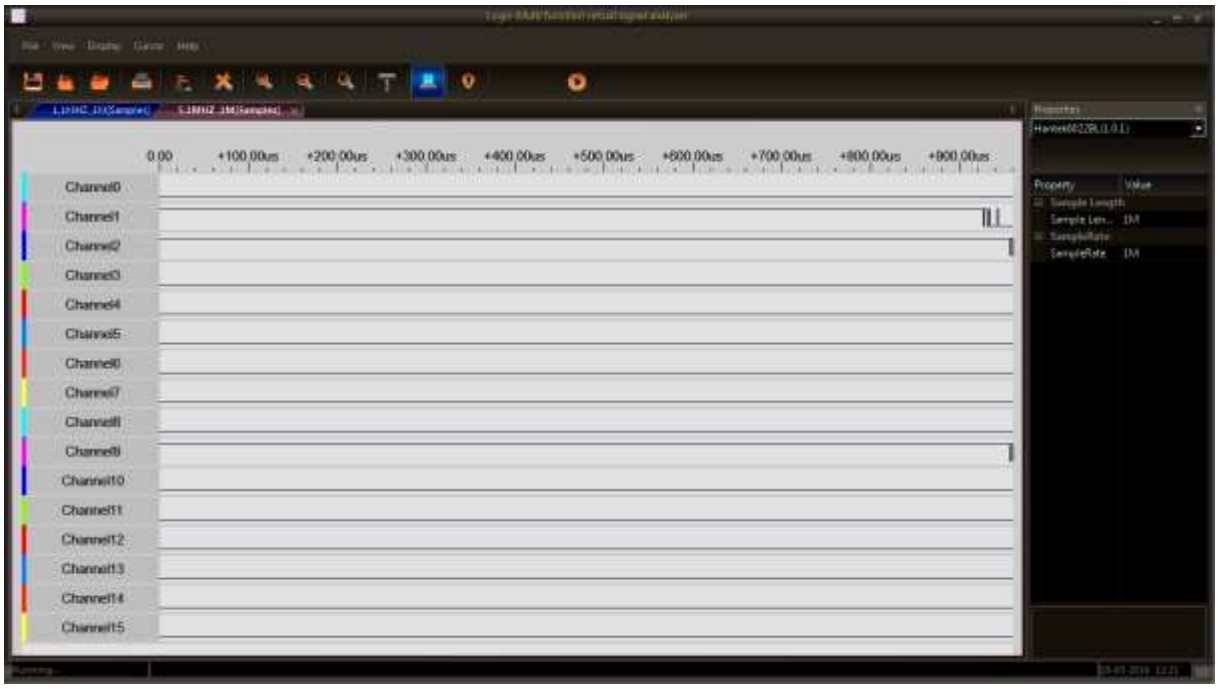

Figure 6.15: Logic analyser results (Channel 1 = wT – Relay IN2, Channel 2 = PV – Relay IN3 and Channel 9 = BATT B STORAGE – Relay IN2)

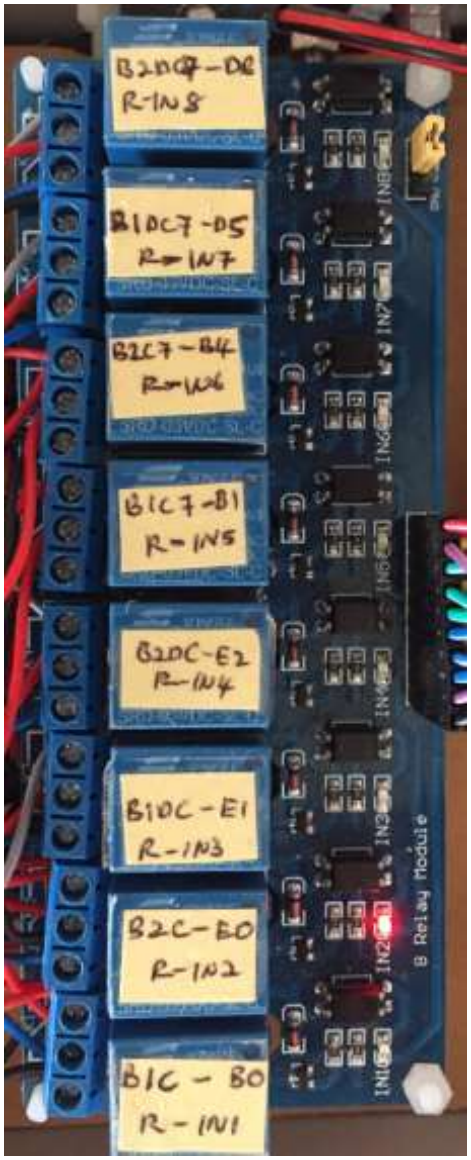

Figure 6.16: Charging/discharging switching circuit – B2C-RE0 (Relay IN2)

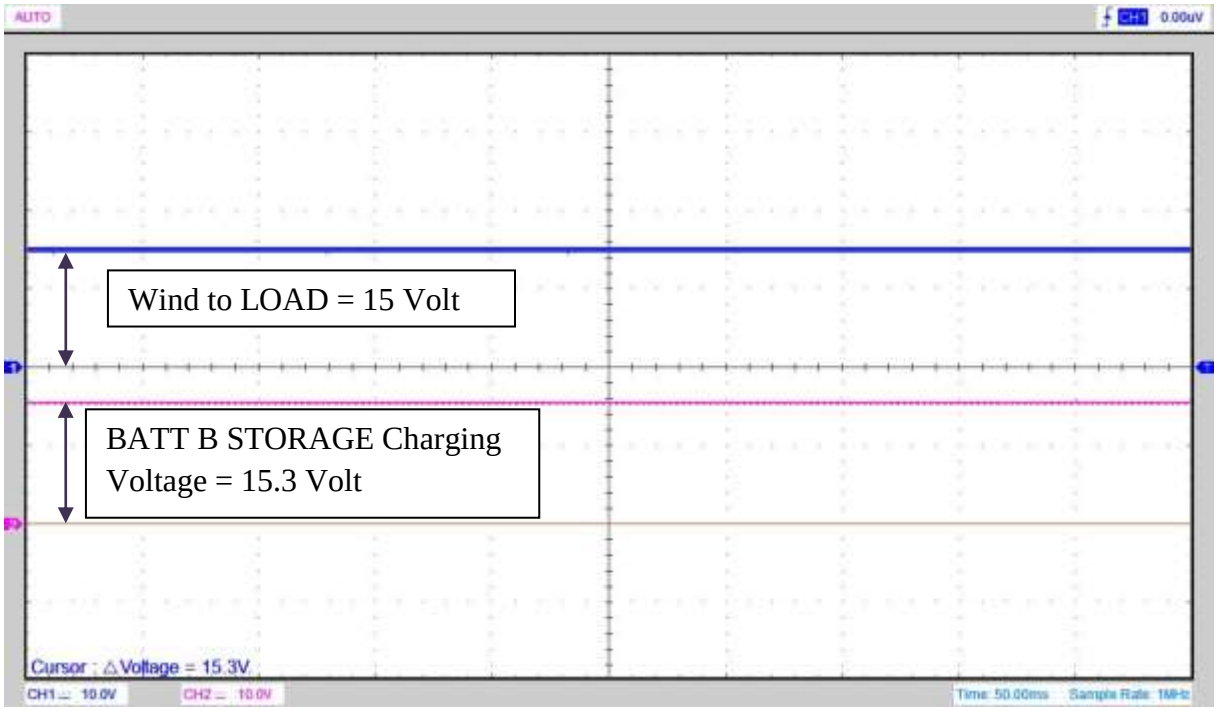

Figure 6.17: Oscilloscope voltage reading - WT = 12~15 Volt and BATT B STORAGE = 15.3 Volt

Reviewing the obtained results in this section, the voltage based self-intervention has successfully demonstrated the voltage sensing and measurement for the output voltages from BESS. The embedded software application incorporated in the microcontroller PIC16F877A have successfully performed the mathematical calculation and operation to convert BESS voltage reading into the percentages as shown in Figure 6.14. Also, the embedded software application have successfully coordinate and manage the switching between the charging/discharging switching circuits for charging or discharging process of BATT B STORAGE when BATT B STORAGE SoC status show 20% equal or less than BATT A STORAGE SoC. The presented results for this section can be validated with the results obtained in Chapter 4 section 4.6.1 (b).

(b) BATT A STORAGE SoC = 72% and BATT B STORAGE SoC = 93%

The sensed and measured solar-wind renewable energy sources regulated output voltages are shown in Figures 6.9 and 6.18. The LCD in Figure 6.18 show BATT A STORAGE SoC is equal to 72% and BATT B STORAGE SoC is equal to 93%. Referring to Figure 5.2, when BATT A STORAGE SoC is 20% equal or less than BATT B STORAGE SoC, then BATT A STORAGE is connected for charging process. The utilisation of wT and PV is explained in the previous section. Therefore, this section will discuss the utilisation of PV for charging the BATT A STORAGE. As it is shown in Figure 6.18, the BA is indicating that the BATT A STORAGE is connected for charging process and bB is connected to perform the discharging process. Based on the developed embedded software application incorporated in the microcontroller PIC16F877A, when the BATT A STORAGE SoC is 20% equal or less than BATT B STORAGE SoC, then the 12~15 Volt regulated output voltage from the solar renewable energy source is connected to the BATT A STORAGE for charging process.

Figure 6.18: LCD reading – wT and PV = 12~15 Volt, BATT A STORAGE SoC = 72% and BATT B STORAGE SoC = 93%

Looking at Figure 6.19, channels 1 and 2 are HIGH activated and respectively are connected to the AC load as a primary power source supply and BESS for charging process, if required. In this condition, the BATT A STORAGE SoC is 20% equal or less than BATT B STORAGE, hence, the BATT A STORAGE is connected for charging process. Analysing the Figure 6.19, channel 8 which is connected at RB0 port at the microcontroller PIC16F877A measure a HIGH activated signal. This indicates that the BATT A STORAGE (B1C) charging

switching circuit is switched on to charge the battery. Thus, B1C-RB0 relay shown in Figure 6.20 is switched from NC to NO. Hence, the 12~15 Volt regulated output voltage from solar renewable energy sources is utilised to charge the BATT A STORAGE as shown in Figure 6.17. According to Figure 6.20, BATT B STORAGE (B2DC) charging switching circuit is not switched ON because there is regulated output voltage available from the wind renewable energy source which is connected to the load as power source supply.

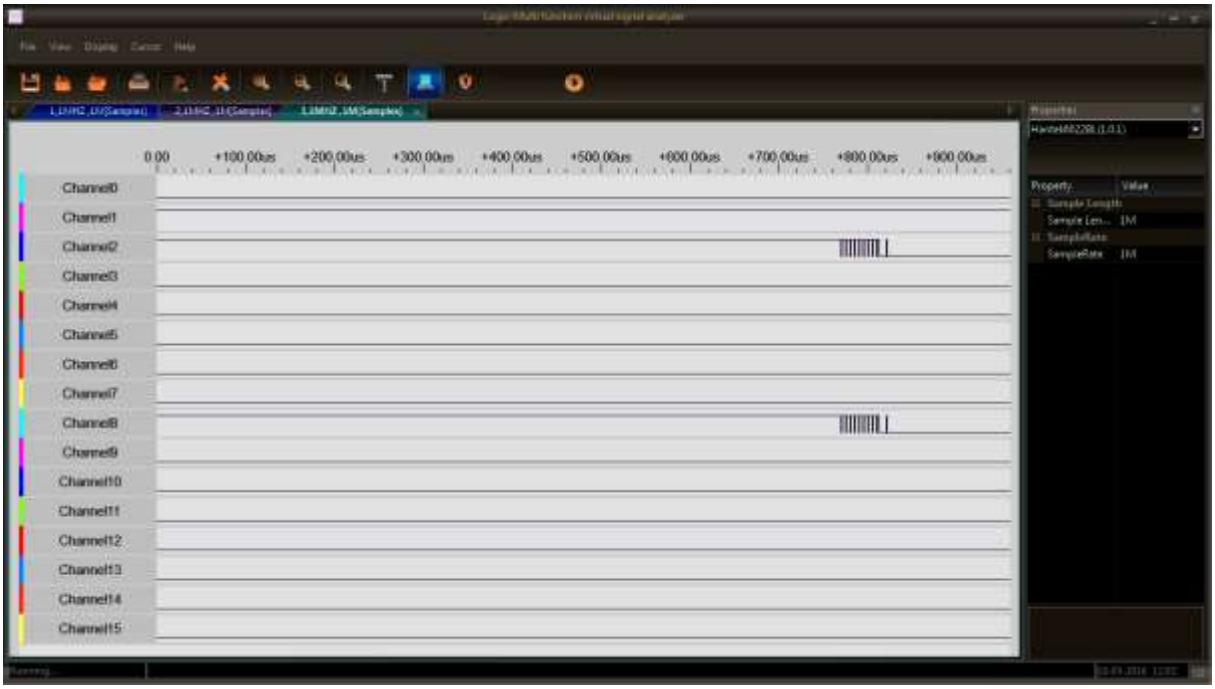

Figure 6.19: Logic analyser results (Channel 1 = wT – Relay IN2, Channel 2 = PV – Relay IN3 and Channel 8 = BATT A STORAGE – Relay IN1)

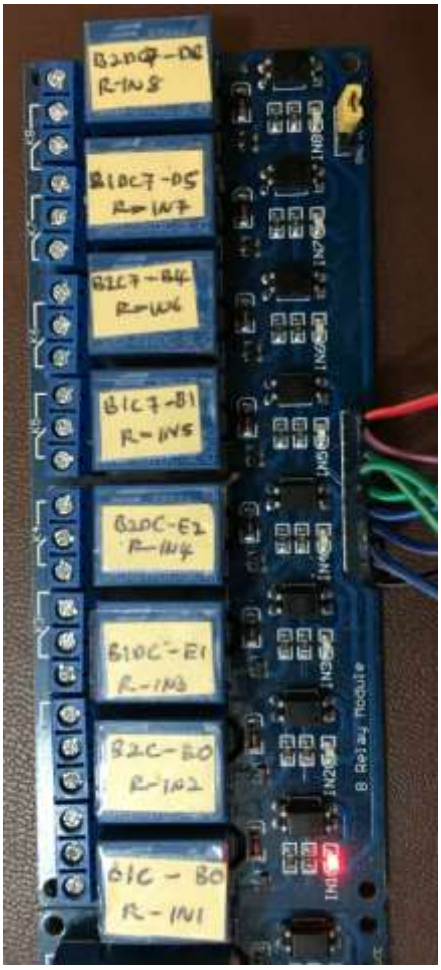

Figure 6.20: Charging/discharging switching circuits – B1C-RB0 (Relay IN1)

Reviewing the obtained results in this section, the voltage based self-intervention has successfully demonstrated the voltage sensing and measurement at the BESS. The embedded software application incorporated in the microcontroller PIC16F877A has successfully performed the mathematical calculation and operation to convert the BESS voltage reading into the percentages as shown in Figure 6.18. Also, the embedded software application have successfully coordinate and manage the switching between the charging switching circuit to charge the BATT A STORAGE when BATT A STORAGE SoC status show 20% equal or less than BATT B STORAGE SoC. The presented results for this section can be validated with the results obtained in Chapter 4 section 4.6.1 (c).

Overall, the obtained results show the real-time DC HRES hardware system have successfully performed the sensing and measurement of the 12~15 Volt regulated output voltages from the solar-wind renewable energy sources. Not only that, real-time DC HRES hardware system have also successfully sense and measure the BESS status to perform the charging or discharging process, whenever is required. Looking at the obtained results, real-time DC HRES hardware system have also successfully coordinated and managed the respected regulated output voltages from the solar-wind renewable energy sources for BESS charging process. In line with that also, real-time DC HRES hardware system managed to perform switching between BESS for charging process which validates the operational of the embedded software application incorporated in the microcontroller PIC16F877A.

6.2.2 CONDITION B: PV = 12~15 Volt and WT = 7~12 Volt - REAL-TIME DC HRES HARDWARE SYSTEM

The sensed and measured solar-wind renewable energy sources regulated output voltages are shown in Figures 6.21 and 6.22. The LCD in Figure 6.21 show BATT A STORAGE SoC is equal to 74% and BATT B STORAGE SoC is equal to 89%. Referring to Figure 5.2, when BATT A STORAGE SoC is 20% equal or less than BATT B STORAGE SoC, then BATT A STORAGE is connected for charging process. In previous section, the regulated output voltage from wind renewable energy source is utilised for the connected AC load and solar renewable energy source was utilised to charge BESS, therefore in this section the available regulated output voltages solar-wind renewable energy sources utilisation are swapped the other way around. The reason for swapping is to allow the 7-12 Volt can be stepped up and the losses in energy conversion will not highly impact the BESS charging.

Figure 6.21: LCD reading – WT = 7~12 Volt and pV = 12~15 Volt, BATT A STORAGE SoC = 74% and BATT B STORAGE SoC = 89%

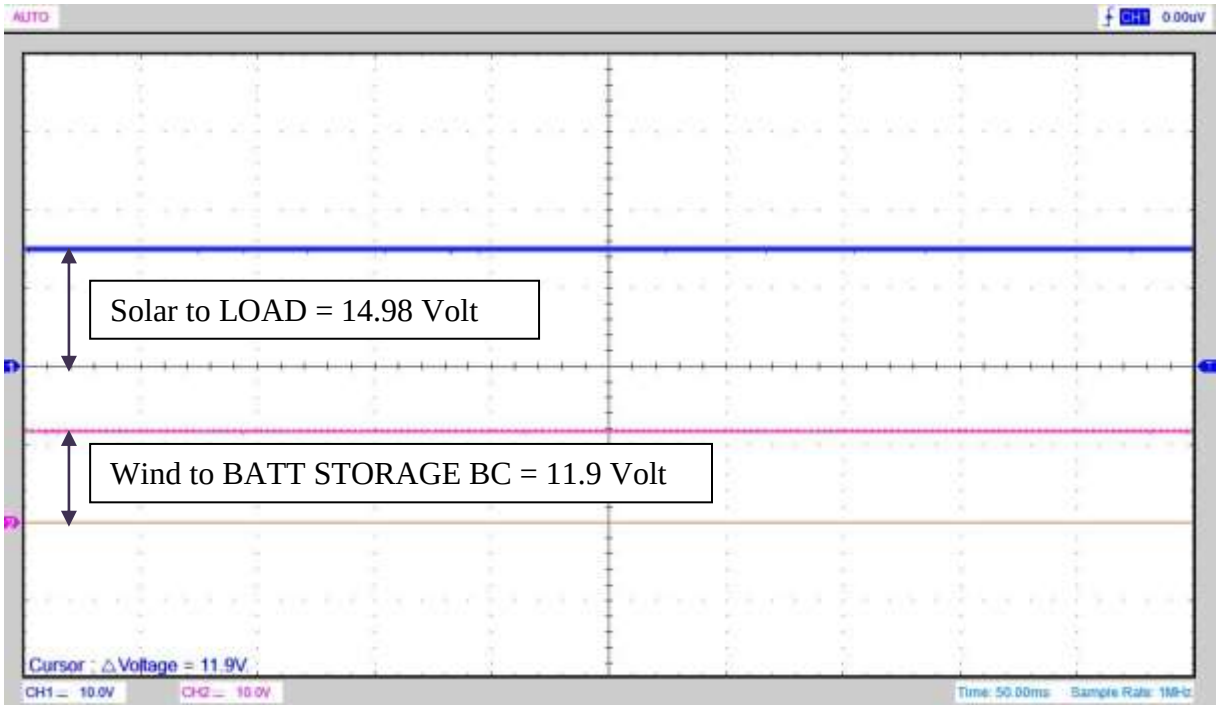

Figure 6.22: Oscilloscope voltage reading - PV = 12~15 Volt and WT = 7~12 Volt

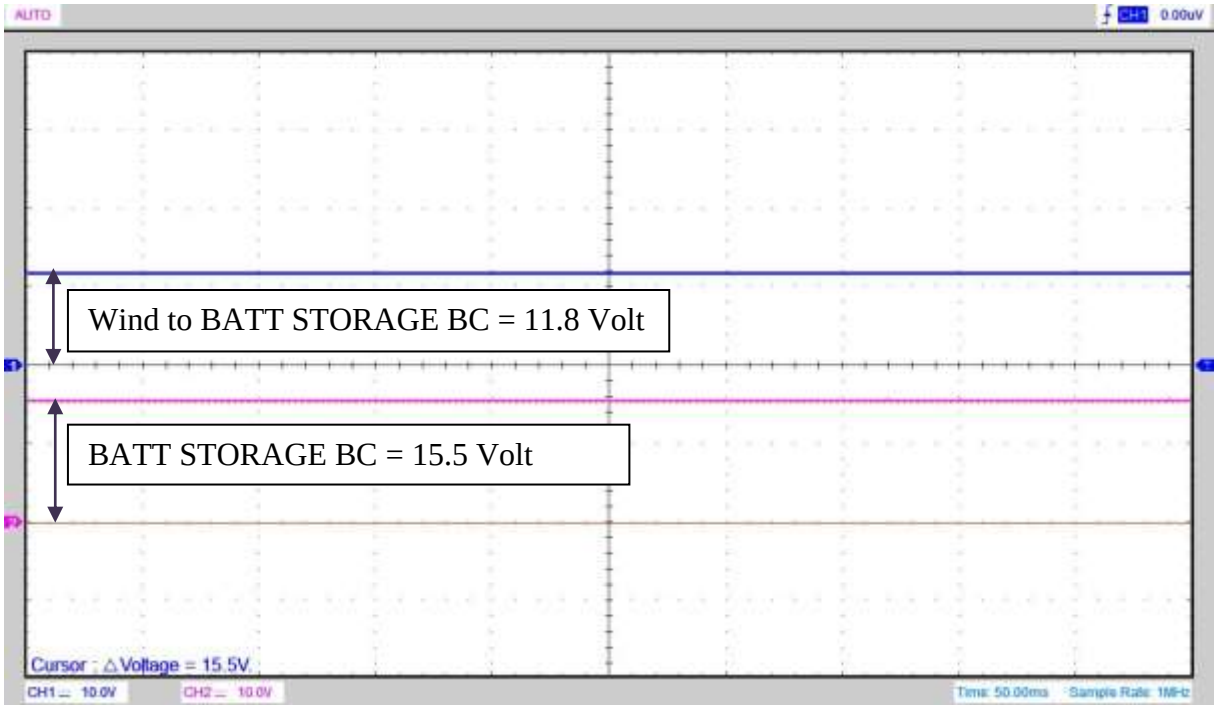

Figure 6.23: Oscilloscope voltage reading - WT = 7~12 Volt and BATT STORAGE BC = 15.5 Volt

Before the regulated output voltage from the wind renewable energy source can be utilised for BESS charging, the voltage is stepped-up to a desired output voltage using the DC to DC BC (BATT STORAGE BC). The stepped-up output voltage from the DC to DC BC is shown in Figure 6.23 and the 15.5 Volt output voltages is utilised to charge the BESS, if required.

As it is shown in Figure 6.24, channels 3 and 4 are HIGH activated and respectively are connected to the AC load as a primary power source supply and BESS for charging process. When channels 3 and 4 are HIGH activated, the respective relay switching and control module is switched on. Thus, relay SL-RC3 shown in Figure 6.24 is switched from NC to NO. Hence, the 12~15 Volt regulated output voltage from the solar renewable energy source is utilised as a primary power source supply for the connected AC load. The WB7-RC4 relay shown in Figure 6.24 is also switched from NC to NO to allow the 7~12 Volt regulated output voltage from the wind renewable energy source to be stepped-up using the DC to DC BC before performing charging process on BESS, if required.

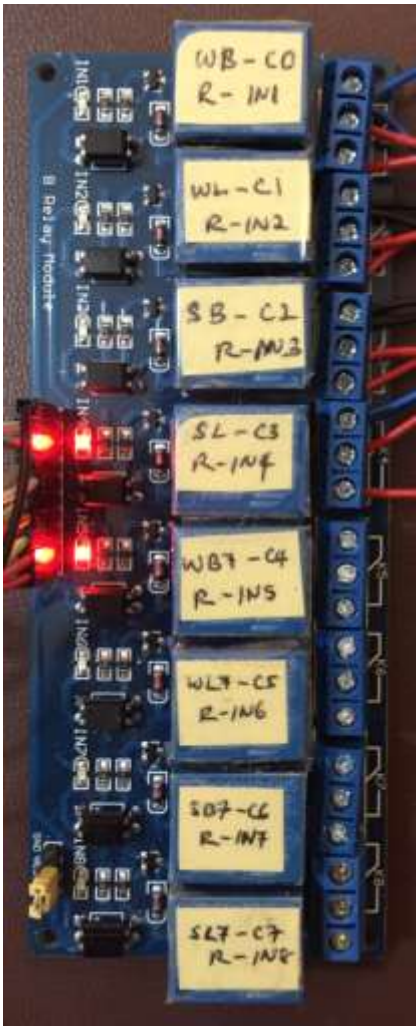

Figure 6.24: Relay switching and control module – SL-RC3 and WB7-RC4

In this condition, the BATT A STOARGE SoC is 20% equal or less than BATT B STORAGE, hence, BATT A STORAGE is connected to the output voltage from the BATT STORAGE BC for charging process. The BATT A STORAGE charging voltage is shown in Figure 6.23. Analysing Figure 6.25, channel 12 which is connected at RB1 port at the microcontroller PIC16F877A measure a HIGH activated signal. This indicates BATT A STORAGE (BIC7) charging switching circuit is switched from NC to NO to start charging the battery. The result of B1C7 charging switching circuit is switched from NC to NO is shown in Figure 6.26. Hence, allowing the 15.5 Volt from the DC to DC BC to charge the BATT A STORAGE.

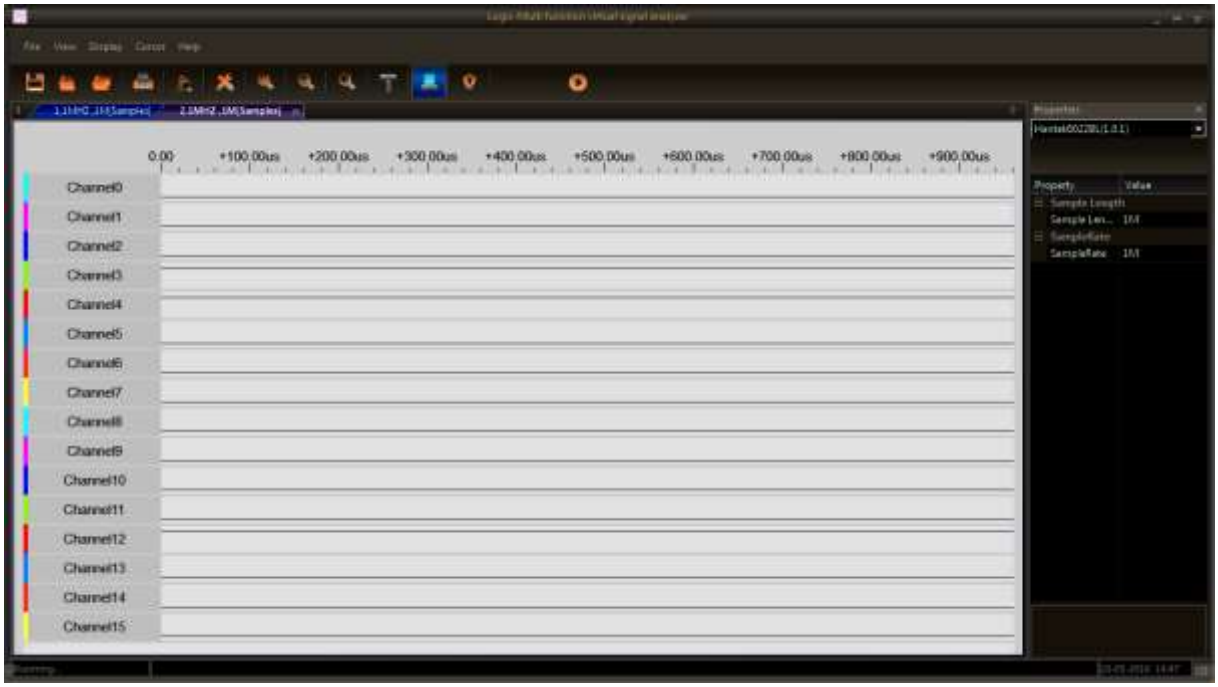

Figure 6.25: Logic analyser results (Channel 3 = pV – Relay IN4, Channel 4 = WT – Relay IN4 and Channel 12 = BATT A STORAGE – Relay IN5)

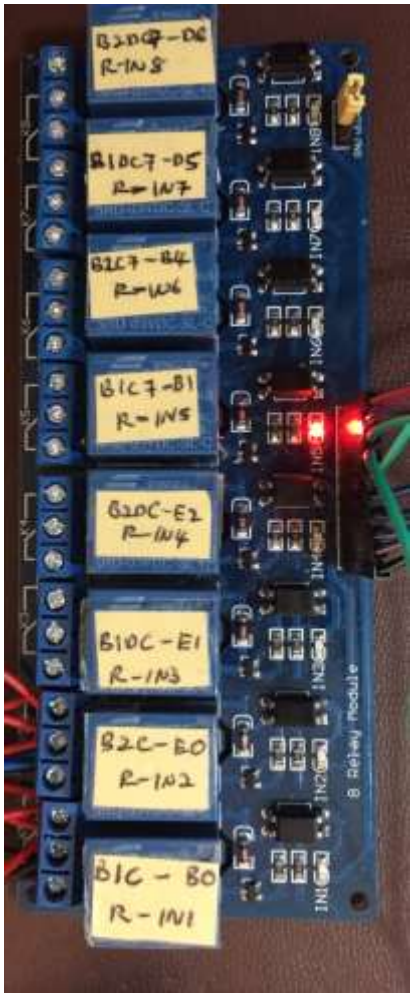

Figure 6.26: Charging/discharging switching circuit – B1C7-RB1 (Relay IN5)

Reviewing the obtained results in this section, the voltage based self-intervention has successfully demonstrated the voltage sensing and measurement between the solar-wind renewable energy sources. Looking at the previous results, regulated output voltage from the wind renewable energy source was used as a power source supply to the connected AC load. While, regulated output voltage from the solar renewable energy source was used as a power source supply for BESS charging. In this section, the regulated output voltage from the wind renewable energy is between 7~12 Volt and the regulated output voltage from the solar renewable energy source is 12~15 Volt. Hence, the regulated output voltage from solar renewable energy is used as a primary power source supply to the connected AC load and regulated output voltage from the wind renewable energy source is used as a power source

supply for BESS charging. The coordination and switching process between solar-wind renewable energy sources are successfully demonstrated only because of the effective performance by the voltage based self-intervention and also the mathematical calculation incorporated in the microcontroller PIC16F877A.

This section also emphasis on the voltage step-up. The 7~12 Volt regulated output voltage from wind renewable energy source is successfully stepped-up to a desired output voltage to perform the charging process on BESS. Based on the recorded results, the 7~12 Volt was successfully stepped-up using DC to DC BC before the output voltage from DC to DC BC is used for BESS charging. The results in this section can be validated with the results from Chapter 4 in section 4.6.2.

6.2.3 CONDITION C: PV = 12~15 Volt and WT = 0~7 - REAL-TIME DC HRES HARDWARE SYSTEM

This section discusses about the availability of only one renewable energy source as power source supply. When this condition occurs, the only available renewable energy source regulated output voltage is used to charge BESS, if required. Also, BESS is connected to the AC load for discharging process as primary power source supply only if the BESS SoC is equal or more than 40%. The sensed and measured solar-wind renewable energy sources regulated output voltages and BESS SoC is shown in Figure 6.27. The status ONLY BATTERY CHARGING (OBC) – ONGRID indicates there is only one renewable energy source available to provide the voltage as power source supply. Therefore, in this case the solar renewable energy source is utilised to charge the BATT A and BATT B STORAGES SoC. As described earlier, during this condition the BESS is connected as primary power source supply to the connected AC load and the available regulated output voltage from solar renewable energy source is used to charge BESS.

Figure 6.27: LCD reading – WT = 0~7 Volt and PV = 12~15 Volt, BATT A STORAGE SoC and BATT B STORAGE SoC = 37%

Looking at BESS SoC, the BESS are equal or less than 40%, therefore, as shown in Figure 6.27 none of the BESS is connected to the AC load for discharging process. However, to continuously supply the power source to the connected AC load, the grid connection/load switching circuit shown in Figure 6.33 is switched from NC to NO to provide power source supply from the grid network. In this condition, BESS is prioritised for charging and the load is connected to the grid network for the BESS charging period.

The captured results using the logic analyser shown in Figure 6.28 show the channel 2 which is connected at RC2 port and channel 8 which is connected at RB0 port at the microcontroller PIC16F877A are activated HIGH. The HIGH activated channel 2 show the regulated output voltage from solar renewable energy source (pV) is directly connected to charge BESS. Thus, relay SB – RC2 shown in Figure 6.29 is switched from NC to NO. Hence, the 12~15 Volt regulated output voltage from solar renewable energy source is utilised as a primary power source supply to charge BESS. The HIGH activated channel 8 show the charging switching circuit shown in Figure 6.30 is switched from NC to NO to charge the BATT A STORAGE.

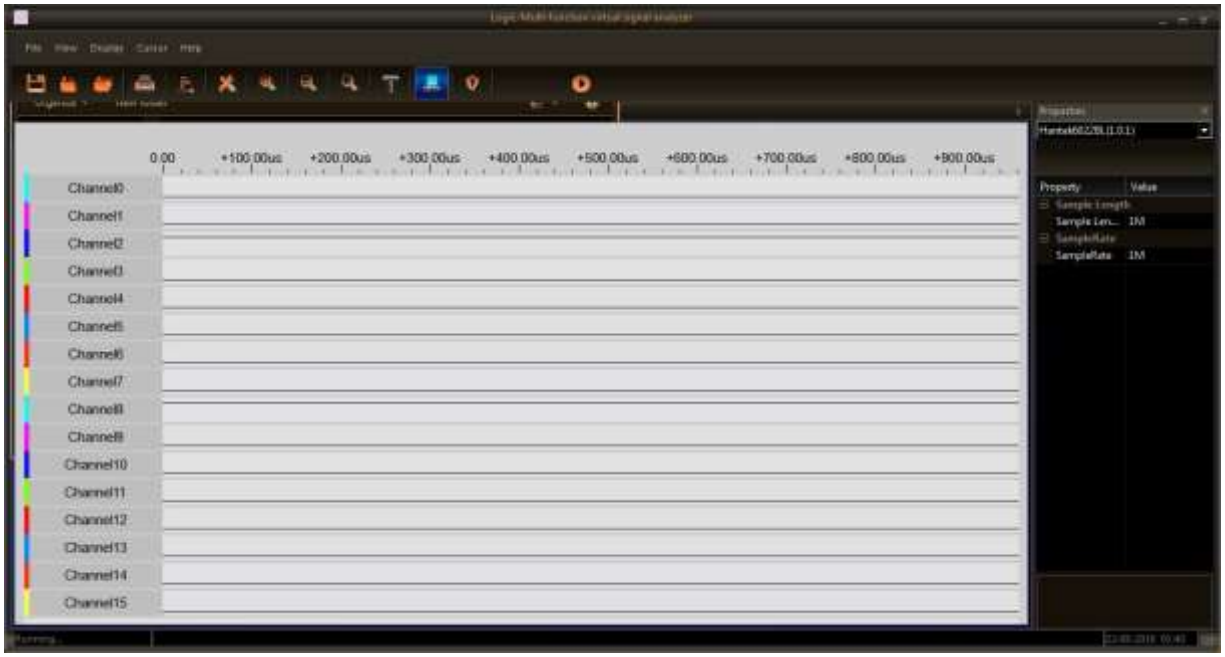

Figure 6.28: Logic analyser results (Channel 2 = pV – Relay IN3 and Channel 8 = BATT A STORAGE – Relay IN1)

In this condition, the BATT A and BATT B STORAGEs SoC are equal or less than 40%. Referring to the BA indicator in Figure 6.27, BATT A STORAGE is connected for charging process and the charging/discharging switching circuit in Figure 6.30 shows the BATT A STORAGE is HIGH activated for charging process.

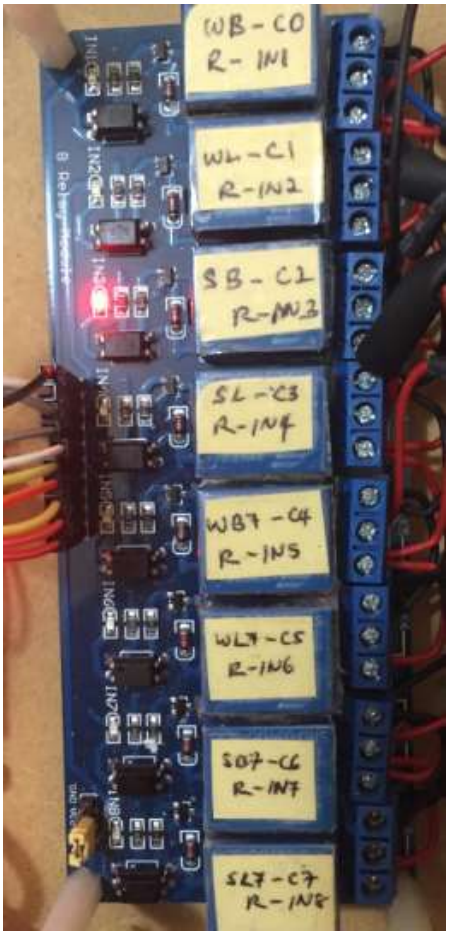

Figure 6.29: Relay switching and control module – SB-RC2

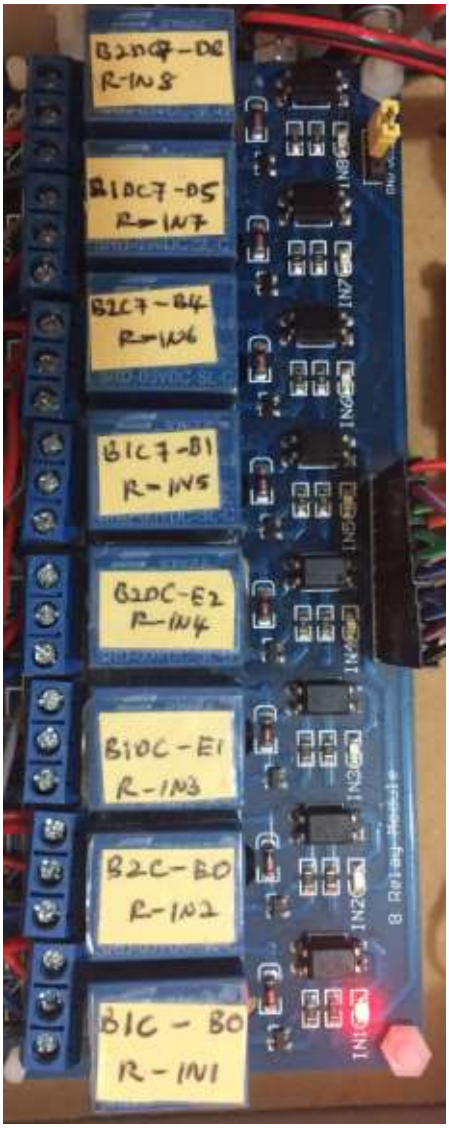

Figure 6.30: Charging/discharging switching circuit – B1C-RB0 (Relay IN1)

Analysing Figure 6.31, sensed and measured solar renewable energy source regulated output voltage is 14.9 Volt. This regulated output voltage is used to charge BATT A STORAGE and charging voltage measured at BATT A STORAGE is shown in Figure 6.32. The charging process of BATT A STORAGE is continued till BATT A STORAGE SoC is 40% equal or more than BATT B STORAGE SoC. Even though in Figure 6.27 the bB indicates BATT B STORAGE is connected for discharging but it is not connected. This can be referred to the charging/discharging switching circuit shown in Figure 6.30, none of the discharging switching circuit is HIGH activated except for BATT A STORAGE for charging process.

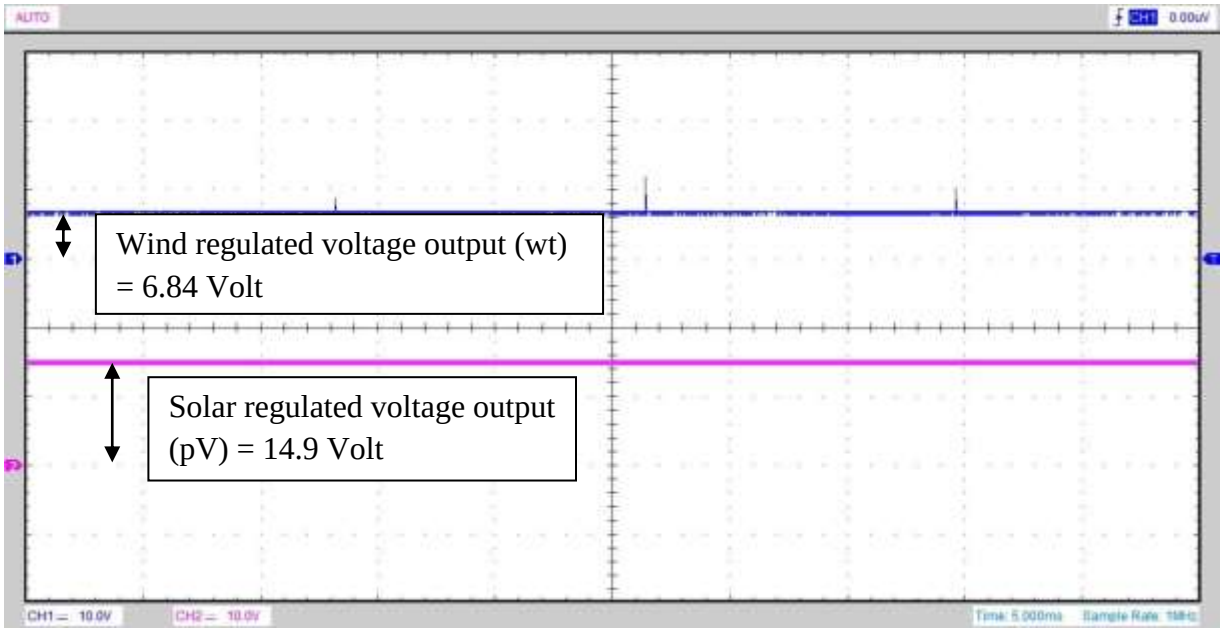

Figure 6.31: Oscilloscope voltage reading – wt=6.84 Volt and pV = 12~15 Volt

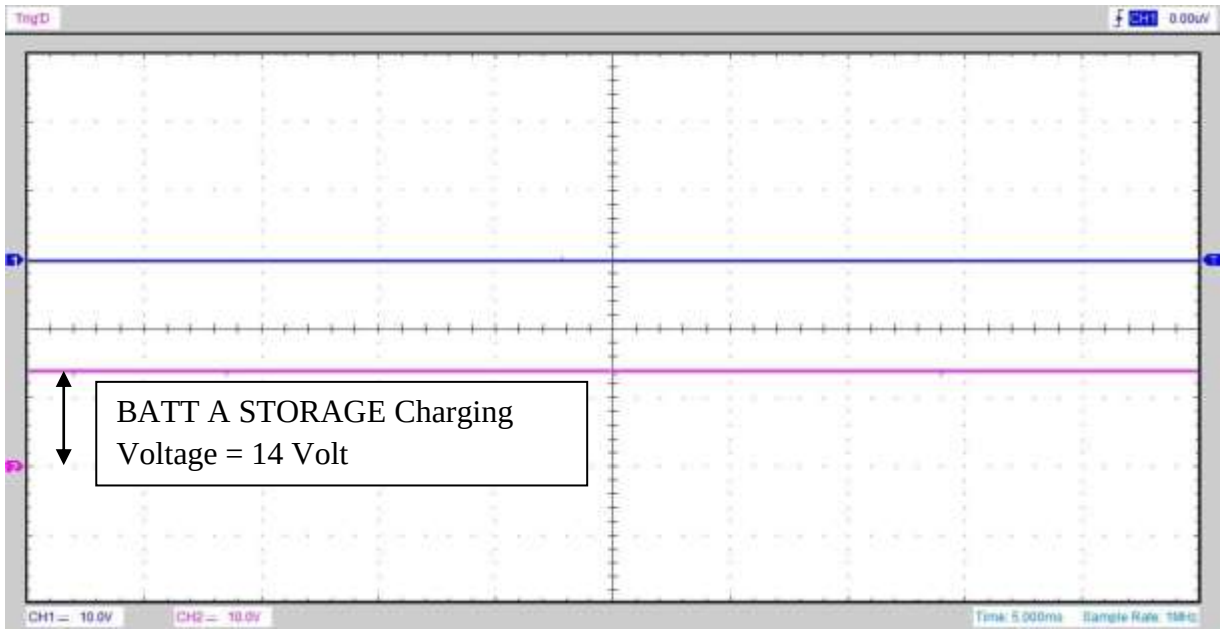

Figure 6.32: Oscilloscope voltage reading – BATT A STORAGE = 14 Volt

When the BESS SoC are equal or less than 40%, the only available regulated output voltage from any of the renewable energy sources are used to charge the BESS. Whereas, the AC load is connected to the grid connection/load switching circuit as shown in Figure 6.33. The RD7

port at the microcontroller PIC16F877A is HIGH activated for this condition to allow the AC power source to be supplied to the connected AC load. Hence, the grid network will supply the AC power source to the connected AC load till BESS SoC is above 40%.

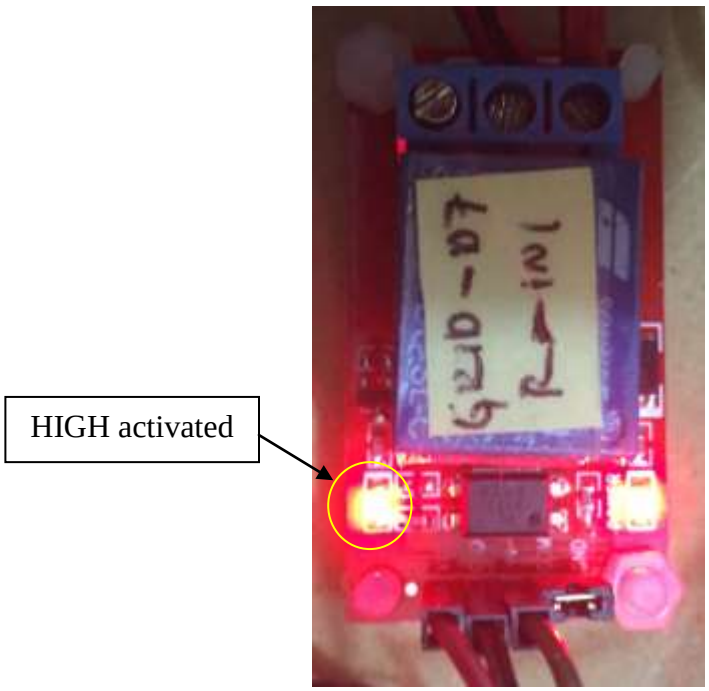

Figure 6.33: GRID connection/LOAD switching circuit – GRID-RD7 (Relay IN1)

Reviewing the results in this section, the only available renewable energy source is utilised for BESS charging process, if required. When this condition occurs, the BESS are the primary power source supply to the connected AC load. Therefore, when BESS are used as primary power source supply to the connected AC load, continuous BESS charging is required to always keep the BESS SoC charged. Otherwise, when BESS SoC decreases to equal or below 40% then the connected AC load is switched for power source supply to the grid network. Thus, in this section the BATT A STORAGE is connected for charging and when BATT A STORAGE SoC is charged upto 40% compare to BATT B STORAGE SoC, then BATT A STORAGE charging is stopped and charging process is switched to BATT B STORAGE. At the same time also, when BESS SoC are equal or below 40%, the grid connection/load switching circuit is HIGH activated to switch the relay from NC to NO to connect the power source supply from grid network to the connected AC load.

(a) BATT A STORAGE SoC = 75% and BATT B STORAGE SoC = 45%

Referring to LCD in Figure 6.34, BATT A STORAGE SoC have been charged up to 75% and bA indicates BATT A STORAGE is connected to perform discharging process. Whereas, BATT B STORAGE SoC is charged up to 45% and BB indicates BATT B STORAGE is connected for charging process.

Figure 6.34: LCD reading – BATT A STORAGE SoC = 75% and BATT B STORAGE SoC = 45%

The captured results using the logic analyser shown in Figure 6.35 show channel 2 which is connected at RC2 port is HIGH activated. The channels 9 and 10 which are connected at RE0 and RE1 ports at the microcontroller PIC16F877A are HIGH activated. The HIGH activated channel 2 show regulated output voltage from solar renewable energy source (pV) is directly connected to charge BESS. Thus, relay SB – RC2 shown in Figure 6.29 is switched from NC to NO. Hence, the 12~15 Volt regulated output voltage from solar renewable energy source is utilised as a primary power source supply to charge BESS.

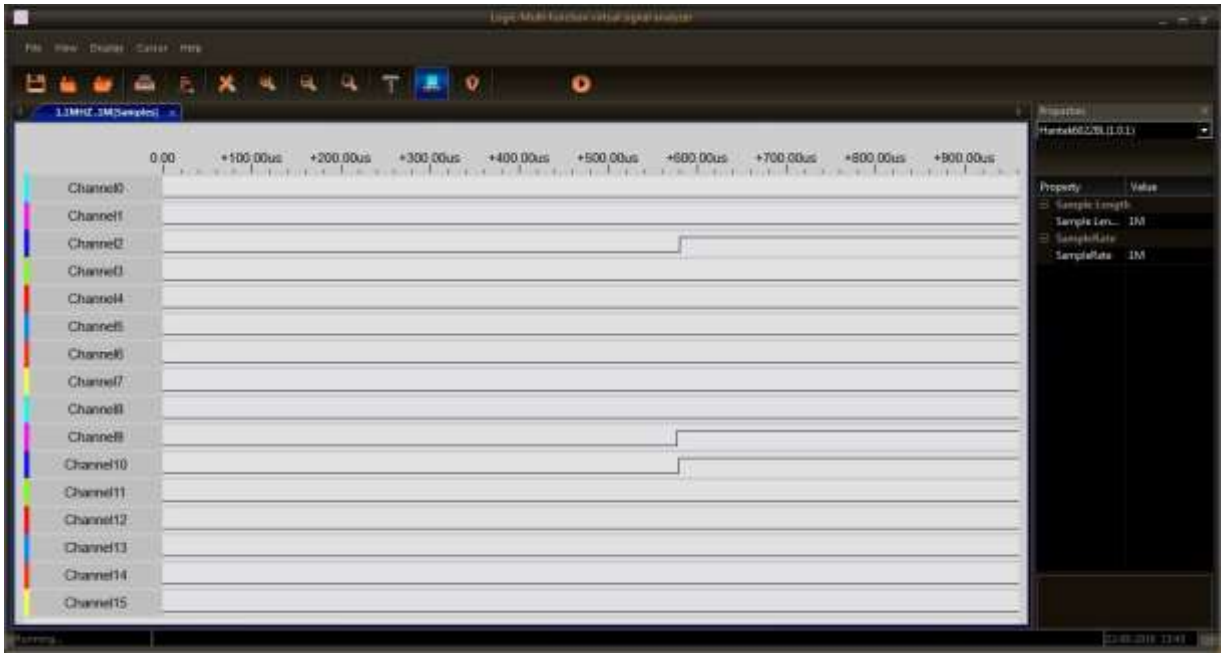

Figure 6.35: Logic analyser results (Channel 2 = pV – Relay IN3, Channel 9 = BATT B STORAGE – Relay IN2 and Channel 10 = BATT A STORAGE – Relay IN3)

The HIGH activated channel 9 show charging switching circuit connected at RE0 at microcontroller PIC16F877A in Figure 6.36 is switched from NC to NO to perform the charging process on BATT B STORAGE. The HIGH activated channel 10 show discharging switching circuit connected at RE1 at microcontroller PIC16F877A for BATT A STORAGE in Figure 6.36 is switched from NC to NO to discharge the stored energy to the connected AC load.

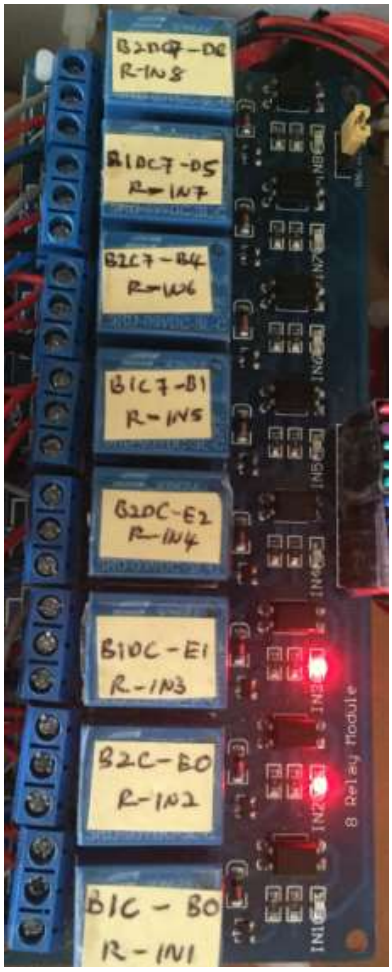

Figure 6.36: Charging/discharging switching circuit – B2C-RE0 (Relay IN2) and B1DC-RE1 (Relay IN3)

Analysing Figure 6.37, the measured voltage at BATT B STORAGE while it is being charged is 12.9 Volt. As mentioned earlier, BATT A STORAGE is charged up to 40% compare with BATT B STORAGE before the charging process is switched to BATT B STORAGE. When BATT A STORAGE SoC is sufficient, then BATT A STORAGE is connected as primary power source supply to the connected AC load. Thus, this disconnects the GRID connection/LOAD switching circuit from grid network by switching the relay from NO to NC. The measured output voltage from BATT A STORAGE is shown in Figure 6.37. The 12 Volt voltages from BATT A STORAGE is send into the DC to AC Inverter (LOAD AC) to be converted into an AC voltage for the connected AC load.

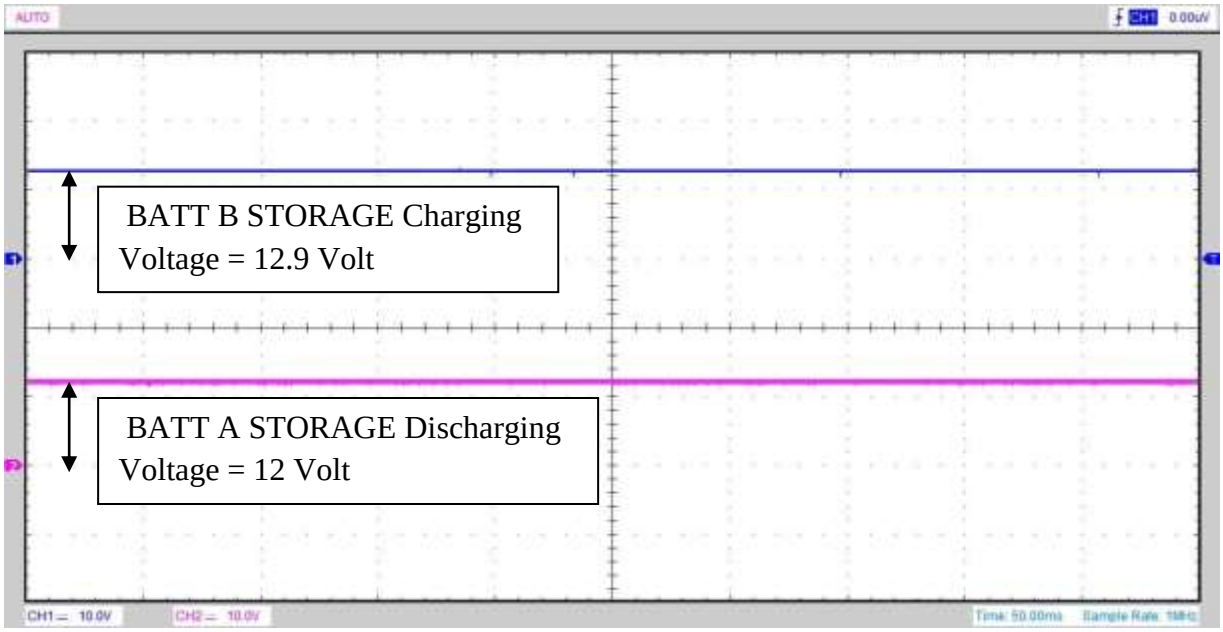

Figure 6.37: Oscilloscope voltage reading – BATT A STORAGE = 12 Volt and BATT B STORAGE = 12.9 Volt

(b) BATT A STORAGE SoC = 100% and BATT B STORAGE SoC = 100%

The sensed and measured BATT A and BATT B STORAGES SoC are shown in Figure 6.38. The BESS SoC shown is fully charged and bB indicates BATT B STORAGE is connected for discharging while BA indicates BATT A STORAGE is connected for charging but referring to Figure 6.40 the charging switching circuit for BATT A STORAGE (BIC) is not activated. As it is mentioned earlier, when only one renewable energy source is available then it is only used as source to charge the BESS, if required otherwise not connected to any storage system.

Figure 6.38: LCD reading – BATT A and BATT B STORAGES SoC = 99%

The captured results using the logic analyser shown in Figure 6.39 show channel 2 which is connected at RC2 port the microcontroller PIC16F877A is HIGH activated. The channel 11 which is connected at RE2 port at the microcontroller PIC16F877A is HIGH activated. The HIGH activated channel 2 show regulated output voltage from the solar renewable energy source (pV) is directly connected to charge the BESS. Thus, relay SB – RC2 shown in Figure 6.29 is switched from NC to NO. Hence, the 12~15 Volt regulated output voltage from the solar renewable energy source is utilised as a primary power source supply to charge the BESS, if required. However, when BESS STORAGES are fully charged the 12~15 volt regulated output voltage from solar renewable energy source is not being utilised for charging process. This can be seen from the captured results shown in Figure 6.39, the charging switching circuit is not switched on for charging process.

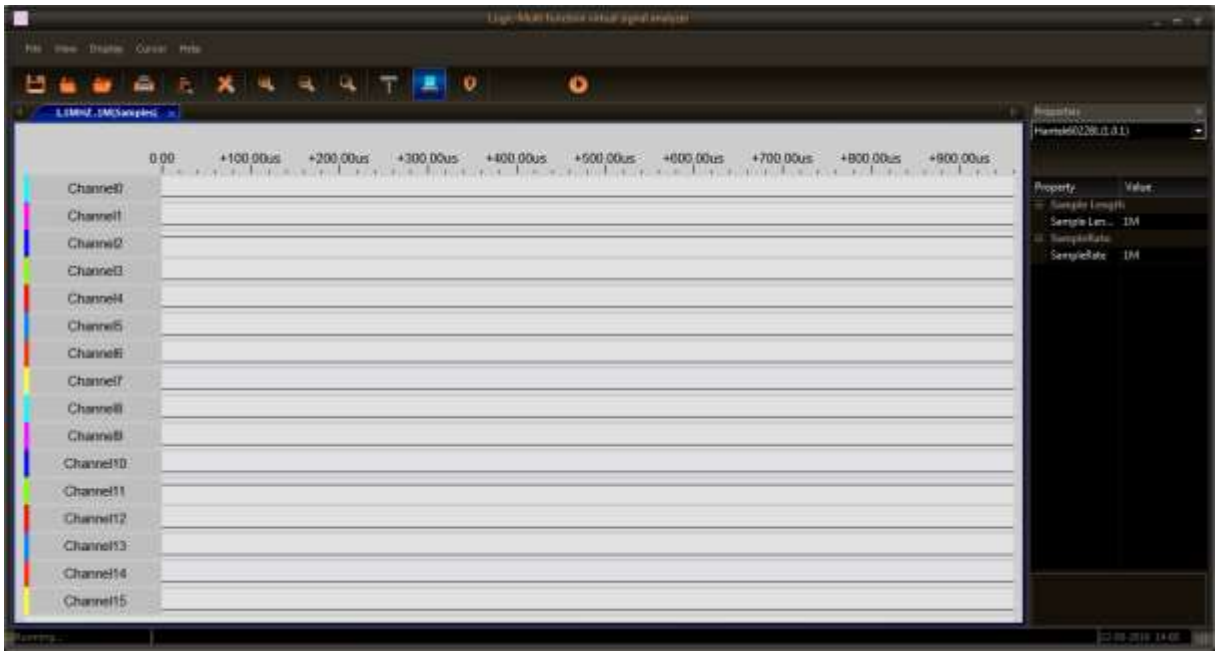

Figure 6.39: Logic analyser results (Channel 2 = pV – Relay IN3, Channel 11 = BATT B STORAGE – Relay IN4)

The channel 11 which is HIGH activated show BATT B STORAGE is connected to perform discharging process. As shown in Figure 6.40, the discharging switching circuit connected at RE2 port is HIGH activated to perform the discharging process. The measured input voltage at the DC to AC Inverter (LOAD AC) is shown in Figure 6.41.

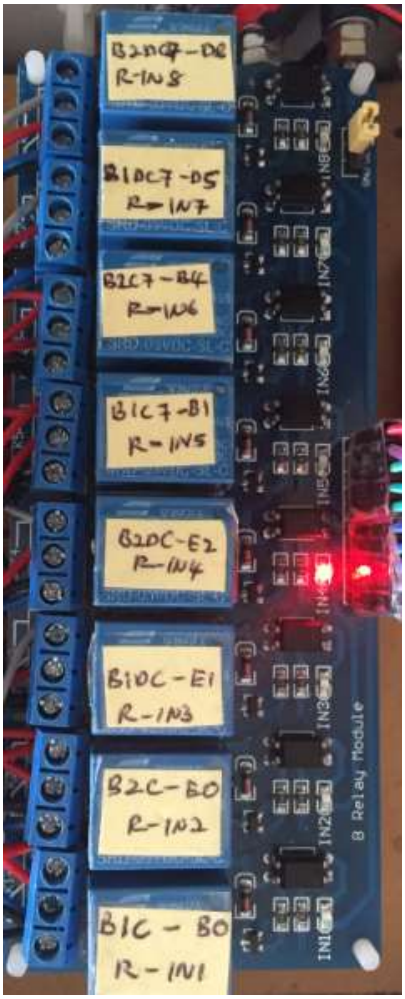

Figure 6.40: Charging/discharging switching circuit – B2DC-RE2 (Relay IN4)

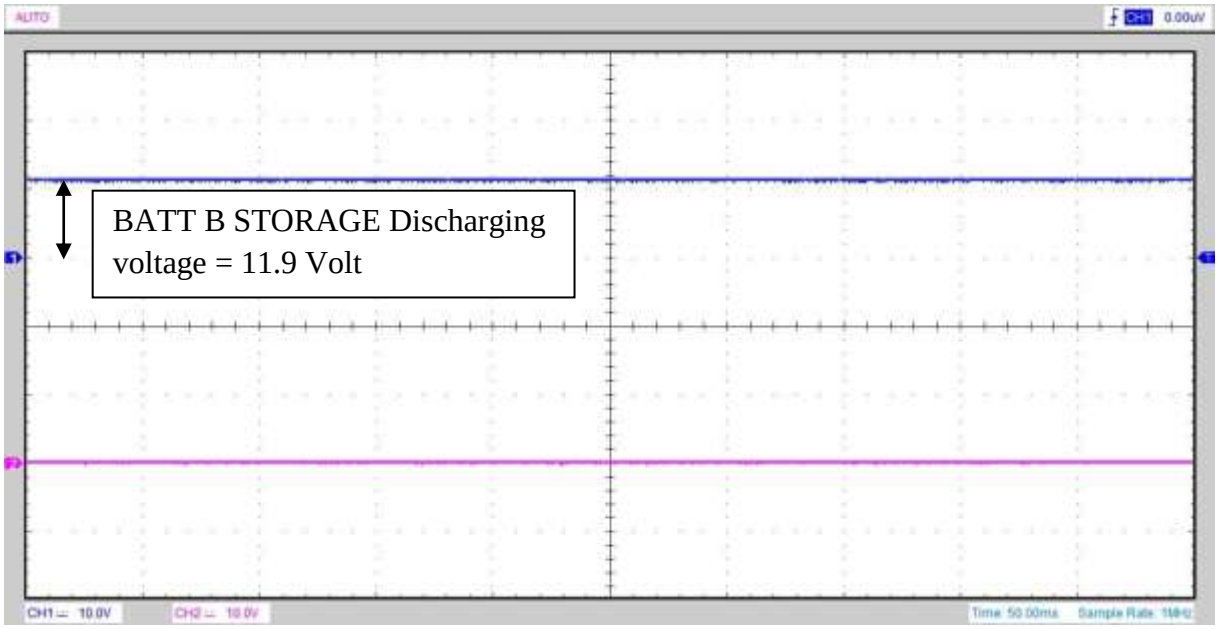

Figure 6.41: Oscilloscope voltage reading – BATT B STORAGE = 11.9 Volt

Reviewing the result in this section, as the objective is to utilise the available renewable energy source as a power source supply to the connected AC load, therefore, available regulated output voltage from the solar renewable energy source is used to charge BESS. The results show when BESS SoC are equal or below 40% then the grid connection/load switching circuit is switched on to connect the AC load to the grid network for power source supply. Besides that also, the embedded software application incorporated in the microcontroller PIC16F877A have successfully demonstrated the charging-discharging switching between the BATT A and BATT B STORAGES, the calculation of available voltages to optimise the system operational and switching between the grid and off-grid system. The results in this section can be validated with the results from Chapter 4 in section 4.6.3.

6.2.4 CONDITION D: WT = 7~12 Volt and PV = 0~7 - REAL-TIME DC HRES HARDWARE SYSTEM

The OBC – ONGRID status is explained in the previous section. Hence, this section discusses about the availability of 7~12 Volt regulated output voltage from solar-wind renewable energy sources for BESS charging process. But before this regulated output voltage is used for BESS charging process, the voltage is stepped-up to a desired output voltage using DC to DC BC.

In this section, regulated output voltage from the wind renewable energy source is used to charge BESS, if required. Therefore, Figure 6.42 is showing the sensed and measured regulated output voltage from wind renewable energy source. The stepped-up output voltage using DC to DC BC is shown in Figure 6.43.

Figure 6.42: LCD reading – wT = 7~12 Volt and pv = 0~7 Volt

Once the 7~12 volt regulated output voltage from wind renewable energy source is stepped-up to a desired output voltage using DC to DC BC then the voltage is used to charge the BESS. The stepped-up output voltage measured in Figure 6.44 is used to charge BATT A STORAGE. The measured charging voltage at BATT A STORAGE is shown in Figure 6.44.

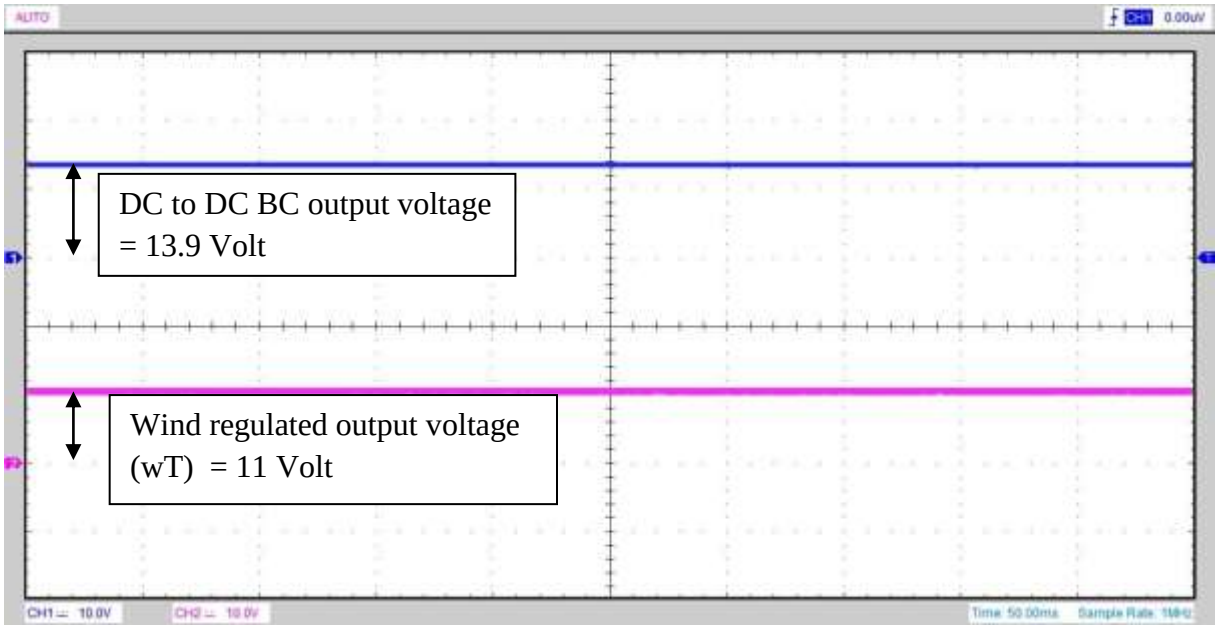

Figure 6.43: Oscilloscope voltage reading – DC to DC BC output voltage = 13.9 Volt and Wind regulated output voltage (wT) = 11 Volt

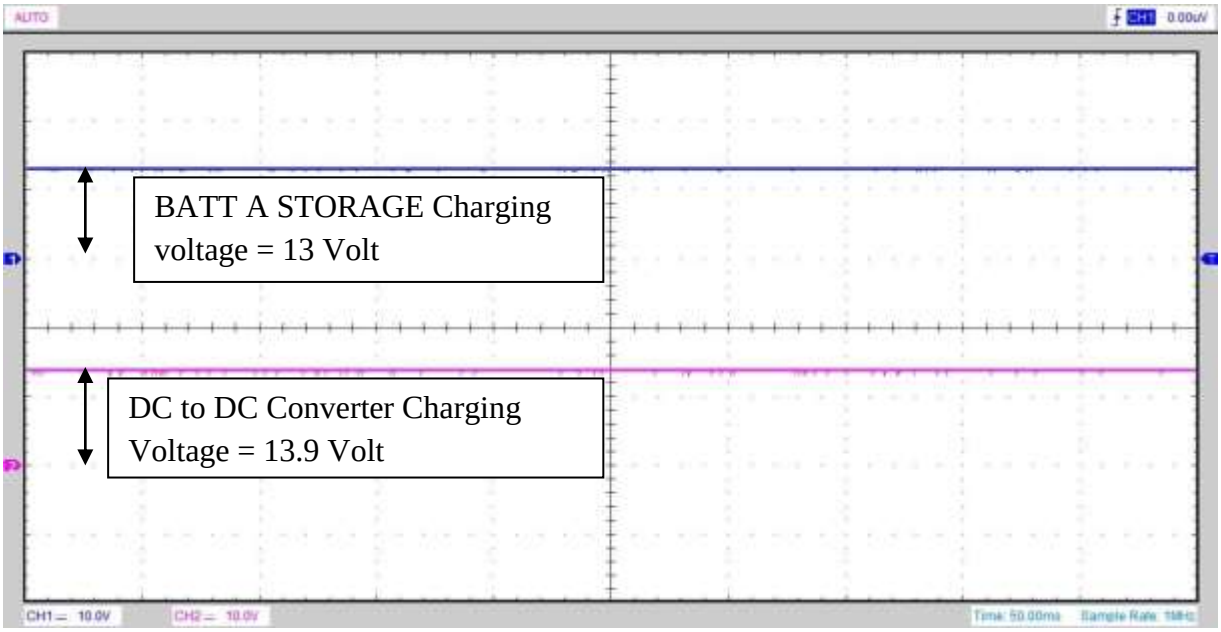

Figure 6.44: Oscilloscope voltage reading – BATT A STORAGE = 13 Volt and DC to DC BC output voltage = 13.9 Volt

Reviewing the results in this section, the 7~12 Volt regulated output voltage from wind renewable energy source is used to charge BESS. The regulated output voltage from wind renewable energy source is send into DC to DC BC to step-up the voltage to a desire output voltage for BESS charging. The results show DC to DC BC have successfully stepped-up the input voltage to a desired output voltage. Other than that, the embedded software application incorporated in the microcontroller PIC16F877A also have successfully performed the self-intervention between the solar-wind renewable energy source using the voltage based self-intervention. Besides that, the embedded software application also have successfully coordinated and managed the switching between the charging/discharging switching circuits. The results in this section can be validated with the results from Chapter 4 in section 4.6.4.

6.2.5 CONDITION E: PV = 0~7 Volt and WT = 0~7 - REAL-TIME DC HRES HARDWARE SYSTEM

Referring to Figure 6.45, when the BESS DisCh status is shown on the LCD screen of the real-time DC HRES hardware system it means the regulated output voltages from solar-wind are between 0~7 Volt. Hence, none of the relay switching and control modules are HIGH activated to flow the 0~7 Volt regulated output voltage from the solar-wind renewable energy sources for either AC load power source supply or BESS STORAGES charging. The bB indicates BATT B STORAGE is connected for discharging process. Therefore, AC load is connected to BESS for power source supply.

Figure 6.45: LCD reading – wt and pv = 0~7 Volt, BATT A and BATT B STORAGES SoC = 99%

The captured results using logic analyser is shown in Figure 6.46 show channel 15 which is connected at RD6 port at the microcontroller PIC16F877A is HIGH activated. Thus, relay B2DC7 – RD6 shown in Figure 6.47 is switched from NC to NO. Hence, the 12 Volt output voltages from BATT B STORAGE is utilised as a primary power source supply to the connected AC load.

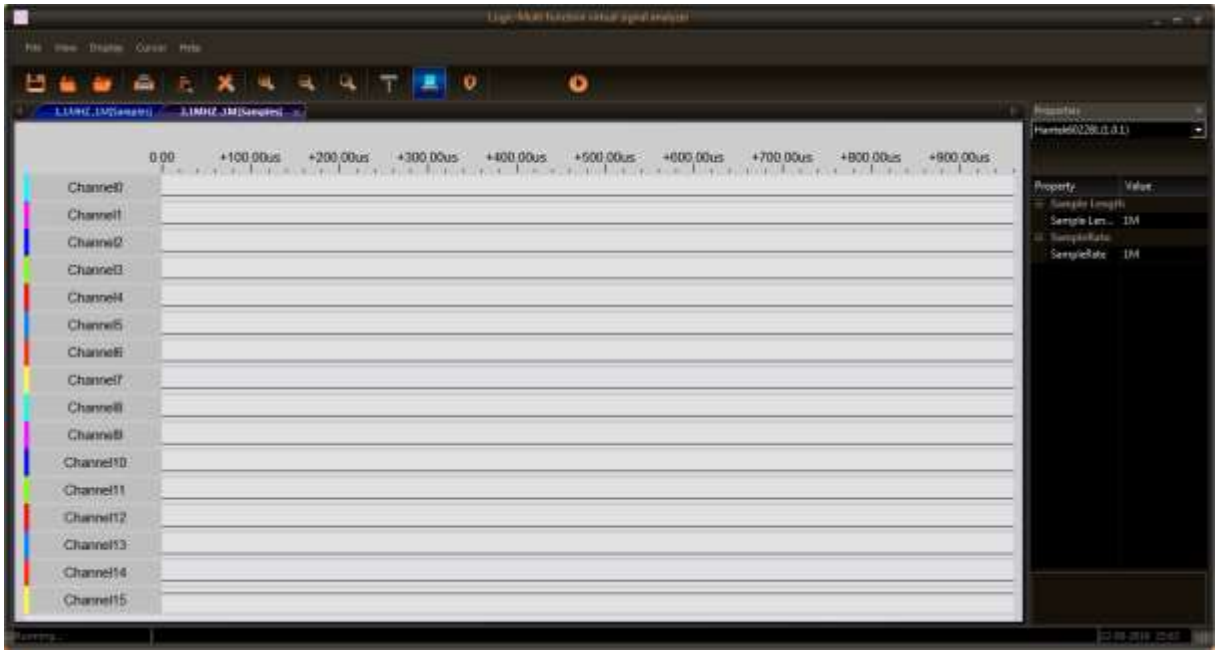

Figure 6.46: Logic analyser result (Channel 15 = BATT B STORAGE – Relay IN8)

Figure 6.47: Charging/discharging switching circuit – B2DC7-RD6 (Relay IN8)

Reviewing the results in this section, BESS SoC is equivalent to 100%. At the same time the renewable energy sources are not available to produce any power source as supply. Hence, BESS are connected to the AC load as primary power source supply. When both BESS are fully charged at 100%, BATT B STORAGE is connected as primary power source supply to the connected AC load for discharging process. The discharging process is switched to the BATT A STORAGE after BATT B STORAGE SoC is 20% discharged.

(a) BATT A STORAGE SoC = 100% and BATT B STORAGE SoC = 80%

The BESS DisCh status is shown in Figure 6.48. The bA indicates BATT A STORAGE is connected for discharging process and BATT B STORAGE is disconnected from discharging process after BATT B STORAGE SoC is 20% discharged.

Figure 6.48: LCD reading – wt and pv = 0~7 Volt, BATT A STORAGE SoC = 99% and BATT B STORAGE SoC = 79%

The captured results using the logic analyser shown in Figure 6.49 show channel 14 which is connected at RD5 port at the microcontroller PIC16F877A is HIGH activated. Thus, relay B1DC7 – RD5 shown in Figure 6.50 is switched from NC to NO. Hence, the 12 Volt output voltages from BATT A STORAGE is utilised as a primary power source supply to the connected AC load.

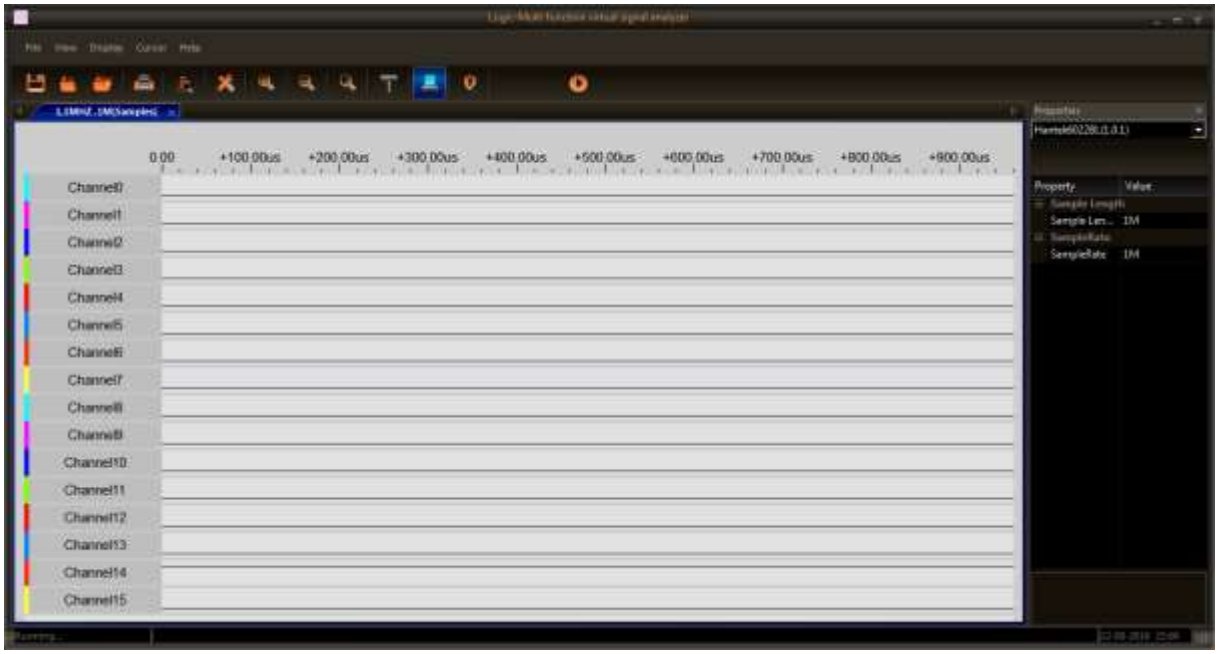

Figure 6.49: Logic analyser result (Channel 14 = BATT A STORAGE – Relay IN7)

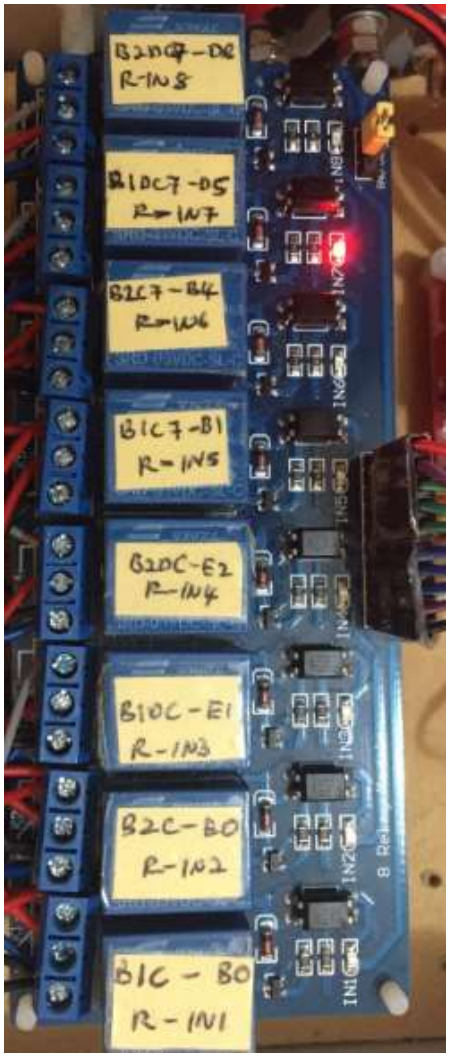

Figure 6.50: Charging/discharging switching circuit – B1DC7-RD5 (Relay IN7)

(b) BATT A STORAGE SoC = 60% and BATT B STORAGE SoC = 80%

The BESS DisCh status is shown in Figure 6.51. The BA indicates BATT A STORAGE is disconnected from discharging process and bB indicates BATT B STORAGE is connected for discharging process after BATT A STORAGE SoC is 20% discharged.

Figure 6.51: LCD reading – wt and pv = 0~7 Volt, BATT A STORAGE SoC = 57% and BATT B STORAGE SoC = 77%

(c) BATT A STORAGE SoC = 40% and BATT B STORAGE SoC = 40%

The BESS DisCh status is shown in Figure 6.52. The BA indicates BATT A STORAGE is disconnected from discharging process and BB indicates BATT B STORAGE is disconnected from discharging process after BESS are discharged up to remaining 40% SoC. When there is no available voltage from solar-wind renewable energy sources and BESS, the AC load is switched to the grid connection/load switching circuit as shown in Figure 6.53.

Figure 6.52: LCD reading – wt and pv = 0~7 Volt, BATT A and BATT B STORAGES SoC ≤ 40%

The grid connection/load switching circuit is connected at RD7 port of microcontroller PIC16F877A. Therefore, RD7 port outputs a HIGH activated signal to the grid

connection/load switching circuit when the conditions described in the following occurs. The conditions are as follows:

i. Voltage based self-intervention sensed and measured voltage for solar-wind renewable energy sources are between 0~7 Volt.

ii. Voltage based self-intervention sensed and measured SoC for BESS are equal or less than 40%.

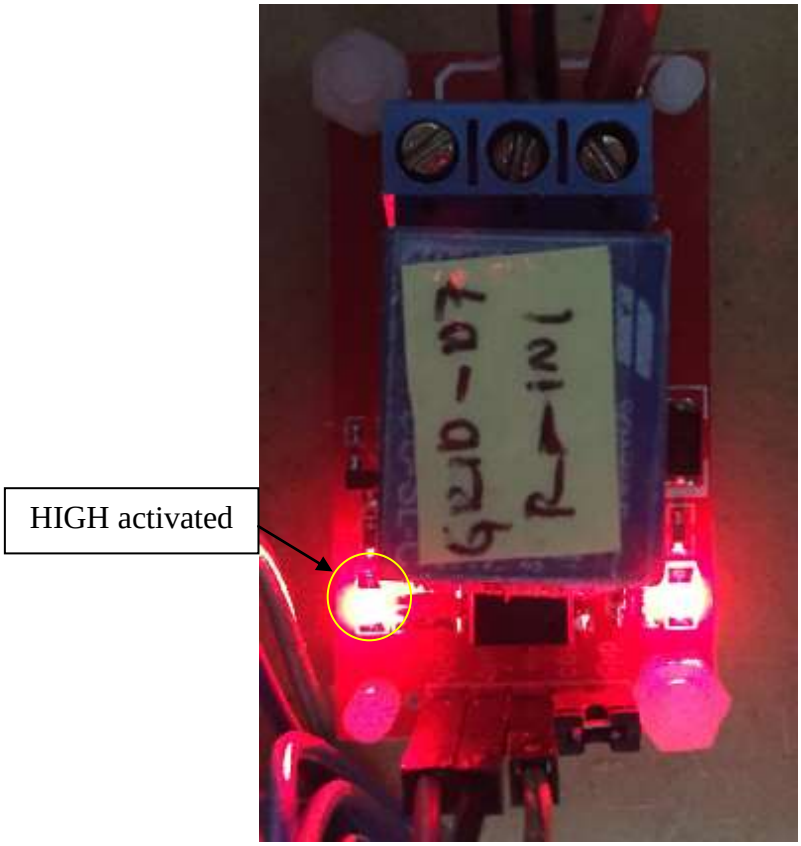

Figure 6.53: Grid connection/load switching circuit – GRID-RD7 (Relay IN1)

Reviewing the result in this section, this condition will occur only when renewable energy sources are not available to produce any power source supply to the connected AC load. In this case, BESS will be the primary power source supply to the connected AC load till BESS SoC decrease equal to or below 40%, and then BESS are stop from discharging process. Once the BESS are stop from discharging, then the AC load is switched to the grid network for

power source supply till the solar-wind renewable energy sources produces 7~12 Volt regulated output voltage for the connected AC load and to perform BESS charging.

6.3 DISCUSSION

This research work was undertaken to develop, integrate, implement and construct real-time DC HRES hardware system to supervise, coordinate, manage, and control the available energy sources for maximum power delivery and optimisation process. As it has been discussed, this research work has undertaken three development stages.

During the first stage of the hardware system development, integration, implementation and construction, MATLAB Simulink/Stateflow software is used to model the proposed real-time DC HRES hardware system. The MATLAB Simulink/Stateflow software in Chapter 3 presents the modelling and simulation of all the subsystem units in real-time DC HRES hardware system. The modelled subsystem units are simulated to analyse the results of each subsystem unit. Once the results are analysed, and if the determined results are as desired then all the subsystems are integrated to perform simulation on the complete system. Thus, the complete system is simulated to record all the new results. The new results are compared and validated with the results obtained while simulating the invidual subsystem units. The results from both simulations are compared and validated to identify any indifferences, hence necessary amendment is made to achieve the desired results. The results comparison and validation is very important because the recorded results are used as fundamental findings to further develop the real-time DC HRES hardware system in the second stage. After all the desired results are achieved and compiled as it is presented in Chapter 3, next stage is proceed.

Next stage involves the electronics circuit design and development using the PROTEUS software. During this stage, all the subsystem units that are modelled using the MATLAB Simulink/Stateflow are designed and developed using the PROTEUS software. The designed and developed subsystems using the PROTEUS software are simulated to analyse the output results. These output results are also analysed and compared with the obtained results in Chapter 3. The results analysis and comparison are very important task because if there is any indifferences then it would be convenient to change any component part or its value at the designing and development stage. The concept of comparing the results from the MATLAB

software modelling and PROTEUS software simulation is a process to reduce hardware system integration and construction error when the hardware implementation process is carried out. At the same time, the developed controllers' methodology using the MATLAB Simulink/Stateflow is transform into the microcontroller PIC16F877A. Thus, all the designed subsystem units using the PROTEUS software are simulated as a complete system with the microcontroller PIC16F877A. But, before the hardware system is simulated, it requires the embedded software application to be incorporated in it. Therefore, the embedded software application is developed for microcontroller PIC16F877A using PCWH CCS C Compiler. The embedded software application incorporated in microcontroller PIC16F877A is designed and developed to perform: (a) voltage sensing and measurement mathematical calculation for the regulated output voltages from solar-wind renewable energy sources, (b) mathematical calculation to convert the sensed and measured BESS voltages status into percentage of SoC and (c) supervise, coordinate, manage and control the relay switching and control modules for solar-wind renewable energy sources and charging/discharging switching circuits for BESS based on the SoC. The embedded software application is described in Chapter 5. Based on the obtained and presented results, the incorporated embedded software application is considered have performed effectively and all the integrated subsystem units have performed well to supervise, coordinate, manage and control as a complete real-time DC HRES hardware system to optimise available the input/output sources.

After all the captured results in Chapters 3 and 4 are analysed, then the hardware integration, implementation and construction task is carried out. The process of integrating, implementation and construction of real-time DC HRES hardware system is explained in Chapter 6. The functionality and operation of each subsystem unit is also explained in Chapter 6. After all the subsystems are integrated into a complete unit of real-time DC HRES hardware system as shown in Figure 6.7, the embedded software application is loaded into microcontroller PIC16F877A to study and analyse the real-time DC HRES hardware system operation based on the conditions and tasks described in Chapters 3 and 4. Due to well organising and structured methodology in Chapters 3, 4 and 5, the integration, implementation and construction of real-time DC HRES hardware system was not much complicated. Hence, this makes the process of gathering and collecting the results easier too. The documented and

presented results for the integration, implemented and constructed real-time DC HRES hardware system in Chapter 6 are analysed and validated with the results presented in Chapters 3 and 4. Based on the presented results, analysis, validation and description, the applied methodology have successfully guided the development, integration, implementation and construction of real-time DC HRES hardware system as presented in Chapter 6. Besides that, real-time DC HRES hardware system also have successfully managed to perform the supervision, coordination, managing and controlling of regulated output voltages from solar-wind renewable energy sources and the input/output voltages from BESS for charging or discharging process.

The performance of real-time DC HRES hardware system is evaluated based on the self intervention among the available sources. The self intervention was performed using the voltage based self-intervention, which sense and measure the sources voltage to detect the differences between the sources. The differences is used to inform the real-time DC HRES hardware system to supervise, coordinate, manage and control the switching between the solar-wind renewable energy sources and BESS. Apart from that also, the embedded software application incorporated into microcontroller PIC16F877A of real-time DC HRES hardware system managed to perform the mathematical calculation to determine real-time status of each sources.

The real-time DC HRES hardware system is also integrated with DC to DC BC. The objective to integrate the DC to DC BC is to step-up the 7~12 Volt regulated output voltages from solar-wind renewable energy sources as a power source supply for the connected AC load or BESS charging process. Analysing the presented results in Chapter 6, DC to DC BC have successfully performed the voltage step-up on the 7~12 Volt regulated output voltage for BESS charging process.

DC to AC Inverter is integrated at the output of the real-time DC HRES hardware system. The DC to AC Inverter converts the DC voltage to an AC voltage as a power source supply to the connected AC load. The presented results demonstrated the regulated output voltage from the solar-wind renewable energy sources and output voltage from BESS are successfully converted into an AC voltage to the connected AC load.

The real-time DC HRES hardware system is developed, integrated, implemented and constructed to optimise the available sources for the connected AC load, which the real-time DC HRES hardware system have successfully demonstrated. But, under some circumstances that are discussed in Chapters 3, 4, and 5 the real-time DC HRES hardware system will not be able to supply the power source to the connected AC load. Hence, the connected AC load will be switched to grid network via the grid connection/load switching circuit shown in Chapter 6. Even though the primary task of real-time DC HRES hardware system is to optimise the power source supply from the available sources, but when there is insufficient power source from the sources the real-time DC HRES hardware system will switch the connected AC load to the grid network via the grid connection/load switching circuit.

Summarising the research, the methodology applied to model, simulate, design, develop, integrate, implement and construct the real-time DC HRES hardware system have successfully demonstrated the aims and objective to optimise the power harvesting from solar-wind renewable energy sources, optimise and utilise the power delivery as a primary power source supply for either the connected AC load or BESS charging or discharging process.

6.4 SUMMARY

The presented results in this chapter validate the preliminary and fundamental research work conducted in Chapters 3 and 4. The integrated, implemented and constructed real-time DC HRES hardware system validates the system's modelling and simulation conducted in Chapter 3. Also, the system's electronic circuits modelling and simulation in Chapter 4 is validated along with the embedded software application developed in Chapter 5. The embedded software application developed in Chapter 5 was incorporated in microcontroller PIC16F877A to allow the real-time DC hardware system to optimise its operation as it is described in the research aims and objective. Therefore, the captured results in this chapter show the preliminary and fundamental research that has been carried out have successfully assisted in developing, integrating, implementing and constructing the real-time DC HRES hardware system for optimal sources utilisation to reduce the dependency on the grid network during the availability of energy sources. This shows the conducted methodology to develop, integrate,

implement and construct the real-time DC HRES hardware system has successfully achieved in completing the real-time DC HRES hardware system.

CHAPTER 7

CONCLUSIONS AND FUTURE WORK

This chapter provides an overall summary of the modelled, simulated, designed, developed, implemented and constructed real-time DC HRES hardware system. The future work section describes about the recommendations that can be consider to enhance the research work.

7.1 CONCLUSIONS

This thesis is documented based on the modelling, simulating, integrating, implementing and constructing the real-time DC HRES hardware system. The real-time DC HRES hardware system is focused to manage and optimise the power harvesting from solar-wind renewable energy sources, power delivery to the connected AC load and BESS for charging process. Besides that, real-time DC HRES hardware system has also successfully managed the BESS discharging process during the off-peak period of solar-wind renewable energy sources. The success of executing the tasks shows that real-time DC HRES hardware system operate-ability is able to execute all the given tasks according to the sensed and measured voltages. This feature of real-time DC HRES hardware system would increase the utilisation of available renewable energy source or stored energy with least dependency on grid network for power source supply.

Modelling and simulation of the real-time DC HRES hardware system which is composed with DC to DC BC and DC to AC Inverter is performed using MATLAB Simulink/Stateflow software. The modelling of the real-time DC HRES hardware system is constructed using the MATLAB Simulink and Stateflow toolbox. Two continuous dynamic decision making controllers are modelled using the Stateflow toolbox which function is to detect the voltage changes from the solar-wind renewable energy sources and BESS. The Simulink toolbox is used to model all the electronic circuitries that are used to supervise, coordinate, manage and control the switching between the solar-wind renewable energy sources and BESS for

charging or discharging process. All the Simulink and Stateflow based modelled subsystems are integrated together and simulated to observe the results. These results are analysed and saved as fundamental findings to proceed to the next stage. DC to DC BC is modelled and integrated to step-up the 7~12 Volt regulated output voltages from the solar-wind renewable energy sources for the connected AC load and BESS charging. DC to AC Inverter is used to step-up the 12~ 15 Volt voltages and convert into 240 AC Volt for the connected AC load. As a conclusion, the real-time DC HRES hardware system is modelled to effectively manage the input and output so that the power source from the solar-wind renewable energy sources and BESS can be optimised.

After the modelled real-time DC HRES hardware system, DC to DC BC and DC to AC Inverter are successfully simulated and the captured results show the desired finding then the real-time DC HRES hardware system, DC to DC BC and DC to AC Inverter are simulated using the electronic circuits PROTEUS software. Prior to simulate the complete real-time DC HRES hardware system which is integrated with DC to DC BC and DC to AC Inverter, each part of the real-time DC HRES hardware system, DC to DC BC and DC to AC Inverter is developed using the electronic circuits PROTEUS software. Each circuit is developed and simulated to observe the circuit characteristics. The output results of each circuit is recorded and analysed. If the results are as desired, these results are compared with the determined results using MATLAB Stateflow/Simulink software. To simulate the real-time DC HRES hardware system, continuous dynamic decision making algorithm is incorporated into the microcontroller PIC16F877A to supervise, coordinate, manage and control the real-time DC HRES hardware system. The importance of continuous dynamic decision making algorithm incorporated into the microcontroller PIC16F877A is to optimise the real-time DC HRES hardware system operation and at the same time optimise the sources power delivery without dependency on the grid network. Summarising the electronic circuits PROTEUS software development, all the electronic circuitries are simulated and their characteristics are analysed before integrating as a complete real-time DC HRES hardware system. Besides that also, executing the PROTEUS software based simulation helps to virtually analyse the overall real-time DC HRES hardware system performances.

The development of continuous dynamic decision making algorithm is essential to perform the microcontroller PIC16F877A based real-time DC HRES hardware system. The continuous dynamic decision making algorithm is developed to supervise, coordinate, manage and control all the integrated subsystems with microcontroller PIC16F877A. The development of the continuous dynamic decision making algorithm is based on the obtained preliminary results from the MATLAB Simulink/Stateflow software modelling and simulation. As a conclusion, the continuous dynamic decision making algorithm is necessary to be incorporated into the microcontroller PIC16F877A because it assist to execute the required task based on the instruction provided when the voltage is sensed and measured.

Finally, the obtained results of modelling, simulation, integrating, implementation and construction of real-time DC HRES hardware system show that the applied methodologies have successfully achieved the aims and objective of this research work. The gathered results also shows that real-time DC HRES hardware system can be effectively used to optimise the power harvesting from solar-wind renewable energy sources and delivery to the connected AC load or BESS for charging process. The self-intervention among solar-wind renewable energy sources and BESS for charging or discharging results shows that the developed continuous dynamic decision making algorithm have successfully performed the respective tasks when it is required. On the contrary, grid connection/load switching circuit which is used to switch the AC load to grid network for power source supply from renewable energy sources or BESS to have also successfully performed this feature when real-time DC HRES hardware system sense the conditions.

Reviewing the presented results for the constructed real-time DC HRES hardware system, it is practical to use real-time DC HRES hardware system as supervision, coordination, management and control mechanism for solar-wind renewable energy sources and BESS for charging or discharging process. Also, real-time DC HRES hardware system have successfully optimise the available sources from the renewable energies and thereby reduce the dependency on the power source supply from the grid network.

7.2 FUTURE WORK

Based on the study conducted in this research work, the following recommendations are made to enhance the research project in the future.

a. Integration of other types of renewable energy sources instead of only solar and wind which can perform the same aim and objectives.

   Studying the nature of different types of renewable energy sources can be used as an addition to the solar or wind renewable energy sources that have been proposed in this research work. Integrating different types of renewable energy sources as complementary product will not only help the system to perform better but also optimize the energy or power harvested from the sources.

b. Integrate BESS faulty detection system which automatically disconnects the faulty battery from charging or discharging.

   Since the aim and objectives of developing HRES is to manage the energy or power delivery for optimum utilization, therefore proper BESS management system is also required. If HRES can deliver excessive energy or power, an efficient BESS management system will be able to assist to store the excessive energy or power and at the same time, strategically manage the energy management between the BESS.

c. Integrate a control system which can divert the excessive energy to the grid network, therefore excessive energy can be sold. Thereby a smart metering can be integrated too.

   As the idea of having more than one renewable energy sources in a system is getting serious consideration among the energy provider, researchers, scientists and energy producer, it would be interesting if the proposed system can be integrated into the grid network for energy or power selling. Also, integrating smart metering would make the control system much intelligent and independently would be able to make decision on the excessive energy.

d. Integrate the real power source, such as wind energy system and solar photovoltaic to the proposed research system.

   This idea can be used as future project expansion, integrating the real power source information would be more realistic in terms of the system modelling and simulation. Thus also, system operation-ability can be optimised and maximised.

REFERENCES

[1] "Solar Wind Energy Tower," *Solar Wind Downdraft Tower*, 2016. [Online]. Available: http://www.solarwindenergytower.com/about-us.html. [Accessed: 11-Dec-2016].

[2] L. K. Gan, J. K. H. Shek, and M. A. Mueller, "Hybrid Wind-Photovoltaic-Diesel-Battery System Sizing Tool Development using Empirical Approach, Life-Cycle Cost and Performance Analysis: A Case Study in Scotland," *Energy Convers. Manag.*, vol. 106, pp. 479–494, 2015.

[3] S. Bhattacharjee and S. Acharya, “PV-Wind Hybrid Power Option for a Low Wind Topography,” *Energy Convers. Manag.*, vol. 89, pp. 942–954, 2015.

[4] D. Delimustafic, J. Islambegovic, A. Aksamovic, and S. Masic, “Model of a Hybrid Renewable Energy System: Control, Supervision and Energy Distribution,” *2011 IEEE Int. Symp. Ind. Electron.*, pp. 1081–1086, Jun. 2011.

[5] K. Agbossou, M. Kolhe, J. Hamelin, and T. K. Bose, “Performance of a Stand-Alone Renewable Energy System Based on Energy Storage as Hydrogen,” *IEEE Trans. Energy Convers.*, vol. 19, no. 3, pp. 633–640, 2004.

[6] K. Mousa, H. AlZu’bi, and A. Diabat, “Design of a Hybrid Solar-Wind Power Plant using Optimization,” *Eng. Syst. Manag. Its Appl. (ICESMA), 2010 Second Int. Conf.*, no. August 2015, 2010.

[7] Olumuyiwa O. Fagbohun1 and and Bankole A. Adebanji, “Integrated Renewable Energy Sources for Decentralized Systems in Developing Countries,” *IOSR J. Electr. Electron. Eng.*, vol. 9, no. 2, pp. 26–35, 2014.

[8] S. Yasmeena and G. T. Das, “A Review of Technical Issues for Grid Connected Renewable Energy Sources,” *Int. J. Energy Power Eng.*, vol. 4, no. 5–1, pp. 22–32, 2015.

[9] L. Zhang, D. Jing, L. Zhao, J. Wei, and L. Guo, “Concentrating PV/T Hybrid System for Simultaneous Electricity and Usable Heat Generation: A Review,” *Int. J. Photoenergy*, vol. 2012, 2012.

[10] C. L. Shen and S. H. Yang, “Multi-Input Converter with MPPT Feature for Wind-PV Power Generation System,” *Int. J. Photoenergy*, vol. 2013, no. Mic, 2013.

[11] T. Pan, H. Wan, and Z. Ji, “Stand-Alone Wind Power System with Battery / Supercapacitor Hybrid Energy Storage,” *Int. J. Sustain. Eng.*, vol. 7, no. 2, pp. 103–110, 2014.

[12] J. Chodkowska-Miszczuk, “Small-Scale Renewable Energy Systems in the

Development of Distributed Generation in Poland," *Morav. Geogr. Reports*, vol. 22, no. 2, pp. 34–43, 2014.

[13] Y. V. Pavan Kumar and R. Bhimasingu, "Renewable Energy based Microgrid System Sizing and Energy Management for Green Buildings," *J. Mod. Power Syst. Clean Energy*, vol. 3, no. 1, pp. 1–13, 2015.

[14] J. C. Reboredo, "Renewable Energy Contribution to the Energy Supply: Is there Convergence Across Countries?," *Renew. Sustain. Energy Rev.*, vol. 45, pp. 290–295, 2015.

[15] G. Bitesize, "Energy: Renewable Energy Sources," *BBC News*, 2015. [Online]. Available: http://www.bbc.co.uk/schools/gcsebitesize/geography/energy_resources/energy_rev2.shtml. [Accessed: 13-Feb-2016].

[16] T. Bocklisch, "Hybrid Energy Storage Systems for Renewable Energy Applications," *Energy Procedia*, vol. 73, pp. 103–111, 2015.

[17] Jim Watson, "Renewable Energy Technologies for Rural Development," 2010.

[18] W. C. Turjenburg, "Renewable Energy Technologies," in *World Energy Assessment: Energy and The Challenge of Sustainability*, vol. 146, 2010, pp. 200–272.

[19] P. Bajpai and V. Dash, "Hybrid Renewable Energy Systems for Power Generation in Stand-Alone Applications: A Review," *Renew. Sustain. Energy Rev.*, vol. 16, no. 5, pp. 2926–2939, Jun. 2012.

[20] T. Z. T. Zhou, P. L. P. Li, and B. Francois, "Power Management Strategies of a DC-Coupled Hybrid Power System in a Microgrid for Decentralized Generation," *2009 13th Eur. Conf. Power Electron. Appl.*, 2009.

[21] S. Majumdar, A. Sapalok, and N. Chakraborty, "Modeling Components of a DC Coupled Photovoltaic System with Maximum Power Point Tracking," *2012 IEEE 5th Power India Conf. PICONF 2012*, 2012.

[22] Schneider Electric, “AC Coupling of Inverters,” 2014.

[23] E. Lorenz, “AC or DC Coupled -- What ?,” *CivicSolar, Inc.*, 2014. [Online]. Available: https://www.civicsolar.com/resource/ac-or-dc-coupled-what. [Accessed: 03-Mar-2016].

[24] P. Balachander, “AC Coupling,” 2012.

[25] F. M. Solution, “Whitepaper on Offgrid and Backup Systems,” 2014.

[26] N. Peterschmidt, “Hybrid Power Systems - An Introduction,” 2013.

[27] “Definition of Hybrid Power Systems,” 2016. [Online]. Available: http://www.cres.gr/hypos/files/fs_inferior01_h_files/definition_of_hps.htm. [Accessed: 05-Mar-2016].

[28] J. McGarry, Kenneth Wermter, Stefan MacIntyre, “Hybrid Neural Systems: From Simple Coupling to Fully Integrated Neural Networks,” *Neural Comput. Surv.*, vol. 2, pp. 62–93, 1999.

[29] A. Chauhan and R. P. Saini, “A Review on Integrated Renewable Energy System based Power Generation for Stand-Alone Applications: Configurations, Storage Options, Sizing Methodologies and Control,” *Renew. Sustain. Energy Rev.*, vol. 38, no. March, pp. 99–120, 2014.

[30] K. S. Devi and G. P. College, “A DC-Coupled Wind / Hydrogen / Super capacitor Hybrid Power System,” *Int. J. Emerg. Trends Electr. Electron.*, vol. 10, no. 8, pp. 31–34, 2014.

[31] S. Kumar, “Modeling and Simulation of Hybrid Wind/Photovoltaic Stand-Alone Generation System,” National Institute Technology, Rourkela, 2014.

[32] A. Cheknane, H. S. Hilal, F. Djeffal, B. Benyoucef, and J.-P. Charles, “An equivalent circuit approach to organic solar cell modelling,” *Microelectronics J.*, vol. 39, no. 10, pp. 1173–1180, Oct. 2008.

[33] C. Jena, A. Das, C. K. Panigrahi, and M. Basu, “Modelling and Simulation of Photovoltaic Module with Buck-Boost Converter,” *Int. J. Adv. Eng. Nano Technol.*, vol. 1, no. 3, pp. 18–21, 2014.

[34] J. Cubas, S. Pindado, C. De Manuel, I. Universitario, D. M. Ignacio, D. Riva, I. D. R. Upm, and E. T. Superior, “Explicit Expressions for Solar Panel Equivalent Circuit Parameters Based on Analytical Formulation and the Lambert,” in *1st International e-Conference on Energies*, 2014, pp. 1–18.

[35] T. Ikegami, T. Maezono, F. Nakanishi, Y. Yamagata, and K. Ebihara, “Estimation of Equivalent Circuit Parameters of PV Module and its Application to Optimal Operation of PV System,” *Sol. Energy Mater. Sol. Cells*, vol. 67, no. 1–4, pp. 389–395, Mar. 2001.

[36] A. Campus and K. Campus, “Mathematical Model Derivation of Solar Cell by Using OneDiode Equivalent Circuit via SIMULINK,” *Int. J. Educ. Res.*, vol. 1, no. 12, pp. 1–12, 2013.

[37] Keithley, “I-V Characterization of Photovoltaic Cells Using the Model 2450 SourceMeter® Source Measure Unit (SMU) Instrum,” 2014.

[38] J.Godson, M.Karthick, T.Muthukrishnan, and M.S.Sivagamasundari, “Solar PV-Wind Hybrid Power Generation System,” *Int. J. Adv. Res. Electr. Electron. Instrum. Eng.*, vol. 2, no. 11, pp. 5350–5354, 2013.

[39] Anonymous, “Wind Turbine Paper,” *AIMU Tech. Serv. Comm.*, no. January, pp. 1–24, 2012.

[40] C. C. Ciang, J.-R. Lee, and H.-J. Bang, “Structural Health Monitoring for a Wind Turbine System: A Review of Damage Detection Methods,” *Meas. Sci. Technol.*, vol. 19, no. 12, p. 122001, 2008.

[41] G. M. Joselin Herbert, S. Iniyan, E. Sreevalsan, and S. Rajapandian, “A Review of Wind Energy Technologies,” *Renew. Sustain. Energy Rev.*, vol. 11, no. 6, pp. 1117–

1145, 2007.

[42] “Wind Turbine Generator,” 2014. [Online]. Available: http://turbinegeneratorz.com/wind-turbine-generator/. [Accessed: 22-Mar-2016].

[43] The Royal Academy of Engineering, “Wind Turbine Power Calculations.”

[44] M. Ragheb and A. M. Ragheb, “Wind Turbines Theory - The Betz Equation and Optimal Rotor Tip Speed Ratio,” in *Fundamental and Advanced Topics in Wind Power*, vol. 1, no. 1, R. Carriveau, Ed. InTech, 2011.

[45] “Use a Cycle Computer to Measure Turbine RPM Small Electric Motors,” 2014. [Online]. Available: http://www.reuk.co.uk/Use-a-Cycle-Computer-to-Measure-Turbine-RPM.htm.

[46] J. A. Baroudi, V. Dinavahi, and A. M. Knight, “A Review of Power Converter Topologies for Wind Generators,” *Renew. Energy*, vol. 32, no. 14, pp. 2369–2385, 2007.

[47] J. M. Lujano-Rojas, R. Dufo-López, and J. L. Bernal-Agustín, “Technical and economic effects of charge controller operation and coulombic efficiency on stand-alone hybrid power systems,” *Energy Convers. Manag.*, vol. 86, pp. 709–716, 2014.

[48] S. T. Cha, A. Saleem, and J. Ostergaard, “Coordinated Control Scheme of Battery Energy Storage System (BESS) and Distributed Generations (DGs) for Electric Distribution Grid Operation,” *IECON 2012 - 38th Annu. Conf. IEEE Ind. Electron. Soc.*, pp. 4758–4764, Oct. 2012.

[49] G. L. Kale and N. N. Shinde, “Implementation of Prototype Device – Off Grid - Charge Controller – Suitable for Wind Solar Hybrid,” *Int. J. Res. Mech. Eng. Technol.*, vol. 5762, no. 1, pp. 89–92, 2011.

[50] N. S. O. and Q. A. I. M. Shusmita Rahman, “Design of a Charge Controller Circuit with Maximum Power Point Tracker (MPPT) for Photovoltaic System,” 2012.

[51] H. Babazadeh, S. Member, W. Gao, and S. Member, “A New Control Scheme in a Battery Energy Storage System for Wind Turbine Generators,” in *2012 IEEE Power and Energy Society General Meeting*, 2012, pp. 1–7.

[52] L. Xing, L. Rui, and C. Xu, “Control of a Battery-Energy-Storage System based on a Cascaded H-Bridge Converter under Fault Condition,” *Proc. 7th Int. Power Electron. Motion Control Conf.*, pp. 952–957, Jun. 2012.

[53] T. Wang, “The Design of Charging Controller in Wind-Photovoltaic Hybrid Power Generation System,” in *International Conference on Civil, Materials and Environmental Sciences (CMES 2015)*, 2015, no. Cmes, pp. 402–404.

[54] I. A. Karim, A. A. Siam, N. A. Mamun, I. Parveen, and S. S. Sharmi, “Design of a Solar Charge Controller for A 100 WP Solar PV System,” *Prejournal Eng. Res.*, vol. 1, no. November, pp. 1–9, 2013.

[55] A. A. Azooz and J. M. Sulayman, “Electronic Control Circuit for Solar Battery Charging,” *Rom. Rep. Phys.*, vol. 59, no. 1, pp. 101–111, 2007.

[56] “DIY Solar Charge Controller,” 2014. [Online]. Available: http://paulorenato.com/joomla/index.php?option=com_content&view=article&id=81:diy-solar-charge-controller&catid=4:projects&Itemid=4.

[57] “Wind Turbine Charge Controllers,” 2014. [Online]. Available: http://www.generate-electricity.co.uk/windcontrollers.htm.

[58] K. R. Hegde, C. P. Prajwal, P. K. H. S, S. Shivakumar, and P. R. Jayapal, “Smart Controller for Wind-Solar Hybrid System under Grid Connected Operations,” *Am. Int. J. Res. Sci. Technol. Eng. Math.*, pp. 61–66, 2014.

[59] M. Hagiwara and H. Akagi, “A Battery Energy Storage System with a Modular Push-Pull PWM Converter,” in *2012 IEEE Energy Conversion Congress and Exposition (ECCE)*, 2012, pp. 747–754.

[60] H. Akagi, L. Maharjan, and A. Background, “A Battery Energy Storage System Based

on a Multilevel Cascade PWM Converter," in *Brazilian Power Electronics Conference, 2009.*, 2009, pp. 9–18.

[61] M. W. Tsang, "ANN Controlled Battery Energy Storage System For Enhancing Power System Stability," in *5th International Conference on Advances in Power System Controls, Operation and Management, APSCOM 2000*, 2000, no. October, pp. 327–331.

[62] S. Tang, H. Yang, R. Zhao, and X. Geng, "Influence of Battery Energy Storage System on Steady State Stability of Power System," *2009 Int. Conf. Electr. Mach. Syst.*, pp. 1–4, Nov. 2009.

[63] L. Olatomiwa, S. Mekhilef, M. S. Ismail, and M. Moghavvemi, "Energy Management Strategies in Hybrid Renewable Energy Systems: A Review," *Renew. Sustain. Energy Rev.*, vol. 62, pp. 821–835, 2016.

[64] E. Dursun and O. Kilic, "Comparative Evaluation of Different Power Management Strategies of a Stand-Alone PV/Wind/PEMFC Hybrid Power System," *Int. J. Electr. Power Energy Syst.*, vol. 34, no. 1, pp. 81–89, 2012.

[65] Z. Liao and X. Ruan, "A Novel Power Management Control Strategy for Stand-Alone Photovoltaic Power System," *2009 IEEE 6th Int. Power Electron. Motion Control Conf.*, vol. 3, pp. 445–449, 2009.

[66] M. S. Ismail, M. Moghavvemi, and T. M. I. Mahlia, "Design of an Optimized Photovoltaic and Microturbine Hybrid Power System for a Remote Small Community: Case Study of Palestine," *Energy Convers. Manag.*, vol. 75, pp. 271–281, 2013.

[67] M. S. Ismail, M. Moghavvemi, and T. M. I. Mahlia, "Techno-economic Analysis of an Optimized Photovoltaic and Diesel Generator Hybrid Power System for Remote Houses in a Tropical Climate," *Energy Convers. Manag.*, vol. 69, pp. 163–173, 2013.

[68] E. M. Nfah and J. M. Ngundam, "Modelling of wind/Diesel/Battery Hybrid Power Systems for far North Cameroon," *Energy Convers. Manag.*, vol. 49, no. 6, pp. 1295–

1301, 2008.

[69] M. Dahmane, M. Ieee, J. Bosche, and M. Dafarivar, “Renewable Energy Management Algorithm for Stand – alone System,” no. October, pp. 20–23, 2013.

[70] M. S. Behzadi and M. Niasati, “Comparative Performance Analysis of a Hybrid PV/FC/Battery Stand-alone System using Different Power Management Strategies and Sizing Approaches,” *Int. J. Hydrogen Energy*, vol. 40, no. 1, pp. 538–548, 2015.

[71] V. Dash and P. Bajpai, “Power Management Control Strategy for a Stand-alone Solar Photovoltaic-Fuel Cell–Battery Hybrid System,” *Sustain. Energy Technol. Assessments*, vol. 9, pp. 68–80, 2015.

[72] S. Nasri, B. S. Sami, and A. Cherif, “Power Management Strategy for Hybrid Autonomous Power System using Hydrogen Storage,” *Int. J. Hydrogen Energy*, vol. 41, no. 2, pp. 857–865, 2016.

[73] S. Abedi, A. Alimardani, G. B. Gharehpetian, G. H. Riahy, and S. H. Hosseinian, “A Comprehensive Method for Optimal Power Management and Design of Hybrid RES-based Autonomous Energy Systems,” *Renew. Sustain. Energy Rev.*, vol. 16, no. 3, pp. 1577–1587, 2012.

[74] C. D. Barley and C. B. Winn, “Optimal Dispatch Strategy in Remote Hybrid Power Systems,” *Sol. Energy*, vol. 58, no. 4–6, pp. 165–179, 1996.

[75] M. Dali, J. Belhadj, and X. Roboam, “Theoretical and Experimental Study of Control and Energy Management of a Hybrid Wind-Photovoltaic System,” in *8th Internatiobal Multi-Conference on Systems,Signals & Devices*, 2007, no. 1.

[76] M. R. Basir Khan, R. Jidin, and J. Pasupuleti, “Multi-agent based Distributed Control Architecture for Microgrid Energy Management and Optimization,” *Energy Convers. Manag.*, vol. 112, pp. 288–307, 2016.

[77] A. Brka, G. Kothapalli, and Y. M. Al-Abdeli, “Predictive Power Management Strategies for Stand-alone Hydrogen Systems: Lab-scale Validation,” *Int. J. Hydrogen*

Energy, vol. 40, no. 32, pp. 9907–9916, 2015.

[78] S. Upadhyay and M. P. Sharma, "Selection of a Suitable Energy Management Strategy for a Hybrid Energy System in a Remote Rural Area of India," *Energy*, vol. 94, pp. 352–366, 2016.

[79] R. Palma-Behnke, C. Benavides, E. Aranda, J. Llanos, and D. Sáez, "Energy Management System for a Renewable based Microgrid with a Demand Side Management Mechanism," in *IEEE SSCI 2011 - Symposium Series on Computational Intelligence - CIASG 2011: 2011 IEEE Symposium on Computational Intelligence Applications in Smart Grid*, 2011, pp. 131–138.

[80] M. Hatti and M. Tioursi, "Dynamic Neural Network Controller Model of PEM Fuel Cell System," *Int. J. Hydrogen Energy*, vol. 34, no. 11, pp. 5015–5021, 2009.

[81] L. C. M. Blasques and J. T. Pinho, "Metering Systems and Demand-Side Management Models Applied to Hybrid Renewable Energy Systems in Micro-grid Configuration," *Energy Policy*, vol. 45, pp. 721–729, 2012.

[82] S. N. David, S. P. Santosh, and L. S. Narayanan, "Control Strategy for Power Flow Management in a PV System Supplying Electrical loads in an Air-conditioned Bus," *2014 Int. Conf. Power Signals Control Comput. EPSCICON 2014*, vol. 60, no. 8, pp. 3185–3194, 2014.

[83] C. Battistelli, L. Baringo, and A. J. Conejo, "Optimal Energy Management of Small Electric Energy Systems Including V2G Facilities and Renewable Energy Sources," *Electr. Power Syst. Res.*, vol. 92, pp. 50–59, 2012.

[84] N. Karami, N. Moubayed, and R. Outbib, "Energy Management for a PEMFC–PV Hybrid System," *Energy Convers. Manag.*, vol. 82, pp. 154–168, Jun. 2014.

[85] P. Finn and C. Fitzpatrick, "Demand Side Management of Industrial Electricity Consumption: Promoting the use of Renewable Energy through Real-time Pricing," *Appl. Energy*, vol. 113, pp. 11–21, 2014.

[86] J. Pascual, J. Barricarte, P. Sanchis, and L. Marroyo, “Energy Management Strategy for a Renewable-based Residential Microgrid with Generation and Demand Forecasting,” *Appl. Energy*, vol. 158, pp. 12–25, 2015.

[87] G. Comodi, M. Renzi, L. Cioccolanti, F. Caresana, and L. Pelagalli, “Hybrid System with Micro Gas Turbine and PV (photovoltaic) Plant: Guidelines for Sizing and Management Strategies,” *Energy*, vol. 89, pp. 226–235, 2015.

[88] H. Kim, S. Baek, E. Park, and H. J. Chang, “Optimal Green Energy Management in Jeju, South Korea - On-grid and Off-grid Electrification,” *Renew. Energy*, vol. 69, pp. 123–133, 2014.

[89] B. E. Turkay and A. Y. Telli, “Economic Analysis of Standalone and Grid Connected Hybrid Energy Systems,” *Renew. Energy*, vol. 36, no. 7, pp. 1931–1943, 2011.

[90] G. J. Dalton, D. A. Lockington, and T. E. Baldock, “Feasibility Analysis of Renewable Energy Supply Options for a Grid-Connected Large Hotel,” *Renew. Energy*, vol. 34, no. 4, pp. 955–964, 2009.

[91] Y. Aagreh and A. Al-Ghzawi, “Feasibility of Utilizing Renewable Energy Systems for a Small Hotel in Ajloun city, Jordan,” *Appl. Energy*, vol. 103, pp. 25–31, 2013.

[92] D. Saheb-Koussa, M. Koussa, M. Belhamel, and M. Haddadi, “Economic and Environmental Analysis for Grid-Connected Hybrid Photovoltaic-Wind Power System in the Arid Region,” *Energy Procedia*, vol. 6, pp. 361–370, 2011.

[93] Q. Jiang, M. Xue, and G. Geng, “Energy Management of Microgrid in Grid-connected and Stand-alone Modes,” *IEEE Trans. Power Syst.*, vol. 28, no. 3, pp. 3380–3389, 2013.

[94] B. Bahmani-Firouzi and R. Azizipanah-Abarghooee, “Optimal Sizing of Battery Energy Storage for Micro-grid Operation Management using a New Improved Bat Algorithm,” *Int. J. Electr. Power Energy Syst.*, vol. 56, pp. 42–54, 2014.

[95] B. B. Alagoz, A. Kaygusuz, and A. Karabiber, “A User-Mode Distributed Energy

Management Architecture for Smart Grid Applications," *Energy*, vol. 44, no. 1, pp. 167–177, 2012.

[96] C.-D. Dumitru and A. Gligor, "SCADA Based Software for Renewable Energy Management System," *Procedia Econ. Financ.*, vol. 3, no. 12, pp. 262–267, 2012.

[97] N. C. Batista, R. Melicio, J. C. O. Matias, and J. P. S. Catalao, "Photovoltaic and Wind Energy Systems Monitoring and Building/Home Energy Management using ZigBee Devices within a Smart Grid," *Energy*, vol. 49, no. 1, pp. 306–315, 2013.

[98] A. R. Al-Ali, A. El-Hag, M. Bahadiri, M. Harbaji, and Y. Ali El Haj, "Smart Home Renewable Energy Management System," *Energy Procedia*, vol. 12, pp. 120–126, 2011.

[99] Anonymous, "Pre - Charge," *Wikipedia*, 2016. [Online]. Available: https://en.wikipedia.org/wiki/Pre-charge. [Accessed: 27-Sep-2016].

[100] Anonymous, "How to Design Battery Charger Applications that Require External Microcontroller and Related System-Level Issues," *Maxim Integrated Products, Inc*, 2016. [Online]. Available: https://www.maximintegrated.com/en/app-notes/index.mvp/id/680. [Accessed: 27-Sep-2016].

[101] H. Grewal, "Li-Ion Battery Charger Solution using the MSP430," 2005.

[102] S. S. Mohammed, "Design , Simulation and Analysis of Microcontroller based DC-DC Boost Converter using Proteus Design," in *International Conference on Advances in Electrical & Electronics, AETAEE*, 2011, vol. 8, no. July,2011, pp. 22–43.

[103] P. Madhu and V. Viswanadha, "Design of Real Time Embedded Solar Tracking System," *Int. J. Emerg. Trends Eng. Res.*, vol. 3, no. 6, pp. 180–185, 2015.

[104] V.Srimaheswaran, V.J.Sivanagappa, and B.Goutham, "Interleaved Boost Converter for PV Cell Application Using DSPIC," *Int. J. Multidiscip. Approach Stud.*, vol. 2, no. 4, pp. 75–86, 2015.

APPENDICES

Appendix : MICROCONTROLLER PIC16F877A PINS DIAGRAM

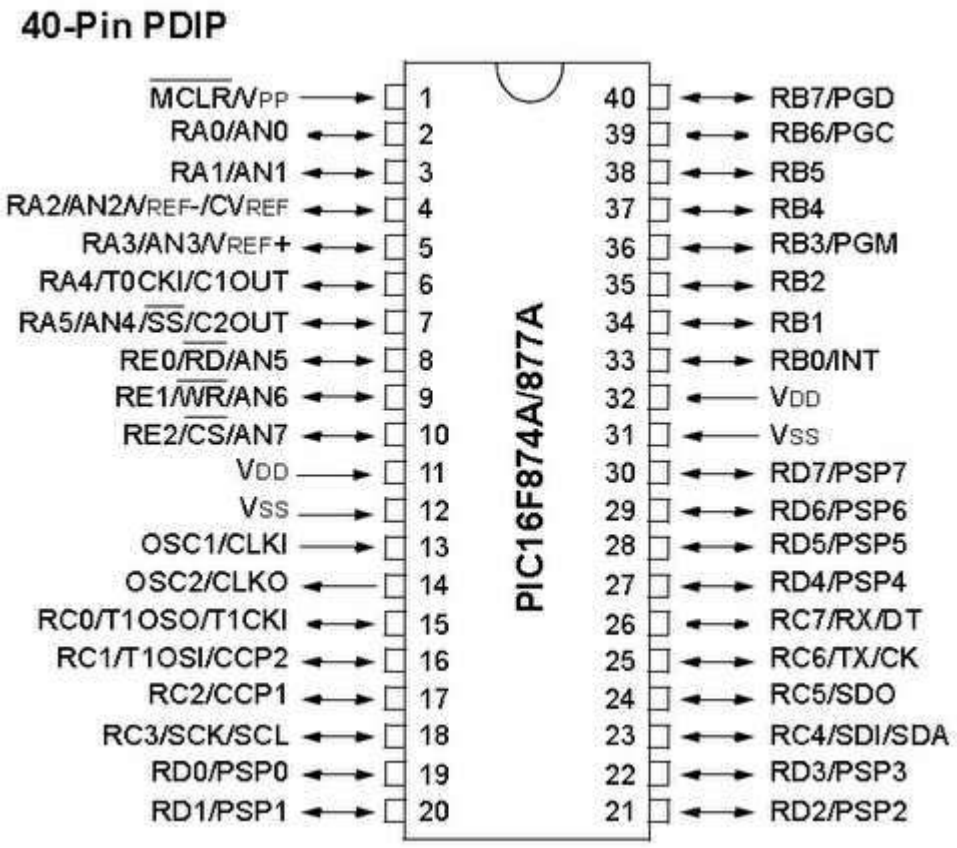

EMBEDDED PROGRAM – MICROCONTROLLER PIC16F877A

```
#include <16f877a.h>
#device adc=10
#use delay(clock=20000000)
```

```
#fuses hs,nowdt,nolvp,noprotect
#include <flex_lcd.c>
#define use_portb_lcd true
int A,B,C,D;
#separate
void halted();
#separate
void halted1();
#separate
void halted2();
#separate
void halted3();
#separate
void system();
#separate
void charging();
#separate
void charging1();
void charging2();
int lcd_ena=1;
float Solar;
float Wind;
float BA;
float BB;
float different=20;
void main()
{
   lcd_init();//Initialize the LCD Module
   lcd_ena=1;
   setup_adc_ports(AN0_AN1_AN2_AN3_AN4);
   setup_adc(adc_clock_internal);
   lcd_putc("    WELCOME   ");delay_ms(1000);lcd_putc("\f");
WHILE(1)
   {
      /////CHECK Voltage(wind energy)//////
      set_adc_channel(0);
      delay_us(20);
      Wind=read_adc();
      Wind=Wind*0.01465;
      delay_us(50);
       /////CHECK Voltage(solar energy)//////
      set_adc_channel(2);
      delay_us(20);
      Solar=read_adc();
      Solar=Solar*0.01465;
```

```
      delay_us(50);
      /////CHECK Voltage(BATTERY1)//////
      set_adc_channel(3);
      delay_us(20);
      BA=read_adc();
      BA=BA*0.0128;
      BA=(BA/13)*100;
      delay_us(50);
      /////CHECK Voltage(BATTERY2)//////
      set_adc_channel(4);
      delay_us(20);
      BB=read_adc();
      BB=BB*0.0128;
      BB=(BB/13)*100;
      delay_us(50);
      }
}
void system()
{
   output_low(GRID);
   if(A==1)
   {
   lcd_gotoxy(1,1);
   lcd_putc("WT=");//connected to the LOAD
   }
   if(A==0)
   {
   lcd_gotoxy(1,1);
   lcd_putc("wT=");//connected to the BESS
   }
   printf(lcd_putc,"%f",Wind);
   if(C==1)
   {
   lcd_gotoxy(10,1);
   lcd_putc("BA="); //connected for charging
   }
   if(C==0)
   {
   lcd_gotoxy(10,1);
   lcd_putc("bA=");//connected for discharging
   }
   printf(lcd_putc,"%f",BA);
   if(B==1)
   {
   lcd_gotoxy(1,2);
```

```
   lcd_putc("PV=");//connected to the LOAD
   }
   if(B==0)
   {
   lcd_gotoxy(1,2);
   lcd_putc("pV=");//Connected to the BESS
   }
   printf(lcd_putc,"%f",Solar);
   if(D==1)
   {
   lcd_gotoxy(10,2);
   lcd_putc("BB=");//connected to charging
   }
   if(D==0)
   {
   lcd_gotoxy(10,2);
   lcd_putc("bB=");//connected to discharging
   }
   printf(lcd_putc,"%f",BB);
   ////////////////////////////////////////////CONDITION1 both at
14V
   if(Solar>=13&&Wind>=13)
   {
      output_high(SOLARTOLOAD);
      output_high(WINDTOBATT);
      output_low(SOLARTOBATT);B=1;
      output_low(WINDTOLOAD);A=0;
      output_high(SOLARTOLOAD7);
      output_high(WINDTOBATT7);
      output_high(SOLARTOBATT7);
      output_high(WINDTOLOAD7);
      charging();
   }

   if(Solar<12 && Wind> 12)
   {
      output_low(WINDTOLOAD);A=0;
      output_high(SOLARTOBATT);
      output_high(SOLARTOLOAD);
      output_high(WINDTOBATT);
      output_high(SOLARTOLOAD7);
      output_high(WINDTOBATT7);
      output_low(SOLARTOBATT7);B=1;
      output_high(WINDTOLOAD7);
      charging2();
```

```
   }
   if(Solar>12 && Wind< 12)
   {
      output_high(WINDTOLOAD);
      output_high(SOLARTOBATT);
      output_low(SOLARTOLOAD);B=0;
      output_high(WINDTOBATT);
      output_high(SOLARTOLOAD7);
      output_low(WINDTOBATT7);A=1;
      output_high(SOLARTOBATT7);
      output_high(WINDTOLOAD7);
      charging2();
   }
   ////////////////////////////////////////////CONDITION2 both at
12V
   if(Solar<=12&&Wind<=12)
   {
      output_high(WINDTOLOAD);
      output_high(SOLARTOBATT);
      output_high(SOLARTOLOAD);
      output_high(WINDTOBATT);
      output_high(SOLARTOLOAD7);
      output_high(WINDTOBATT7);
      output_low(SOLARTOBATT7);B=1;
      output_low(WINDTOLOAD7);A=0;
      charging1();
   }
   if(Solar<7 && Wind>=12)
   {
      output_high(WINDTOLOAD);
      output_high(SOLARTOBATT);
      output_high(SOLARTOLOAD);
      output_low(WINDTOBATT);A=0;
      output_high(WINDTOLOAD7);
      output_high(SOLARTOBATT7);
      output_high(SOLARTOLOAD7);
      output_high(WINDTOBATT7);
      halted3();
   }
   if(Solar>=12 && Wind<7)
   {
      output_high(WINDTOLOAD);
      output_low(SOLARTOBATT);B=0;
      output_high(SOLARTOLOAD);
      output_high(WINDTOBATT);
```

```
      output_high(WINDTOLOAD7);
      output_high(SOLARTOBATT7);
      output_high(SOLARTOLOAD7);
      output_high(WINDTOBATT7);
      halted3();
   }
      if(Solar<7 && Wind>=7)
   {
      output_high(WINDTOLOAD);
      output_high(SOLARTOBATT);
      output_high(SOLARTOLOAD);
      output_high(WINDTOBATT);
      output_high(WINDTOLOAD7);
      output_high(SOLARTOBATT7);
      output_high(SOLARTOLOAD7);
      output_low(WINDTOBATT7);A=0;
      output_low(GRID);
      halted1();
   }
      if(Solar>=7 && Wind<7)
   {
      output_high(WINDTOLOAD);
      output_high(SOLARTOBATT);
      output_high(SOLARTOLOAD);
      output_high(WINDTOBATT);
      output_high(WINDTOLOAD7);
      output_high(SOLARTOBATT7);B=0;
      output_high(SOLARTOLOAD7);
      output_low(WINDTOBATT7);
      output_low(GRID);
      halted1();
   }
}
void charging()
{
   if((BA-BB)>=different)
   {
      output_high(BATT1CHARGING);
      output_low(BATT2CHARGING);D=1;
      output_high(BATT1DISCHARGING);C=0;
      output_high(BATT2DISCHARGING);
      output_high(BATT1CHARGING7);
      output_high(BATT2CHARGING7);
      output_high(BATT1DISCHARGING7);
      output_high(BATT2DISCHARGING7);
```

```
   }
   if((BB-BA)>=different)
   {
      output_high(BATT2CHARGING);
      output_low(BATT1CHARGING);C=1;
      output_high(BATT2DISCHARGING);D=0;
      output_high(BATT1DISCHARGING);
      output_high(BATT1CHARGING7);
      output_high(BATT2CHARGING7);
      output_high(BATT1DISCHARGING7);
      output_high(BATT2DISCHARGING7);
   }
   if(BA>=100&&BB>=100)//////////////stop charging
   {
      output_high(BATT1CHARGING);
      output_high(BATT2CHARGING);
      output_high(BATT1DISCHARGING);
      output_high(BATT2DISCHARGING);
      output_high(BATT1CHARGING7);C=1;
      output_high(BATT2CHARGING7);
      output_high(BATT1DISCHARGING7);
      output_high(BATT2DISCHARGING7);
   }
   if(BA<=40&&BB<=40)
   {
      output_high(BATT1DISCHARGING);
      output_high(BATT2DISCHARGING);
      output_low(BATT1CHARGING);C=1;
      output_high(BATT2CHARGING);
      output_high(BATT1CHARGING7);
      output_high(BATT2CHARGING7);
      output_high(BATT1DISCHARGING7);
      output_high(BATT2DISCHARGING7);
   }
}
void charging1()
{
   if((BA-BB)>=different)
   {
      output_high(BATT1CHARGING);
      output_high(BATT2CHARGING);
      output_high(BATT1DISCHARGING);
      output_high(BATT2DISCHARGING);
      output_high(BATT1CHARGING7);
      output_low(BATT2CHARGING7);D=1;
```

```
      output_high(BATT1DISCHARGING7);
      output_high(BATT2DISCHARGING7);
   }
   if((BB-BA)>=different)
   {
      output_high(BATT1CHARGING);
      output_high(BATT2CHARGING);
      output_high(BATT1DISCHARGING);
      output_high(BATT2DISCHARGING);
      output_high(BATT2CHARGING7);
      output_low(BATT1CHARGING7);C=1;
      output_high(BATT2DISCHARGING7);
      output_high(BATT1DISCHARGING7);
   }
   if(BA>=100&&BB>=100)//////////////stop charging
   {
      output_high(BATT1CHARGING);
      output_high(BATT2CHARGING);
      output_high(BATT1DISCHARGING);
      output_high(BATT2DISCHARGING);
      output_high(BATT1CHARGING7);
      output_high(BATT2CHARGING7);
      output_high(BATT1DISCHARGING7);
      output_high(BATT2DISCHARGING7);
   }
   if(BA<=40&&BB<=40)
   {
      output_high(BATT1CHARGING);
      output_high(BATT2CHARGING);
      output_high(BATT1DISCHARGING);
      output_high(BATT2DISCHARGING);
      output_high(BATT1DISCHARGING7);
      output_high(BATT2DISCHARGING7);
      output_low(BATT1CHARGING7);C=1;
      output_high(BATT2CHARGING7);
   }
}
void charging2()
{
   if((BA-BB)>=different)
   {
      output_high(BATT1CHARGING);
      output_high(BATT2CHARGING);
      output_high(BATT1DISCHARGING);
      output_high(BATT2DISCHARGING);
```

```
      output_high(BATT1CHARGING7);
      output_low(BATT2CHARGING7);D=1;
      output_high(BATT1DISCHARGING7);
      output_high(BATT2DISCHARGING7);
   }
   if((BB-BA)>=different)
   {
      output_high(BATT2CHARGING);
      output_high(BATT1CHARGING);
      output_high(BATT2DISCHARGING);
      output_high(BATT1DISCHARGING);
      output_low(BATT1CHARGING7);C=1;
      output_high(BATT2CHARGING7);
      output_high(BATT1DISCHARGING7);
      output_high(BATT2DISCHARGING7);
   }
   if(BA>=100&&BB>=100)//////////////stop charging
   {
      output_high(BATT1CHARGING);
      output_high(BATT2CHARGING);
      output_high(BATT1DISCHARGING);
      output_high(BATT2DISCHARGING);
      output_high(BATT1CHARGING7);
      output_high(BATT2CHARGING7);
      output_high(BATT1DISCHARGING7);
      output_high(BATT2DISCHARGING7);
   }
   if(BA<=40&&BB<=40)
   {
      output_high(BATT1DISCHARGING);
      output_high(BATT2DISCHARGING);
      output_high(BATT1CHARGING);
      output_high(BATT2CHARGING);
      output_low(BATT1CHARGING7);C=1;
      output_high(BATT2CHARGING7);
      output_high(BATT1DISCHARGING7);
      output_high(BATT2DISCHARGING7);
   }
}
void halted()
{
   lcd_putc("\f");
   while(1)
   {
   lcd_gotoxy(1,1);
```

```
lcd_putc(" HALTED - ONGRID ");
/////CHECK Voltage(wind energy)//////
   set_adc_channel(0);
   delay_us(20);
   Wind=read_adc();
   Wind=Wind*0.0146;
   delay_us(20);
   /////CHECK Voltage(solar energy)//////
   set_adc_channel(2);
   delay_us(20);
   Solar=read_adc();
   Solar=Solar*0.0147;
   delay_us(20);
   /////CHECK Voltage(BATTERY1)//////
   set_adc_channel(3);
   delay_us(20);
   BA=read_adc();
   BA=BA*0.0128;
   BA=(BA/13)*100;
   delay_us(20);
   /////CHECK Voltage(BATTERY2)//////
   set_adc_channel(4);
   delay_us(20);
   BB=read_adc();
   BB=BB*0.0128;
   BB=(BB/13)*100;
   delay_us(20);
   lcd_gotoxy(1,2);
   lcd_putc("wt=");
   printf(lcd_putc,"%f",Wind);
   lcd_gotoxy(10,2);
   lcd_putc("pv=");
   printf(lcd_putc,"%f",Solar);
 if((Solar<=7 && Wind<=7)&& (BA<=40&&BB<=40))
   {
   output_high(WINDTOLOAD);
   output_high(SOLARTOLOAD);
   output_high(SOLARTOBATT);
   output_high(WINDTOBATT);
   output_high(WINDTOLOAD7);
   output_high(SOLARTOLOAD7);
   output_high(SOLARTOBATT7);
   output_high(WINDTOBATT7);
   output_low(GRID);
   }
```

```
   if(Solar>9 || Wind>9)
      {
      lcd_putc("\f");
      lcd_putc("    BACK   ");
      delay_ms(1000);
      output_high(GRID);
      break;
      }
   }
}
void halted1()
{
   lcd_putc("\f");
   while(1)
   {
   lcd_gotoxy(1,1);
   lcd_putc(" OBC - ONGRID ");
   /////CHECK Voltage(wind energy)//////
      set_adc_channel(0);
      delay_us(20);
      Wind=read_adc();
      Wind=Wind*0.0146;
      delay_us(20);
      /////CHECK Voltage(solar energy)//////
      set_adc_channel(2);
      delay_us(20);
      Solar=read_adc();
      Solar=Solar*0.0146;
      delay_us(20);
      /////CHECK Voltage(BATTERY1)//////
      set_adc_channel(3);
      delay_us(20);
      BA=read_adc();
      BA=BA*0.0128;
      BA=(BA/13)*100;
      delay_us(20);
      /////CHECK Voltage(BATTERY2)//////
      set_adc_channel(4);
      delay_us(20);
      BB=read_adc();
      BB=BB*0.0128;
      BB=(BB/13)*100;
      delay_us(20);

      lcd_gotoxy(1,2);
```

```
    lcd_putc("wT=");
    printf(lcd_putc,"%f",Wind);
    lcd_gotoxy(10,2);
    lcd_putc("pv=");
    printf(lcd_putc,"%f",Solar);
if(BA>=100&&BB>=100)
 {
    output_high(BATT1CHARGING);
    output_high(BATT2CHARGING);
    output_high(BATT1DISCHARGING);
    output_high(BATT2DISCHARGING);
    output_high(BATT1DISCHARGING7);
    output_low(BATT2DISCHARGING7);D=0;
    output_high(BATT1CHARGING7);
    output_high(BATT2CHARGING7);
 }
 if((BA-BB)>=different)
 {
    output_high(BATT1CHARGING);
    output_high(BATT2CHARGING);
    output_high(BATT1DISCHARGING);
    output_high(BATT2DISCHARGING);
    output_low(BATT1DISCHARGING7);C=0;
    output_high(BATT2DISCHARGING7);
    output_high(BATT1CHARGING7);
    output_low(BATT2CHARGING7);D=1;
 }
 if((BB-BA)>=different)
 {
    output_high(BATT1CHARGING);
    output_high(BATT2CHARGING);
    output_high(BATT1DISCHARGING);
    output_high(BATT2DISCHARGING);
    output_high(BATT1DISCHARGING7);
    output_low(BATT2DISCHARGING7);D=0;
    output_low(BATT1CHARGING7);C=1;
    output_high(BATT2CHARGING7);
 }
 if(BA<=40&&BB<=40)
 {
    output_high(BATT1CHARGING);
    output_high(BATT2CHARGING);
    output_high(BATT1DISCHARGING);
    output_high(BATT2DISCHARGING);
    output_high(BATT1DISCHARGING7);
```

```
      output_high(BATT2DISCHARGING7);
      output_low(BATT1CHARGING7);C=1;
      output_high(BATT2CHARGING7);
      output_high(GRID);
   }
   if(Solar>9 && Wind>9)
      {
      lcd_putc("\f");
      lcd_putc("    BACK   ");
      delay_ms(1000);
      output_low(GRID);
      break;
      }
   }
}
void halted3()
{
   lcd_putc("\f");
   while(1)
   {
   lcd_gotoxy(1,1);
   lcd_putc(" OBC - ONGRID ");
   /////CHECK Voltage(wind energy)//////
      //set_adc_channel(0);
      //delay_us(20);
      //Wind=read_adc();
      //Wind=Wind*0.0146;
      //delay_us(20);
      /////CHECK Voltage(solar energy)//////
      //set_adc_channel(2);
      //delay_us(20);
      //Solar=read_adc();
      //Solar=Solar*0.0146;
      //delay_us(20);
      /////CHECK Voltage(BATTERY1)//////
      set_adc_channel(3);
      delay_us(20);
      BA=read_adc();
      BA=BA*0.0128;
      BA=(BA/13)*100;
      delay_us(20);
      /////CHECK Voltage(BATTERY2)//////
      set_adc_channel(4);
      delay_us(20);
      BB=read_adc();
```

```
   BB=BB*0.0128;
   BB=(BB/13)*100;
   delay_us(20);
   delay_us(100);
   lcd_gotoxy(1,2);
   lcd_putc("wt=");
   printf(lcd_putc,"%f",Wind);
   lcd_gotoxy(10,2);
   lcd_putc("pV=");
   printf(lcd_putc,"%f",Solar);
   if(BA>=80&&BB>=80)
 {
   output_high(BATT1CHARGING);
   output_high(BATT2CHARGING);
   output_high(BATT1DISCHARGING);
   output_low(BATT2DISCHARGING);D=0;
   output_high(BATT1DISCHARGING7);
   output_high(BATT2DISCHARGING7);
   output_high(BATT1CHARGING7);
   output_high(BATT2CHARGING7);
 }
 if((BA-BB)>=different)
 {
   output_high(BATT1CHARGING);
   output_low(BATT2CHARGING);C=0;
   output_low(BATT1DISCHARGING);D=1;
   output_high(BATT2DISCHARGING);
   output_high(BATT1DISCHARGING7);
   output_high(BATT2DISCHARGING7);
   output_high(BATT1CHARGING7);
   output_high(BATT2CHARGING7);
 }
if((BB-BA)>=different)
 {
   output_high(BATT1CHARGING);C=1;
   output_high(BATT2CHARGING);
   output_high(BATT1DISCHARGING);
   output_low(BATT2DISCHARGING);D=0;
   output_high(BATT1DISCHARGING7);
   output_high(BATT2DISCHARGING7);
   output_high(BATT1CHARGING7);
   output_high(BATT2CHARGING7);
 }
 if(BA<40&&BB<40)
 {
```

```
      output_low(BATT1CHARGING);C=1;
      output_high(BATT2CHARGING);
      output_high(BATT1DISCHARGING);
      output_high(BATT2DISCHARGING);
      output_high(BATT1DISCHARGING7);
      output_high(BATT2DISCHARGING7);
      output_high(BATT1CHARGING7);
      output_high(BATT2CHARGING7);
      output_high(GRID);
   }
   if(Solar>9 && Wind>9)
      {
      lcd_putc("\f");
      lcd_putc("    BACK   ");
      delay_ms(1000);
      output_low(GRID);
      break;
      }
   }
}
void halted2()
{
   lcd_putc("\f");
   while(1)
   {
   lcd_gotoxy(1,1);
   lcd_putc(" BESS ");
   lcd_gotoxy(1,2);
   lcd_putc("DisCh");
         /////CHECK Voltage(BATTERY1)//////
      set_adc_channel(3);
      delay_us(20);
      BA=read_adc();
      BA=BA*0.0128;
      BA=(BA/13)*100;
      delay_us(20);
      /////CHECK Voltage(BATTERY2)//////
      set_adc_channel(4);
      delay_us(20);
      BB=read_adc();
      BB=BB*0.0128;
      BB=(BB/13)*100;
      delay_us(20);
      if(C==1)
        {
```

```
      lcd_gotoxy(9,1);
      lcd_putc("BA="); //connected for charging
      }
   if(C==0)
      {
      lcd_gotoxy(9,1);
      lcd_putc("bA=");//connected for discharging
      }
      printf(lcd_putc,"%f",BA);
   if(D==1)
      {
      lcd_gotoxy(9,2);
      lcd_putc("BB=");//connected to charging
      }
   if(D==0)
      {
      lcd_gotoxy(9,2);
      lcd_putc("bB=");//connected to discharging
      }
      printf(lcd_putc,"%f",BB);
if((BA>=80&&BB>=80)&&(Solar<=7&&Wind<=7))
 {
   output_high(BATT1CHARGING);
   output_high(BATT2CHARGING);
   output_high(BATT1DISCHARGING);
   output_high(BATT2DISCHARGING);
   output_high(BATT1DISCHARGING7);
   output_low(BATT2DISCHARGING7);D=0;
   output_high(BATT1CHARGING7);C=1;
   output_high(BATT2CHARGING7);
 }
 if((BA-BB)>=different)
 {
   output_high(BATT1CHARGING);
   output_high(BATT2CHARGING);
   output_high(BATT1DISCHARGING);
   output_high(BATT2DISCHARGING);
   output_low(BATT1DISCHARGING7);C=0;
   output_high(BATT2DISCHARGING7);
   output_high(BATT1CHARGING7);
   output_high(BATT2CHARGING7);D=1;
 }
 if((BB-BA)>=different)
 {
   output_high(BATT1CHARGING);
```

```
      output_high(BATT2CHARGING);
      output_high(BATT1DISCHARGING);
      output_high(BATT2DISCHARGING);
      output_high(BATT1DISCHARGING7);
      output_low(BATT2DISCHARGING7);D=0;
      output_high(BATT1CHARGING7);C=1;
      output_high(BATT2CHARGING7);
   }
   if(BA<=40&&BB<=40)
   {
      output_high(BATT1CHARGING);
      output_high(BATT2CHARGING);
      output_high(BATT1DISCHARGING);
      output_high(BATT2DISCHARGING);
      output_high(BATT1DISCHARGING7);
      output_high(BATT2DISCHARGING7);
      output_high(BATT1CHARGING7);
      output_high(BATT2CHARGING7);D=1;
      output_high(GRID);
   }
   if(Solar>9||Wind>9)
      {
      lcd_putc("\f");
      lcd_putc("    BACK   ");
      delay_ms(1000);
      output_low(GRID);
      break;
      }
   }
}
```